REMARKS

Status of the claims

Claims 1-8 and 10-85 are pending of which 1, 6-8, 10-33, and 71-75 stand rejected and claims 2-5, 10, 34-70, and 76-85 are withdrawn. Claims 1, 6-8, 11-13, 15, 18, and 33 are amended and claims 2, 34-38, 51-52 are amended and withdrawn. Claim 9 was canceled previously and claims 10, 14, 20, 24, 26-28, 31, 39, 44, 49, 54, 58-61, 64, 69, 72-75 and 81 are canceled herein. New claims 86-89 are added. No new matter is added.

Amendments to the claims

In claim 1, the preamble is amended to remove the limiting phrases "covalent antibodies that form complexes with polypeptide antigens wherein said complexes do not dissociate on treatment with a protein denaturant, and". The preamble and body are amended, however, to recite antibodies that bind a peptide or protein covalently" (PP 0032; Fig. 2) and catalytic antibodies "that covalently bind to and hydrolyze the peptide or protein" to clarify that what is produced by the method using the same pCRA is both types of antibodies. Also, claim 1 is amended to clarify in the pCRA structure that antigenic determinant is "of the peptide or protein" recited in the preamble because Lx is defined as an amino acid residue. In addition, Y" is limited to a linker (PP Fig. 4). Applicants respectfully draw the Examiner's attention to the argument presented *infra* in the §112, second paragraph, rejections of claims 1 and 11.

In addition, claim 1 is amended to incorporate the limitations of selecting and screening the produced antibodies as recited in dependent claims 11 and 12 and to further clarify that 1) screening and selecting antibodies is for those antibodies that covalently bind to the pCRA or to the peptide or protein having one or more (PP 0032) of the antigenic determinant comprising the pCRA to identify covalent antibodies produced in the organism, and 2) screening and selecting for antibodies that covalently bind to the pCRA and screening from among the covalently binding antibodies for antibodies that catalytically hydrolyze a peptide bond in the peptide or protein having the antigenic determinant comprising the pCRA to identify catalytic antibodies produced in the organism. Withdrawn claim 2 is amended to correspond to the amendments to the pCRA structural formula (1) of claim 1.

Claim 6 is amended to clarify that "covalent and catalytic" antibody binding is to "the peptide or protein" to correspond to amended claim 1. Claim 7 is amended to correspond to claim 6. Claim 8 is amended to recite that the "protein" is HIV-1 gp120 to correspond to claim 1.

Claim 11 is amended to delete steps a) and b) and to recite "covalent antibodies or catalytic antibodies" in view of the amendments to claim 1.

Claim 12 is amended in the preamble to recite that the steps "of screening and selecting further comprise" to correspond to the inclusion of claim 12 steps b) and c) in amended claim 1 and is amended in the body of the claim to delete steps b) and c). In addition in claim 12, step a) is amended to indicate that the method step is performed "prior to screening and selecting for the covalently binding antibodies or antibody fragments thereof" and step d) is amended, as new step b) to correspond to amended claim 1.

PAGE 14/92 * RCVD AT 4/28/2010 6:45:45 PM [Eastern Daylight Time] * SVR:USPTO-EFXRF-6/33 * DNIS:2738300 * CSID:7132705361 * DURATION (mm-ss):48-00

Claim 13 is amended to depend from amended claim 1 and to recite that the antigenic "determinant" of the pCRA "comprises" the recited proteins to correspond to claim 1 amendments.

Claim 15 and withdrawn claim 38 are amended to replace "transonic" with "transgenic".

Claim 18 is amended to depend from amended claim 1 and the preamble is amended to delete the phrase "expressing covalent or catalytic activity" and replace the term "isolated" with "obtained" to correspond to amended claim 1. Also, claim 18 is amended to delete method steps d) and e) to end the method at step c).

Claim 33 is amended to replace "immunogenic" with "antigenic" to correspond to amended claim 1.

Claims 34-36 are amended to depend from pending amended claim 12 and claims 69 and 84-85 already depend directly from claim 12. Claim 37 is amended to clarify that the full length IgG, IgM and IgA antibodies prepared by the claim 12 method are prepared by the specific method steps recited in claim 37.

Claims 51-52 are amended to properly depend from claim 50 which depends from claim 38 which recites a method of obtaining, inter alia, antibody fragments.

New claims 86-89 are added to depend directly or indirectly from amended independent claim 1. Claim 86 recites that Y", Y' or Y does contain a water-binding group as a terminal or internal component which is an option recited in claim 1. Claims 87-89 correspond to claims 2-5. No new matter is contained in these claims.

Amendments to the specification

The specification was amended to replace the term "transonic" with "transgenic". No new matter was added

Restriction/Election of claims

The Examiner maintains the restriction of the claims such that claims 2-5, 34-70 and 76-85 remain withdrawn. The Examiner has rejected the Applicants contention that the original claims are unified by several technical features as described at length in Applicants' previous submission of 07/30/2009. The Examiner states that because **Taguchi** *et al.* teaches a CRA antigen having the same structure as Applicants' pCra, **Taguchi** *et al.* teach Applicants technical feature of conformational flexibility.

Applicants strongly aver that the pCRA of the instant amended independent claim 1 (and the pCRAW of amended withdrawn claim 2) and the conformational flexibility resulting from the structural arrangement provide the unifying feature of the claims. As discussed *infra* in traversing the §102 rejection over **Taguchi** *et al.*, the pCRA (and the pCRAW) are not identical to the CRA of **Taguchi** *et al.* Specifically, *inter alia*, the electrophile in the CRA of **Taguchi** et al. is not located at the functional group of an amino acid as in Applicant's pCRA. Instead, the electrophile of Taguchi et al is located at the C terminus. Moreover, the CRA of Taguchi et al does not contain a linker between the electrophile and the peptide C terminus. Without the linker, the electrophile in **Taguchi** et al. does not possess the requisite conformation flexibility provided to the electrophile in the instant pCRAs and pCRAWs. It is the pCRA (and pCRAW) structure, including the greater degree of conformational

PAGE 15/92 * RCVD AT 4/28/2010 6:45:45 PM [Eastern Daylight Time] * SVR:USPTO-EFXRF-6/33 * DNIS:2738300 * CSID:7132705361 * DURATION (mm-ss):48-00

flexibility conferred by the combined side chain functional group-linker-electrophile unit, per se that is the unifying element in claims 1-85.

Therefore, Applicants respectfully request that withdrawn claims 2-5, 34-38, 40-43, 45-48, 50-53, 55-57, 62-63, 65-70 and 76-80, and 82-85 be rejoined with the pending claims as Applicants have canceled claims 39, 44, 49, 54, 58-61, 64, and 81. Particularly, Applicants respectfully draw the Examiner's attention to claims 2-5 which encompass the pCRA structure of claim 1 including the optional water-binding group recited in claim 1. Also, Applicants wish to point out that claims 38 and 76 depend from claim 1 and recites a method for preparing the antibodies using the pCRA of claim 1 in an organism with autoimmune disease or medical condition, etc. by the method steps recited in original pending claim 12 and claims 67, 84-85 depend directly or indirectly from claim 12, as originally filed. Claims 40-43, 45-48, 50-53, 55-57, 62-63, 65, 68, and 70 and claims 77-78 depend directly or indirectly from claims 38 and claims 76. Furthermore, claims 79-82 and 84 utilize the pCRA in methods of treating medical conditions, such as autoimmune diseases. Thus, practice of the methods recited in the withdrawn claims all require the pCRA of amended independent claim 1. Applicants also request that new claims 86-89 be examined since they narrow the structure of the pCRA of amended claim 1.

Objections to the specification

The specification is objected to for reciting the incorrect term "transonic". The specification is amended to replace "transonic" with "transgenic", as described *supra*. Accordingly, in view of these amendments, Applicants respectfully request that the objection to the specification be withdrawn.

Objections to the claims

Claims 10, 14-15, 18, and 38 are objected to for the reasons described *infra*. Claim 14 is canceled.

Claim 10 is objected to as a duplicate of claim 8. Claim 10 is canceled herein.

Claim 18 is objected to for not reciting "and" before step "e)" and not starting "e)" in a different line. Claim 18 is amended to delete steps d) and e) thereby rendering the objection moot.

Claim 15 and withdrawn claim 38 are objected to for reciting "transonic". In claims 15 and 38 "transonic" is replaced with "transgenic".

Accordingly, in view of these amendments, Applicants respectfully request that the objections to claims be withdrawn.

The 35 U.S.C. §112, second paragraph, rejections

Claims 1, 6-8, 10-33, and 71-75 stand rejected under 35 U.S.C. §112, second paragraph, as being indefinite. Applicants respectfully traverse these rejections.

The Examiner states that claims 1 and 11 are unclear in their recitation of covalent antibodies as it is unclear what is meant by covalent antibodies because claim 1 produces catalytic antibodies using pCRA which is what the antibodies are considered to be for examination purposes. The Examiner continues that Applicant's amendment of claim 1 is indefinite because it is not clear whether "...covalent antibodies that form complexes with polypeptide antigens..." is covalently bound or not.

PAGE 16/92 * RCVD AT 4/28/2010 6:45:45 PM [Eastern Daylight Time] * SVR:USPTO-EFXRF-6/33 * DNIS:2738300 * CSID:7132705361 * DURATION (mm-ss):48-00

Applicants have canceled claims 10, 14, 20, 24, 26-28, 31, and 72-75. As discussed *supra*, independent claim 1 is amended to delete the phrases in the preamble considered indefinite and to amend the preamble and the body to recite antibodies that bind a peptide or a protein covalently and catalytic antibodies that covalently bind and hydrolyze the peptide or protein and to clarify in the body of the claim that both types of antibodies are prepared by the method. As discussed *supra*, dependent claim 11 is amended to recite that the covalent antibodies or catalytic antibodies screened and selected in steps a) and b) that are now amended into claim 1 are polyclonal antibodies.

Covalent and catalytic antibodies are functionally distinct entities. Covalent antibodies covalently bind naturally occurring peptide and protein antigens devoid of artificially incorporated electrophiles covalently. The binding by covalent antibodies is stable and resistant to dissociation to denaturants. Covalent antibodies do NOT express appreciable catalytic activity. Catalytic antibodies initially form an unstable covalent intermediate with naturally occurring peptide and protein antigens devoid of artificially incorporated electrophiles. After a water molecule attacks the complex of a catalytic antibody and the peptide or protein antigen, the result is degradation of the peptide or protein antigen by the catalytic antibody.

pCRAs and pCRAWs of the present invention bind covalently to both types of antibodies, covalent antibodies, as well as catalytic antibodies. However, unlike naturally occurring peptide and protein antigens, catalytic antibodies do not degrade pCRAs and pCRAWs, because the complex is usually resistant to water attack. The definition of 'covalent antibodies' as used in the present invention is supported by Figs. 41- 42 which shows gp120 binding by antibodies produced by immunization with a pCRA. The immune complexes were not dissociated by sodium dodecylsulfate, indicating irreversible antibody binding due to a covalent reaction. Sodium dodecylsulfate is well known to dissociate non-covalent complexes. Also, the antibodies owe their covalent reactivity to their increased nucleophilic reactivity attained by immunization with electrophilic pCRAs (PP0008, 0525, 0526). The mechanism whereby pCRAs and pCRAWs induce production of covalent antibodies is supported at PP 0099 and the distinction between covalent antibodies and catalytic antibodies is clarified in PP 0083. Examples of covalent antibodies raised to two pCRAs are described at PP 0087. Applicants submit, therefore, that covalent antibodies and catalytic antibodies, as recited in the claims, is clearly defined and would be readily understood by one of ordinary skill in the art given the recitation in the claim and disclosure in the specification.

The Examiner states that claim 6 is indefinite in the recitation of "denaturant" as there is no antecedent basis for the term in claim 1. Secondly, the Examiner states that claim 6 depends from claim 1 which requires the complexes not to dissociate upon treatment with a protein denaturant. The Examiner concludes that claim 6, in reciting "resistant to dissociation" is broader than claim 1.

As discussed *supra*, the phrase containing "...do not dissociate on treatment with a protein denaturant" was deleted from amended independent claim 1, so, as a first instance, the recitation of "a denaturant" is proper. Applicants submit that the body of claim 1 is amended to recite that the antibodies produced by the method of claim 1 are, *inter alia*, effective to covalently bind to the peptide or protein or pCRA antigen determinant comprising the same. As such, claim 6 is amended as discussed *supra* to clarify that covalent antibodies and catalytic antibodies binding to the peptide or the protein is further limited by being resistant to dissociation by "a denaturant".

PAGE 17/92 * RCVD AT 4/28/2010 6:45:45 PM [Eastern Daylight Time] * SVR:USPTO-EFXRF-6/33 * DNIS:2738300 * CSID:7132705361 * DURATION (mm-ss):48-00

Thus, with the deletion of the phrase containing the recitation "do not dissociate on treatment with a protein denaturant", dependent claim 6 is not broader than amended claim 1.

The Examiner states that claim 13 is indefinite for reciting "the antigenic pCRA is the CRA derivative of gp120..." because it is unclear how the term "CRA derivative" is related to the formula (1). As discussed *supra*, amended claim 13, which now depends from claim 1, recites that the antigenic determinant of the pCRA comprises the recited proteins to correspond to claim 1 amendments. Thus, the claim clearly identifies specific peptide antigenic determinants.

The Examiner states that claim 14 is indefinite for reciting "the polypeptide" as there is no antecedent basis for "the polypeptide" in claim 12 from which this claim depends. Claim 14 is canceled.

The Examiner states that claim 18 is indefinite for reciting "single chain Fv fragments expressing covalent or catalytic activity. The Examiner is unclear how an Fv fragment expresses these activities and what is a covalent activity in relation to an Fv fragment. As discussed *supra*, the phrase "expressing covalent or catalytic activity" is deleted from the claim, as are method steps d) and e). Claim 1 is amended to recite antibodies screened and selected by the method will bind covalently to the antigenic pCRA or to a peptide or protein having the antigenic determinant comprising the pCRA and will catalytically hydrolyze the peptide or protein. As amended, claim 18 limits the antibody fragments to Fv fragments and describes how they are isolated.

Accordingly, in view of the amendments and arguments presented herein, Applicants respectfully request that the rejection of claims 1, 6, 11, 13-14, and 18 under 35 U.S.C. §112, second paragraph, are withdrawn.

The 35 U.S.C. §112, first paragraph, rejections

Claim 1 is rejected and claims 6-7, 11-12, 15-23, 25-29, and 71-75 remain rejected under 35 U.S.C. §112, first paragraph, written requirement. Applicants respectfully traverse this rejection.

The Examiner states the independent claim 1 is directed to a method of generating catalytic antibodies to a polypeptide covalently attached to any transition state analog of any reaction and injecting the antigen into any organism such that the antibodies produced show the catalytic activity of cleaving any peptide bond of any polypeptide. The Examiner continues that the specification does not disclose how catalytic antibodies produced against any pCRA comprising any polypeptide epitope can catalyze the cleavage of any peptide bond of any antigenic polypeptide. The Examiner concludes that given this lack of description of representative species encompassed by the genus of the claim, the specification fails to sufficiently describe the claimed invention in such full, clear, concise, and exact terms that a skilled artisan would recognize that applicants were in possession of the claimed invention.

Applicant has amended independent claim 1 to limit Y" to a linker as is disclosed in Fig. 4 and 48-49 and in paragraphs 0034-0035, 0079-0080, 0098, 0590, 0618. Claim 1 is amended to limit the antigenic determinant of a peptide or protein and to incorporate steps recited in dependent claims of screening for and selecting for antibodies that both covalently bind the pCRA or a peptide or protein comprising the antigenic determinant thereof and catalytically cleave the peptide or protein as discussed *supra*. The specification well describes preparing covalent antibodies and covalent and catalytic antibodies using antigenic determinants from gp120, VIP, CD4, β-amyloid peptide 1-40 or β-amyloid peptide 1-42.

PAGE 18/92 * RCVD AT 4/28/2010 6:45:45 PM [Eastern Daylight Time] * SVR:USPTO-EFXRF-6/33 * DNIS:2738300 * CSID:7132705361 * DURATION (mm-ss):48-00

The specification describes that a linker, for example, but not limited to, a suberic acid or gamma-maleimidobutyryl group (Fig. 4) is placed between the electrophile Y and the side chain functional group of the antigenic determinant using known linker techniques (PP 0262) to enable control of the distance therebetween and the spatial positioning of these groups to provide conformational flexibility and freedom to permit simultaneous covalent binding of the Y electrophile to the antibody nucleophile and of the antigenic determinant to the antibody paratope (PP 0034, 0099). Optionally, the Y electrophile may be derivatized with a charged or neutral group, such as a (4-amidinophenyl)methylamine group, a 1-amino-4-guanidinobutyl group or an ethylamine group (Fig. 4) which provides an additional regulation of reactivity of the pCRA independent of the electrophilicity of Y (PP 0034).

In addition the specification discloses electrophiles, which as one particular example, generally are mono- or di-phenylphosphonates or boronates. The Figures (Figs. 5B-5C) disclose these structures and depict the phenyl(s) moiety as unsubstituted or substituted. The specification discloses that polypeptide analogs in which a covalently reactive electrophile can readily be located in side chains of the amino acids instead of the peptide backbone without unduly disturbing the native peptide or protein antigenic structure. (PP 0010). In general, as shown in Fig. 5A, the electrophile need only comprise an electron deficient atom (Z), which forms a covalent bond with the nucleophile and may contain one or more substituents (--R1 and --R2) attached to Z. R1 and R2 can be any atoms or groups that modulate the proclivity of Z to form covalent bond with a nucleophile. Typical examples of R1 and R2 include alkyl groups, alkoxyl groups, aryl groups, aryloxyl groups, hydrogen, and hydroxyl group. R1 and R2 can be pairs of the same or different substituents and R1 and R2 can be substituents that increase or decrease the covalent reactivity of the electrophile. The electronic characteristics of R1 and R2 control the electrophilic reactivity of the electrophile.

In general, the claimed pCRAs structures represent a broad genus unified by the common feature of covalent reactivity of the electrophile incorporated in the pCRAs with nucleophilic antibodies. Essentially all antibodies tested directed against diverse antigens express an innately occurring nucleophilic site with functional similarity to the serine protease family of enzymes. Consequently, the pCRAs react covalently with diverse antibodies, with specificity derived from noncovalent binding of the antigenic epitope of the pCRA to the traditional antibody paratope. Structural examples of pCRAs encompassing the entire genus that is reactive with covalent and catalytic antibodies directed to any antigen of claim 1 are provided in Example I for EGFR-pCRA, Example II for gp120-pCRA, Example III for VIP-pCRA and Example X for Aβ-pCRA.

In addition, the specification describes the induction of gp120 selective nucleophilic polyclonal antibodies in Example VI, the induction of VIP-selective nucleophilic polyclonal antibodies in Example VI, the induction of VIP-pCRA variant structures in Example XI, the structures of Aβ-pCRAs/pCRAWs and the antibody induction in Example X, covalent phage selection with gp120-pCRA: Isolation of gp120 selective catalytic antibodies in Examples VIII, and specific inhibition of anti-VIP catalytic antibodies by VIP-pCRAin Example III.

Thus, the written description provides sufficient guidance for one of ordinary skill in the art to prepare covalently binding, catalytic antibodies to a antigenic polypeptide of medical interest. The pCRA can be synthesized using the described electrophiles and linkers to bond to appropriate functional groups in the peptide or protein antigenic sequence, immunization of an organism is well-known in the art and the subsequent screening and

PAGE 19/92 * RCVD AT 4/28/2010 6:45:45 PM [Eastern Daylight Time] * SVR:USPTO-EFXRF-6/33 * DNIS:2738300 * CSID:7132705361 * DURATION (mm-ss):48-00

selecting for produced covalent antibodies and covalent and catalytic polyclonal or monoclonal antibodies or Fv fragments is well-described in the specification. It is well known in the art that near homologs or analogs of a chemical structural are likely to be functionally similar, if not identical. One of ordinary skill in the art is well-suited to design alternative linkers for the instant pCRAs based on the particular side chain functional groups L' and particular electrophile Y or, optionally, Y'-Y without undue experimentation and with a reasonable expectation of success. Similarly, it is known in the art that, *inter alia*, phosphonate or boronates are excellent electrophiles to covalently bind to nucleophilic antibodies. One of ordinary skill in the art is well able to design a suitable electrophile given the art and the disclosure of many electrophilic structures in the specification.

Therefore, the written description contained in Applicant's specification allows one of ordinary skill in the art to practice the invention of amended independent claim 1 and dependent claims 6-7, 11-12, 15-23, 25-29, and 71-75. Accordingly, in view of the amendments and arguments presented, Applicants respectfully request that the rejection of claims 1, 6-7, 11-12, 15-23, 25-29, and 71-75 under 35 U.S.C. §112, first paragraph, written description, be withdrawn.

Claim 1 is rejected and claims 6-7, 11-12, 15-23, 25-29, and 71-75 remain rejected under 35 U.S.C. §112, first paragraph, enablement requirement. Applicants respectfully traverse this rejection.

The Examiner states that the specification, while being enabling for a method of generating catalytic antibodies to the antigens of Figs. 36 or 48-49 or compounds of claims 30-33 where the method comprises administering the pCRA to an organism, such as a mouse, and where the catalytic antibodies cleave the peptide bond of gp120 peptide, does not reasonably enable a method of generating a catalytic antibody that shows proteolytic activity against any peptide bond of any protein or peptide. The Examiner continues that production of catalytic antibodies depends on the structure of the transition state analog and the enzymatic reaction depends on mimicking the transition state analog of bond cleavage or formation of that reaction. The Examiner concludes that the specification does not teach the structures of all the constituents of the pCRA recited in claim 1 and, hence, the transition state analog of peptide bond cleavage reaction, the specification does not enable any person skilled in the art to which it pertains or is most nearly connected to make and use the invention commensurate in scope with these claims.

Applicant has amended independent claim 1 as discussed *supra*. Applicants maintain that the written description in the specification provides sufficient guidance for one of ordinary skill in the art to prepare covalent antibodies and catalytic antibodies as recited in the method steps of amended independent claim 1. Applicants also submit that the enablement in the specification to prepare such antibodies to gp120, vasoactive intestinal peptide (VIP), β-amyloid peptide 1-40 or β-amyloid peptide 1-42 antigenic determinants, as described *supra*, enables one of ordinary skill in the art to prepare covalent antibodies and catalytic antibodies to other prophylactic or therapeutic antigenic polypeptides, such as, but not limited to, cytokines, growth factors, cytokine and growth factor receptors, proteins involved in the transduction of stimuli intiated by growth factor receptors, clotting factors, integrins, antigen receptors, enzymes, transcriptional regulators particularly those involved in cellular program, such as differentiation, proliferation and programmed cell death, control, other inducers of these cellular programs, cellular pumps capable of expelling anticancer agents, microbial and viral peptide antigens (PP 0137).

PAGE 20/92 * RCVD AT 4/28/2010 6:45:45 PM [Eastern Daylight Time] * SVR:USPTO-EFXRF-6/33 * DNIS:2738300 * CSID:7132705361 * DURATION (mm-ss):48-00

Independent claim 1 is amended to limit the antigenic determinant to a peptide or protein antigenic determinant. One of ordinary skill in the art must know the antigenic sequence of the peptide of interest, although Applicants submit that one of ordinary skill in the art could readily make a pCRA with a potential antigenic sequence where the isolation of covalently binding, catalytic antibodies would be an indicator that the tested polypeptide sequence is antigenic. As discussed, the specification describes the structural components of a pCRA and how to make the pCRA with appropriate electrophiles and linking molecules. Producing an antibody in an organism is well-known in the art and the specification describes and enables one of ordinary skill in the art to screen and select for covalently binding, catalytic antibodies or fragments thereof from serum or lymphocytes depending on whether one is screening for polyclonal or monoclonal antibodies or fragments.

As such, at a minimum the specification enables induction of gp120 selective nucleophilic polyclonal antibodies in Example VI, induction of VIP-selective nucleophilic polyclonal antibodies in Example VI, induction of VIP-pCRA variant structures in Example XI, the tructures of Aβ-pCRAs/pCRAWs and antibody induction in Example X, covalent phage selection with gp120-pCRA: Isolation of gp120 selective catalytic antibodies in Examples VIII, and specific inhibition of anti-VIP catalytic antibodies by VIP-pCRAin Example III.

Also, the enablement rejections appear to derive from the Examiner's assertions that the pCRAs and pCRAWs of the present invention are synonymous with transition state analogs (TSAs) described by Mader *et al.* Chem Rev. 1997, 97, 1281-1301. Applicants maintain that pCRAs/pCRAWs of the present invention are chemically and functionally distinct from the TSAs as described in detail in the Applicant's submission of 7/30/2009. The differences between TSAs and pCRAs are summarized in the Table below which clearly demonstrates that Transition State Analogs (TSAs) are not pCRAs/pCRAWs.

PAGE 21/92 * RCVD AT 4/28/2010 6:45:45 PM [Eastern Daylight Time] * SVR:USPTO-EFXRF-6/33 * DNIS:2738300 * CSID:7132705361 * DURATION (mm-ss):48-00

Feature	TSA Mader et al. Chem Rev. 1997, 97, 1281-1301	pCRA/pCRAW US 10/581294
Structure		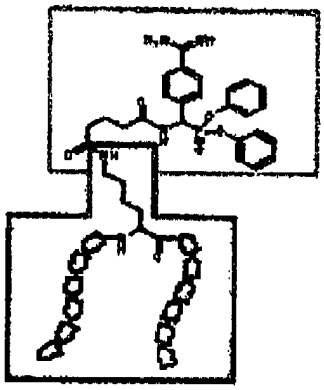
Chemical properties	• Full negative charge • No covalent reactivity • Reactive group within peptide backbone or terminus	• Covalent reactivity • Reactive group on peptide side chain
Properties of induced Antibodies	• *de novo* synthesis of Abs induced by oxyanion hole • Noncovalent TS stabilization • Esterase activity, no example of proteolytic activity	• Preferential recruitment of innate nucleophilic Abs coordinated with adaptive development of peptide specificity • Covalent catalysis, Proteolytic activity

The broad utility of pCRAs can be appreciated if it is understood that all antibodies tested were found to have nucleophilic sites that react with electrophiles in coordination with noncovalent binding of the antibody to the antigenic epitope or determinant (see Example 1). Therefore, pCRAs containing the appropriate electrophile and the appropriate antigenic epitope can be used broadly to identify any covalently binding antibody and any catalytic antibody to any peptide or protein antigen. Multiple examples of such covalently binding antibodies and catalytic antibodies are provided throughout the specifications. As described in the specifications, the pCRAs recruit the innate nucleophilic reactivity of antibodies and induce adaptive improvement of the nucleophilic reactivity coordinated with improvement of the noncovalent binding affinity for defined antigenic epitopes.

Chica *et al* Curr Opin Biotechnol, 1997, 97, 1281-1301 discuss difficulties in obtaining enzymatic activity by ab initio design and by directed evolution methods. The Examiner's enablement rejections are based in

PAGE 22/92 * RCVD AT 4/28/2010 6:45:45 PM [Eastern Daylight Time] * SVR:USPTO-EFXRF-6/33 * DNIS:2738300 * CSID:7132705361 * DURATION (mm-ss):48-00

part on the difficulties discussed by Chica *et al.* The present invention does not rely on the methods discussed by Chica *et al.* Therefore, the Applicants maintain that Chica *et al* is not germane to the present invention.

In addition, Applicants provided verification of enablement is available from additional examples of the utility of pCRAs published in scientific journals by the Applicants and other research groups (copies enclosed) as shown in the following outline.

I. Enablement of immunization/catalytic antibody induction

A. Immunization with pCRA

1. Induction of Induction of gp120 selective catalytic antibodies: Examples II and VI (Paul *et al.*, J Biol Chem 2003 May 30; 278(22):20429-20435).

2. Induction of gp120 selective covalent antibodies: Example VI (Nishiyama *et al*, J Mol Recognit. 2006 Sep-Oct; 19(5):423-31).

3. gp120 peptide CRA: Mol Immunol. 2009 Nov; 47(1):87-95. This paper reports catalytic antibody production by immunization of mice with a peptide CRA.

B. Immunization with V3 epitope pCRA

1. Induction of virus reactive covalent antibodies: Nishiyama *et al*, J Biol Chem. 2007 Oct 26; 282(43):31250-6.

II. Enablement of catalytic antibody selection/isolation

A. Covalent phage selection with Aβ-pCRA: Isolation of Aβ selective catalytic antibodies: Taguchi *et al*, J Biol Chem. 2008 Dec 26; 283(52):36724-33.

B. Aβ CRA: Kasturirangan *et al*, Biotechnol Prog. 2009 Jul-Aug;25 (4):1054-63. This paper reports isolation of Aβ selective catalytic antibodies by covalent phage selection.

III. Enablement of catalytic antibody selection/isolation

A. Specific inhibition of anti-VIP catalytic antibodies by VIP-pCRA: Example III (Nishiyama *et al.*, J Biol Chem 2004 Feb 27; 279(9):7877-83).

B. Specific inhibition of anti-FVIII catalytic antibodies by FVIII-pCRA and FVIII-C2-pCRA: Planque *et al.*, J Biol Chem. 2008 May 2; 283(18):11876-11886.

Thus, the specification enables amended independent claim 1. As claims 6-7, 11-12, 15-23, 25-29, and 71-75 depend directly or indirectly from amended claim 1, these dependent claims also are enabled. Accordingly, in view of the amendments and arguments presented herein, Applicants respectfully request that the rejection of claims 1, 6-7, 11-12, 15-23, 25-29, and 71-75 under 35 U.S.C. §112, first paragraph, enablement, be withdrawn.

The 35 U.S.C. §102 rejections

Claim 1 is rejected and claims 8-14, 16, 24, and 31 stand rejected under 35 U.S.C. §102(a) as being anticipated by **Taguchi** *et al.* (Bioorg. and Med. Chem. Lett., 2002, 12:3167-3170). Applicants respectfully traverse this rejection.

The Examiner states that **Taguchi** *et al.* teach catalytic antibodies raised by using a gp120 polypeptide epitope (L of claim 1 having a carboxyl functional group of amino acid residues as Y") attached covalently to a phosphonate ester (Y reactive electrophilic group, Transition state analog) which comprises a covalently reactive

PAGE 23/92 * RCVD AT 4/28/2010 6:45:45 PM [Eastern Daylight Time] * SVR:USPTO-EFXRF-6/33 * DNIS:2738300 * CSID:7132705361 * DURATION (mm-ss):48-00

antigen (CRA) (pg. 3168, Fig. 1) where the phosphonate ester moiety binds to the antibody. The Examiner also states that **Taguchi** *et al.* disclose a method of producing the antibody by administering the CRA to a mouse (pg. 3168, col. 1, PP 3).

Applicants submit that **Taguchi** *et al.* disclose an antigenic peptide analog consisting of HIV gp120 residues 421-431 with a diphenyl amino(4-amidinophenyl)methanephosphonate located at the C-terminus. Antibodies to the peptide determinant recognized the peptidyl phosphonate probe.

Claims 24 and 31 are canceled. As discussed *supra*, independent claim 1 is amended to recite a Y" linker. Also, claim 1 is amended to incorporate steps to obtain, screen and select for the covalently binding, catalytic antibodies produced by the pCRA in the organism.

It is well established that to anticipate a claim, a single reference must disclose each and every claim element as they are arranged in the claim. The Examiner maintains that, in the CRA of **Taguchi** *et al.*, the gp120 polypeptide epitope is the "L" in Applicant's pCRA where the carboxyl functional group of the amino acid residue corresponds to L' in the pCRA. As recited in amended independent claim 1, the L1...Lx...Lm component of Applicants' pCRA is an antigenic determinant of a polypeptide or a protein where L' within the antigenic determinant is a functional group of any amino acid side chain, e.g., those of Lys, Asp, Glu, Cys, Ser, Thr, and Tyr (PP 0095). L' is linked by a linker Y", for example, but not limited to, a suberic acid or a gamma-maleimidobutyryl group directly to the electrophilic group Y or L' is indirectly linked to Y" via the optional Y' group (which may be the 4-amidinophenyl)methylamine group as in **Taguchi** *et al.*) to the electrophilic group.

At a minimum Applicants submit that the CRA of **Taguchi** *et al.* does not have a Y" group as in Applicants' claim 1. Applicants present the diagram below to explain their position. Panel (A) shows the general formula for pCRAs of the present invention. Panel (B) shows the compound disclosed in **Taguchi** *et al*, an analog of gp120 residues 421-433. This compound consists of a peptide corresponding to residues 421-431, in which the backbone carboxyl group of Gly431 is connected to the aminoalkylphosphonate group via a C-N covalent bond. The chemical designation system identifying the pCRA elements in the present invention is employed to identify various components of the **Taguchi** *et al* compound. Panel (C) shows an example pCRA of the present invention corresponding to gp120 residues 421-433. Element Lx in the **Taguchi** compound is devoid of a side chain and cannot be used prepare a pCRA of the present invention, as a defining feature of the pCRAs is the side chain location of the unit composed of elements L'-Y"-Y-Y. Moreover element L' of the present invention is missing altogether in the **Taguchi** *et al* compound. Moreover, element Lm is also missing in **Taguchi** et al compound, as the unit composed of elements Y"-Y'-Y is attached to the C-terminus. In comparison, the unit of elements Y"-Y'-Y is attached to the side chain in the pCRAs, making possible incorpopration of element Lm in the present invention. The lack of chemical identity between the **Taguchi** *et al* compound and the pCRAs of the present invention is evident.

PAGE 24/92 * RCVD AT 4/28/2010 6:45:45 PM [Eastern Daylight Time] * SVR:USPTO-EFXRF-6/33 * DNIS:2738300 * CSID:7132705361 * DURATION (mm-ss):48-00

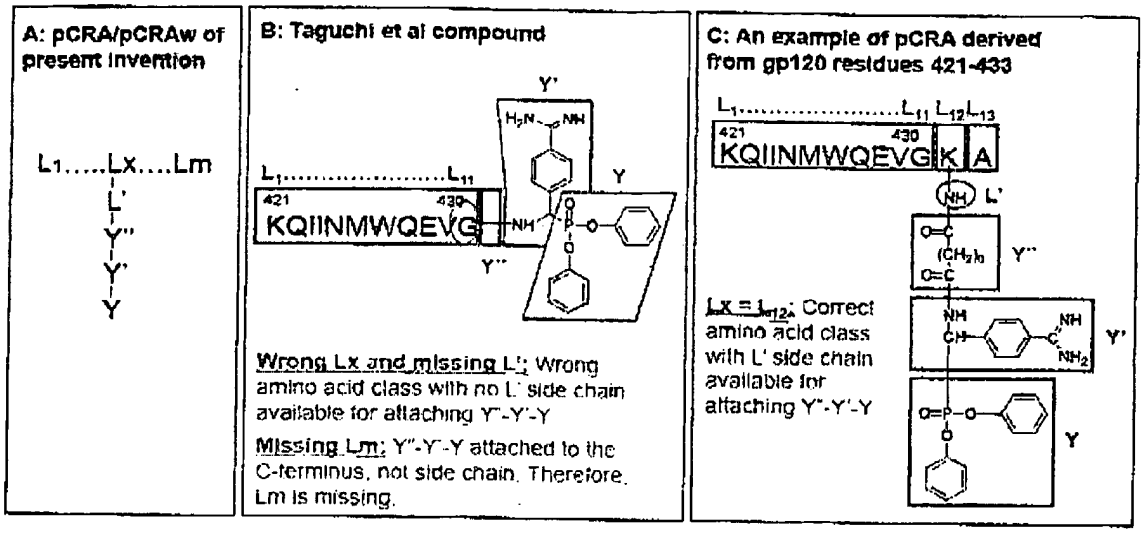

For these reasons, neither can **Taguchi** *et al.* render obvious amended independent claim 1 and, by extension, dependent claims 8-14, 16 and 24. Given the synthetic and structural requirements for the CRA of **Taguchi** *et al*, one of ordinary skill in the art cannot predict that modifying any side chain functional group with a linker and electrophile would produce an effective pCRA because such positioning would not mimic the Lys432-Ala433 cleavage target in gp120. In the CRA in **Taguchi** *et al.*, the positively charged amidino group adjacent to the phosphonate diester group serves as an analog of Lys432 (pg. 3167, 2nd col., last PP).

Thus, Applicants' pCRA as recited in claim 1 is arranged differently from and comprises components not found in the CRA disclosed in **Taguchi** *et al.* In the absence of these teachings, **Taguchi** *et al.* do not teach all the claim elements of the pCRA of amended independent claim 1 as they are arranged and, therefore, cannot anticipate the method recited in amended independent claim 1. Claims 8-14, 16, 24, and 31 depend directly or indirectly from amended independent claim 1 and as claim 1 is not anticipated by **Taguchi** *et al.*, these dependent claims are also not anticipated by **Taguchi** *et al.* Accordingly, in view of the arguments and amendments presented herein, Applicants respectfully request that rejection of the claims 1, 8-14, 16, 24, and 31 under 35 USC §102 be withdrawn.

Claim 1 is rejected and claims 8-14, 16-18, 21-22, 24-29, 71-72, and 74 stand rejected as being anticipated by **Paul** *et al.* (U.S. Patent No. 6,235,714). Applicants respectfully traverse this rejection.

In considering independent claim 1, the Examiner states that **Paul** *et al.* teach a catalytic antibody and a method of producing said antibody (monoclonal or polyclonal, single chain Fv fragments; col. 16, ll. 48-66) by administering to an organism (MRL/lpr mouse, col. 14, ll. 45-60) a covalently reactive peptide antigen, CRAA (col. 3, ll. 25-45) where the CRAA is X1-Y-E-X2, where X1 and X2 are peptide molecules having reactive functional group attached to and electrophonic reactive center E that reacts covalently to a nucleophile, and Y is a basic residue of the peptide molecule. The Examiner maintains that the CRRA of **Paul** *et al.* is identical to Applicants' pCRA. The Examiner also states that **Paul** *et al.* teach that the antigen molecule comprises tumor necrosis factor, epidermal growth factor receptor, gp120 (claim 4), etc. and that **Paul** *et al.* disclose that the catalytic antibodies produced

PAGE 25/92 * RCVD AT 4/28/2010 6:45:45 PM [Eastern Daylight Time] * SVR:USPTO-EFXRF-6/33 * DNIS:2738300 * CSID:7132705361 * DURATION (mm-ss):48-00

against the antigens can be used for the treatment of medical disordes like cancer, autoimmune disease (col. 6, ll. 1-13; Figs. 19A-19B.

Applicants submit that **Paul** *et al.* disclose covalently reactive antigen analogs (CRAA) that stimulate production of catalytic antibodies specific for predetermined antigens that are associated with certain medical disorders. The CRAA has a X1-Y-E-X2 component structure where E is an electrophilic reaction center, Y is a basic residue (Arg or Lys) at the first amino acid on the N terminal side of the reaction center or at the P1 position and X1 and X2 are three to ten flanking amino acids on the N-terminal and C-terminal side of the reaction center (col. 3, ll. 26-35).

Applicants' amended independent claim 1 is described *supra*. It is well established that to anticipate a claim, a single reference must disclose each and every claim element as they arranged in the claim. Applicants strongly maintain that, the Examiner's contention notwithstanding, Applicants' pCRA, as recited in amended independent claim 1, is **not** (Applicants' emphasis) identical to the CRAA of **Paul** *et al.* Applicants' pCRA contains a covalently reactive electrophilic group, such as a mono- or di-substituted phosphonate or boronate group that is linked to an amino acid side chain functional group via a linking moiety, e.g., *inter alia*, a gamma-malimidobutyryl group or a suberic acid group. In addition, optionally, the pCRA may comprise a charged or neutral group between the phosphonate/boronate moiety, e.g. and the linker, as shown in Fig. 4. As such, the side chain functional group may comprise any amino acid, e.g., the negatively charged carboxyl of aspartic acid or glutamic acid, the positively charged amino group of lysine or arginine, the hydroxy group of polar amino acids serine, threonine and tyrosine or the nonpolar sulfhydryl of cysteine (Fig. 4).

In distinct contrast, **Paul** *et al.* disclose that the CRAA described therein is composed of an electrophilic phosphonate ester flanked by amino acid residues, e.g., EGFR residues 294-303 on the N terminal side and EGFR residues 304-310 on the C terminal side (col. 15, ll. 5-8; Fig. 4). In addition the N terminal residue must be positively charged which limits the amino acids to arginine or lysine (claim 1, Fig. 10). The phosphonate residue is inserted between residues in the polypeptide, but does not form bonds with any of the sidechain molecules (Figs. 15-17).

More particularly, Applicants present the figure below to explain their position. Panel (A) shows the general formula for pCRAs of the present invention. Panel (B) shows an example of the CRAA disclosed by **Paul** *et al*, an analog of gp120 residues 421-436. This compound consists of a peptide corresponding to residues 421-436. The chemical designation system identifying the pCRAs in the present invention is employed to identify various components of the CRAA disclosed by **Paul** *et al.* Panel (C) shows an example pCRA of the present invention corresponding to gp120 residues 421-433. Elements Y", Y' and Y of the pCRAs of the present invention are located within the peptide backbone of the **Paul** *et al* CRAA. In contrast, these elements are located on the side chain of an amino acid in the pCRAs of the present invention. The L' element of the present invention is missing altogether in the **Paul** *et al* CRAA. The lack of chemical identity between the **Paul** *et al* CRAAs and the pCRAs of the present invention is evident from this comparison.

PAGE 26/92 * RCVD AT 4/28/2010 6:45:45 PM [Eastern Daylight Time] * SVR:USPTO-EFXRF-6/33 * DNIS:2738300 * CSID:7132705361 * DURATION (mm-ss):48-00

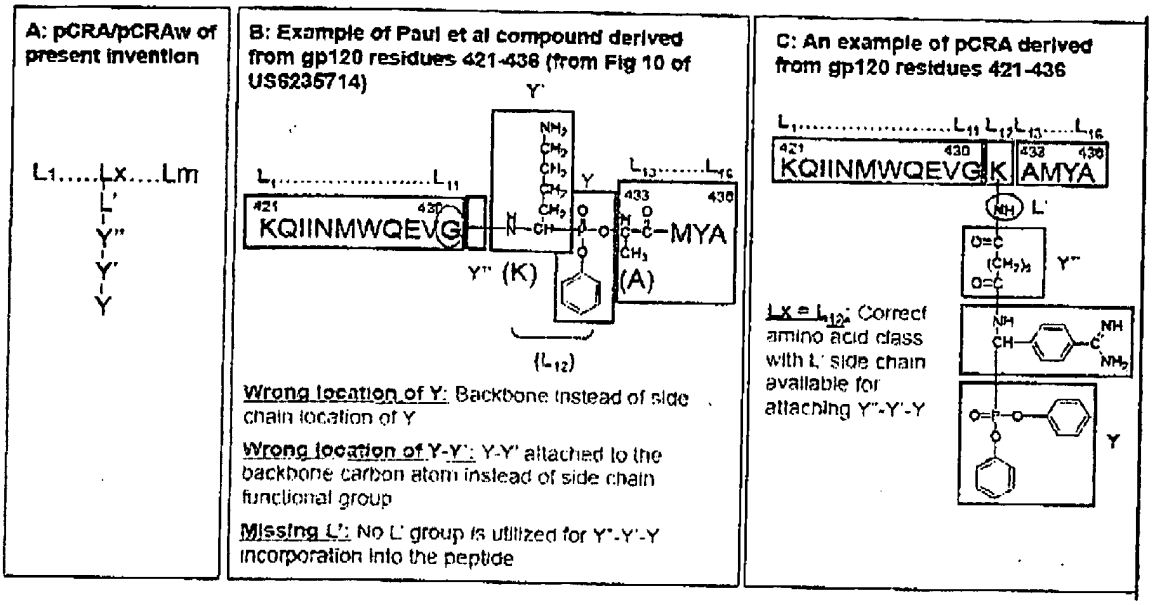

The Applicants wish the Examiner to please note that the chemical designations from the present pCRA/pCRAW are used to illustrate chemical non-identity in panel B (L1...L11, Y", Y').

For these reasons neither can **Paul** *et al.* render obvious amended independent claim 1 and, by extension, dependent claims 8-14, 16-18, 21-22, 24-29, 71-72, and 74. Given the structural requirements for the CRAA of **Paul** *et al*, one of ordinary skill in the art cannot predict that modifying any side chain functional group with a linker and electrophile would produce an effective pCRA because such positioning would removes the electrophile from the flanked position at the reaction center within the peptide and require that a linker be incorporated to link the electrophile to the side chain functional group. In the CRAA in **Paul** *et al.*, the specific positional combination of individual structural elements act in concert to (a) bind chemically reactive serine residues encoded by the germline genes for certain serine protease types of catalytic antibodies; (b) utilize ion pairing and noncovalent forces to bind structures such as positively charged Asp/Glu residues that are responsible for the basic residue cleavage specificity of the germline encoded catalytic sites; and (c) bind antibody combining sites at multiple amino acids via ion pairing and noncovalent forces. (col. 3, ll. 27-45).

Thus, Applicants aver that Applicants' pCRA as recited in claim 1 is not identical to the CRAA disclosed in **Paul** *et al.* **Paul** *et al.* do not teach all the claim elements of the pCRA of amended independent claim 1 as they are arranged and, therefore, cannot anticipate the method recited in amended independent claim 1. Claims 8-14, 16-18, 21-22, 24-29, 71-72, and 74 depend directly or indirectly from amended independent claim 1 and as claim 1 is not anticipated by **Paul** *et al.*, then neither would these dependent claims be anticipated by **Paul** *et al.* Accordingly, in view of the arguments and amendments presented herein, Applicants respectfully request that rejection of the claims 1, 8-14, 16-18, 21-22, 24-29, 71-72, and 74 under 35 USC §102 be withdrawn.

PAGE 27/92 * RCVD AT 4/28/2010 6:45:45 PM [Eastern Daylight Time] * SVR:USPTO-EFXRF-6/33 * DNIS:2738300 * CSID:7132705361 * DURATION (mm-ss):48-00

Double patenting rejections

Claims 1, 6-29 and 71-75 remain rejected under the judicially created doctrine of obviousness-type double patenting as being unpatentable over claim 1 of U.S. Patent No. 6,855,528. The Examiner contends that U.S. Patent No. 6,855,528 teaches a method of producing a catalytic antibody (CRAA) which is identical to Applicant's pCRA.

Claim 1 in U.S. Patent No. 6,855,528 does not provide the structure of the CRAA, however this patent is a divisional of U.S. Patent No. 6,235,714 which is cited as anticipating Applicants' independent claim 1 under 35 U.S.C. §102(b). As discussed *supra*, Applicant's pCRA is distinctly and structurally different from the CRAA. Nor, given the requirements for a CRAA, would Applicants' pCRA be an obvious variant thereof, particularly since the electrophilic group must be flanked by residues of the antigenic determinant and the N terminal residue must be positively charged overall. One of ordinary skill in the art cannot reasonably predict that linking a side chain functional group of any amino acid to the electrophilic group with the Y" groups would yield an effective polypeptide covalently reactive analogs (pCRA). Thus, Applicants' submit that a terminal disclaimer is not required. Accordingly, in view of the arguments and amendments presented herein, Applicants respectfully request that rejection of the claims 1, 6-29 and 71-75 under the judicially created doctrine of obviousness-type double patenting as being unpatentable over claim 1 of U.S. Patent No. 6,855,528 withdrawn.

Applicants submit that this Response to Office Action, mailed October 28, 2009, is complete. If any issues remain outstanding, please telephone the undersigned attorney of record for resolution. Applicants enclose a Petition for a Three Month Extension of Time. Please charge the $555 extension fee under 37 C.F.R. §1.17(a) to the credit card identified on the enclosed Form PTO-2038. **Only in the absence** of Form PTO-2038, please debit any applicable fees from Deposit Account No. 07-1185, upon which the undersigned is allowed to draw.

Respectfully submitted,

Date: Apl 28, 2010

ADLER & ASSOCIATES
8011 Candle Lane
Houston, Texas 77071
Tel: (713) 270-5391
Fax: (713) 270-5361
Ben@adlerandassociates.com

Benjamin Aaron Adler, Ph.D., J.D.
Registration No. 35,423
Counsel for Applicant

PAGE 28/92 * RCVD AT 4/28/2010 6:45:45 PM [Eastern Daylight Time] * SVR:USPTO-EFXRF-6/33 * DNIS:2738300 * CSID:7132705361 * DURATION (mm-ss):48-00

Supplemental Material can be found at:
http://www.jbc.org/cgi/content/full/M800589200/DC1

THE JOURNAL OF BIOLOGICAL CHEMISTRY VOL. 283, NO. 18, pp. 11876–11886, May 2, 2008
© 2008 by The American Society for Biochemistry and Molecular Biology, Inc. Printed in the U.S.A.

Covalent Inactivation of Factor VIII Antibodies from Hemophilia A Patients by an Electrophilic FVIII Analog*[S]

Received for publication, January 23, 2008, and in revised form, March 5, 2008 Published, JBC Papers in Press, March 11, 2008, DOI 10.1074/jbc.M800589200

Stephanie Planque‡, Miguel A. Escobar‡, Keri C. Smith‡, Hiroaki Taguchi‡, Yasuhiro Nishiyama‡, Elizabeth Donnachie‡, Kathleen P. Pratt§, and Sudhir Paul‡1

From the ‡Chemical Immunology Research Center, Departments of Pathology and Medicine and Gulf States Hemophilia and Thrombophilia Center, University of Texas-Houston Medical School, Houston, Texas 77030 and §Puget Sound Blood Center and Division of Hematology, University of Washington, Seattle, Washington 98104-1256

The antigen-binding sites of antibodies (Abs) can express enzyme-like nucleophiles that react covalently with electrophilic compounds. We examined the irreversible and specific inactivation of antibodies (Abs) to Factor VIII (FVIII) responsible for failure of FVIII replacement therapy in hemophilia A (HA) patients. Electrophilic analogs of FVIII (E-FVIII) and its C2 domain (E-C2) were prepared by placing the strongly electrophilic phosphonate groups at surface-exposed Lys side chains of diverse antigenic epitopes. IgG Abs to FVIII from HA patients formed stable immune complexes with E-FVIII and E-C2 that were refractory to dissociation by SDS treatment and boiling, procedures that dissociate noncovalent Ab-antigen complexes. The rate-limiting step in the reaction was formation of the initial noncovalent complexes. Conversion of the initial complexes to the irreversible state occurred rapidly. The antigenic epitopes of E-FVIII were largely intact, and most of the Abs were consumed covalently. E-FVIII expressed poor FVIII cofactor activity in clotting factor assays. Nonspecific interference by E-FVIII in clotting factor function was not evident. Treatment with E-FVIII, and to a lesser extent E-C2, irreversibly relieved the FVIII inhibitory effect of HA IgG in clotting factor assays. Small FVIII peptides did not display useful reactivity, highlighting the diverse epitope specificities of the Abs and the conformational character of FVIII epitopes. E-FVIII is a prototype reagent able to attain irreversible and specific inactivation of pathogenic Abs.

Specific antibodies (Abs)[2] to individual antigens are thought to cause harmful effects in autoimmune diseases, transfusion of incompatible blood products, and organ transplantation. Inhibitory Abs to Factor VIII (FVIII) in hemophilia A (HA) are a well characterized example. HA is a chromosome X-linked genetic disorder characterized by the synthesis of functionally inactive FVIII. This impairs the intrinsic pathway of blood coagulation. The primary therapy for control of bleeding in HA patients is infusion of recombinant or plasma-derived FVIII (1). About 20–30% of patients receiving FVIII replacement therapy produce antibodies (Abs) to FVIII that inhibit FVIII cofactor activity. These are referred to clinically as "inhibitors." The inhibitory effect is thought to derive from reversible steric hindrance of FVIII interactions with phospholipids and other coagulation factors, including thrombin, Factor IXa (FIXa), and von Willebrand factor (2). In addition, some Abs inactivate FVIII permanently by catalyzing its proteolytic breakdown (3). Epitope mapping studies using FVIII fragments (heavy chain, light chains, and A2, A3, C1, and C2 domains) and FVIII hybrid molecules have suggested that many Abs are directed to conformational epitopes (4, 5). Most inhibitor positive patients mount a highly diverse immune response consisting of Abs to multiple FVIII epitopes located in the A2, C1, C2, and A3 domains (2, 6, 7).

The Abs pose major problems in managing acute bleeding episodes and surgical procedures in the patients. Short term bleeding in inhibitor-positive patients can be controlled by infusing activated prothrombin complex concentrates or recombinant factor VIIa, agents that bypass the requirement for FVIII in the coagulation pathway (8, 9). Refractory bleeds occur in about 20% of inhibitor-positive HA patients receiving bypass therapy, and an overdose carries the risk of inducing thrombotic events (9). In principle, FVIII itself could be infused to saturate the Abs and restore the coagulation pathway. However, massive quantities of FVIII are required to overcome the inhibitory effect of the circulating Abs even for a short duration. An important clinical advance has been the development of immune tolerance protocols in which high dose FVIII infusions are administered over prolonged periods to suppress Ab production by memory B lymphocytes (10, 11). Experimental peptides (5, 12) and anti-idiotypic Abs (13) have been reported to block FVIII inhibitory Abs by mimicking the structure of certain FVIII epitopes. Regrettably, there is no single immu-

* This work was supported by grants from the Hemophilia Associations of New York and Georgia and National Institutes of Health Grant AI31268. The costs of publication of this article were defrayed in part by the payment of page charges. This article must therefore be hereby marked "*advertisement*" in accordance with 18 U.S.C. Section 1734 solely to indicate this fact.

[S] The on-line version of this article (available at http://www.jbc.org) contains supplemental Fig. S1.

1 To whom correspondence should be addressed: Dept. of Pathology, University of Texas, Houston Medical School, 6431 Fannin, Houston, TX 77030. E-mail: Sudhir.Paul@uth.tmc.edu.

2 The abbreviations used are: Ab, antibody; APTT, activated partial thromboplastin time; E-C2, C2-domain analog containing electrophilic phosphonates; E-hapten, electrophilic hapten; E-FVIII, electrophilic Factor VIII; FVIII, Factor VIII; FIXa, activated Factor IX; FX, Factor X; FXa, activated Factor X; HA, hemophilia A; VIP, vasoactive intestinal peptide; ELISA, enzyme-linked immunosorbent assay; CHAPS, 3-[(3-cholamidopropyl)dimethylammonio]-1-propanesulfonic acid; HPLC, high pressure liquid chromatography; MALDI-TOF, matrix-assisted laser desorption ionization time-of-flight; Z, benzyloxycarbonyl; PBS, phosphate-buffered saline; ESI, electrospray ionization.

PAGE 29/92 * RCVD AT 4/28/2010 6:45:45 PM [Eastern Daylight Time] * SVR:USPTO-EFXRF-6/33 * DNIS:2738300 * CSID:7132705361 * DURATION (mm-ss):48-00

Downloaded from www.jbc.org at HAM-TMC Library on May 1, 2008

nodominant FVIII epitope, and these approaches do not adequately address the problem of diverse epitope reactivities of the Abs.

The combining sites of certain Abs contain enzyme-like activated nucleophiles. The Ab nucleophilic reactivities were evident from formation of covalent complexes with electrophilic phosphonate diesters (14–16), compounds that were originally developed as class-specific inhibitors of serine proteases (17). The phosphonates react with activated nucleophiles generated by intramolecular interactions between certain amino acids. For instance, the Ser side chain acquires enhanced nucleophilicity by virtue of the hydrogen-bonded network in the Ser-His-Asp catalytic triads of serine proteases (18). The nucleophilic sites permit certain Abs to catalyze the hydrolysis of their cognate antigens (19). Ser-His-Asp and Ser-Arg-Glu catalytic triads have been identified in proteolytic Abs by site-directed mutagenesis (20) and crystallography studies (21). Nucleophilic catalytic Abs that hydrolyze FVIII and inhibit FVIII cofactor activity are found in HA patients (3). However, only a subset of nucleophilic Abs displays catalytic activity (14), indicating that additional events in the catalytic cycle occurring after the initial nucleophilic attack on the peptide bond carbonyl group can be rate-limiting (*e.g.* water attack and product release).

We hypothesize that electrophilic FVIII (E-FVIII) analogs may relieve the anti-coagulant effect of Abs by reacting specifically and covalently with their nucleophilic sites. The covalent reaction is predicted to preclude dissociation of the immune complexes, thereby permitting prolonged Ab inactivation. We describe here E-FVIII analogs that relieve the FVIII inhibitory effect of Abs from patients with HA. E-FVIII is a prototypic therapeutic reagent for control of bleeding in inhibitor-positive HA patients. The observed properties of E-FVIII suggest that electrophilic antagonism can potentially be developed as a general basis for attaining specific inactivation of various antigen-specific pathogenic Abs found in immunological diseases.

EXPERIMENTAL PROCEDURES

Electrophilic FVIII Analogs—Recombinant FVIII (Helixate, CSL Behring) in 10 mM HEPES, 150 mM NaCl, 0.025% Tween 20 was derivatized at Lys residues with the 3-sulfosuccinimidyl ester of diphenyl *N*-suberoyl-amino(4-amidinophenyl)methanephosphonate, and unincorporated phosphonate was removed by gel filtration (16). The phosphonate content of three E-FVIII preparations employed in this study was 52–76 mol of phosphonate/mol of FVIII determined by fluorescamine labeling of the residual amine groups (16). To prepare biotinylated E-proteins, biotin was first introduced into recombinant FVIII and C2 protein (22) by partial acylation in 10 mM HEPES, 150 mM NaCl, 0.1 mM CHAPS (14). This yielded FVIII and C2, respectively, containing 8.8 and 0.6 mol of biotin/mol of protein. Phosphonate labeling of biotinylated FVIII was as above (81 mol of phosphonate/mol of protein). Fast protein liquid chromatography-gel filtration of E-FVIII was on a Superose-6 column at a flow rate of 0.3 ml/min as described (23). Initial attempts to prepare E-C2 as described above for E-FVIII resulted in precipitation of the protein (>90%). Therefore, a phosphonate reagent with a more hydrophilic linker was prepared by treating diphenyl amino(4-amidinophenyl)methanephosphonate with di(*N*-succinimidyl) ethylene glycol disuccinate (Sigma), followed by reversed phase HPLC purification (observed *m/z* 722.5 (MH^+) and calculated MH^+ 722.2). Treatment of biotinylated C2 with this reagent yielded E-C2 preparations containing 6.7–8.2 mol of phosphonate/mol of C2. The E-VIP preparation has been described (15). The following peptides were prepared by Fmoc (*N*-(9-fluorenyl)methoxycarbonyl)-based solid phase synthesis: FVIII residues 484–508 with a Cys residue at the N terminus (*N*-acetyl-CRPLYSRRLPKGVKHLKDFPILPGEI); residues 1804–1819 (KNFVKPNETKTYFWKV); FVIII residues 2303–2332 with lysyl-biotin at the C terminus (TRYLRIHPQSWVHQIALKMEVLGCEAQDLYK-biotinamidohexanoyl); and the mimotope of a C2 epitope recognized by monoclonal Ab BO2C11 (SCHAWSNRRTCR) (12). The peptides were purified by HPLC (>95% purity) and characterized by matrix-assisted laser desorption ionization time-of-flight (MALDI-TOF) or electrospray ionization (ESI) mass spectroscopy (FVIII-(484–508), *m/z* (MALDI) 3076.0 (MH^+; calculated MH^+ 3075.7); FVIII-(2303–2332), *m/z* (ESI) 1356.2 (MH_3^{3+}, calculated MH_3^{3+} 1356.4), 1018.0 (MH_4^{4+}, 1017.5), and 814.5 (MH_5^{5+}, 814.2); FVIII-(1804–1819), *m/z* (ESI) 677.4 (MH_3^{3+}, calculated MH_3^{3+} 677.4), and 508.5 (MH_4^{4+}; 508.3); BO2C11 epitope: *m/z* (MALDI) 1474.8 (MH^+; calculated MH^+ 1474.7)). E-(2303–2332) was prepared by regiospecific acylation (15) as follows. The resin with the 2303–2332 peptide protected at Lys-2320 side chain with the 4-methyltrityl group was treated with 1% trifluoroacetic acid in dichloromethane to remove this protecting group, and the Lys-2320 side chain amine was acylated with the *N*-hydroxysuccinimidyl ester of the phosphonate reagent used for E-FVIII preparation. Protecting groups and the solid support were removed with trifluoroacetic acid containing 2% phenol, 5% thioanisole, and 5% ethanedithiol, and E-(2303–2332) was purified by HPLC (*m/z* (ESI) 1529.5 (MH_3^{3+}, calculated MH_3^{3+} 1529.5), 1147.3 (MH_4^{4+}, 1147.4), 917.6 (MH_5^{5+}, 918.1)]. The electrophilic analogs were stored at −80 °C as lyophilized powders. Protein concentrations were measured by the bicinchoninic acid assay.

Patients and Antibodies—This study was approved by the University of Texas Institutional Review Board. Plasma was prepared from blood in 3.2% sodium citrate from 8 inhibitor-positive HA patients (our lab codes: HA1828, HA1834, HA1835, HA2084, HA2085, HA2222, HA2223, and HA3112; age range 5–59 years). The patients had a history of FVIII inhibitors for at least 5 years but had not received FVIII replacement therapy for at least 2 months prior to the blood draw). The plasma FVIII titers were determined by Bethesda assay (24) and are reported in Table 1. Control plasma was from a nonhemophiliac human subject without known coagulation or autoimmune disorders (code NH1941). Electrophoretically homogeneous IgG from the plasma samples was purified by affinity chromatography using immobilized protein G (25). Fab fragments were prepared by digestion with immobilized papain and chromatography using immobilized protein A (26). Murine monoclonal anti-C2 IgG (clone ESH8) was from American Diagnostica. The isotype-matched control was monoclonal anti-VIP IgG (clone c23.5) (27).

Hapten Phosphonate Binding—Synthesis of hapten electrophilic probe E-hapten-1, E-hapten-2, and E-hapten-3 was

Downloaded from www.jbc.org at HAM-TMC Library on May 1, 2008

PAGE 30/92 * RCVD AT 4/28/2010 6:45:45 PM [Eastern Daylight Time] * SVR:USPTO-EFXRF-6/33 * DNIS:2738300 * CSID:7132705361 * DURATION (mm-ss):48-00

described (14, 23, 28). FVIII (0.5 μM) was treated with the E-hapten probes (100 μM) for 4 h, and formation of irreversible adducts was measured by reducing SDS-electrophoresis as described (14).

E-FVIII and FVIII Binding—Abs were incubated with electrophilic or control polypeptides devoid of electrophilic groups in 10 mM HEPES, pH 7.5, 150 mM NaCl, 0.025% Tween 20 (HEPES/Tween) at 37 °C. The reaction mixtures were boiled (5 min) in 2% SDS and 3.3% 2-mercaptoethanol and subjected to SDS-electrophoresis. Adducts were detected and quantified in gel blots with peroxidase-conjugated streptavidin or goat anti-human IgG (Fc and κ/λ chain-specific, 1:1000; Sigma (16)). ELISAs were done using microtiter plates (Nunc) coated with 0.1 ml of FVIII, E-FVIII, C2, E-C2 (1 μg/ml), or synthetic FVIII peptides (4 μg/ml) in 100 mM $NaHCO_3$, pH 9.5, and blocked with 5% skimmed milk in 10 mM sodium phosphate, pH 7.4, 137 mM NaCl, 2.7 mM KCl, 0.05% Tween 20 (PBS/Tween). Ab binding was measured using peroxidase-conjugated goat anti-human IgG as above or goat anti-human Fab (Sigma) followed by peroxidase-conjugated rabbit anti-goat IgG (Pierce) (16). Binding to biotinylated E-(2303–2332) was measured similarly using streptavidin-coated plates (1 μg/ml). To measure irreversible binding, Abs were permitted to bind the immobilized antigens; the fluid was removed, and the wells were incubated for 30 min in PBS/Tween without (total binding) or with 2% SDS (SDS-refractory binding), followed by washing with PBS/Tween (16). Percent residual binding in SDS-treated wells was (A_{490}, SDS-treated wells) × 100/(A_{490}, PBS/Tween-treated wells). Samples displaying A_{490} > mean ± 3 S.D. for control IgG (from subject NH1941) were considered positive. Binding rate data were fitted to the equation $A_{490}/A_{490,max} = 1 - \exp^{(-Kt)}$, where K is the pseudo-first order rate constant ($K = (k_3 \times [Ab])/K_d$); k_3 is the first order rate constant for covalent bonding; K_d is the equilibrium dissociation constant for noncovalent binding step; [Ab] is the Ab concentration). $t_{1/2}$ was computed as $\ln 2/K$. In the immunoadsorption experiment, HA IgG (0.7 μM) was incubated in diluent or biotinylated E-FVIII (0.1 μM) for 20 h, and the reaction mixture (0.04 ml) was incubated for 1 h with immobilized streptavidin in spin columns (30 μl of settled gel, UltraLink Plus columns, Pierce). The unbound fraction and three washes (0.05 ml each) were pooled and assayed for binding to FVIII and E-FVIII by ELISA.

Clotting Factor Assays—FVIII and E-FVIII cofactor activity was determined using the Diapharma Coamatic FVIII kit® as instructed by the manufacturer using 0.045-ml solutions of the proteins in HEPES/Tween. The method measures the ability of FVIIIa generated by thrombin cleavage to form the FIXa tenase complex responsible for FXa generation, which in turn hydrolyzes the chromogenic substrate N-α-Z-D-Arg-Gly-Arg-*p*-nitroanilide. To measure FVIII inhibitor activity of Abs, IgG preparations from patients HA1828 (0.2 mg/ml), HA2222 (0.1 mg/ml), and HA3112 (0.1 mg/ml) were incubated with diluent or the electrophilic FVIII analogs in HEPES/Tween (0.1 ml; 20 h, 37 °C). Unbound electrophilic analogs in the reaction mixtures (0.1 ml) were removed by chromatography on protein G-Sepharose (0.04 ml of settled gel packed in Micro Biospin columns, Bio-Rad). The columns were washed with 5 ml of 50 mM Tris-HCl, pH 7.4, 0.1 mM CHAPS. Bound IgG was eluted with 0.1 M glycine, pH 2.7, 0.1 mM CHAPS (0.2 ml) in tubes containing 0.01 ml of 1 M Tris base, pH 9. The FVIII inhibitory activity of eluates was determined using the Coamatic assay or the one-stage activated partial thromboplastin time (APTT) clotting assay using APTT-SP reagent (29) (Instrumentation Laboratory) and an ACL300 plus coagulometer (Instrumentation Laboratory) according to the manufacturer's instructions. The standard curve was constructed from the clotting times of reference FVIII-containing plasma diluted in FVIII-depleted plasma (both from George King Bio-Medical, Inc.). Prior to the chromogenic FVIII inhibitor assay, FVIII (0.2 IU/ml, 0.025 ml) was incubated with the IgG eluates from protein G columns (0.025 ml; 1 h). Prior to the APTT clotting assay, pooled plasma from normal subjects (0.06 ml) was incubated with the IgG eluates (0.06 ml; 2 h). The concentrations of the FVIII inhibitory IgG in these assays yielded FVIII inhibition in the linear range of the inhibition curve (25–75% residual activity of reference FVIII-containing plasma).

RESULTS

E-FVIII and E-C2—Multiple electrophilic phosphonate groups were placed on FVIII and C2 Lys residues (E-FVIII, 52 mol/mol; E-C2, 7 mol/mol; total available Lys residues, respectively, 158 and 9; Fig. 1*A*), producing diverse electrophilic epitopes. Reducing SDS-electrophoresis and silver staining of E-C2 indicated a single band with mass similar to underivatized C2 (18.6 kDa; Fig. 1*B*, *lane 3*). SDS gels of E-FVIII revealed major 225- and 86-kDa bands (respectively, intact FVIII and FVIII light chain), minor ~96–200-kDa bands corresponding to known proteolytic FVIII fragments (3, 30), and smeared aggregate bands (nominal mass values ~350 and 580 kDa close to the loading position; Fig. 1*B*, *lane 1*). Other than the aggregates, these bands were present in underivatized FVIII obtained from the supplier (Fig. 1*B*, *lane 2*). The aggregates constituted 21–32% of the total silver-stainable protein present in three preparations of E-FVIII examined.

We reported recently the presence of nucleophilic sites in various nonenzymatic proteins, evident from their covalent reaction with small molecule phosphonate diester compounds (E-haptens) containing a positive charge neighboring the electrophilic phosphorus atom (31). The presence of a naturally occurring nucleophilic site(s) in FVIII was suggested by the formation of a major 225-kDa adduct and a faint 86-kDa adduct of FVIII treated with a positively charged E-hapten-1 (Fig. 1*C*, *lane 1*). Only faint adduct bands were observed in reaction mixtures containing the poorly electrophilic control phosphonic acid (E-hapten-2) or the neutral phosphonate E-hapten-3. Control ovalbumin, a protein with minimal nucleophilic reactivity (31), did not form detectable E-hapten-1 adducts. The E-FVIII aggregates may therefore be interpreted to derive from intermolecular covalent bonding between the electrophilic phosphonate and a naturally occurring nucleophilic site(s) of FVIII.

To assess antigenic integrity, the binding of E-FVIII and E-C2 by Abs was determined by ELISA using affinity-purified IgG preparations from eight HA patients positive for FVIII inhibitory antibodies. All of the IgG preparations at 25 μg/ml displayed E-FVIII and E-C2 binding exceeding the mean ± 3 S.D.

Downloaded from www.jbc.org at HAM-TMC Library on May 1, 2008

PAGE 31/92 * RCVD AT 4/28/2010 6:45:45 PM [Eastern Daylight Time] * SVR:USPTO-EFXRF-6/33 * DNIS:2738300 * CSID:7132705361 * DURATION (mm-ss):48-00

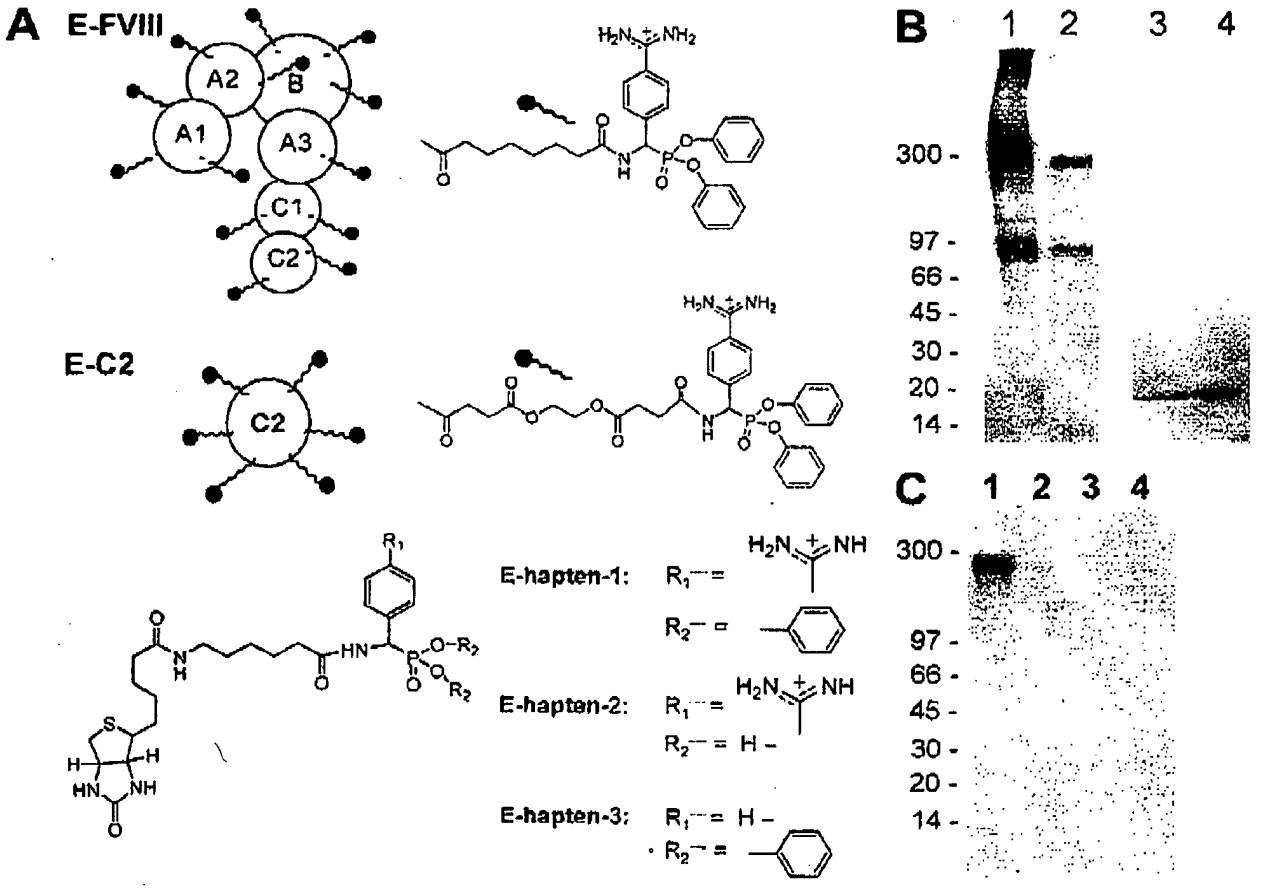

FIGURE 1. **Electrophilic FVIII (E-FVIII) and C2 (E-C2 analogs).** *A*, multidomain protein FVIII and the single domain protein C2 contain several phosphonate diester groups at Lys side chains to allow electrophile presentation within diverse antigenic epitopes. For detection of immune adducts, biotin was incorporated in the proteins as needed. E-hapten-1 is the biotin-containing small molecule phosphonate diester. E-hapten-2 is the poorly electrophilic phosphonic acid counterpart of E-hapten-1. E-hapten-3 is the counterpart devoid of the positively charged amidino function. *B*, silver-stained reducing SDS-polyacrylamide gels of E-FVIII (*lane 1*), FVIII (*lane 2*), E-C2 (*lane 3*), and C2 (*lane 4*) stained with silver. Marker protein migration is indicated on the *left*. *C*, streptavidin-peroxidase stained reducing SDS-polyacrylamide electrophoresis gels of FVIII (0.5 μM) treated with hapten probes (100 μM, 4 h). E-hapten-1, *lane 1*; E-hapten-2, *lane 2*; E-hapten-3, *lane 3*. *Lane 4* shows the poorly nucleophilic protein ovalbumin treated identically with E-hapten-1.

TABLE 1

E-FVIII and E-C2 binding activity and FVIII inhibitor titer of antibodies from HA patients

NH is nonhemophiliac subject. FVIII inhibitor titers were measured in plasma samples and are reported in Bethesda assay units (BU). The E-FVIII and E-C2 binding activity at various dilutions of purified IgG (5–100 μg of IgG/ml) was determined in duplicate by ELISA, and the concentration yielding A_{490} values of 0.25 ($IgG_{0.25}$) were computed from plots of A_{490} *versus* $\log_{10}$[Ab] fitted by linear regression.

Patient ID	Plasma FVIII inhibitor	E-FVIII binding, $IgG_{0.25}$ in μg/ml	E-C2 binding, $IgG_{0.25}$ in μg/ml
	BU/ml		
HA1828	800	2.7	2.6
HA1834	150	3.3	7.9
HA1835	149	4.5	5.6
HA2084	1024	4.3	12.9
HA2085	49	19.2	17.4
HA2222	1011	0.5	1.6
HA2223	70	29.9	56.1
HA3112	198	5.1	52.8
NH1941	<0.5	>100	>100

values for control IgG from the nonhemophilia subject (code NH1941; A_{490}, respectively, 0.01 ± 0.01 and 0.07 ± 0.01). The IgG concentrations yielding an A_{490} value of 0.25 computed from dose-response curves are reported in Table 1. Fast protein liquid chromatography-gel filtration of E-FVIII permitted separation of an aggregate peak eluting close to the column void volume (retention time 18.3–21.6 min; 13% of protein loaded on the column) from unaggregated E-FVIII (retention time 43.3–46.0 min). The aggregates did not display reduced reactivity with IgG from an HA patient (HA1828) compared with unfractionated E-FVIII (A_{490} 1.22 ± 0.02 and 0.85 ± 0.10, respectively; 30 μg/ml IgG, 93 ng/well E-FVIII aggregates or unfractionated FVIII), suggesting that the Ab-reactive epitopes aggregates are present in the aggregates. The ability of E-FVIII to consume anti-FVIII Abs was measured following solution phase reactions of HA1828 IgG with biotinylated E-FVIII. Immune complexes were removed using immobilized streptavidin, and free Abs in the unbound fraction were measured. This procedure resulted in essentially complete removal of Abs capable of binding FVIII or E-FVIII (Fig. 2). E-FVIII, therefore, is recognized by the majority of anti-FVIII Abs present in the HA IgG.

Irreversible Immune Complexation—Formation of irreversible immune adduct of E-FVIII and Abs was initially studied by

PAGE 32/92 * RCVD AT 4/28/2010 6:45:45 PM [Eastern Daylight Time] * SVR:USPTO-EFXRF-6/33 * DNIS:2738300 * CSID:7132705361 * DURATION (mm-ss):48-00

Downloaded from www.jbc.org at HAM-TMC Library on May 1, 2008

The Journal of Biological Chemistry

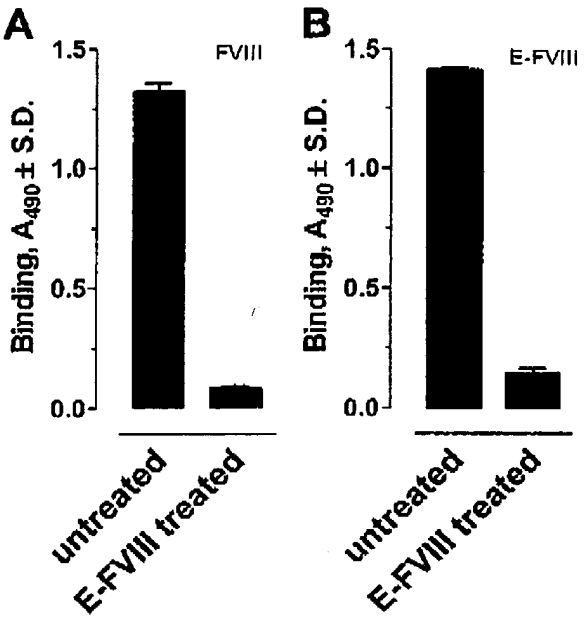

FIGURE 2. **Near-complete consumption of anti-FVIII Abs by E-FVIII.** IgG HA1828 (0.7 μM) was incubated in solution phase with diluent or biotinylated E-FVIII (0.1 μM) for 20 h. Immune complexes and free E-FVIII were removed by affinity chromatography using streptavidin-agarose. The flow-through and wash fractions were pooled and assayed for binding to immobilized FVIII in *A* or E-FVIII in *B* by ELISA.

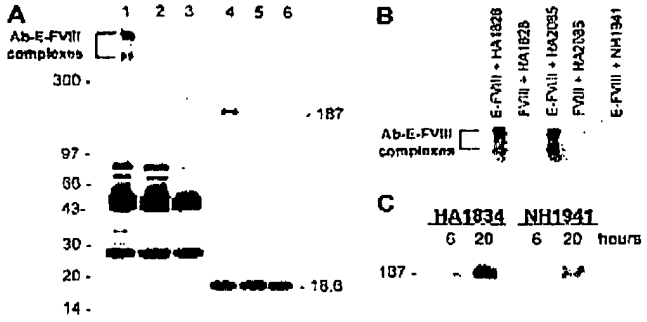

FIGURE 3. **Irreversible binding of E-FVIII and E-C2 to anti-FVIII Abs.** *A*, anti-mouse IgG-stained blots of an SDS-electrophoresis gel showing boiled reaction mixtures of E-FVIII (*lane 1*) or FVIII (*lane 2*) incubated with the anti-C2 domain monoclonal antibody (clone ESH8). *Lane 3* shows E-FVIII incubated with an irrelevant isotype-matched antibody (IgG clone c23.5). *Lanes 4–6* are, respectively, streptavidin-peroxidase-stained blots of an SDS gel showing boiled reaction mixtures of biotinylated E-C2 incubated with monoclonal Ab ESH8, biotinylated C2 incubated with monoclonal Ab ESH8, and biotinylated E-C2 incubated with the irrelevant isotype-matched Ab. Reaction conditions are as follows: IgG, 0.7 μM; E-FVIII, FVIII, biotinylated E-C2 or biotinylated C2, 0.2 μM (2 h, 37 °C). The anti-IgG-stained bands at 80 and 25 kDa in *lanes 1* and *2* are the heavy and light chains, respectively. The bands at 80 and 70 kDa represent anomalously migrating Ab subunits. The streptavidin-stained band at 18.6 kDa in *lanes 4–6* is the uncomplexed form of E-C2 and C2. *B*, representative anti-human IgG-stained blots of reducing SDS gels showing large-mass E-FVIII complexes with IgG from FVIII inhibitor-positive patients. *Lanes 1* and *2*, respectively, HA1828 IgG incubated with E-FVIII or FVIII. *Lanes 3* and *4*, respectively, HA2085 IgG incubated with E-FVIII or FVIII. *Lane 5*, E-FVIII incubated with NH1941 IgG (nonhemophilic IgG control). Reaction conditions are as in *A*. *C*, streptavidin-peroxidase-stained nonreducing SDS gels showing time-dependent formation of E-C2 immune complexes following incubation with FVIII inhibitor-positive IgG (mass 187 kDa). IgG was from HA subject HA1834 or control subject NH1941. Reaction conditions are as in *A*.

reducing SDS-electrophoresis and detection of large-mass bands by immunoblotting with anti-human IgG. The E-FVIII aggregates do not interfere in immune complex detection, as they are not stained by the anti-IgG reagent. Treatment of an anti-FVIII monoclonal Ab (directed to the C2 domain; clone ESH8) with E-FVIII but not FVIII devoid of the electrophilic groups resulted in formation of two large-mass bands stainable with anti-IgG Ab, one close to the sample loading position and the second with a nominal mass of 500 kDa (Fig. 3*A*). The theoretical mass of IgG adducts containing one and two 2 FVIII molecules are ~415 and ~680 kDa, respectively. The observed large-mass adducts were absent in E-FVIII treated with a control monoclonal Ab of the same isotype as the anti-FVIII Ab (IgG2a,κ). IgG purified from all eight inhibitor-positive HA patients formed similar immune adducts with E-FVIII but not with FVIII (examples shown in Fig. 3*B*). Control IgG from the non-HA subjects did not form the adducts. The adducts were observed despite boiling and SDS denaturation, consistent with covalent E-FVIII binding by nucleophilic Ab sites. The electrophoresis studies do not reveal the precise molecular composition of the adducts, but they fulfill our purpose of unambiguously establishing the formation of irreversible and specific immune adducts. As in the case of E-FVIII, treatment of biotinylated E-C2 with the monoclonal anti-FVIII Ab resulted in formation of the predicted large-mass band stainable with streptavidin-peroxidase (nominal mass 187 kDa; anticipated mass of bivalent IgG complexed with 2 E-C2 molecules, 188 kDa; Fig. 3*A*). No 187-kDa complex was observed by treatment of E-C2 with an equivalent concentration of the control isotype-matched monoclonal Ab. IgG from all eight inhibitor-positive HA patients formed the 187-kDa complex with E-C2 but not C2 devoid of the electrophilic groups. Control IgG from the non-HA subjects did not form the complex or did so at very low levels (example in Fig. 3*C*). This rules out an indiscriminate covalent reaction of the phosphonate group as the explanation for formation of stable immune adducts by the HA IgGs.

E-FVIII binding by Abs can be modeled as a two-step reaction, in which the initial step generates specific noncovalently associated immune complexes (state 1 in Fig. 4*A*) followed by conversion of these complexes to irreversible adducts (state 2) via covalent phosphonate bonding with Ab nucleophiles. The model is supported by the following observations. Inclusion of excess FVIII devoid of the phosphonates in the reaction mixture at $t = 0$ inhibited E-FVIII binding by the HA IgG preparations, indicating specificity typical of conventional Ab-antigen noncovalent binding reactions (Fig. 4*B*). We measured the dissociation of E-FVIII immune complexes formed by the polyclonal HA IgG by removing the free IgG and incubating the reaction mixture for 20 h in excess FVIII (which precludes reassociation of dissociated complexes). Seventy five percent of the immune complexes remained in the associated state (Fig. 4*C*). Under these conditions, there was near-complete dissociation of the noncovalent immune complexes formed by the high affinity monoclonal anti-FVIII Ab (clone ESH8, K_d 0.4 nM; Ref. 32) with FVIII devoid of the phosphonates. This is consistent with the observed dissociation rates of other high affinity noncovalent immune complexes (33). As the experimental protocol effectively distinguishes between noncovalent and irreversible

PAGE 33/92 * RCVD AT 4/28/2010 6:45:45 PM [Eastern Daylight Time] * SVR:USPTO-EFXRF-6/33 * DNIS:2738300 * CSID:7132705361 * DURATION (mm-ss):48-00

Downloaded from www.jbc.org at HAM-TMC Library on May 1, 2008

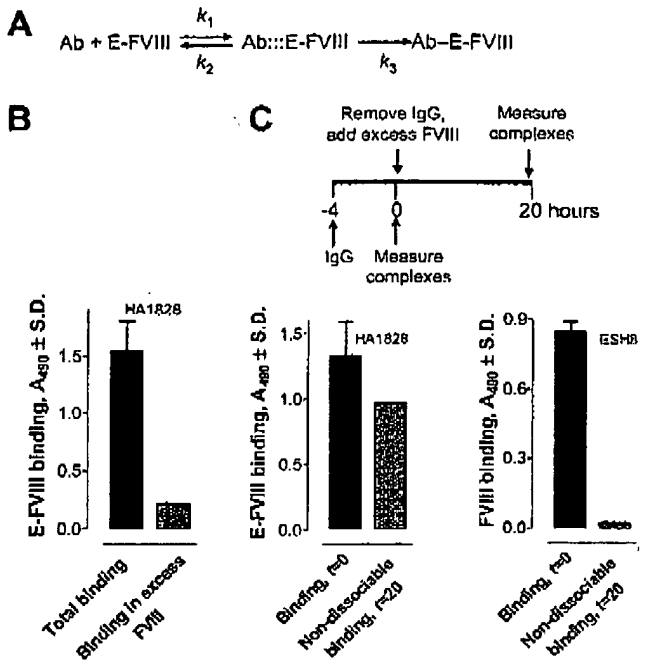

FIGURE 4. Specific irreversible E-FVIII binding by HA IgG preparations. *A*, two-step reaction model for generation of irreversible adducts E-FVIII and Abs. The initial noncovalent binding reaction imparts specificity to the reaction (state 1). The covalent reaction occurs if the electrophilic phosphonate is in register with a naturally occurring nucleophile in the Ab combining site (state 2). *B*, saturability of E-FVIII binding by HA1828 IgG (0.07 μM) evident from competitive inhibition with excess FVIII (0.25 μM) included in the reaction mixture. Total binding was determined in PBS. Incubation time was 4 h. *C*, nondissociable E-FVIII complexation by HA1828 IgG. *Top*, assay protocol. *Left*, after formation of immobilized E-FVIII immune complexes with HA1828 IgG for 4 h as in *A*, free IgG was removed by extensive washing, and the complexes were allowed to dissociate over 20 h in the presence of excess FVIII (0.25 μM). Binding in PBS prior to IgG removal is labeled *Binding*, $t = 0$. Binding after removal of IgG and incubation for 20 h in excess FVIII is labeled *Nondissociable binding*, $t = 20$. *Right*, same experimental protocol was applied to determine nondissociable binding of FVIII devoid of the electrophilic groups with the monoclonal anti-FVIII IgG ESH8 (0.07 μM). Values are corrected for nonsaturable binding in wells that received excess FVIII at $t = 0$ the reaction (nonsaturable A_{490} for HA IgG, 0.21; for ESH8 IgG, 0.14).

complexes, it may be concluded that the majority of the complexes is converted to the irreversible state.

Irreversible immune complexation was studied further by an ELISA method entailing dissociation of the noncovalent state 1 complexes with 2% SDS (30 min of treatment). The protocol has been validated in our previous report of covalent complexation of human immunodeficiency virus gp120 by Abs (16). Treatment with SDS dissociated the noncovalent complexes of FVIII devoid of the electrophilic phosphonates and the high affinity anti-FVIII monoclonal Ab (<10% residual binding after SDS treatment). After incubation with IgG preparations from HA patients ($n = 8$) for 2 h, 77.6 ± 9.1% complexes formed by E-FVIII and 66.3 ± 17.6% of the complexes formed by E-C2 (mean ± S.D.) were refractory to dissociation by SDS (Fig. 5*A*). The proportion of SDS-refractory complexes reached plateau levels within 30 min (Fig. 5*B*), indicating rapid conversion of the state 1 noncovalent complexes to state 2 irreversible adducts. $t_{1/2}$ values for formation of the complexes in nondenaturing solvent (PBS; state 1 + state 2 complexes) and SDS (state 2 complexes) were comparable (2.5 and 2.3 h, respectively). This suggests that noncovalent binding of E-FVIII and Abs is the rate-limiting step in accumulation of the covalent adducts. Taken together, it may be concluded that the electrophilic phosphonates are in sufficient proximity with Ab nucleophiles in a majority of noncovalent complexes to allow conversion to the covalently associated state. Approximately 15% of the E-FVIII immune complexes remained SDS-dissociable in Fig. 5*B*, suggesting that the covalent bonding is disallowed in a minority of complexes. Fab fragments prepared from the IgG of patient HA1828 displayed SDS-refractory binding to E-FVIII equivalent to intact IgG (Fig. 5*C*). This suggests that an avidity effect because of bivalent IgG binding is not a factor, and the irreversible binding can be attributed to monovalent Ab combining sites.

Irreversible Loss of Antibody Inhibitory Activity—The functional effect of E-FVIII and E-C2 was studied by measuring irreversible loss of FVIII inhibitory activity of IgG from patients HA1828, HA2222, and HA3112 (plasma FVIII inhibitor titer: 800, 1011, and 198 Bethesda assay units/ml, respectively). The IgGs were treated with E-FVIII (0.1 μM), E-C2 (1 μM), or control E-VIP (0.1 and 1 μM). Protein G-Sepharose columns were used to capture free IgG and immune complexes, and free polypeptides were removed by extensive washing. Column eluates from reaction mixtures of IgG and the E polypeptides were tested for the ability to inhibit FVIII cofactor activity by the chromogenic Factor Xa (FXa) generation assay or the one-stage APTT assay. The FXa generation assay measures the ability of FVIII to generate the catalytic complex with FIXa responsible for converting FX to FXa. The APTT assay measures the time to clot formation of plasma after initiating the coagulation cascade by phospholipid contact activators that promote Factor XII conversion to Factor XIIa. Several control experiments were conducted prior to studying E-FVIII and E-C2 effects. Dose-dependent inhibition of FVIII cofactor activity was observed in both assays using protein G eluates from control reactions containing increasing HA IgG concentrations (16–100 μg/ml) and diluent. The recovery of FVIII inhibitory activity in the eluates was 67–95% of the activity predicted from the plasma Bethesda titers of the three HA patients. Identically processed IgG from a non-HA subject treated with diluent was devoid of FVIII inhibitor activity. Eluates obtained by chromatography of 0.1 μM FVIII in diluent without IgG did not display detectable FVIII activity, confirming removal of free polypeptides by the chromatography procedure. Similarly processed E-FVIII or E-C2 in diluent without IgG did not express detectable FVIII activity.

Treatment of the IgG preparations with the irrelevant E-polypeptide E-VIP was without noticeable effect on the FVIII inhibitor activity (<15% loss of activity compared with diluent-treated inhibitory IgGs). In comparison, treatment with 0.1 μM E-FVIII relieved the FVIII inhibitor activity of the three IgG preparations by an average of 87.9 ± 7.1% (S.D.) and 69.2 ± 5.2%, respectively, determined by the chromogenic FXa and APTT assays (Fig. 6*A*). E-C2 was less potent than E-FVIII, and higher concentrations of E-C2 were necessary to obtain IgG inactivation. Treatment with 1.0 μM E-C2 relieved the FVIII inhibitor activity of the IgG preparations by 40.1 ± 17.8 and 29.6 ± 13.5%, respectively, determined by the FXa and APTT assays (Fig. 6*B*). From these results, it may be concluded that

Downloaded from www.jbc.org at HAM-TMC Library on May 1, 2008

PAGE 34/92 * RCVD AT 4/28/2010 6:45:45 PM [Eastern Daylight Time] * SVR:USPTO-EFXRF-6/33 * DNIS:2738300 * CSID:7132705361 * DURATION (mm-ss):48-00

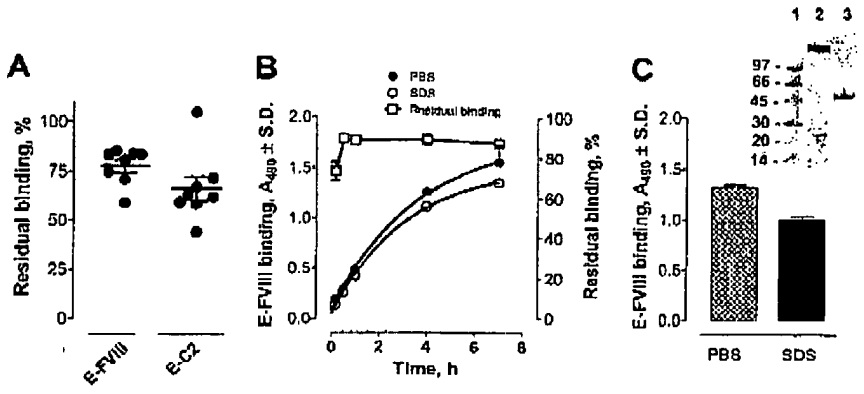

FIGURE 5. **Irreversibility of E-FVIII complexation with Abs in denaturing solvent.** *A*, SDS-refractory binding of E-FVIII and E-C2 by HA IgG. Plotted are values of residual binding that survived treatment with 2% SDS for 30 min, expressed as percent of total binding without SDS treatment. A_{490} values for total E-FVIII and E-C2 binding by IgGs from individual patients were as follows, respectively: HA1828, 1.20 and 1.24; HA1834, 1.20 and 0.68; HA1835, 1.09 and 0.96; HA2084, 0.97 and 1.02; HA2085, 1.30 and 0.84; HA2222, 1.12 and 0.73; HA2223, 0.83 and 0.45; and HA3112, 0.79 and 0.36. IgG concentrations, 6.3–100.0 μg/ml (adjusted to yield reliable A_{490} values from preliminary dose-response experiments). Residual binding was calculated as: $100 \times (A_{490,PBS} - A_{490,SDS})/A_{490,PBS}$. *B*, time course of total and SDS-refractory E-FVIII binding by HA1828. Residual binding was computed as in *A*. IgG HA1828 was 25 μg/ml. *C*, irreversible E-FVIII binding by Fab fragments from IgG HA1828. Total binding and SDS-refractory binding by Fab fragments (75 μg/ml) were determined as in *A*. *Inset*, Coomassie Blue-stained SDS-electrophoresis gels (nonreducing) of IgG (*lane 2*) and Fab (*lane 3*). Molecular mass markers, *lane 1*.

irreversible occupancy of the Ab combining sites by E-FVIII and E-C2 results in loss of the IgG FVIII inhibitory activity.

E-FVIII Reactivity with Coagulation Factors—The cofactor role of FVIII in blood coagulation depends on interactions of discrete FVIII regions with various coagulation proteins and phospholipids (34). We compared the ability of E-FVIII and FVIII to generate FXa. E-FVIII or FVIII was incubated with a mixture of FIXa, thrombin, calcium chloride, phospholipids, and FX. FXa enzymatic activity was quantified using a chromogenic peptidyl ester substrate. FXa activities in the presence of E-FVIII were 2–3 orders of magnitude lower than in the presence of FVIII (EC_{50} values, respectively, 14.8 and 0.03 IU/ml; Fig. 7*A*). Thrombin, FIXa, and FXa are serine proteases. We examined the possibility that nonspecific serine protease inhibition by the electrophilic phosphonates is the reason for low FXa activity observed in the presence of E-FVIII. Comparable activities of FXa generation were evident in the presence of FVIII alone or FVIII mixed with E-FVIII, indicating the presence of fully functional serine proteases (Fig. 7*B*). As an additional test of nonspecific serine protease inhibition, FVIII-containing normal human plasma was incubated for 2 h at 37 °C with an equal volume of diluent or E-FVIII (100 nM; corresponding 110 IU FVIII/ml; physiological concentration of FVIII ~1 IU/ml). E-FVIII did not prolong the time to clot formation determined by the APTT test compared with control assays conducted in the absence of E-FVIII (59.0 ± 0.1 s). This suggests that E-FVIII does not interfere with serine protease factors involved in blood coagulation.

FVIII Peptide Analogs—At high concentrations, the 2315–2332 region of the C2 domain is suggested to relieve partially the FVIII inhibitory effect of Abs found in some but not all inhibitor-positive HA patients (35). We prepared the electrophilic analog of the synthetic FVIII peptide 2303–2332 containing the phosphonate at Lys-2320 (E-(2303–2332), Fig. 8*A*). No E-(2303–2332) binding by IgG from our inhibitor-positive HA patients was detected by ELISA ($n = 7$ patients; $A_{490} < 0.1$; data not shown). Denaturing electrophoresis of boiled reaction mixtures containing excess biotinylated E-(2303–2332) revealed small amounts of immune adducts formed by IgG from two of the seven HA patients but not control IgG from the non-HA subject (56-kDa IgG heavy chain band, Fig. 8*B*). However, treatment of these IgG preparations without and with excess E-(2303–2332) (20 μM) did not influence their FVIII inhibitory activity (Fig. 8*C*). This suggests that E-(2303–2332) binding Abs do not constitute a functionally significant proportion of the FVIII inhibitory Abs in these subjects. Certain other FVIII synthetic peptides are recognized by anti-FVIII Abs found in HA patients with low affinity. In this study, we tested the following peptides (devoid of phosphonate groups): A2 domain residues 484–508 (36), A3 domain residues 1804–1819 (37), and BO2C11 peptide, a mimetic of a C2 domain conformational epitope (12). The peptides were not bound detectably by the seven HA IgG preparations studied ($A_{490} < 0.1$). At a concentration of 200 μM, the peptides failed to relieve the FVIII inhibitor activity of the HA IgG preparations (measured as in Fig. 8C; <15% difference for diluent-treated IgG; data not shown). We concluded that the reactivity of the peptides with the Abs is insufficient to afford useful Ab inactivation. Previous reports have also suggested that the inhibitory Abs recognize large FVIII polypeptide fragments (6) better than small peptides, suggesting that the Abs are directed mainly to conformational rather than linear epitopes (12, 35, 36).

DISCUSSION

Infused FVIII is ineffective in correcting defective blood coagulation in a subpopulation of FVIII-deficient HA patients producing inhibitory Abs to the protein. Here we describe electrophilic FVIII analogs that bind specifically and covalently to the nucleophilic sites of Abs. E-FVIII and E-C2 were bound irreversibly by IgG preparations from each of eight inhibitor-positive HA patients studied. The unique mechanism of action of the electrophilic analogs was also evident from irreversible relief of FVIII inhibition by the Abs in coagulation assays. Full-length E-FVIII inactivated the Abs with superior potency compared with E-C2 and synthetic FVIII peptides. This is consistent with findings that HA patients produce Abs directed to diverse FVIII epitopes outside the C2 domain (2, 35). Our studies provide proof-of-principle that targeting of Ab nucleophilic sites can relieve the pathogenic effects of Abs. The strengths of this approach and potential means to address its weaknesses are discussed below.

Irreversible reactions of E-FVIII and E-C2 with Abs from HA patients were evident from the failure of denaturing treatments

Downloaded from www.jbc.org at HAM-TMC Library on May 1, 2008

PAGE 35/92 * RCVD AT 4/28/2010 6:45:45 PM [Eastern Daylight Time] * SVR:USPTO-EFXRF-6/33 * DNIS:2738300 * CSID:7132705361 * DURATION (mm-ss):48-00

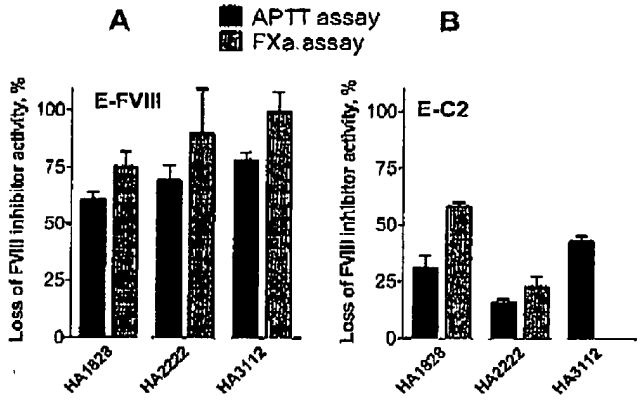

FIGURE 6. **Loss of FVIII inhibitory activity of antibodies by treatment with E-FVIII (*A*) and E-C2 (*B*) determined by the APTT clotting assay and chromogenic FXa assay.** IgG from three inhibitor-positive patients (HA1828, 200 μg/ml; HA2222, 100 μg/ml; HA3112, 100 μg/ml) was treated with E-FVIII or E-VIP (0.1 μM; *A*) and E-C2 or E-VIP (1.0 μM; *B*) in 0.1-ml reaction mixtures for 20 h. Free E-polypeptides were removed by protein G affinity purification. IgGs along with any stable immune complexes were recovered with 0.2 ml of elution buffer. FVIII cofactor activity was determined by the one-stage APTT clotting assay with 0.06-ml eluates mixed with an equal volume of FVIII-containing normal plasma (incubation for 2 h, 37 °C). FVIII cofactor activity was determined by the chromogenic FXa assay (Diapharma Coamatic kit) as in Fig. 4 with 0.025-ml column eluates incubated with recombinant FVIII (0.025 ml; 0.2 IU/ml; 1 h, 37 °C). Percent relief from FVIII inhibitory activity was computed as follows: (FVIII inhibitor activity in the presence of E-VIP − FVIII inhibitor activity in the presence of E-FVIII or E-C2) × 100/(FVIII inhibitor activity in the presence of E-VIP), where FVIII inhibitor activity denotes (FVIII cofactor activity in the absence of IgG − FVIII cofactor activity in the presence of IgG). FVIII inhibitor activity was read from the linear portion of the curve constructed using various dilutions of standard FVIII-containing plasma (0.95 IU/ml). Values plotted are means of duplicates ± S.D. *A*, FVIII activity levels without IgG treatment in the APTT and chromogenic FXa assays were, respectively, 0.37 ± 0.01 and 0.045 ± 0.015 IU/ml. In the APTT assay, FVIII activities in the presence of IgG from subjects HA1828 (100 μg/ml), HA2222 (50 μg/ml), and HA3112 (50 μg/ml) treated with control E-VIP were, respectively, 0.11 ± 0.06, 0.04 ± 0.01, and 0.07 ± 0.01 IU/ml. The FVIII activities in presence of these IgG preparations (4.5 μg/ml) treated with control E-VIP in the chromogenic FXa assay were 0.019 ± 0.007, 0.030 ± 0.003, and 0.000 ± 0.001 IU/ml. *B*, FVIII activity in the absence of IgG in the APTT and chromogenic FXa assays were, respectively, 0.36 ± 0.02 and 0.054 ± 0.009 IU/ml. In the APTT assay of *B*, FVIII activities in the presence of IgG from subjects HA1828 (33 μg/ml), HA2222 (16 μg/ml) or HA3112 (16 μg/ml) treated with control E-VIP were, respectively, 0.25 ± 0.03, 0.18 ± 0.01 and 0.21 ± 0.8 IU/ml. The FVIII activities in the presence of IgG from subjects HA1828 or HA2222 (4.5 μg/ml) treated with control E-VIP in the chromogenic FXa assay were 0.013 ± 0.005 and 0.018 ± 0.001 IU/ml.

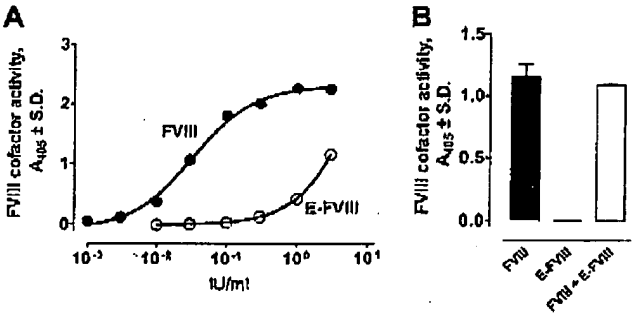

FIGURE 7. **Clotting factor activity of E-FVIII.** *A*, recombinant FVIII and E-FVIII were assayed for formation of the FVIIIa-FIXa tenase complex responsible for FXa activation. Shown are A_{405} values (means of duplicates ± S.D.) corresponding to FXa-catalyzed hydrolysis of *N*-α-benzyloxycarbonyl-D-Arg-Gly-Arg-*p*-nitroanilide. *B*, inability of E-FVIII to interfere with clotting factor activity of FVIII. Activation of FXa by FVIII alone, E-FVIII alone, or FVIII mixed with an equivalent mass of E-FVIII was measured as in *A*.

to dissociate the immune adducts. Similarly, a majority of the adducts remained undissociated in nondenaturing solvent after removal of free Abs and prolonged incubation in excess competitor FVIII. There was no evidence that E-FVIII or E-C2 react nonspecifically with irrelevant Abs. This supports a two-step reaction model in which initial noncovalent binding confers specificity to the reaction, followed by covalent bonding of the electrophilic phosphonates with Ab nucleophiles. Conversion of the noncovalent complexes to irreversible adducts was rapid, and noncovalent E-FVIII binding by the Abs was rate-limiting. This is consistent with the strong electrophilicity of phosphonate diesters evident from the study of nucleophilic enzymes. The first order rate constant for the reaction of a phosphonate diester with trypsin is 0.03 s^{-1} (15, 38). IgG nucleophilic reactivities can exceed that of trypsin (14), consistent with rapid conversion of noncovalent E-FVIII immune complexes to irreversible adducts. We did not address in detail the extent of damage to the antigenic structure of FVIII caused by introducing phosphonate groups. However, all eight HA IgG preparations displayed E-FVIII binding. The observed E-FVIII aggregation reaction is likely because of the reactivity of phosphonate groups with an endogenous nucleophile of FVIII. Formation of the aggregates did not appear to impact the reaction with Abs negatively, as the aggregates were bound by an HA IgG preparation comparably to unfractionated E-FVIII. Treatment with excess E-FVIII resulted in near-complete consumption of FVIII binding Abs, indicating that most epitopes recognized by the Abs are expressed on E-FVIII.

To determine the functional consequence of irreversible occupancy of Ab combining sites, free E-FVIII was removed from the E-FVIII/IgG reaction mixtures prior to clotting factor assays. E-FVIII-treated HA IgG preparations displayed reduced FVIII inhibitor activity (by 61–99%). An irrelevant E-polypeptide was without effect, suggesting specific Ab inactivation. The functional results are consistent with biochemical studies indicating that the majority of noncovalent complexes are converted to irreversible adducts. It may be concluded that electrophilic phosphonates are available for covalent bonding in most FVIII epitopes recognized by Abs. This is significant, as diverse Abs directed to various FVIII epitopes must be inactivated irreversibly to obtain a functionally useful effect. The linker attaching the phosphonate groups to FVIII contains single bonds around which rotation is permissible. The resultant spatial freedom enjoyed by the phosphonates should facilitate approach of the electrophilic phosphorus atom within covalent binding distance of Ab nucleophiles. Conversely, the failure of a minority of the reversibly associated complexes to convert to the irreversible state suggests room for improvement in the structure of the E-FVIII. Factors that may limit the covalent reaction are as follows: (*a*) some epitopes may not be labeled with the electrophilic phosphonate if they do not contain a sufficiently exposed Lys residue; (*b*) the distance between the phosphonate and Ab nucleophile or the spatial orientation of these groups may be nonpermissive for covalent bonding; and (*c*) a minority of the Abs may lack nucleophilic sites. We hold the last mentioned possibility unlikely as the nucleophilic reactivity was expressed by the variable domains of every recombinant Ab fragment and monoclonal Ab examined previously (14, 23).

Downloaded from www.jbc.org at HAM-TMC Library on May 1, 2008

PAGE 36/92 * RCVD AT 4/28/2010 6:45:45 PM [Eastern Daylight Time] * SVR:USPTO-EFXRF-6/33 * DNIS:2738300 * CSID:7132705361 * DURATION (mm-ss):48-00

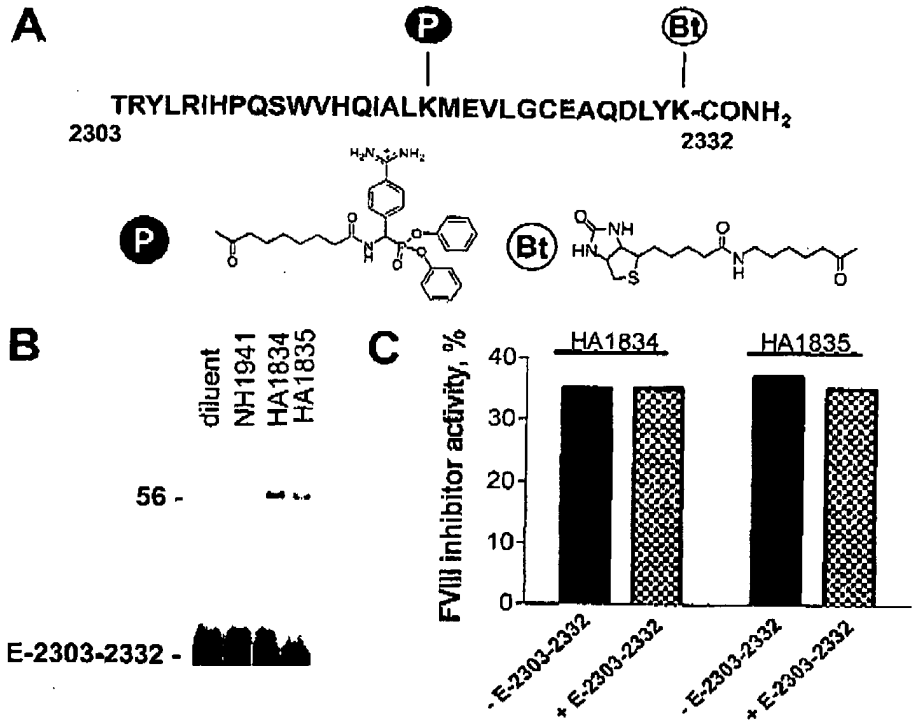

FIGURE 8. **Covalent binding of peptide E-(2303–2332) to inhibitory IgG and effect on FVIII inhibitor activity.** *A*, structure of the E-(2303–2332) peptide analog. *P* and *Bt* denote, respectively, the phosphonate and biotin groups. *B*, streptavidin-peroxidase-stained blot of a reducing SDS-electrophoresis gel showing boiled reaction mixtures of biotinylated E-(2303–2332) (10 μM) incubated with HA1834 IgG, HA1835 IgG or control NH1941 IgG (75 μg/ml; 20 h, 37 °C). The bands at the *bottom* of the lanes and the 56-kDa position represent, respectively, the free E-(2303–2332) and E-(2303–2332) complexed to the heavy chains of the IgG. *C*, FVIII inhibitory activity of IgG preparations treated with E-(2303–2332). FVIII cofactor activity was measured by the APTT assay after incubation of HA IgG1834 or HA IgG 1835 (400 μg/ml) with E-(2303–2332) (20 μM; 20 h at 37 °C) and treatment of FVIII-containing normal plasma with varying concentrations of the reaction mixtures (diluted 1/2 and 1/6). FVIII inhibitory activity was computed as follows: 100 − 100 × (FVIII activity in presence of IgG/FVIII activity in absence of IgG). FVIII activity in absence of IgG was 0.54 IU/ml. Experimental procedures were as in Fig. 6. Values plotted are means of duplicates ± S.D.

That the irreversible E-FVIII binding activity in this study is a property of Ab variable domains is confirmed by observations that the antigen binding Fab fragments of IgG displayed this activity.

FX activation occurs via formation of the FVIIIa-FIXa complex on phospholipid surfaces ("tenase complex"). E-FVIII was a poor activator of FX compared with underivatized FVIII. A low level risk of thrombotic events is associated with overdose of bypass reagents such as recombinant Factor VII (9). The poor cofactor activity of E-FVIII may be a functionally useful property, as this diminishes the risk of a thrombotic effect. Possible reasons for the poor cofactor activity of E-FVIII are as follows: (*a*) structural perturbations because of introduction of phosphonate groups may render E-FVIII resistant to thrombin hydrolysis; (*b*) even if E-FVIIIa is produced by thrombin hydrolysis, it may not form the tenase complex; or (*c*) E-FVIII may inhibit serine proteases indiscriminately. Possibilities *a* and *b* are innocuous, in that they should not produce undesirable effects. The potential inhibition of serine proteases involved in the coagulation pathway, however, merits attention. High micromolar to millimolar concentrations of small molecule phosphonates are reported to bind covalently to the nucleophilic sites of serine proteases (17). E-FVIII did not interfere with FVIII-dependent hydrolysis of the peptidyl ester substrate catalyzed by FXa, indicating that it does not inhibit the enzymes necessary for this reaction (thrombin, FIXa, and FXa). Moreover, no prolongation of the time to fibrin clot formation was observed in the APTT test at an E-FVIII concentration that relieved the FVIII inhibitor activity of the Abs irreversibly. These observations indicate that E-FVIII can selectively inactivate Abs without functionally significant inhibition of serine protease clotting factors.

The phosphonate-containing E-FVIII is a first generation reagent. Future genetic and chemical manipulations may help develop improved E-FVIII analogs. As the selectivity of the reaction derives from noncovalent Ab binding, the conformation of E-FVIII should preferably be as close to native FVIII as feasible. As the covalent reactivity of E-FVIII is not rate-limiting, it may be useful to reduce the electrophilicity of E-FVIII to further minimize reactions with non-Ab serine proteases while maintaining sufficiently rapid covalent Ab bonding capability. Carbon-based electrophiles placed at defined positions within FVIII may offer sufficient electrophilicity to inactivate Abs directed to individual epitopes with minimal overall structural perturbation of FVIII. Electrophilic pyruvate analogs and dicarbonyl compounds react covalently with protein nucleophilic sites (38, 39), and suppressor tRNA technologies for incorporation of such compounds into the protein backbone are available (40). The half-life of FVIII in human circulation ($t_{1/2}$) is ~12 h (41). Aggregation of proteins can influence their clearance *in vivo*. E-FVIII aggregation appears to involve a naturally occurring nucleophile that reacts with the phosphonate groups. Availability of an FVIII mutant with deficient nucleophilicity will help minimize the aggregation reaction. Site-directed mutagenesis has been applied previously to generate enzymes and Abs with deficient nucleophilic reactivity (20, 42). A significant proportion of inhibitory Abs to FVIII in HA patients is directed to the C2 domain (43). However, Ab diversity and the conformational character of the immunodominant epitopes pose significant challenges. This is illustrated by our observations using E-C2 and E-(2303–2332), a C2 peptide analog. E-C2 was consistently less reactive with HA IgG than E-FVIII. E-(2303–2332) displayed very limited reactivity. For these reasons, developing mixtures of large E-FVIII polypeptides or optimization of the full-length E-FVIII struc-

PAGE 37/92 * RCVD AT 4/28/2010 6:45:45 PM [Eastern Daylight Time] * SVR:USPTO-EFXRF-6/33 * DNIS:2738300 * CSID:7132705361 * DURATION (mm-ss):48-00

The Journal of Biological Chemistry

Downloaded from www.jbc.org at HAM-TMC Library on May 1, 2008

ture are preferred routes to clinical application of the covalent inactivation approach described here.

The FVIII inhibitory potencies of Abs in HA patients can vary over 3 log orders, and the titers can exceed 1000 Bethesda assay units/ml (44, 45). The magnitude of the titers depends on the concentration and affinity of Abs directed to the neutralizing FVIII epitopes. The irreversible reaction of E-FVIII offers the advantage of more potent Ab inactivation if certain conditions are met. For example, 84% of 1 nM Ab with K_d 10 nM will be in free state after equilibrium is attained with 2 nM reversibly binding antigen (see supplemental Fig. S1). Assuming a covalent binding rate constant that does not limit the overall reaction rate (as observed in this study), only 6% of the Ab will exist in free state after incubation for 12 h with an irreversible binding antigen. Consumption of the Abs by the irreversible antigen will occur at superior levels as long as the Ab concentration does not exceed the K_d. With increasing Ab concentration or decreasing K_d values, Ab consumption by the irreversible and reversible antigen will approach equivalence, and the potential advantage of the former antigen is lost. Even if the Abs are initially consumed at equivalent levels by E-FVIII and FVIII, the former reagent should provide more long lasting Ab inactivation *in vivo*. With reducing concentrations of free FVIII in blood because of metabolic clearance, a progressive reduction in the concentration of reversibly associated immune complexes will occur. The irreversibly associated E-FVIII immune complexes, on the other hand, are not subject to dissociation because of metabolic clearance of E-FVIII. With respect to catalytic Abs, a nonhydrolyzable antigen analog such as E-FVIII offers superior inactivation potency even when [Ab] > K_d (see supplemental Fig. S1).

In addition to Abs to FVIII, other antigen-specific Abs exert harmful effects in various diseases, *e.g.* autoantibodies to the acetylcholine receptor in myasthenia gravis (46) and to platelet antigens in autoimmune thrombocytic purpura (47). Nonspecific immunosuppressive agents are used to control Ab production, but this is often accompanied by profound side effects and enhanced susceptibility to infection. As several electrophilic polypeptides are documented to bind their cognate Abs irreversibly (14, 15), it is reasonable to consider the generality of the irreversible Ab targeting approach in future studies. Consideration of the effect of electrophilic antigens on the cells responsible for Ab synthesis is also warranted. Antigen binding to the antigen receptor (immunoglobulins complexed to signal transducing proteins) drives maturation of B lymphocytes into Ab-secreting cells. Saturation of the antigen receptor induces B cell apoptosis and immune tolerance (48, 49). Administration of very large amounts of FVIII on the order of grams induces immune tolerance to FVIII in a subpopulation of HA patients (10, 11). We reported covalent binding of an electrophilic hapten to nucleophilic B cell antigen receptors (23). Electrophilic antigen analogs are predicted to saturate cellular antigen receptors more readily than the reversibly binding antigen. In preliminary studies (50) we observed that prior treatment with E-FVIII attenuated Ab synthesis by B cells challenged with FVIII. Taken together, these considerations support further development of electrophilic antigen analogs for irreversible inactivation of pathogenic Abs.

Acknowledgments—We thank Y. Bangale, R. Dannenbring, and T. Yoshikawa for assistance and CSL Behring for recombinant FVIII.

REFERENCES

1. Ettingshausen, C. E., and Kreuz, W. (2006) *Haemophilia* **12**, Suppl. 6, 102–106
2. Scandella, D. (1999) *Vox Sang.* **77**, Suppl. 1, 17–20
3. Lacroix-Desmazes, S., Moreau, A., Sooryanarayana, Bonnemain, C., Stieltjes, N., Pashov, A., Sultan, Y., Hoebeke, J., Kazatchkine, M. D., and Kaveri, S. V. (1999) *Nat. Med.* **5**, 1044–1047
4. Spiegel, P. C., Jr., Jacquemin, M., Saint-Remy, J. M., Stoddard, B. L., and Pratt, K. P. (2001) *Blood* **98**, 13–19
5. Villard, S., Piquer, D., Raut, S., Leonetti, J. P., Saint-Remy, J. M., and Granier, C. (2002) *J. Biol. Chem.* **277**, 27232–27239
6. Lavigne-Lissalde, G., Schved, J. F., Granier, C., and Villard, S. (2005) *Thromb. Haemostasis* **94**, 760–769
7. Kopecky, E. M., Greinstetter, S., Pabinger, I., Buchacher, A., Romisch, J., and Jungbauer, A. (2006) *J. Immunol. Methods* **308**, 90–100
8. Lloyd Jones, M., Wight, J., Paisley, S., and Knight, C. (2003) *Haemophilia* **9**, 464–520
9. Berntorp, E., Gringeri, A., Leissinger, C., Negrier, C., and Key, N. (2006) *Semin. Thromb. Hemostasis* **32**, Suppl. 2, 22–27
10. Brackmann, H. H. (1984) *Prog. Clin. Biol. Res.* **150**, 181–195
11. Brackmann, H. H., and Gormsen, J. (1977) *Lancet* **2**, 933
12. Villard, S., Lacroix-Desmazes, S., Kieber-Emmons, T., Piquer, D., Grailly, S., Benhida, A., Kaveri, S. V., Saint-Remy, J. M., and Granier, C. (2003) *Blood* **102**, 949–952
13. Gilles, J. G., Grailly, S. C., De Maeyer, M., Jacquemin, M. G., VanderElst, L. P., and Saint-Remy, J. M. (2004) *Blood* **103**, 2617–2623
14. Planque, S., Taguchi, H., Burr, G., Bhatia, G., Karle, S., Zhou, Y. X., Nishiyama, Y., and Paul, S. (2003) *J. Biol. Chem.* **278**, 20436–20443
15. Nishiyama, Y., Bhatia, G., Bangale, Y., Planque, S., Mitsuda, Y., Taguchi, H., Karle, S., and Paul, S. (2004) *J. Biol. Chem.* **279**, 7877–7883
16. Paul, S., Planque, S., Zhou, Y. X., Taguchi, H., Bhatia, G., Karle, S., Hanson, C., and Nishiyama, Y. (2003) *J. Biol. Chem.* **278**, 20429–20435
17. Oleksyszyn, J., and Powers, J. C. (1994) *Methods Enzymol.* **244**, 423–441
18. Bertrand, J. A., Oleksyszyn, J., Kam, C. M., Boduszek, B., Presnell, S., Plaskon, R. R., Suddath, F. L., Powers, J. C., and Williams, L. D. (1996) *Biochemistry* **35**, 3147–3155
19. Paul, S., Volle, D. J., Beach, C. M., Johnson, D. R., Powell, M. J., and Massey, R. J. (1989) *Science* **244**, 1158–1162
20. Gao, Q. S., Sun, M., Rees, A. R., and Paul, S. (1995) *J. Mol. Biol.* **253**, 658–664
21. Ramsland, P. A., Terzyan, S. S., Cloud, G., Bourne, C. R., Farrugia, W., Tribbick, G., Geysen, H. M., Moomaw, C. R., Slaughter, C. A., and Edmundson, A. B. (2006) *Biochem. J.* **395**, 473–481
22. Pratt, K. P., Shen, B. W., Takeshima, K., Davie, E. W., Fujikawa, K., and Stoddard, B. L. (1999) *Nature* **402**, 439–442
23. Planque, S., Bangale, Y., Song, X. T., Karle, S., Taguchi, H., Poindexter, B., Bick, R., Edmundson, A., Nishiyama, Y., and Paul, S. (2004) *J. Biol. Chem.* **279**, 14024–14032
24. Kasper, C. K., and Pool, J. G. (1975) *Thromb. Diath. Haemorrh.* **34**, 875–876
25. Paul, S., Said, S. L., Thompson, A. B., Volle, D. J., Agrawal, D. K., Foda, H., and de la Rocha, S. (1989) *J. Neuroimmunol.* **23**, 133–142
26. Paul, S., Mei, S., Mody, B., Eklund, S. H., Beach, C. M., Massey, R. J., and Hamel, F. (1991) *J. Biol. Chem.* **266**, 16128–16134
27. Paul, S., Sun, M., Mody, R., Tewary, H. K., Stemmer, P., Massey, R. J., Gianferrara, T., Mehrotra, S., Dreyer, T., and Meldal, M. (1992) *J. Biol. Chem.* **267**, 13142–13145
28. Paul, S., Tramontano, A., Gololobov, G., Zhou, Y. X., Taguchi, H., Karle, S., Nishiyama, Y., Planque, S., and George, S. (2001) *J. Biol. Chem.* **276**, 28314–28320
29. Ten Boekel, E., Bock, M., Vrielink, G. J., Liem, R., Hendriks, H., and Kieviet, W. D. (2007) *Thromb. Res.* **12**, 361–367
30. Bhopale, G. M., and Nanda, R. K. (2003) *J. Biosci.* **28**, 783–789

PAGE 38/92 * RCVD AT 4/28/2010 6:45:45 PM [Eastern Daylight Time] * SVR:USPTO-EFXRF-6/33 * DNIS:2738300 * CSID:7132705361 * DURATION (mm-ss):48-00

Downloaded from www.jbc.org at HAM-TMC Library on May 1, 2008

The Journal of Biological Chemistry

31. Nishiyama, Y., Mitsuda, Y., Taguchi, H., Planque, S., Hara, M., Karle, S., Hanson, C. V., Uda, T., and Paul, S. (2005) *J. Mol. Recognit.* 18, 295–306
32. Saenko, E. L., Shima, M., Gilbert, G. E., and Scandella, D. (1996) *J. Biol. Chem.* 271, 27424–27431
33. Nishiyama, Y., Karle, S., Mitsuda, Y., Taguchi, H., Planque, S., Salas, M., Hanson, C., and Paul, S. (2006) *J. Mol. Recognit.* 19, 423–431
34. Schenone, M., Furie, B. C., and Furie, B. (2004) *Curr. Opin. Hematol.* 11, 272–277
35. Nogami, K., Shima, M., Nakai, H., Tanaka, I., Suzuki, H., Morichika, S., Shibata, M., Saenko, E. L., Scandella, D., Giddings, J. C., and Yoshioka, A. (1999) *Br. J. Haematol.* 107, 196–203
36. Healey, J. F., Lubin, I. M., Nakai, H., Saenko, E. L., Hoyer, L. W., Scandella, D., and Lollar, P. (1995) *J. Biol. Chem.* 270, 14505–14509
37. Zhong, D., Saenko, E. L., Shima, M., Felch, M., and Scandella, D. (1998) *Blood* 92, 136–142
38. Walter, J., and Bode, W. (1983) *Hoppe-Seyler's Z. Physiol. Chem.* 364, 949–959
39. Biemel, K. M., Friedl, D. A., and Lederer, M. O. (2002) *J. Biol. Chem.* 277, 24907–24915
40. Tsao, M. L., Tian, F., and Schultz, P. G. (2005) *ChemBioChem* 6, 2147–2149
41. van Dijk, K., van der Bom, J. G., Lenting, P. J., de Groot, P. G., Mauser-Bunschoten, E. P., Roosendaal, G., Grobbee, D. E., and van den Berg, H. M. (2005) *Haematologica* 90, 494–498
42. Carter, P., and Wells, J. A. (1988) *Nature* 332, 564–568
43. Prescott, R., Nakai, H., Saenko, E. L., Scharrer, I., Nilsson, I. M., Humphries, J. E., Hurst, D., Bray, G., and Scandella, D. (1997) *Blood* 89, 3663–3671
44. Shetty, S., Ghosh, K., and Mohanty, D. (2003) *Haemophilia* 9, 654
45. Sahud, M. A., Pratt, K. P., Zhukov, O., Qu, K., and Thompson, A. R. (2007) *Haemophilia* 13, 317–322
46. Appel, S. H., Almon, R. R., and Levy, N. (1975) *N. Engl. J. Med.* 293, 760–761
47. Coopamah, M. D., Garvey, M. B., Freedman, J., and Semple, J. W. (2003) *Transfus. Med. Rev.* 17, 69–80
48. Nossal, G. J. (1997) *CIBA Found. Symp.* 204, 220–230
49. Goodnow, C. C., Crosbie, J., Adelstein, S., Lavoie, T. B., Smith-Gill, S. J., Brink, R. A., Pritchard-Briscoe, H., Wotherspoon, J. S., Loblay, R. H., Raphael, K., Trent, R. J., and Basten, A. (1988) *Nature* 334, 676–682
50. Smith, K. C., Planque, S., Bangale, Y., Nishiyama, Y., Taguchi, H., Escobar, E. A., and Paul, S. (2007) *J. Immunol.* 178, 88.14 (abstr.)

Downloaded from www.jbc.org at HAM-TMC Library on May 1, 2008

PAGE 39/92 * RCVD AT 4/28/2010 6:45:45 PM [Eastern Daylight Time] * SVR:USPTO-EFXRF-6/33 * DNIS:2738300 * CSID:7132705361 * DURATION (mm-ss):48-00

JOURNAL OF MOLECULAR RECOGNITION
J. Mol. Recognit. 2006; 19: 423–431
Published online 13 July 2006 in Wiley InterScience
(www.interscience.wiley.com) DOI:10.1002/jmr.795

Towards irreversible HIV inactivation: Stable gp120 binding by nucleophilic antibodies

Yasuhiro Nishiyama[1], Sangeeta Karle[1], Yukie Mitsuda[1], Hiroaki Taguchi[1], Stephanie Planque[1], Maria Salas[2], Carl Hanson[2] and Sudhir Paul[1]*

[1]Chemical Immunology and Therapeutics Research Center, Department of Pathology and Laboratory Medicine, University of Texas-Houston Medical School, 6431 Fannin, Houston, Texas 77030, USA
[2]Viral and Rickettsial Disease Laboratory, California Department of Health Services, Richmond, California 94804, USA

Conventional antibodies react with antigens reversibly. We report the formation of unusually stable complexes of HIV gp120 and nucleophilic antibodies raised by immunization with an electrophilic HIV gp120 analog (E-gp120). The stability of the complexes was evident from their very slow dissociation in a nondenaturing solvent (approximate t½ 18.5 days) and their resistance to dissociation by a denaturant commonly employed to disrupt noncovalent protein–protein binding (sodium dodecyl sulfate). Kinetic studies indicated time-dependent and virtually complete progression of the antibody-gp120 complexes from the initial noncovalent state to a poorly dissociable state. The antibodies to E-gp120 displayed improved covalent reactivity with an electrophilic phosphonate probe compared to control antibodies, suggesting their enhanced nucleophilicity. One of the stably binding antibodies neutralized the infectivity of CCR5-dependent primary HIV strains belonging to clades B and C. These findings suggest the feasibility of raising antibodies capable of long-lasting inactivation of antigens by electrophilic immunization. **Copyright © 2006 John Wiley & Sons Ltd.**

Keywords: **nucleophilic antibody; gp120; HIV**

Received 27 January 2006; revised 30 March 2006; accepted 13 April 2006

INTRODUCTION

Following noncovalent substrate recognition, many enzymes employ nucleophile-electrophile interactions to form covalent reaction intermediates (Hedstrom, 2002). The presence of nucelophiles in Ab combining sites is suggested by observations that haptenic electrophilic phosphonate diesters originally developed as probes for serine proteases (Oleksyszyn and Powers, 1994) bind covalently to IgM Abs synthesized early in the ontogeny of the immune response (Planque *et al.*, 2004). Adaptive immunological processes occurring over the course of the immune response hold the potential of improving the naturally occurring nucleophilic reactivity of Abs and permitting development of specific catalytic Abs (Planque *et al.*, 2004). Examples of antigen-specific catalysis by Abs produced in various immunological diseases have been reported (Paul *et al.*, 1989; Shuster *et al.*, 1992; Lacroix-Desmazes *et al.*, 1999) but most Abs raised by routine immunization with polypeptides do not express proteolytic activity. Hypothesizing that adaptive immune processes can strengthen the nucleophilic reactivity in coordination with development of noncovalent antigen binding forces, we raised monoclonal Abs (MAbs) by immunization with HIV gp120 containing electrophilic phosphonate diesters within its antigenic epitopes (E-gp120; Paul *et al.*, 2003). This approach is based on the discovery of serine protease-like sites in naturally occurring Abs (Paul *et al.*, 1991; Gao *et al.*, 1994) and Abs raised by immunization with a hapten phosphonate monoester (Zhou *et al.*, 1994). A minority of the MAbs displayed slow proteolytic cleavage of gp120. The phosphonate electrophiles integrated into the gp120 immunogen may be anticipated to select for Ab active sites with adaptively improved nucleophilic reactivity but not sites that facilitate the subsequent water attack and product release steps, with the result that catalysis occurs slowly. Regardless of the ability to complete the catalytic cycle, the covalent character of the MAbs may result in formation of immune complexes that are more stable than customary reversibly associated complexes. Here, we describe the formation of exceptionally stable immune complexes by gp120 devoid of artificial electrophiles with the Abs raised by immunization with E-gp120. One of the stably binding MAbs displayed

*Correspondence to: S. Paul, Department of Pathology and Laboratory Medicine, University of Texas-Houston Medical School, 6431 Fannin, Houston, TX 77030, USA.
E-mail: Sudhir.Paul@uth.tmc.edu

Contract/grant sponsor: National Institutes of Health; *contract/grant numbers:* AI31268; AI058865; AI058684; AG025304.
Contract/grant sponsors: Texas Higher Education Coordinating Board; Hemophilia Association of New York.

Abbreviations used: Ab, antibody; Bt-gp120, biotinylated gp120; E-gp120, electrophilic analog of gp120; HIV, human immunodeficiency virus; MAb, monoclonal antibody; SDS, sodium dodecylsulfate.

Copyright © 2006 John Wiley & Sons, Ltd.

cross-clade HIV neutralizing activity, a property rarely encountered in anti-HIV Abs.

MATERIALS AND METHODS

MAbs

The preparation of anti-E-gp120 MAbs from mice hyperimmunized with E-gp120 has been described previously (Paul *et al.*, 2003). The E-gp120 contained 23–32 mol phosphonate/mol protein located at Lys side chains. Additional MAbs were obtained from the AIDS Research and Reference Reagent Program (Division of AIDS, NIAID, NIH), Dr Susan Zolla-Pazner (anti-V3 MAbs 257-DIV, 268-DIV), Dr Dennis Burton and Dr Carlos Barbas (anti-CD4 binding site MAb b12), Immunodiagnostics (anti-V3 MAb 1121), Sigma-Aldrich (MAb MOPC21; IgG1, κ isotype control for MAb SK-T03) and ATCC (MAb CRL1689; IgG2a, κ isotype control for MAb YZ23). All experiment reported here utilized IgG purified to electrophoretic homogeneity from tissue culture supernatants or ascites by affinity chromatography on immobilized protein G (Paul *et al.*, 2003). Fab fragments of MAb SK-T03 were prepared by the method described previously (Planque *et al.*, 2004).

Stability in SDS

The method for measuring MAb binding to E-gp120 refractory to dissociation with SDS has been described (Paul *et al.*, 2003). Formation of stable complexes following incubation of gp120 devoid of artificial electrophiles with MAbs was studied essentially in the same manner by treatment of the ELISA plates with 2% SDS (w/v) for 30 min prior to measurement of bound MAbs. Total binding (reversible + irreversible) was measured by incubation with diluent instead of SDS. Recombinant gp120 was from MN strain (40 ng/well; purified from baculovirus expression system; Protein Science). Bound MAbs were detected using peroxidase-conjugated goat anti-mouse IgG or goat anti-human IgG (Fc specific, Sigma-Aldrich). For identification of adducts by electrophoresis, biotinylated gp120 (Bt-gp120, 6.7 mol biotin/mol gp120, see Paul *et al.*, 2003 for preparation method) and MAb reaction mixtures in 50 mM Tris-HCl, 0.1 M glycine, pH 7.7, 1 mM 3-[(3-cholamidopropyl)dimethylammonio]-1-propanesulfonic acid (CHAPS) and 1.3% gelatin were subjected to SDS-gel electrophoresis (4–20%, Bio-Rad). The gels were electroblotted onto nitrocellulose and probed for the presence of biotin or IgG using peroxidase-conjugated streptavidin (Sigma-Aldrich) or peroxidase-conjugated goat anti-mouse IgG (heavy and light chains; Pierce), respectively, and a chemiluminscent substrate. The hapten probe for nucleophilic reactivity, diphenyl *N*-(6-biotinamidohexanoyl)amino(4-amidinophenyl)methanephosphonate (phosphonate **1**), and measurement of its SDS-resistant binding to Abs by electrophoresis is described in Planque *et al.*, 2004. In certain experiments, MAb SK-T03 was incubated with gp120 peptide 465–479 or control gp120 peptide 297–311 for 17 h prior to the reaction with **1**. Band intensities were determined by densitometry using Fluoro-STM Multi-Imager (Bio-Rad) and expressed in arbitrary volume units (AVU; volume represents the pixel intensity × area inside the bands).

Stability in nondenaturing solvent

To measure dissociation rates, the MAbs (clone SK-T03, 20 μg/mL; clone 268-D IV, 1 μg/mL) were first incubated with Bt-gp120 (0.2 μg/mL) in 50 mM Tris-HCl, 0.1 M glycine, pH 7.7, 1 mM CHAPS and 5% bovine serum albumin (v/v) for 12 h, the immune complexes were captured on Protein G-Sepharose beads (300 μL settled volume; Amersham Biosciences), free Bt-gp120 was removed by washing (1.5 mL × 5 washes) and the gel was resuspended in 3.1 mL diluent containing excess competitor peptide (10 μg/mL). The suspension was kept at 25°C for various lengths of time, aliquots (0.1 mL) were transferred to Whatman filter plates (0.45 μm, PVDF), the gel was washed (5×) and residual Bt-gp120 contained in immune complexes was determined by incubation of the gel with peroxidase-conjugated streptavidin as described in the preceding section. Background nonspecific binding was determined by identical treatment of Bt-gp120 with an irrelevant MAb (clone MOPC21). First-order dissociation rate constants (k) and half-lives ($t½$) were obtained, respectively, from the equations, [(residual binding, %) = $100 \times e^{(-k \cdot t)}$] and [$t½ = \ln(2)/k$]. The competitor peptides were identified by screening 122 synthetic gp120 peptides for inhibition of MAb binding to immobilized Bt-gp120 (fifteen-mer overlapping peptides; 50 μg/mL; corresponding to the gp120 MN strain sequence, NIH AIDS Research and Reference Reagent Program; catalog numbers 6215 through 6336). Conversion of the MAb-gp120 complexes from their readily dissociable state to the poorly dissociable state was studied as follows. MAbs were preincubated for varying time periods (0–8 hours, 37°C) in a reaction volume of 50 μL with Bt-gp120 (40 ng/well) immobilized on streptavidin-coated plates (1 μg/well). Thereupon, 50 μL diluent or excess competitor peptide was added to the wells, the reactions were incubated for another 2 h, and the immune complexes were quantified using peroxidase-conjugated goat anti-mouse IgG or goat anti-human IgG (Fc specific, Sigma-Aldrich). A490 values in reaction mixtures containing excess competitor were taken to represent the concentrations of the poorly dissociable state, and the values in reactions containing diluent, the sum of the concentrations of the dissociable and poorly dissociable states. Background nonspecific binding was determined by eliminating the preincubation step, i.e., by co-incubating the MAb, immobilized gp120 and excess competitor peptide for 2 h. Similar studies were done with the Fab fragment of a MAb using goat anti-mouse Fab (Sigma-Aldrich) to measure the Fab-containing complexes. Pseudo-first order rate constants (k_{obs}) for complex formation were obtained from least-square-fits to the equation [$A_{490}/A_{490}^{max} = 1 - e^{(-k_{obs} \cdot t)}$], where A_{490}^{max} represents the extrapolated maximum value of A_{490}. Second-order rate constants (k_2/K_D) were estimated as $k_{obs}/[MAb]$.

Copyright © 2006 John Wiley & Sons, Ltd.

PAGE 41/92 * RCVD AT 4/28/2010 6:45:45 PM [Eastern Daylight Time] * SVR:USPTO-EFXRF-6/33 * DNIS:2738300 * CSID:7132705361 * DURATION (mm-ss):48-00

HIV neutralization

Infection of peripheral blood mononuclear cells by primary isolates of HIV was measured (Karle *et al.*, 2004) by treating the virus (100 $TCID_{50}$) with an equal volume of increasing concentrations of protein G-purified MAbs for 1 h. Phytohemagglutinin-stimulated cells from healthy human donors were added and cultures incubated for 3 days, the cells were washed, incubated in fresh RPMI for 24 h, lysed with Triton X-100, and p24 in the supernatants was measured.

RESULTS

Immune complex stability

MAb-producing hybridomas were prepared from the splenocytes of two mice immunized with E-gp120 containing phosphonate diester groups at Lys side chains (Paul *et al.*, 2003). Eight MAbs displayed binding to the electrophilic analog of gp120 (E-gp120) that was not dissociable by SDS (2% w/v), a detergent that disrupts noncovalent Ab-antigen complexes. The SDS-resistant E-gp120 binding is consistent with a covalent Ab reaction at the strongly electrophilic phosphonates in E-gp120.

Interestingly, the MAbs also displayed unusually stable binding to gp120 devoid of artificial electrophiles. This was suggested by two independent lines of study conducted in denaturing and nondenaturing solvents as follows. First, all anti-E-gp120 MAbs (8/8) formed complexes with gp120 devoid of artificial electrophiles (the phosphonate groups) that were resistant to dissociation with the denaturant (2% SDS; A490 62–92 % of the values observed without detergent treatment; Fig. 1A). Formation of SDS-resistant complexes by four control anti-gp120 MAbs obtained from mice and humans by conventional procedures was not evident [MAbs 1121, 257-D IV and 268-D IV directed to V3 domain (Gorny *et al.*, 1991; Gorny *et al.*, 1993); MAb b12 directed to the CD4 binding site (Burton *et al.*, 1994)]. The reaction mixture of Bt-gp120 and one of the anti-E-gp120 MAbs (clone SK-T03) was analyzed by denaturing electrophoresis. Large mass biotin-containing, anti-mouse IgG stainable immune complexes were evident that were absent in the reaction mixtures of an isotype-matched MAb (clone MOPC21) (Fig. 1B). Disulfide exchange reaction occurring at low levels in the protein mixture may result in the S-S bonded immune complexes. However, the biotin-containing and anti-mouse IgG (Fc) stainable large mass complexes were also observed in electrophoresis gels run under reducing conditions (2-mercaptoethanol, 3.3%; nominal mass 155 kD; gp120 migrates as a 100–110 kD band and the predicted mass of heavy chain-gp120 complexes is 150–160 kD), indicating that disulfide bonding does not explain the stable immune complexation. Moreover, from the ELISA data, it is evident that the stable immune complexation is a consistent feature of the anti-E-gp120 MAbs but not the control anti-gp120 MAbs. It is

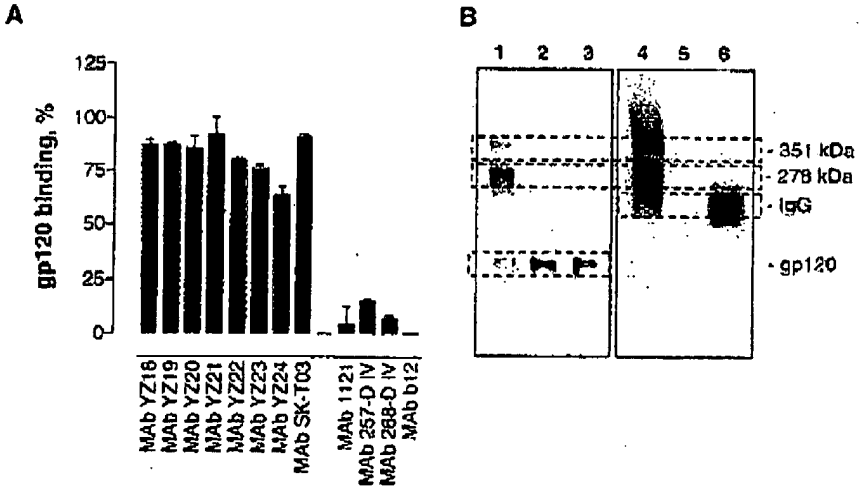

Figure 1. Formation of SDS-resistant immune complexes by anti-E-gp120 MAbs. (A) ELISA showing MAb complexes formed by incubation with gp120. MAbs (75 μg/mL) were mixed with immobilized gp120 in an ELISA plate (40 ng/well) and the wells were treated with PBS (total binding) or buffer containing 2% SDS (SDS-resistant binding). Values (means of 3 replicates) represent residual SDS-resistant binding expressed as percentage of total binding (A490 for total binding by MAbs YZ16, YZ19, YZ20, YZ21, YZ22, YZ23, YZ24, SK-T03; respectively, 1.86 ± 0.05, 0.86 ± 0.01, 0.17 ± 0.01, 0.32 ± 0.03, 0.84 ± 0.01, 1.86 ± 0.04, 0.29 ± 0.01, 2.08 ± 0.04). (B) Streptavidin–peroxidase-stained (lanes 1–3) and anti-mouse IgG–peroxidase-stained (lanes 4–6) blots of nonreducing SDS-electrophoresis gels showing SDS-resistant adducts formed by treatment of gp120 with MAb SK-T03. Lanes 1 and 4, MAb SK-T03 incubated with Bt-gp120; lane 2, Isotype-matched control MAb MOPC21 incubated with Bt-gp120; lanes 3 and 5, Control Bt-gp120 alone incubated in the diluent; lane 6, MAb SK-T03 alone incubated in the diluent. Ab, 75 (lanes 1–3) or 15 μg/mL (lanes 4–6); Bt-gp120, 5 (lanes 1–3) or 27 μg/mL (lanes 4–6); Incubations for 17 h. Nominal molecular weights computed by comparison with standard proteins are indicated.

Copyright © 2006 John Wiley & Sons, Ltd.

DOI: 10.1002/jmr

PAGE 42/92 * RCVD AT 4/28/2010 6:45:45 PM [Eastern Daylight Time] * SVR:USPTO-EFXRF-6/33 * DNIS:2738300 * CSID:7132705361 * DURATION (mm-ss):48-00

difficult to explain the reaction, therefore, as an unusual property arising from the unique properties of an individual MAb.

Second, to obtain data relevant to the biological behavior of the MAbs, we studied the stability of the immune complexes in a nondenaturing solvent. Synthetic peptides were used in these studies as competitive ligands to preclude reassociation of released gp120 to the MAbs.[1] Dissociation kinetics were determined by mixing solutions of Bt-gp120 and MAb SK-T03 or control MAb 268-D IV, capture of the immune complexes on protein G-Sepharose beads followed by incubation of the beads for varying lengths of time in diluent containing the appropriate peptide competitor at excess concentration. Rapid and near-complete dissociation of gp120 from the control MAb (268-D IV) was evident (Fig. 2). The control MAb has previously been reported to display high affinity for gp120 (K_D 9.2×10^{-10} M; VanCott *et al.*, 1994). Dissociation of complexes formed by the anti-E-gp120 MAb SK-T03 was very slow and substantial amounts of the biotin-containing complexes were observed at the final time point examined (10 days). The apparent $t½$ values for the control MAb was 4.8 hours ($r^2 = 0.99$). Accurate measurement of the dissociation rate of the complexes formed by the anti-E-gp120 MAb was difficult from the data in Fig. 2 because of the slow reaction rate. The nominal $t½$ for this MAb was 18.5 days ($r^2 = 0.57$). The corresponding first-order dissociation rate constants for the control and anti-E-gp120 MAb complexes were, respectively, $(4.2 \pm 0.2) \times 10^{-5}$ sec^{-1} and $(4.3 \pm 0.9) \times 10^{-7}$ sec^{-1}. The observed dissociation rate constant of the complex of gp120 with the control MAb was comparable to the previously published value [$(11 \pm 0.1) \times 10^{-5}$ sec^{-1}: VanCott *et al.*, 1994]. These results indicate that the immune complexes formed by the anti-E-gp120 MAb are exceptionally stable, with the MAb remaining bound to antigen for a period of time ~100-fold greater than the control high-affinity MAb.

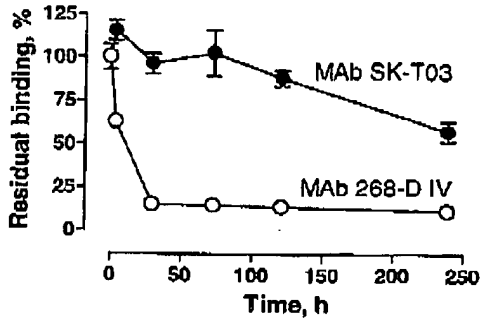

Figure 2. Stability of MAb SK-T03 immune complexes in nondenaturing solution. Immune complexes were formed by incubating MAb SK-T03 (20 μg/mL) or MAb 268-D IV (1 μg/mL) with Bt-gp120 (0.2 μg/mL) for 12 h. The complexes were captured on protein G-Sepharose, free gp120 removed by washing and the resin was incubated further in the presence of gp120 peptide 465–479 (MAb SK-T03; 10 μg/mL) or peptide 309–323 (MAb 268-D IV; 10 μg/mL). Aliquots of the gel slurry were withdrawn at 0, 4, 30, 73, 121 and 239 h, the gel was washed (5×) and the residual gel-bound immune complexes were detected using a streptavidin-peroxidase conjugate. Values are expressed as per cent of binding at t = 0 (100% values for MAb SKT-T03 and MAb 268-D IV, respectively; 1.05 ± 0.08 and 1.78 ± 0.07), after correction for nonspecific binding determined using an irrelevant MAb instead of the anti-gp120 MAbs (MOPC 21; 20 μg/mL). The nonspecific binding was nearly constant at all of the time point studied (A490, 0.23 ± 0.01).

Kinetics of immune complex stabilization

Formation of stable immune complexes by the anti-E-gp120 MAbs may be explained by a two-state model in which the initial MAb-gp120 noncovalent complex is converted to another state that is stabilized by nucleophile-electrophile interactions (designated States 1 and 2 in Fig. 3A). As the first test of this model, we measured the rate of formation of the hypothetical State 2 complexes as a function of time. To distinguish between the two states, the peptide competitor was added at excess concentration at various time points following initiation of the reaction between immobilized gp120 and the MAbs. The poorly-dissociable State 2 complexes are predicted to survive treatment with the competitor peptide, whereas the reversibly-bound State 1 complexes are not (as the latter will be replaced by MAb-competitor peptide complexes). Progressive accumulation of immune complexes that remained associated despite the presence of excess peptide competitor was observed using the anti-E-gp120 MAbs SK-T03 and YZ23 but not the control MAb (Fig. 3B). At prolonged incubation times, virtually complete transformation of the anti-E-gp120 complexes from the dissociable form (State 1) to nondissociable form (State 2) was evident, whereas the control MAb complexes remained virtually completely in the dissociable state. These observations are in agreement with the proposed two-state model, i.e., the initial formation of the dissociable immune complexes, followed by their transition to the poorly dissociable state. With the assumption of pseudo-first-order conditions, the overall efficiencies for formation of the State 2 complexes for MAbs SK-T03 and YZ23, corresponding to the second-order rate constant k_3/K_D, were, respectively, 2.1×10^7 M^{-1} min^{-1} and 2.1×10^6 M^{-1} min^{-1}.

IgGs contain two antigen binding sites, and an avidity effect may restrict the dissociation of MAbs complexed to immobilized antigens. Therefore, we repeated the binding studies using monovalent Fab fragments. After treatment of immobilized gp120 for 4 h with the Fab fragments of MAb SK-T03, the reaction had progressed virtually completely to

[1]The competitors were identified by screening 122 peptides encompassing gp120 residues 25–523 (15-mer peptides with 11-mer overlapping regions; MN strain). Peptide 465–479 and peptide 297–311, respectively, inhibited the formation of complexes of gp120 and MAb SK-T03 and MAb YZ23 (IC_{50} values for MAbs SK-T03 and YZ23, respectively, 2.2 nM and 1.1 μM). In the case of MAb YZ23, the overlapping peptide 301–315 also inhibited the complexation with gp120 (IC_{50} 1.2 μM), suggesting residues 301–311, as the minimal epitope sequence. Peptide 309–323 has been previously identified as a competitor inhibitor of gp120 binding by the control MAb (268-D IV) (Gorny *et al.*, 1991; Gorny *et al.*, 1993). In the case of MAb YZ23, binding to gp120 was inhibited partially by another synthetic peptide composed of gp120 residues 421–435, and this region may constitute a portion of the MAb epitope. As peptide 297–311 displaced the binding of gp120 by the MAb completely, its use as a competitor in the immune complex stability measurement is valid even if the peptide does not represent the entire binding epitope.

Copyright © 2006 John Wiley & Sons, Ltd.

DOI: 10.1002/jmr

PAGE 43/92 * RCVD AT 4/28/2010 6:45:45 PM [Eastern Daylight Time] * SVR:USPTO-EFXRF-6/33 * DNIS:2738300 * CSID:7132705361 * DURATION (mm-ss):48-00

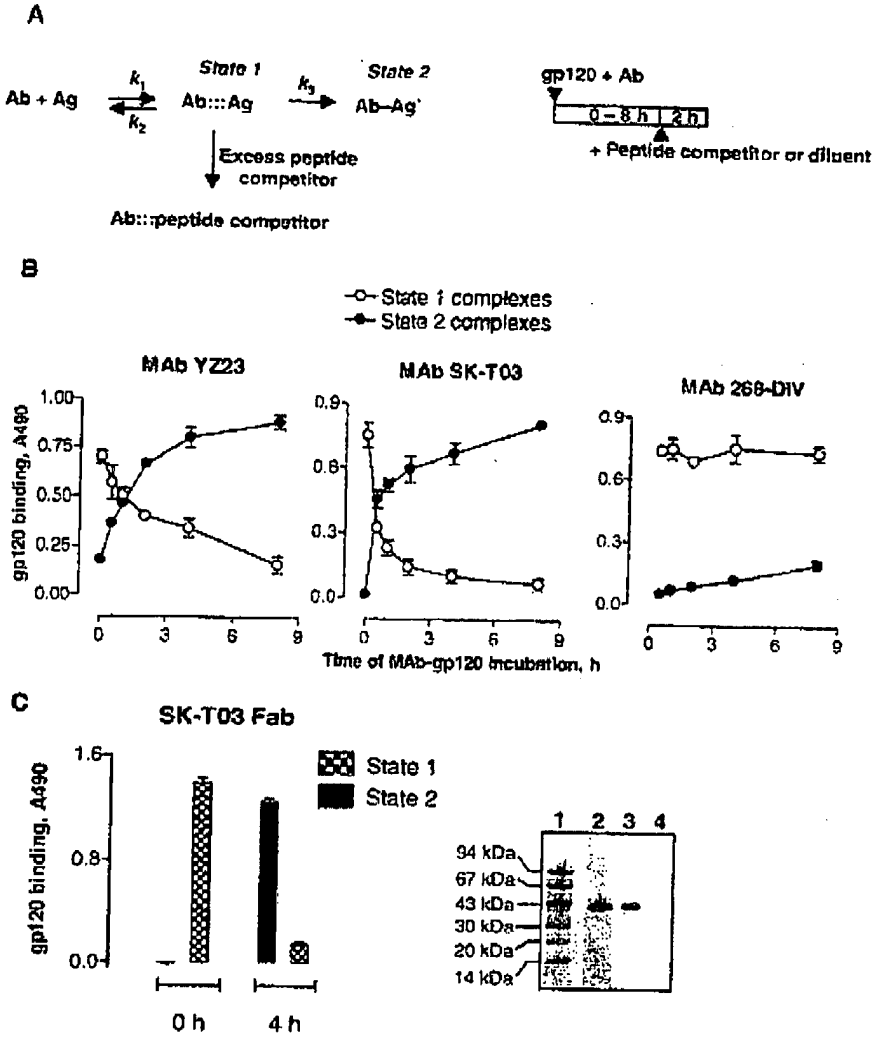

Figure 3. Rate of stable immune complex formation. (A) Hypothetical two state model of the Ab-Ag reaction. gp120 (Ag) binding by anti-E-gp120 MAb (Ab) is suggested to proceed as a two-step reaction: the formation of noncovalent complexes (Ab:::Ag, State 1) followed by transition to a poorly-dissociable state (Ab–Ag', State 2). Ab–Ag' can be the acyl-MAb complex generated by nucleophilic attack on electrophilic carbonyls or the chemically unmodified, resonance-stabilized form of the complex (see Discussion). Production of State 2 complexes was determined using the experimental protocol shown in the right panel by treatment of immobilized gp120 with MAb for varying lengths of time (0–8 h); incubation with excess competitor peptide or diluent for another 2 h; and determination of bound MAb. In solutions containing excess competitor peptide, the State 1 complexes are replaced by MAb-peptide complexes but the State 2 complexes remain intact. Thus the ELISA signals detected with and without competitor treatment represent, respectively, the State 2 complex concentration and the sum of the State 1 + State 2 concentrations. Formation of the initial noncovalent complex is determined by the association and dissociation rate constants ($k_2/k_1 = K_D$). Transformation of the initial complex to the poorly dissociable complex is determined by the first-order rate constant k_3. (B) Progress curves showing accumulation of State 2 complexes formed by incubation of gp120 with MAb YZ23 and MAb SK-T03. After incubating the MAbs with immobilized gp120 in ELISA plates for varying lengths of time (x-axis), diluent or the appropriate competitor peptide at excess concentration (●) was added and the immune complexes (corresponding to State 2 complexes) were measured after further incubation for 2 h. The amounts of State 1 complexes (○) were computed as (total binding in diluent—binding corresponding to State 2 complexes). Competitor gp120 peptides were: MAb YZ23, peptide 297–311 (50 μg/mL); MAb SK-T03, peptide 465–479 (10 μg/mL); MAb 268-DIV, peptide 309–323 (20 μg/mL). MAb concentrations were: MAb YZ23, 5 μg/mL; MAb SK-T03, 0.2 μg/mL. (C) ELISA (left) showing State 2 complexes formed by incubation of gp120 with the Fab fragment of MAb SK-T03 (0.2 μg/mL). Competitor peptide 465–479 (10 μg/mL). Right: lane 1, Coomassie Blue-stained SDS-gel of the Fab; lane 2, anti-Fab stained blot of the gel; lane 3, anti-Fc stained blot of the gel.

Copyright © 2006 John Wiley & Sons, Ltd.

DOI: 10.1002/jmr

PAGE 44/92 * RCVD AT 4/28/2010 6:45:45 PM [Eastern Daylight Time] * SVR:USPTO-EFXRF-6/33 * DNIS:2738300 * CSID:7132705361 * DURATION (mm-ss):48-00

complexes that remained undissociated in the presence of excess competitor peptide (Fig. 3C). It is difficult to explain formation of the stable immune complexes based on avidity effects.

MAb nucleophilicity

Studies with polyclonal IgG have previously suggested the induction of increased nucleophilic reactivity in Abs raised by immunization with E-gp120, judged from the rate of formation of covalent complexes with the hapten phosphonate **1** (Paul *et al.*, 2003; Fig. 4A). Here, similar studies indicated ~8-fold superior nucleophilic reactivity of MAb SK-T03 compared to its isotype-matched control IgG (Fig. 4B). The heavy chain subunit of the MAb formed adducts with hapten **1** more rapidly than the light chain subunit (4-fold, computed from initial reaction rates). Covalent hapten **1**-binding by MAb SK-T03 was inhibited by its epitope peptide (gp120 residues 465–479) devoid of the electrophilic phosphonate, but not by an irrelevant peptide (Fig. 4C). This suggests that the nucleophile is located within or close to the noncovalent antigen-binding site of the MAb. The anti-E-gp120 MAbs did not react detectably with an irrelevant polypeptide (albumin) or the electrophilic phosphonate analog of an irrelevant peptide (VIP; see Nishiyama *et al.*, 2004 for description of this compound) under conditions permitting formation of stable complexes with gp120 and E-gp120 shown in Fig. 1. The absence of indiscriminate reactivity may be explained from the contribution of noncovalent binding in accelerating the initial noncovalent interaction of the MAbs with gp120 (see reaction model in Fig. 3A). In previous studies, noncovalent paratope-epitope interactions were observed to accelerate

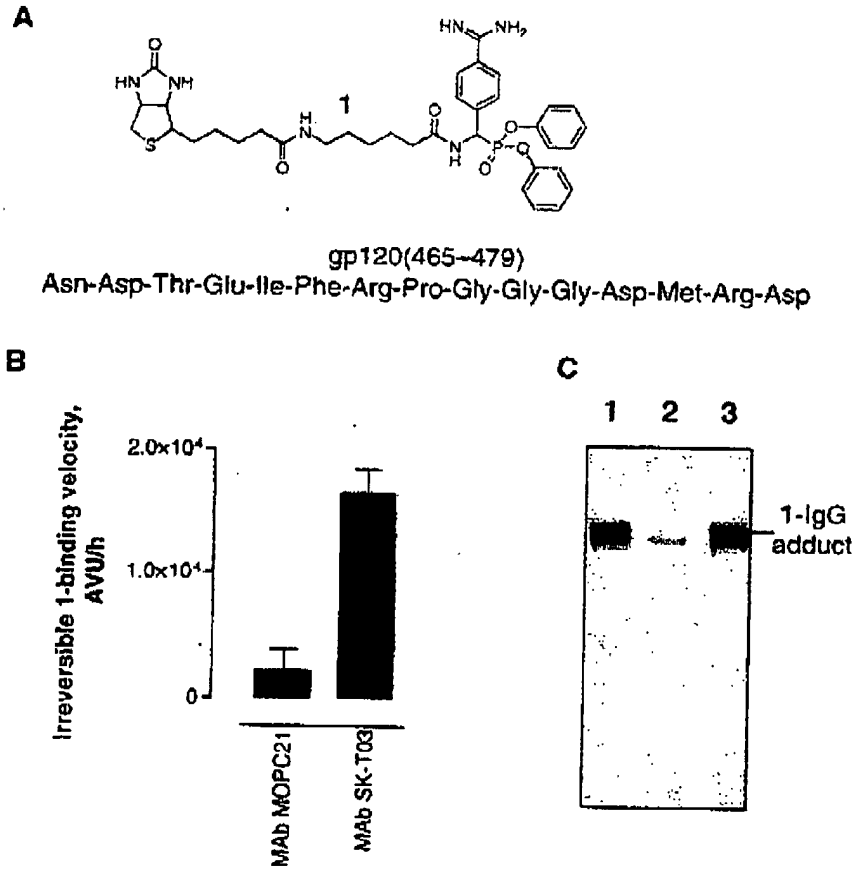

Figure 4. Nucleophilic reactivity of MAb SK-T03. (A) Electrophilic hapten phosphonate probe **1** and competitor gp120 peptide 465–479. (B) MAb-1 reactivity. MAb SK-T03 (4.5 μg/mL) incubated with **1** (100 μM) for 1 h was subjected to reducing SDS-electrophoresis and covalent 1-MAb adducts were quantified by densitometry of streptavidin-peroxidase stained blots (arbitrary volume units, AVU). (C) Streptavidin–peroxidase-stained blot of nonreducing SDS electrophoresis gel showing inhibition of covalent 1-MAb SK-T03 binding by gp120 peptide 465–479. Lane 1, MAb incubated with **1** (1 h); lane 2, MAb pretreated with gp120 peptide 465–479 (0 μM, 17 h), then incubated with **1**; lane 3, MAb preincubated with control gp120 peptide 297–311 as in lane 2, then incubated with **1**. MAb SK-T03, 45 μg/mL.

Copyright © 2006 John Wiley & Sons, Ltd.

DOI: 10.1002/jmr

PAGE 45/92 * RCVD AT 4/28/2010 6:45:45 PM [Eastern Daylight Time] * SVR:USPTO-EFXRF-6/33 * DNIS:2738300 * CSID:7132705361 * DURATION (mm-ss):48-00

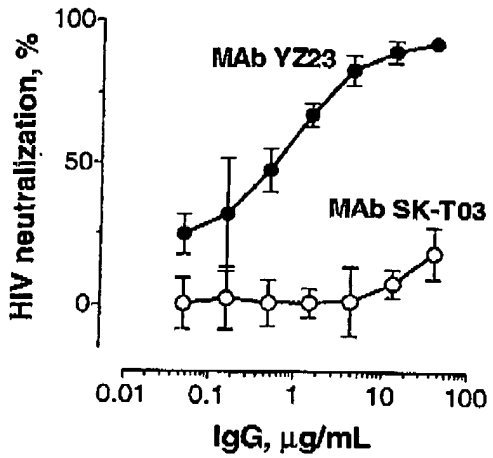

Figure 5. HIV neutralization by MAb YZ23. Values are means of four replicates. HIV strain, ZA009. Phytohemagglutinin-stimulated peripheral blood mononuclear cells were added to MAb–virus mixtures and incubated for 3 days. After washing, the cells were incubated for 24 h, lysed and p24 was measured. Neutralization was computed as % decrease of p24 concentrations in MAb-containing wells compared to vehicle control. MAb CRL1689, which has the same isotype as MAb YZ23, was without neutralizing activity.

the formation of covalent polyclonal and monoclonal Ab adducts with the electrophilic analogs of the cognate antigens by several orders of magnitude (Planque *et al.*, 2003; Nishiyama *et al.*, 2004).

HIV neutralization

Three of the eight anti-E-gp120 MAbs neutralized the infection of peripheral blood mononuclear cells by a primary HIV-1 isolate belonging to clade C (strain ZA009), i.e., MAbs YZ18, YZ22 and YZ23. The concentration-dependence of HIV neutralization by MAb YZ23 is shown in Fig. 5. An irrelevant, control MAb of the same isotype as MAb YZ23 (clone CRL1689) did not neutralize the virus. Host cells cultured in the presence of the anti-E-gp120 MAbs without the virus showed no decrease in viability, indicating the absence of a nonspecific cytotoxic effect (determined by staining with acridine orange/ethidium bromide; viability ~80–85%). MAb YZ23 neutralized two CCR5-dependent clade C and another CCR5-dependent clade B strain with $IC_{90} \sim 10\ \mu g/mL$ (Table 1). Neutralization of the two clade C strains by MAb b12, directed to the CD4 binding site of gp120, did not reach reliable levels (IC90 > highest MAb concentration tested). MAb YZ23 at the highest concentration tested (200 μg/mL) did not neutralize the clade D UG046 strain. Nine of the 11 residues at gp120 positions 301–311, the minimum MAb-reactive epitope, are identical in the neutralization-sensitive HIV strains (Table 1). The neutralization-refractory clade D strain expresses 4/11 identities in this region of gp120.

DISCUSSION

Studies in denaturating and nondenaturating solvents independently indicated the formation of stable gp120 complexes by Abs to the electrophilic analog of gp120. Reaction mixtures of gp120 mixed with each of the 8 MAbs contained complexes refractory to dissociation with SDS, a detergent that disrupts most noncovalent protein–protein interactions. When mixed with gp120, the MAbs initially formed readily dissociable complexes similar to conventional reversibly bound complexes. The initial complexes were nearly completely converted to their poorly dissociable state as a function of time. Complexes formed by treating gp120 with MAb SK-T03 dissociated more slowly than the biotin-streptavidin complex ($t_{1/2}$ 18.5 days versus 1.4–3.3 days, respectively; (Piran and Riordan, 1990; Chilkoti and Stayton, 1995) and at a rate comparable to the clearance rate of free IgG from the vascular compartment *in vivo* ($t_{1/2}$ of 1–3 weeks).

We intended the immunization with E-gp120 to induce MAbs that recapitulate the mechanism of serine proteases (see top reaction scheme in Fig. 6; Paul *et al.*, 2003). These enzymes are thought to form a covalent acyl-enzyme intermediate in course of peptide bond hydrolysis, accompanied by liberation of the peptide fragment C-terminal to the site of nucleophilic attack, as suggested by study of pre-steady state kinetics (Hedstrom, 2002). A single turnover MAb capable of forming a covalent acyl intermediate with a small molecule lactam antigen has been described previously (Lefevre *et al.*, 2001). Three of the eight anti-E-gp120 MAbs examined here were observed

Table 1. MAb YZ23 neutralization of clade B and C strains. Inhibitory concentrations yielding 50% and 90% neutralization obtained from MAb dose response studies (4 replicates at each concentration), with curve fitting as in Karle *et al.*, 2004. Also shown are amino acid sequences of gp120 residues 301–311. Bold font indicates amino acid identities.

	MAb YZ23		MAb b12		
HIV (clade)	IC_{50} (μg/mL)	IC_{90} (μg/mL)	IC_{50} (μg/mL)	IC_{90} (μg/mL)	Residues 301–311
SF162 (B)	0.15	4.8	1.1	14.1	CTRPNNNTRKS
BR004 (C)	1.4	5.3	9	>20	CTRPNNNTRES
ZA009 (C)	0.7	15	0.7	>20	CTGPNNNTRES
UG046 (D)	>200		NT		CSRPYENKRRR

Copyright © 2006 John Wiley & Sons, Ltd.

DOI: 10.1002/jmr

PAGE 46/92 * RCVD AT 4/28/2010 6:45:45 PM [Eastern Daylight Time] * SVR:USPTO-EFXRF-6/33 * DNIS:2738300 * CSID:7132705361 * DURATION (mm-ss):48-00

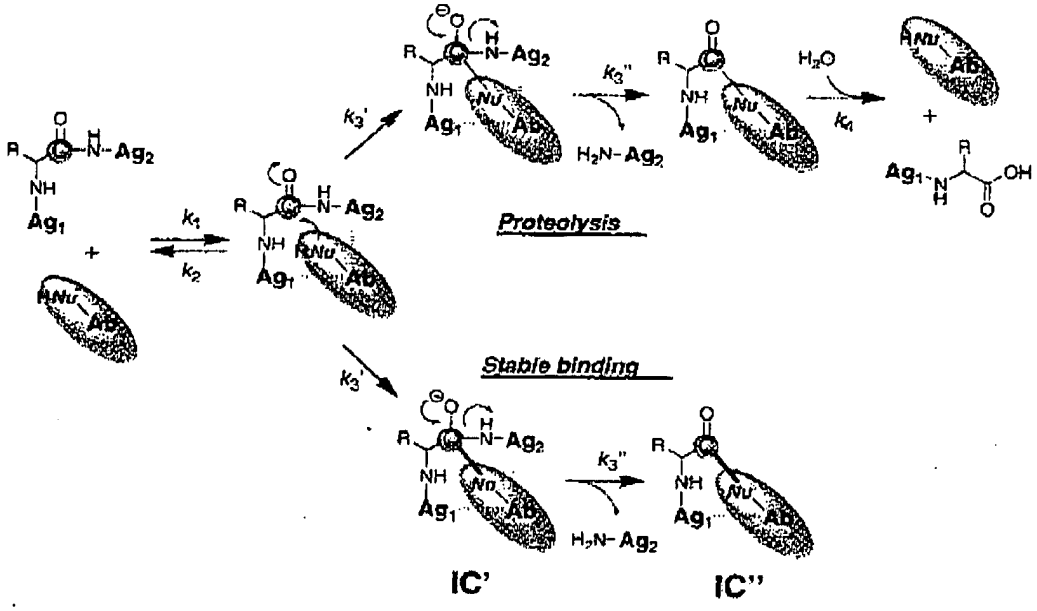

Figure 6. Proposed reaction mechanism of nucleophilic Abs: Antigen hydrolysis (top) and irreversible binding (bottom). The Ab forms the initial noncovalent complex by conventional epitope–paratope interactions. In proteolysis, the active site nucleophile attacks the carbonyl of the scissile bond in the antigen to form the tetrahedral transition-state complex. The C-terminal antigen fragment is released and the acyl-Ab complex is formed. Hydrolysis of the acyl-Ab complex (deacylation) releases the N-terminal antigen fragment and regenerates the catalytic Ab. In irreversible binding, accumulation of the tetrahedral complex (IC') or the trigonal acyl-Ab complex (IC'', after release of the C-terminal antigen fragment) may occur because of increased stability of the bond formed by the attacking nucleophile or deficient support for a step(s) after completion of the nucleophile attack. *Nu*H, nucleophile; Ag_1-NH-CH(R)-CO_2H, N-terminal antigen fragment; NH_2-Ag_2, C-terminal antigen fragment.

to cleave gp120 slowly (Paul *et al.*, 2003), but the remaining five MAbs were devoid of this activity, and there was no evidence for release of a gp120 fragment despite a 5-fold MAb excess. This suggests that the polypeptide backbone is not susceptible to the cleavage, and the observed stable immune complexes correspond to the IC′ structure in Fig. 6. Alternatively, the nucleophilic attack may occur at the amide carbonyl of Gln or Asn side chains, accompanied by liberation of ammonia. In this case, the observed stable complexes may correspond to either IC′ or IC″. Accumulation of complexes with IC′ structure is feasible because resonant electrophile–nucleophile pairing may impart covalent character to the ground state of protein-protein complexes (Nishiyama *et al.*, 2005). Regardless of the mechanism, from the results reported here, it is evident that MAbs generated by E-gp120 immunization can routinely form the unusually stable immune complexes.

Several reversibly binding MAbs to polypeptide antigens have been developed for clinical use, e.g., MAbs to vascular endothelial growth factor and epidermal growth factor receptor employed in the treatment of cancer. Developing immunotherapeutic MAbs to HIV, however, has proved difficult. gp120 expresses many antigenic epitopes that stimulate Ab responses following HIV infection (Burton and Montefiori, 1997; Kent and Robinson, 1996). The mutability of gp120 along with conformational transitions in the protein is thought to be important in the failure of humoral immune responses to control HIV infection (Burton and Moore, 1998). Certain rare MAbs neutralize primary HIV isolates belonging to clade B but are poorly effective against clade C strains (Binley *et al.*, 2004) often found in geographical regions where HIV infection is growing rapidly. Formation of stable gp120 complexes in the present study did not predict HIV neutralization by the MAbs. Five MAbs did not neutralize the virus, including MAb SK-T03. This MAb appears to recognize the region of gp120 composed of residues 465–479, which may be insufficiently exposed on the viral surface or may not be essential for establishing infection. Another MAb, clone YZ23, neutralized both clade C strains tested in Table 1. The minimum candidate epitope of this MAb, residues 301–311, encompasses certain contact sites involved in gp120 binding by the chemokine coreceptor (CCR5: Cormier and Dragic, 2002). Residues 301–311 tend to be conserved in clade C HIV strains [% identity 85 ± 7; $n = 111$ strains; for each strain, the number of identities with CTXPNNNTRES, representing the shared sequence of the clade C strains in Table 1, was counted and the per cent identity was calculated as $100 \times$ (number of identities)/10; data from the Los Alamos HIV database]. The immunogen employed to generate the MAbs, E-gp120, differs from conventional gp120 preparations in that it contains self-assembled oligomers (Paul *et al.*, 2003). The oligomers may expose epitopes not customarily encountered in monomer gp120 preparations. Consequently, further study of the anti-E-gp120 MAbs may help identify additional neutralizing epitopes appropriate for development as candidate electrophilic vaccines.

Copyright © 2006 John Wiley & Sons, Ltd.

PAGE 47/92 * RCVD AT 4/28/2010 6:45:45 PM [Eastern Daylight Time] * SVR:USPTO-EFXRF-6/33 * DNIS:2738300 * CSID:7132705361 * DURATION (mm-ss):48-00

To the extent that the poorly dissociable MAbs are directed to a neutralizing epitope, they may be predicted to provide long-lasting antigen inactivation compared to conventional reversibly bound MAbs. The upper limit for the stability of the immune complexes formed by nucleophilic Abs remains to be determined. In recent studies, we raised MAbs to the electrophilic analog of a second polypeptide antigen using methods similar to those in the present report. These MAbs displayed SDS-resistant binding to the polypeptide antigen devoid of artificial electrophiles.[2] Electrophilic immunization may prove useful as a general strategy, therefore, for raising neutralizing MAbs.

Acknowledgment

The authors thank Bob Dannenbring for technical assistance.

REFERENCES

Binley JM, Wrin T, Korber B, Zwick MB, Wang M, Chappey C, Stiegler G, Kunert R, Zolla-Pazner S, Katinger H, Petropoulos CJ, Burton DR. 2004. Comprehensive cross-clade neutralization analysis of a panel of anti-human immunodeficiency virus type 1 monoclonal antibodies. *J. Virol.* **78**: 13232–13252.

Burton DR, Pyati J, Koduri R, Sharp SJ, Thornton GB, Parren PW, Sawyer LS, Hendry RM, Dunlop N, Nara PL, Lamacchia M, Garratty E, Stiehm ER, Bryson YJ, Cao Y, Moore JP, Ho DD, Barbas CFIII. 1994. Efficient neutralization of primary isolates of HIV-1 by a recombinant human monoclonal antibody. *Science* **266**: 1024–1027.

Burton DR, Montefiori DC. 1997. The antibody response in HIV-1 infection. *AIDS* **11** (Suppl. A): S87–98.

Burton DR, Moore JP. 1998. Why do we not have an HIV vaccine and how can we make one? *Nat. Med.* **4**: 495–498.

Chilkoti A, Stayton PS. 1995. Molecular origins of the slow streptavidin-biotin dissociation kinetics. *J. Am. Chem. Soc.* **117**: 10622–10628.

Cormier EG, Dragic T. 2002. The crown and stem of the V3 loop play distinct roles in human immunodeficiency virus type 1 envelope glycoprotein interactions with the CCR5 coreceptor. *J. Virol.* **76**: 8953–8957.

Gao QS, Sun M, Tyutyulkova S, Webster D, Rees A, Tramontano A, Massey RJ, Paul S. 1994. Molecular cloning of a proteolytic antibody light chain. *J. Biol. Chem.* **269**: 32389–32393.

Gorny MK, Xu JY, Gianakakos V, Karwowska S, Williams C, Sheppard HW, Hanson CV, Zolla-Pazner S. 1991. Production of site-selected neutralizing human monoclonal antibodies against the third variable domain of the human immunodeficiency virus type 1 envelope glycoprotein. *Proc. Natl. Acad. Sci. U.S.A.* **88**: 3238–3242.

Gorny MK, Xu JY, Karwowska S, Buchbinder A, Zolla-Pazner S. 1993. Repertoire of neutralizing human monoclonal antibodies specific for the V3 domain of HIV-1 gp120. *J. Immunol.* **150**: 635–643.

Hedstrom L. 2002. Serine protease mechanism and specificity. *Chem. Rev.* **102**: 4501–4524.

Karle S, Planque S, Nishiyama Y, Taguchi H, Zhou YX, Salas M, Lake D, Thiagarajan P, Arnett F, Hanson CV, Paul S. 2004. Cross-clade HIV-1 neutralization by an antibody fragment from a lupus phage display library. *AIDS* **18**: 329–331.

Kent KA, Robinson J. 1996. Antigenic determinants on HIV-1 envelope glycoproteins: a dickens of a time with oligomer twist. *AIDS* **10** (Suppl. A): S107–114.

Lacroix-Desmazes S, Moreau A, Sooryanarayana, Bonnemain C, Stieltjes N, Pashov A, Sultan Y, Hoebeke J, Kazatchkine MD, Kaveri SV. 1999. Catalytic activity of antibodies against factor VIII in patients with hemophilia A. *Nat. Med.* **5**: 1044–1047.

Lefevre S, Debat H, Thomas D, Friboulet A, Avalle B. 2001. A suicide-substrate mechanism for hydrolysis of beta-lactams by an anti-idiotypic catalytic antibody. *FEBS Lett.* **489**: 25–28.

Nishiyama Y, Bhatia G, Bangale Y, Planque S, Mitsuda Y, Taguchi H, Karle S, Paul S. 2004. Toward selective covalent inactivation of pathogenic antibodies: a phosphate diester analog of vasoactive intestinal peptide that inactivates catalytic autoantibodies. *J. Biol. Chem.* **279**: 7877–7883.

Nishiyama Y, Mitsuda Y, Taguchi H, Planque S, Hara M, Karle S, Hanson CV, Uda T, Paul S. 2005. Broadly distributed nucleophilic reactivity of proteins coordinated with specific ligand binding activity. *J. Mol. Recognit.* **18**: 295–306.

Oleksyszyn J, Powers JC. 1994. Amino acid and peptide phosphonate derivatives as specific inhibitors of serine peptideses. *Methods Enzymol.* **244**: 423–441.

Paul S, Johnson DR, Massey R. 1991. Binding and multiple hydrolytic sites in epitopes recognized by catalytic anti-peptide antibodies. *Ciba. Found. Symp.* **159**: 156–167.

Paul S, Volle DJ, Beach CM, Johnson DR, Powell MJ, Massey RJ. 1989. Catalytic hydrolysis of vasoactive intestinal peptide by human autoantibody. *Science* **244**: 1158–1162.

Paul S, Planque S, Zhou YX, Taguchi H, Bhatia G, Karle S, Hanson C, Nishiyama Y. 2003. Specific HIV gp120-cleaving antibodies induced by covalently reactive analog of gp120. *J. Biol. Chem.* **278**: 20429–20435.

Piran U, Riordan WJ. 1990. Dissociation rate constant of the biotin-streptavidin complex. *J. Immunol. Methods* **133**: 141–143.

Planque S, Taguchi H, Burr G, Bhatia G, Karle S, Zhou YX, Nishiyama Y, Paul S. 2003. Broadly Distributed Chemical Reactivity of Natural Antibodies Expressed in Coordination with Specific Antigen Binding Activity. *J. Biol. Chem.* **278**: 20436–20443.

Planque S, Bangale Y, Song XT, Karle S, Taguchi H, Poindexter B, Bick R, Edmundson A, Nishiyama Y, Paul S. 2004. Ontogeny of proteolytic immunity: IgM serine proteases. *J. Biol. Chem.* **279**: 14024–14032.

Shuster AM, Gololobov GV, Kvashuk OA, Bogomolova AE, Smirnov IV, Gabibov AG. 1992. DNA hydrolyzing autoantibodies. *Science* **256**: 665–667.

VanCott TC, Bethke FR, Polonis VR, Gorny MK, Zolla-Pazner S, Redfield RR, Birx DL. 1994. Dissociation rate of antibody-gp120 binding interactions is predictive of V3-mediated neutralization of HIV-1. *J. Immunol.* **153**: 449–459.

Zhou GW, Guo J, Huang W, Fletterick RJ, Scanlan TS. 1994. Crystal structure of a catalytic antibody with a serine protease active site. *Science* **265**: 1059–1064.

[2]Immunization of mice with an electrophilic analog of amyloid β peptide (Aβ1–40) derivitized at the side chains of Lys16, Lys28 and the *N*-terminus (E-Aβ) yielded 19 Ab-secreting hybridomas with E-Aβ binding activity. Twelve of these Abs displayed binding to Aβ1–40 that was nondissociable by treatment with 2% SDS, suggesting the formation of stable immune complexes.

Copyright © 2006 John Wiley & Sons, Ltd.

DOI: 10.1002/jmr

PAGE 48/92 * RCVD AT 4/28/2010 6:45:45 PM [Eastern Daylight Time] * SVR:USPTO-EFXRF-6/33 * DNIS:2738300 * CSID:7132705361 * DURATION (mm-ss):48-00

Supplemental Material can be found at:
http://www.jbc.org/content/suppl/2008/11/04/M806766200.DC1.html

THE JOURNAL OF BIOLOGICAL CHEMISTRY VOL. 283, NO. 52, pp. 36724–36733, December 26, 2008
© 2008 by The American Society for Biochemistry and Molecular Biology, Inc. Printed in the U.S.A.

Exceptional Amyloid β Peptide Hydrolyzing Activity of Nonphysiological Immunoglobulin Variable Domain Scaffolds*[S]

Received for publication, September 2, 2008, and in revised form, October 28, 2008 Published, JBC Papers in Press, October 30, 2008, DOI 10.1074/jbc.M806766200

Hiroaki Taguchi, Stephanie Planque, Gopal Sapparapu, Stephane Boivin, Mariko Hara, Yasuhiro Nishiyama, and Sudhir Paul[1]

From the Chemical Immunology Research Center, Department of Pathology and Laboratory Medicine, University of Texas Houston Medical School, Houston, Texas 77030

Nucleophilic sites in the paired variable domains of the light and heavy chains (V_L and V_H domains) of Ig can catalyze peptide bond hydrolysis. Amyloid β (Aβ)-binding Igs are under consideration for immunotherapy of Alzheimer disease. We searched for Aβ-hydrolyzing human IgV domains (IgVs) in a library containing a majority of single chain Fv clones mimicking physiological V_L-V_H-combining sites and minority IgV populations with nonphysiological structures generated by cloning errors. Random screening and covalent selection of phage-displayed IgVs with an electrophilic Aβ analog identified rare IgVs that hydrolyzed Aβ mainly at His^{14}–Gln^{15}. Inhibition of IgV catalysis and irreversible binding by an electrophilic hapten suggested a nucleophilic catalytic mechanism. Structural analysis indicated that the catalytic IgVs are nonphysiological structures, a two domain heterodimeric V_L (IgV_{L2}-*t*) and single domain V_L clones with aberrant polypeptide tags (IgV_L-*t'*). The IgVs hydrolyzed Aβ at rates superior to naturally occurring Igs by 3–4 orders of magnitude. Forced pairing of the single domain V_L with V_H or V_L domains resulted in reduced Aβ hydrolysis, suggesting catalysis by the unpaired V_L domain. Ångstrom level amino acid displacements evident in molecular models of the two domain and unpaired V_L domain clones explain alterations of catalytic activity. In view of their superior catalytic activity, the V_L domain IgVs may help attain clearance of medically important antigens more efficiently than natural Igs.

The antigen-combining sites of immunoglobulins found in higher organisms are composed of the variable domains of light and heavy chain subunits (V_L and V_H domains). The individual V_L and V_H domains can bind antigens independently of each other, but the paired V_L-V_H structure consistently expresses superior antigen binding affinity because of cooperative antigen-binding forces contributed by the two domains (1). High affinity Igs are generated by adaptive V domain sequence diversification over the course of B lymphocyte differentiation, a process in which antigen binding to mutated B cell receptors (surface Igs associated with signal-transducing proteins) drives the selective expansion of the cells. Adaptive Ig maturation entails the use of one each of ~50 inherited V_L and V_H genes, diversification at the junctions of the V_L-D_L gene segments and V_H-D_H-J_H gene segments, and somatic mutation over the entire length of the V domains.

Following initial noncovalent binding of antigen, some Igs proceed to catalyze its chemical transformation. Examples of Ig-catalyzed reactions include hydrolysis of polypeptide antigens (2, 3), hydrolysis of nucleic acids (4, 5), and various acyl transfer reactions of other antigen classes (6). Proteolytic Igs that utilize serine protease-like covalent hydrolytic pathways have been described (7, 8). Serine protease-like catalytic triads have been identified in the V domains of Igs by site-directed mutagenesis and crystallography (9, 10). The catalytic mechanism involves nucleophilic attack on the electrophilic carbonyl of peptide bonds. Electrophilic phosphonate diesters originally developed as covalent probes for the nucleophilic site of serine proteases bind catalytic Igs irreversibly and inhibit their catalytic activity (7, 11, 12). The strength of Ig-antigen noncovalent binding often exceeds that of enzyme-substrate binding. An important limitation holding back the application of catalytic Igs for clearance of undesirable antigens is that their catalytic rate constants (turnover number; k_{cat}) are small compared with enzymes. Evidently, Ig adaptive selection is geared toward noncovalent immune complexation (the ground state stabilization step), and the ability of Igs to recognize the high energy transition state complex that must be stabilized to accelerate chemical reactions is limited. This is supported by observations that IgMs, the first and least diversified Ig class produced during B cell differentiation, express superior catalytic rate constants than IgGs produced by the cells at later stages of their adaptive differentiation (12).

Accumulation of amyloid β peptide (Aβ)[2] aggregates in the brain is thought to be a central contributor to neurodegenera-

* This work was supported, in whole or in part, by National Institutes of Health Grant R01AG025304. The costs of publication of this article were defrayed in part by the payment of page charges. This article must therefore be hereby marked "*advertisement*" in accordance with 18 U.S.C. Section 1734 solely to indicate this fact.

The nucleotide sequence(s) reported in this paper has been submitted to the GenBank™/EBI Data Bank with accession number(s) FJ231714, FJ231715, FJ231716, FJ231717, FJ231718, FJ231719, FJ231720, FJ231721, FJ231722, and FJ231723.

[S] The on-line version of this article (available at http://www.jbc.org) contains supplemental Tables S1–S3 and Figs. S1–S5.

[1] To whom correspondence should be addressed: Dept. of Pathology, University of Texas Houston Medical School, 6431 Fannin, Houston, TX 77030. E-mail: Sudhir.Paul@uth.tmc.edu.

[2] The abbreviations used are: Aβ, amyloid β peptide; AD, Alzheimer disease; AMC, 7-amino-4-methylcoumarin; CHAPS, 3-[(3-cholamidopropyl)dimethylammonio]-1-propanesulfonic acid; ESI-MS, electron spray ionization-mass spectrometry; FPLC, fast protein liquid chromatography; IgV, Ig variable domain; IgV_L-*t'*, IgV with a single V_L domain and tag *t'*; IgV_{L2}-*t*, IgV with two V_L domains and tag *t*, L-*t*, full light chain with tag *t*; MALDI-TOF MS, matrix-assisted laser desorption ionization time-of-flight mass spectrometry; PBS, phosphate-buffered saline; RP-HPLC, reversed-phase high performance liquid chromatography; r.m.s. deviation, root mean square deviation; PDB, Protein Data Bank; Bt, 6-biotinamidohexanoyl group.

Downloaded from www.jbc.org by guest, on April 28, 2010

PAGE 49/92 * RCVD AT 4/28/2010 6:45:45 PM [Eastern Daylight Time] * SVR:USPTO-EFXRF-6/33 * DNIS:2738300 * CSID:7132705361 * DURATION (mm-ss):48-00

Supplemental Material can be found at:
http://www.jbc.org/content/suppl/2008/11/04/M806786200.DC1.html

tive changes underlying Alzheimer disease (AD). Administration of monoclonal IgGs that bind Aβ reversibly to transgenic mice overexpressing human Aβ clears brain Aβ deposits and improves cognitive function (13, 14). Suggested mechanisms explaining the favorable effect of peripherally administered IgG are as follows: (*a*) Aβ containing immune complexes formed by small amounts of IgGs that cross the blood-brain barrier are removed by Fc receptor-mediated uptake by resident macrophages in the brains, the microglia (14); (*b*) Aβ binding to the IgG constrains the peptide into a nonaggregable conformation (15); (*c*) IgG bound to FcRn receptors on the blood-brain barrier accelerates Aβ exit from the brain to periphery blood (16); and (*d*) binding of peripherally circulating Aβ by IgG disrupts equilibrium between the central and peripheral compartments, causing compensatory Aβ release from the brain (17). In principle, Igs that catalyze the hydrolysis of Aβ can be applied to clear Aβ. We reported naturally occurring IgMs and isolated Ig light chain subunits (IgLs) that hydrolyze Aβ impede Aβ aggregation and inhibit Aβ-induced neurotoxicity (18, 19). However, these Igs hydrolyze Aβ slowly, and development of more efficient catalysts will help advance the use of catalytic Igs for Aβ clearance.

We report here the search for efficient Aβ-hydrolyzing Ig fragments in a human IgV domain (IgV) library in which the majority of clones are single chain Fv constructs (scFv-*t*; a V_L domain attached via a linker peptide to a V_H domain). The scFv scaffold mimics the physiological structure of antigen-combining sites. A minority of clones in the library are nonphysiological V domain structures generated by repertoire cloning errors. Unexpectedly, the nonphysiological two domain and single domain IgV_L fragments expressed exceptional Aβ hydrolyzing efficiency. scFv-*t* derivatives obtained by repairing a high activity single domain IgV_L displayed reduced catalytic activity. The observations suggest that novel Ig structures freed of constraints imposed by the physiological organization of V domains can be the source of efficient catalysts to medically important antigens.

MATERIALS AND METHODS

Electrophilic Compounds—Syntheses and Ig binding characteristics of these compounds are reported: E-hapten 1 and 2 (20) and E-hapten 3 (12). Bt-E-Aβ40 was prepared by reacting biotinylated Aβ-(1–40) (Aβ40; 10 mg, 2.1 μmol) with diphenyl-*N*-{*O*-(3-sulfosuccinimidyl)suberoyl]-amino(4-amidinophenyl)methane phosphonate (10.6 mg, 12.5 μmol) in DMSO. The reaction mixture was purified by RP-HPLC (Waters) and lyophilized. Its identity and purity were confirmed by RP-HPLC (retention time 36.36 min, purity >99.9%, Vydac C4 column; 0.05% trifluoroacetic acid in water, 0.05% trifluoroacetic acid in MeCN 90:10–40:60 in 50 min, 1.0 ml/min; 220 nm absorbance) and electrospray ionization-mass spectrometry (ESI-MS; observed *m/z*, 1427.6, 1142.6 and 952.4; calculated $(M + H)^{4+}$, $(M + 2H)^{5+}$, and $(M + 3H)^{6+}$ for $C_{266}H_{380}N_{62}O_{71}P_2S_2$, 1427.2, 1141.9, and 951.8).

Igs—Methods for IgV preparation and characterization have been described (7, 21). Briefly, the library consists of 1.4×10^7 IgVs cloned in the phagemid vector pHEN2 prepared from the peripheral blood lymphocyte of patients with lupus. A His_6 sequence and a c-*myc* epitope are located at the IgV C terminus. Expression levels were 1–3 mg of IgV/liter of bacterial culture, determined by anti-c-*myc* immunoblotting. Soluble IgVs were purified from periplasmic extracts of HB2151 cells by metal affinity chromatography. Further purification was by anion exchange FPLC (MonoQ HR 5/5 column; 0–1 M NaCl in 50 mM Tris buffer, pH 7.4, containing 0.1 mM CHAPS). Purity was determined by SDS-gel electrophoresis and immunoblotting. IgV phages (10^{12} colony-forming units) were packaged using the hyperphage method (22) and incubated (2 h, 37 °C) with Bt-E-Aβ40 in 0.07 ml of 10 mM sodium phosphate, 137 mM NaCl, 2.7 mM KCl, pH 7.4 (PBS). Phages with bound Bt-E-Aβ40 were captured using anti-biotin antibody coupled to agarose gel (0.22 ml settled gel; Sigma) and washed with 100 ml of PBS containing 0.1% bovine serum albumin. Reversibly bound phages were eluted by incubation of the gel in 0.2 ml of 100 μM Aβ40 for 1 h with slow mixing, and the residual phages covalently complexed to Bt-E-Aβ were eluted with 0.4 ml of 0.1 M glycine, pH 2.7. scFv-*t* derivatives of single domain IgV_L-*t*' 5D3 were prepared by inserting the deleted V_H residues 8–115 (Kabat numbering). For this, full-length V_H cDNA was amplified by PCR using as template the IgV-pHEN2 DNA library and back/forward primers containing ApaLI/NotI restriction sites (respectively, GGTAGTGCACTTCAGGTGCAGCTGTTGCAGTCT/ATGTGCGGCCGCGGGGAAAAGGGTTGGGGGCATGC), and the cDNA digested with ApaLI/NotI was ligated into similarly digested plasmid IgV_L-*t*' 5D3 DNA with T4 DNA ligase (Invitrogen). Full-length light chain L-*t*' 5D3 was prepared by Mutagenex by a chimeragenesis method (23) using as starting materials the V_L domain of IgV_L-*t*' 5D3 and human κ chain constant domain (obtained from pLC-huCκ (24)) and cloned into pHEN2 vector as the NcoI/NotI-digested fragment. cDNAs for the homodimeric IgV_{L2}-*t* form of clone 5D3 were prepared by PCR by Mutagenex. Briefly, V_L cDNA was amplified by PCR from the IgV_L-*t*'5D3 template using back/forward primers containing ApaLI/NotI restriction sites (respectively, AAAGTGCACTTGAAATTGTGTTGACGCAGTCTC/AAAGCGGCCGCGCGTTTGATCTCCAGCTTGGT), and the cDNA digested with ApaLI/NotI was ligated into pHEN2 vector. The nucleotide sequence of all constructs determined by dideoxy nucleotide sequencing in the 5' to 3' and 3' to 5' directions was identical (Applied Biosystems, ABI PRISM® 3100 Genetic Analyzer). Following electroporation of IgV phagemid DNA into HB2151 cells, soluble IgVs were purified from periplasmic extracts as before. Total protein was determined by the microBCA kit (Pierce). For mass spectroscopy (25), the IgV band was excised from the SDS-electrophoresis gel stained with GelCode Blue (Pierce), subjected to dehydration in 50% acetonitrile and SpeedVac drying, reduced (dithiothreitol) and alkylated (Iodoacetamide), and digested with sequencing grade trypsin (Promega) and Lys-C (Wako) for 20 h at 37 °C. Following extraction of gel fragments with acetonitrile/formic acid, digested peptides obtained by ZipTip C18 (Millipore) fractionation using 5 μl of aqueous 50% acetonitrile containing 2% formic acid were analyzed by mass spectrometry using a matrix of α-cyano-4-hydroxycinnamic acid (ABI 4700 MALDI-TOF/TOF mass spectrometer). Predicted monoisotopic peptide

Downloaded from www.jbc.org by guest, on April 28, 2010

PAGE 50/92 * RCVD AT 4/28/2010 6:45:45 PM [Eastern Daylight Time] * SVR:USPTO-EFXRF-6/33 * DNIS:2738300 * CSID:7132705361 * DURATION (mm-ss):48-00

Supplemental Material can be found at:
http://www.jbc.org/content/suppl/2008/11/04/M808766200.DC1.html

tive changes underlying Alzheimer disease (AD). Administration of monoclonal IgGs that bind Aβ reversibly to transgenic mice overexpressing human Aβ clears brain Aβ deposits and improves cognitive function (13, 14). Suggested mechanisms explaining the favorable effect of peripherally administered IgG are as follows: (*a*) Aβ containing immune complexes formed by small amounts of IgGs that cross the blood-brain barrier are removed by Fc receptor-mediated uptake by resident macrophages in the brains, the microglia (14); (*b*) Aβ binding to the IgG constrains the peptide into a nonaggregable conformation (15); (*c*) IgG bound to FcRn receptors on the blood-brain barrier accelerates Aβ exit from the brain to periphery blood (16); and (*d*) binding of peripherally circulating Aβ by IgG disrupts equilibrium between the central and peripheral compartments, causing compensatory Aβ release from the brain (17). In principle, Igs that catalyze the hydrolysis of Aβ can be applied to clear Aβ. We reported naturally occurring IgMs and isolated Ig light chain subunits (IgLs) that hydrolyze Aβ impede Aβ aggregation and inhibit Aβ-induced neurotoxicity (18, 19). However, these Igs hydrolyze Aβ slowly, and development of more efficient catalysts will help advance the use of catalytic Igs for Aβ clearance.

We report here the search for efficient Aβ-hydrolyzing Ig fragments in a human IgV domain (IgV) library in which the majority of clones are single chain Fv constructs (scFv-*t*; a V_L domain attached via a linker peptide to a V_H domain). The scFv scaffold mimics the physiological structure of antigen-combining sites. A minority of clones in the library are nonphysiological V domain structures generated by repertoire cloning errors. Unexpectedly, the nonphysiological two domain and single domain IgV_L fragments expressed exceptional Aβ hydrolyzing efficiency. scFv-*t* derivatives obtained by repairing a high activity single domain IgV_L displayed reduced catalytic activity. The observations suggest that novel Ig structures freed of constraints imposed by the physiological organization of V domains can be the source of efficient catalysts to medically important antigens.

MATERIALS AND METHODS

Electrophilic Compounds—Syntheses and Ig binding characteristics of these compounds are reported: E-hapten **1** and **2** (20) and E-hapten **3** (12). Bt-E-Aβ40 was prepared by reacting biotinylated Aβ-(1–40) (Aβ40; 10 mg, 2.1 μmol) with diphenyl-*N*-[*O*-(3-sulfosuccinimidyl)suberoyl]-amino(4-amidinophenyl)methane phosphonate (10.6 mg, 12.5 μmol) in DMSO. The reaction mixture was purified by RP-HPLC (Waters) and lyophilized. Its identity and purity were confirmed by RP-HPLC (retention time 36.36 min, purity >99.9%, Vydac C4 column; 0.05% trifluoroacetic acid in water, 0.05% trifluoroacetic acid in MeCN 90:10–40:60 in 50 min, 1.0 ml/min; 220 nm absorbance) and electrospray ionization-mass spectrometry (ESI-MS; observed *m/z*, 1427.6, 1142.6 and 952.4; calculated $(M + H)^{4+}$, $(M + 2H)^{5+}$, and $(M + 3H)^{6+}$ for $C_{256}H_{380}N_{62}O_{71}P_2S_2$, 1427.2, 1141.9, and 951.8).

Igs—Methods for IgV preparation and characterization have been described (7, 21). Briefly, the library consists of 1.4×10^7 IgVs cloned in the phagemid vector pHEN2 prepared from the peripheral blood lymphocyte of patients with lupus. A His_6 sequence and a c-*myc* epitope are located at the IgV C terminus. Expression levels were 1–3 mg of IgV/liter of bacterial culture, determined by anti-c-*myc* immunoblotting. Soluble IgVs were purified from periplasmic extracts of HB2151 cells by metal affinity chromatography. Further purification was by anion exchange FPLC (MonoQ HR 5/5 column; 0–1 M NaCl in 50 mM Tris buffer, pH 7.4, containing 0.1 mM CHAPS). Purity was determined by SDS-gel electrophoresis and immunoblotting. IgV phages (10^{12} colony-forming units) were packaged using the hyperphage method (22) and incubated (2 h, 37 °C) with Bt-E-Aβ40 in 0.07 ml of 10 mM sodium phosphate, 137 mM NaCl, 2.7 mM KCl, pH 7.4 (PBS). Phages with bound Bt-E-Aβ40 were captured using anti-biotin antibody coupled to agarose gel (0.22 ml settled gel; Sigma) and washed with 100 ml of PBS containing 0.1% bovine serum albumin. Reversibly bound phages were eluted by incubation of the gel in 0.2 ml of 100 μM Aβ40 for 1 h with slow mixing, and the residual phages covalently complexed to Bt-E-Aβ were eluted with 0.4 ml of 0.1 M glycine, pH 2.7. scFv-*t* derivatives of single domain IgV_L-*t*′ 5D3 were prepared by inserting the deleted V_H residues 8–115 (Kabat numbering). For this, full-length V_H cDNA was amplified by PCR using as template the IgV-pHEN2 DNA library and back/forward primers containing ApaLI/NotI restriction sites (respectively, GGTAGTGCACTTCAGGTGCAGCTGTTGCAGTCT/ATGTGCGGCCGCGGGGGAAAAGGGTTGGGGGCATGC), and the cDNA digested with ApaLI/NotI was ligated into similarly digested plasmid IgV_L-*t*′ 5D3 DNA with T4 DNA ligase (Invitrogen). Full-length light chain L-*t*′ 5D3 was prepared by Mutagenex by a chimeragenesis method (23) using as starting materials the V_L domain of IgV_L-*t*′ 5D3 and human κ chain constant domain (obtained from pLC-huCκ (24)) and cloned into pHEN2 vector as the NcoI/NotI-digested fragment. cDNAs for the homodimeric IgV_{L2}-*t* form of clone 5D3 were prepared by PCR by Mutagenex. Briefly, V_L cDNA was amplified by PCR from the IgV_L-*t*′5D3 template using back/forward primers containing ApaLI/NotI restriction sites (respectively, AAAGTGCACTTGAAATTGTGTTGACGCAGTCTC/AAAGCGGCCGCGCGTTTGATCTCCAGCTTGGT), and the cDNA digested with ApaLI/NotI was ligated into pHEN2 vector. The nucleotide sequence of all constructs determined by dideoxy nucleotide sequencing in the 5′ to 3′ and 3′ to 5′ directions was identical (Applied Biosystems, ABI PRISM® 3100 Genetic Analyzer). Following electroporation of IgV phagemid DNA into HB2151 cells, soluble IgVs were purified from periplasmic extracts as before. Total protein was determined by the microBCA kit (Pierce). For mass spectroscopy (25), the IgV band was excised from the SDS-electrophoresis gel stained with GelCode Blue (Pierce), subjected to dehydration in 50% acetonitrile and SpeedVac drying, reduced (dithiothreitol) and alkylated (iodoacetamide), and digested with sequencing grade trypsin (Promega) and Lys-C (Wako) for 20 h at 37 °C. Following extraction of gel fragments with acetonitrile/formic acid, digested peptides obtained by ZipTip C18 (Millipore) fractionation using 5 μl of aqueous 50% acetonitrile containing 2% formic acid were analyzed by mass spectrometry using a matrix of α-cyano-4-hydroxycinnamic acid (ABI 4700 MALDI-TOF/TOF mass spectrometer). Predicted monoisotopic peptide

Downloaded from www.jbc.org by guest, on April 28, 2010

PAGE 51/92 * RCVD AT 4/28/2010 6:45:45 PM [Eastern Daylight Time] * SVR:USPTO-EFXRF-6/33 * DNIS:2738300 * CSID:7132705361 * DURATION (mm-ss):48-00

Supplemental Material can be found at: http://www.jbc.org/content/suppl/2008/11/04/M806769200.DC1.html

mass values were obtained using MS-Fit for protein data base searches (Protein Prospector, University of California, San Francisco). IgM was purified from human sera as described (18).

Hydrolysis and Binding Assays—Hydrolysis of ^{125}I-Aβ40 was determined as described (18). Briefly, ^{125}I-Aβ40 prepared by the chloramine-T method was purified by RP-HPLC (2.2 Ci/μmol). The ^{125}I-Aβ40 (~0.1 nM, ~30,000 cpm/tube) was treated with IgVs in PBS containing 0.1 mM CHAPS and 0.1% (w/v) bovine serum albumin; intact peptide was separated from fragments by precipitation with trichloroacetic acid, and acid-soluble radioactivity was counted and corrected for background values in control assay tubes incubated in diluent without Ig (mean ± S.D., 18 ± 6%; n = 7 assays). This procedure affords estimates of hydrolysis concordant with RP-HPLC separation of the reaction mixtures. Apparent kinetic parameters were estimated by fitting hydrolysis rates observed at varying Aβ40 concentrations mixed with a constant amount of ^{125}I-Aβ40 to the following equation: $v = (V_{max}[A\beta40])/K_m + [A\beta40]$, where V_{max} is the maximum velocity at saturating Aβ40 concentrations, and K_m is the concentration at which half-maximal velocity was observed. To identify the reaction products, reaction mixtures of nonradiolabeled synthetic Aβ40 or Aβ42 (100 μM; American Peptide Co.) incubated with IgVs in PBS/CHAPS were desalted by gel filtration (Bio-Rad micro Bio-spin 6 columns), lyophilized, and subjected to MALDI-TOF MS with α-cyano-4-hydroxycinnamic acid as matrix (positive ion mode, 20,000 V). RP-HPLC of Aβ40-Ig reaction mixtures and ESI-MS identification of the product have been described previously (18). Hydrolysis of the amide bond linking 7-amino-4-methylcoumarin (AMC) to the C-terminal amino acid of peptide-AMC substrates (Peptides International) was measured in PBS/CHAPS buffer by fluorimetry with authentic AMC as reference (λem 470 nm; λex 360 nm (12)). Hydrolysis of biotinylated proteins was determined by SDS-electrophoresis using peroxidase-conjugated streptavidin to stain blots of the gels (18). IgV covalent binding to biotinylated E-hapten 2 or E-hapten 3 was assayed in PBS/CHAPS (12). The reaction mixtures were boiled in SDS in reducing buffer (5 min) and subjected to SDS-electrophoresis, and blots of the gels were stained with the streptavidin-peroxidase conjugate. IgV binding to immobilized Bt-Aβ40 was determined by enzyme-linked immunosorbent as described (18) except that anti-c-*myc* antibody (1:100) was employed to detect IgVs bound to immobilized antigens (26).

IgV Modeling—The two V_L domains of the heterodimeric IgV_{L2}-*t* 2E6 located, respectively, on the N- and C-terminal side of the linker (designated VL1 and VL2) were initially modeled as monomers by sequence alignment to the most-homologous V_L domains in the Protein Data Bank (PDB codes, respectively, 1MCB and 2BX5; 85–95% sequence identity) and homology modeling with DS 1.7 (Accelrys; modeler module followed by minimization in CHARMm force field; 1000 cycles). The VL1 and VL2 structures were then refined in dimeric form using as template the light chain dimer PDB 1MCW. The flexible inter-domain linker peptide and C-terminal tag region were incorporated into the model, and minor steric clashes were removed by energy minimization using CNS 1.1 (200 cycles; see Ref. 27). The V_L domain of the single domain IgV_L-*t*′ 5D3 was initially modeled in its paired V_L-V_H scFv-*t* 5D3-E6 form by the WAM server. V_L models in the IgV_L-*t*′, IgV_{L2}-*t*, and full-length light chain L-*t* forms of the molecule were prepared by superimposing the V_L domain from the WAM model to the coordinates of the homodimeric light chain crystal structure (PDB 1B6D; 85% sequence identity). The structures were submitted to steepest-descent energy minimization using the Adopted Basis-set Newton-Raphson method under the CHARMm force field (2000 cycles) until an r.m.s. deviation of 0.1 kcal/mol/Å was obtained. The quality of all structures was checked using PROCHECK. Percent V_L residues in the final models located in the most favored or generous regions of the Ramachandran plot were as follows: IgV_{L2}-*t* 2E6, 90.8%; IgV_L-*t*′ 5D3, 96.5%; scFv-*t* 5D3-E6, 97.7%; IgV_{L2}-*t* 5D3 homodimer, 95.5%; L-*t* 5D3, 96.9%. No unacceptable atomic collisions were detected. The van der Waals energy was negative, suggesting the absence of bad non-bonded contacts. Superimposition and determination of global r.m.s. deviation and translational Cα-Cα movements were performed using PyMOL (DeLano Scientific LLC). The feasibility of Aβ40 interactions with IgV_{L2}-*t* 2E6 was assessed by molecular docking as described (18) using ZDOCK with Gln^{15} of Aβ40 constrained within 12 Å of each putative nucleophilic residue (VL1 domain: Ser^{27A}, Tyr^{87}, Ser^{93}, and Thr^{105}; VL2 domain: Thr^{85}, Ser^{76}, and Ser^{91}). The docked model containing VL1 domain Thr^{105} apposed to Aβ40 Gln^{15} was the energetically most favored structure.

RESULTS

Aβ40 Hydrolyzing IgVs—We reported previously the hydrolysis of Aβ40 by polyclonal IgM purified from humans without dementia (18). Here we searched for Aβ40-hydrolyzing human IgVs in a library composed of ~10^7 clones. A majority of the clones in the library are scFv-*t* constructs with the domain organization V_L-*Li*-V_H-*t*, where *Li* denotes the 16-residue peptide $SS(GGGGS)_2GGSA$ joining the V_L domain C terminus to the V_H domain N terminus, and *t* denotes the 26-residue C-terminal peptide containing the c-*myc* peptide and His_6 tags (7). A minority of clones possess unusual IgV structures generated by cloning errors (see below). Sixty three IgVs purified from the periplasmic extracts of randomly picked clones by His_6 binding to nickel affinity columns were tested for ^{125}I-Aβ40 hydrolyzing activity. Two IgVs with activity markedly superior to the remaining clones were identified (Fig. 1*A*). The activity of the empty vector control extract (pHEN2 devoid of an IgV insert) was within the assay error range (50 cpm/h, corresponding to mean background acid soluble radioactivity + 3 S.D.). The phagemid DNA of the high activity IgV clone 2E6 was re-expressed in 15 individual bacterial colonies. All recloned colonies secreted IgV with robust ^{125}I-Aβ40 hydrolyzing activity (Fig. 1*B*), ruling out trivial sample preparation variations as the cause of proteolytic activity. As before, the purified extract of the control empty vector clone did not hydrolyze ^{125}I-Aβ40.

In previous studies, electrophilic phosphonate groups incorporated within polypeptides were bound covalently by catalytic Ig nucleophilic sites, with noncovalent binding at the peptide epitopes conferring specificity to the reaction (21). We employed the biotinylated Aβ40 analog containing phospho-

Downloaded from www.jbc.org by guest, on April 28, 2010

PAGE 52/92 * RCVD AT 4/28/2010 6:45:45 PM [Eastern Daylight Time] * SVR:USPTO-EFXRF-6/33 * DNIS:2738300 * CSID:7132705361 * DURATION (mm-ss):48-00

Supplemental Material can be found at:
http://www.jbc.org/content/suppl/2008/11/04/M806766200.DC1.html

nates at Lys^{16} and Lys^{28} side chains to isolate Aβ40 catalysts displayed on phage surface (Bt-E-Aβ40; Fig. 2*A*). Phage IgVs treated with Bt-E-Aβ40 were captured using immobilized anti-biotin antibody, and noncovalently bound phage IgVs were eluted by treatment with excess Aβ40 (designated noncovalently selected IgVs), and the irreversible phage IgV immune complexes were eluted by acid disruption of the biotin-antibiotin antibody complexes (designated covalently selected IgVs). The frequency of IgVs with robust Aβ hydrolyzing activity was increased by covalent selection (Fig. 2*B*). Four of 7 IgVs obtained by covalent selection at 2 μM Aβ40 hydrolyzed ^{125}I-Aβ40 at rates >400 cpm/h, compared with 2 of 63 IgVs with this level of activity identified by random screening. Phage selections conducted at increased Aβ40 concentration (10 μM) yielded less active IgVs (Fig. 2*B*), consistent with the prediction of more efficient selection of catalysts at the lower ligand concentration. Eighteen IgVs recovered by noncovalent selection displayed no or little hydrolytic activity.

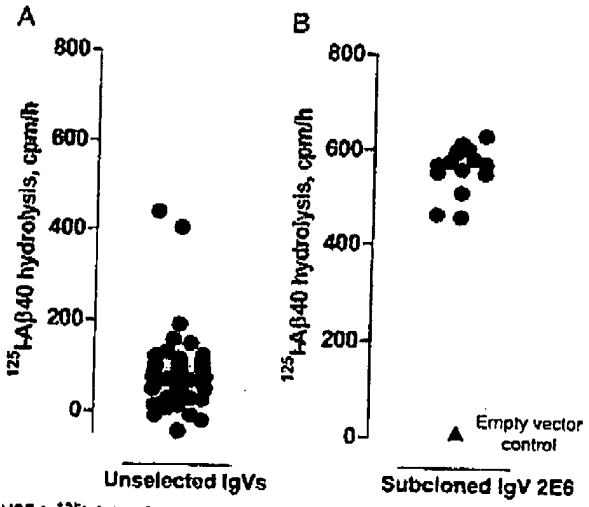

FIGURE 1. **^{125}I-Aβ40 hydrolysis by randomly picked IgV clones.** *A*, identification of rare Aβ-hydrolyzing IgVs. Sixty three IgVs were purified from periplasmic extracts (15 ml) of bacterial colonies picked randomly from the IgV library grown on an agar plate. Aliquots of eluates (75 μl) obtained by metal affinity chromatography of the periplasmic extracts (total eluate volume 0.9 ml) were tested for Aβ hydrolyzing activity. Values are means of closely agreeing duplicates (S.D. < 7.3% of mean). Each point represents one clone. ^{125}I-Aβ40, 0.1 nM; 18 h of incubation. *B*, validation of IgV 2E6 hydrolytic activity by recloning. Phagemid DNA isolated from the high activity clone 2E6 was electroporated into bacteria, and purified IgV from 15 individual colonies obtained from the recloning procedure were analyzed for Aβ hydrolyzing activity as in *A* along with the identically purified empty vector control (pHEN2).

IgV Primary Structure and Activity Validation—The cDNAs for IgV clone 2E6 obtained without phage selection and three covalently selected IgVs with the greatest Aβ40 hydrolyzing activity (clones 5D3, 1E4, and 5H3) were sequenced. Identical nucleotide sequences were obtained for each clone sequenced from the 5′ to 3′ direction and the 3′ to 5′ direction. The cDNA sequences indicated that IgV 2E6 is a dimer of two different V_L domains with the intervening linker peptide and the expected C-terminal tag (designated heterodimeric IgV_{L2}-*t*, Fig. 3*A*; sequences in supplemental Fig. S1). IgVs 5D3, 1E4, and 5H3 are single domain V_L clones with unexpected C-terminal polypeptide segments, designated IgV_L-*t′* clones, where *t′* denotes the following: (*a*) the expected linker peptide, (*b*) a 15–28-residue aberrant peptide sequence in place of the V_H domain composed of ~115 residues, and (*c*) the expected 26 residue peptide sequence containing the c-*myc* and His_6 sequences (Fig. 3*A* and supplemental Fig. S1).

Two clones were studied further, IgV_{L2}-*t* 2E6 and IgV_L-*t′* 5D3. Their deduced protein masses predicted from the cDNA sequences are, respectively, 27 and 17 kDa. Denaturing electrophoresis of the IgVs purified by 2 cycles of nickel-affinity chromatography and anion exchange FPLC (IgV_{L2}-*t* 2E6 and IgV_L-*t′* 5D3 fractions corresponding, respectively, to retention times 10–11 and 23–23.5 min; supplemental Fig. S2) revealed silver and anti-c-*myc* stainable protein bands close to the predicted mass of the monomer proteins (IgV_{L2}-*t* 2E6, 29 kDa; IgV_L-*t′* 5D3, 18 kDa; Fig. 3*B*). The presence of the c-*myc* peptide epitope confirms that these are IgV bands. In view of its unusual structure, the identity of IgV_L-*t′* 5D3 monomer band was confirmed further by tryptic digestion and mass spectroscopy (supplemental Table S1). All observed spectroscopic signals originated from peptides within the predicted IgV_L-*t′* structure deduced from the cDNA sequence, and the peptide signals were consistent with deletion of V_H residues 8–115 predicted from the cDNA sequence. Additional IgV bands were detected prior to anion exchange chromatography (low mass IgV_{L2}-*t* 2E6 band at 18 kDa; high mass IgV_L-*t′* 5D3 bands at 36, 50, 58, 67, and 74 kDa). All of these bands were stained by anti-c-*myc* antibody (Fig. 3*B*). As irrelevant proteins are not stained by the anti-c-*myc* antibody, there is no evidence of non-IgV contaminants. We concluded that the anomalous low mass band is an IgV_{L2}-*t* self-degradation product, and the high mass bands are IgV_L-*t′* aggregates. ^{125}I-Aβ40 hydrolyzing activities of both IgVs remained constant after one and two cycles of nickel-affinity chro-

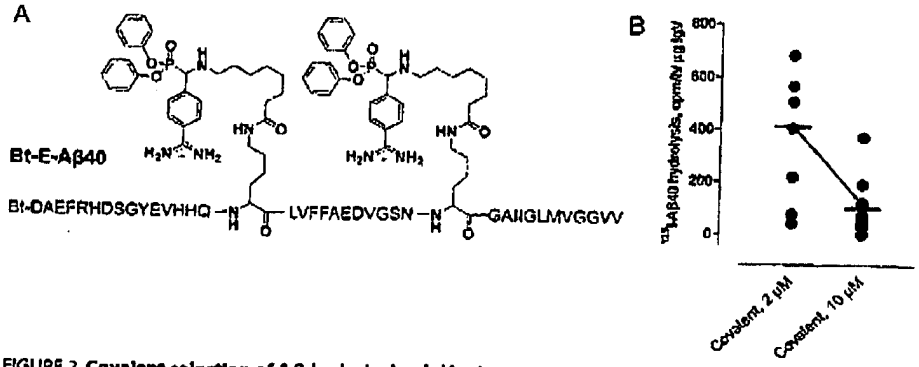

FIGURE 2. **Covalent selection of Aβ-hydrolyzing IgVs.** *A*, structure of Bt-E-Aβ40. The electrophilic phosphonates placed within Aβ40 permit specific covalent binding to nucleophilic Igs facilitated by noncovalent Aβ40 recognition. *B*, frequent Aβ-hydrolyzing IgVs obtained by covalent selection. The IgV-phage library was treated with Bt-E-Aβ40 (2 or 10 μM), and covalently bound phages were recovered as described under "Materials and Methods," and hydrolysis of ^{125}I-Aβ40 (0.1 nM) by purified IgVs obtained from selected clones was measured as in Fig. 1*A*. Each point represents an individual IgV clone.

Downloaded from www.jbc.org by guest, on April 28, 2010

PAGE 53/92 * RCVD AT 4/28/2010 6:45:45 PM [Eastern Daylight Time] * SVR:USPTO-EFXRF-6/33 * DNIS:2738300 * CSID:7132705361 * DURATION (mm-ss):48-00

Supplemental Material can be found at:
http://www.jbc.org/cgi/content/suppl/2008/11/04/M806763200.DC1.html

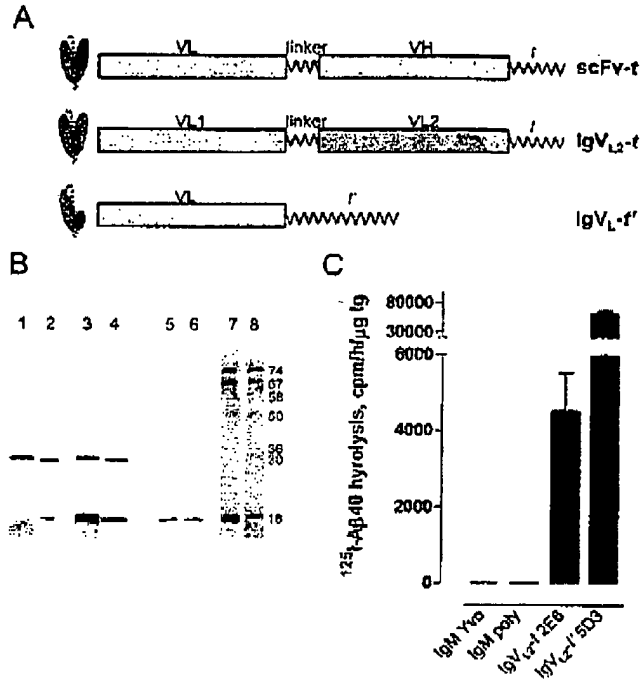

FIGURE 3. **Structure and hydrolytic activity of IgV$_{L2}$-*t* 2E6 and IgV$_L$-*t'* 5D3.** *A*, schematic representation of IgV structures. scFv-*t*, V_L, and V_H domains connected by a peptide linker with *t*, the His^6/c-*myc* tag located at the C terminus; IgV$_{L2}$-*t* 2E6, a heterodimer of two V_L domains with the linker and *t*; IgV$_L$-*t'* 5D3, a single domain V_L with *t'* at the C terminus, corresponding to the peptide linker, a short peptide region in place of the V_H domain and the *t* tag. *B*, SDS-electrophoresis of IgVs. *Lanes 1* and *2*, respectively, IgV$_{L2}$-*t* 2E6 purified by metal affinity chromatography followed by anion exchange FPLC and stained with silver and anti-c-*myc* antibody. *Lanes 3* and *4*, respectively, IgV$_{L2}$-*t* 2E6 purified by two cycles of metal affinity chromatography and stained with silver and anti-c-*myc* antibody. *Lanes 5* and *6*, respectively, IgV$_L$-*t'* 5D3 purified by metal affinity chromatography followed by anion exchange FPLC and stained with silver and anti-c-*myc* antibody. *Lanes 7* and *8*, respectively, IgV$_L$-*t'* 5D3 purified by two cycles of metal affinity chromatography and stained with silver and anti-c-*myc* antibody. *C*, ^{125}I-Aβ40 hydrolysis (cpm/h/μg Ig; means ± S.D.) by monoclonal IgM Yvo, a pooled human polyclonal IgM preparation, IgV$_{L2}$-*t* 2E6, and IgV$_L$-*t'* 5D3. ^{125}I-Aβ40, ~30,000 cpm (~0.1 nM). The monoclonal and polyclonal IgM preparations are described previously (18). Data are from assays at 90–405 μg/ml IgMs and 0.075–0.55 μg/ml IgVs.

TABLE 1

^{125}I-Aβ-(1–40) hydrolyzing activity of IgVs following metal affinity and anion exchange FPLC purification

Recombinant IgV preparations purified by one round of metal affinity chromatography on nickel-agarose (preparation MA1) were subjected either to a second round of metal affinity chromatography (MA2) or anion exchange chromatography (AEQ) on a Mono Q FPLC column. Aβ hydrolysis was assayed as in Fig. 2. Shown are specific activities expressed in cpm/h/μg of protein.

Catalyst	Specific activity, cpm/h/μg of protein IgV (mean ± S.D.)		
	MA1	MA2	AEQ
IgV$_{L2}$-*t* 2E6	1318 ± 375	1220 ± 134	4495 ± 1035
IgV$_L$-*t'* 5D3	2660 ± 114	2273 ± 308	61401 ± 5274

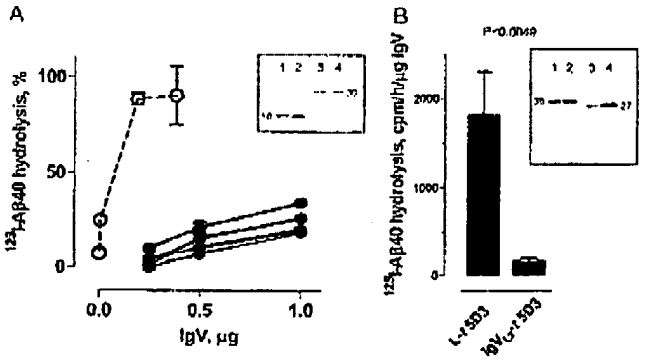

FIGURE 4. **^{125}I-Aβ40 hydrolysis by single domain IgV$_L$-*t'* 5D3 and its paired V domain derivatives.** *A*, hydrolytic activity of the IgV$_L$-*t'* (○) and its scFv-*t* derivatives (●), ^{125}I-Aβ40, ~30,000 cpm, (~0.1 nM). Values are means ± S.D. Incubation, 18 h. *Inset*, *lanes 1* and *2*, respectively, SDS-electrophoresis gels of the IgV$_L$-*t'* stained with silver and anti-c-*myc* antibody. *Lanes 3* and *4*, respectively, an example scFv-*t* derivative of 5D3 (clone 5D3-E6) stained with silver and anti c-*myc* antibody. The bands at 18 and 30 kDa are, respectively, the IgV$_L$-*t'* and scFv-*t*. *B*, hydrolytic activity of full-length L-*t* 5D3 and homodimeric IgV$_{L2}$-*t* 5D3. ^{125}I-Aβ40 hydrolysis assayed as in *A*. *Inset*, *lanes 1* and *2*, respectively, SDS-electrophoresis gels of the L-*t* stained with silver and anti-c-*myc* antibody. *Lanes 3* and *4*, respectively, the IgV$_{L2}$-*t* stained with silver and anti-c-*myc* antibody. The bands at 30 and 27 kDa are, respectively, the L-*t* and IgV$_{L2}$-*t*.

matography but were increased following further FPLC purification that removed the degradation product and aggregates (Table 1; by 3.1- and 31.2-fold, respectively, for the IgV$_{L2}$-t and IgV$_L$-*t'*). These observations are consistent with Aβ hydrolysis by the unaggregated IgVs.

Sequencing of 24 randomly picked clones indicated that most IgVs in the library are scFv-*t* constructs (83.3% clones), with only rare representation of IgV$_{L2}$-*t* and IgV$_L$-*t'* constructs (respectively, 12.5 and 4.2% clones; supplemental Table S2). The cumulative probability that all four Aβ40-hydrolyzing IgVs identified in the present study are IgV$_{L2}$-*t* or IgV$_L$-*t'* clones by random chance is very small ($p = 0.9 \times 10^{-5}$; computed as 0.125×0.042^3). It may be concluded that the rare IgV structures favor expression of Aβ hydrolysis compared with the physiological V_L-V_H paired structure of scFv-*t* clones. This is supported by comparisons of IgV catalytic activities with the previously reported polyclonal human IgM preparations and a monoclonal IgM from a patient with Waldenstrom's macroglobulinemia (18). IgV$_{L2}$-*t* 2E6 and IgV$_L$-*t'* 5D3 hydrolyzed ^{125}I-Aβ40 with potencies superior to the IgMs by 3–4 orders of magnitude (Fig. 3*C*).

Repaired IgV 5D3 Versions—The aberrant *t'* region of IgV$_L$-*t'* 5D3 contains a deletion of V_H domain residues 8–115 (Kabat numbering). Four scFv-*t* constructs were generated from the IgV$_L$-*t'* by inserting the deleted residues derived from full-length V_H domains represented in the library (supplemental Fig. S3). The repaired scFv-*t* 5D3 derivatives migrated at the expected mass in electrophoresis gels (30 kDa, example in Fig. 4*A*, *inset*). Their ^{125}I-Aβ40 hydrolyzing activity was consistently lower than the parent IgV$_L$-*t'* (by ~82–167-fold, computed by rate comparisons in the linear region of the hydrolysis curves; Fig. 4*A*). This suggests that Aβ40 hydrolysis occurs at an autonomous catalytic site in the IgV$_L$-*t'* V_L domain that is suppressed by pairing with V_H domains.

Intermolecular noncovalent bonding between isolated light chains can generate dimeric light chain structures (29). To assess whether noncovalently associated IgV$_L$-*t'* dimers containing paired V_L-V_L structures might account for the hydrolytic activity, we prepared the homodimeric IgV$_{L2}$-*t* molecule containing two 5D3 V_L domains connected by the peptide linker. Homodimeric IgV$_{L2}$-*t* 5D3 hydrolyzed ^{125}I-Aβ40 poorly

Downloaded from www.jbc.org by guest, on April 28, 2010

PAGE 54/92 * RCVD AT 4/28/2010 6:45:45 PM [Eastern Daylight Time] * SVR:USPTO-EFXRF-6/33 * DNIS:2738300 * CSID:7132705361 * DURATION (mm-ss):48-00

Supplemental Material can be found at:
http://www.jbc.org/content/suppl/2008/11/04/M806786200.DC1.html

(Fig. 4*B*). In comparison, the full-length light chain containing the 5D3 V_L domain linked to the κ constant domain (designated L-*t*), displayed detectable hydrolytic activity. In denaturing electrophoresis gels, the homodimeric IgV_{L2}-*t* 5D3 migrated as a single protein band at the predicted 27-kDa position (Fig. 4*B*, *inset*). As expected, L-*t* 5D3 migrated as a mixture of monomers and S–S-bonded dimers with nominal mass, respectively, 30 and 60 kDa. These observations suggest that the monomeric, unpaired state of the V_L domain is required to maintain catalytic site integrity.

Catalytic Properties—The hydrolytic activity of both IgV clones was saturable with increasing Aβ40 concentrations (1–100 μM nonradioactive Aβ40 mixed with 0.1 nM ^{125}I-Aβ40). Kinetic parameters are reported in Table 2. MALDI-MS of nonradioactive Aβ40 treated with IgV_{L2}-*t* 2E6 or IgV_L-*t'* 5D3 indicated similar product profiles (Fig. 5, *A* and *B*). The prominent products were Aβ-(1–14) and Aβ-(15–40), suggesting hydrolysis of the His^{14}–Gln^{15} peptide bond (Fig. 5*E*; observed and calculated *m/z* values in Fig. 5 legend). Smaller signals for the following peptide products were also detected as follows: Aβ-(1–15), Aβ-(1–20), Aβ-(16–40), and Aβ-(21–40). The corresponding scissile bonds in Aβ40 are Gln^{15}–Lys^{16} and Phe^{20}–Ala^{21}. Similar product profiles were evident in reaction mixtures of the longer Aβ42 peptide treated with the IgV_{L2}-*t* 2E6 (Fig. 5, *C* and *D*), except that additional minor products suggesting cleavage at the Lys^{28}–Gly^{29} and Gly^{29}–Ala^{30} bonds were evident. As accurate product quantification by MALDI-MS is difficult, we also conducted RP-HPLC of Aβ40 treated with IgV_{L2}-*t* 2E6. This indicated depletion of the intact Aβ40 peak, accompanied by appearance of a major peptide product absent in control chromatograms of the IgV alone or Aβ40 alone (supplemental Fig. S4*A*). The product peak was identified as Aβ-(1–14) by ESI-MS, confirming the His^{14}–Gln^{15} bond as the major cleavage site.

The ^{125}I-Aβ40 hydrolysis measurements were conducted using a small amount of the Aβ40 substrate (0.1 nM) mixed with excess albumin (1 mg/ml; 15 μM), which can serve as an alternate substrate for promiscuous catalysts. As hydrolysis of ^{125}I-Aβ40 was detected readily, the IgVs do not appear to be nonspecific catalysts. In addition, there was no evidence for hydrolysis of several irrelevant biotinylated polypeptides (ovalbumin, soluble extracellular domain of the epidermal growth factor receptor, human immunodeficiency virus gp120, protein A; supplemental Fig S4*B*). Previous reports have identified promiscuous Igs present in human blood using model fluorigenic peptide substrates (12). IgV_{L2}-*t* 2E6 and IgV_L-*t'* 5D3 failed to hydrolyze the model peptide substrate appreciably (Table 3), whereas a representative human polyclonal IgM preparation 9010 hydrolyzed large amounts of Arg/Lys-containing peptide substrates. The data indicate specific Aβ hydrolysis by the IgVs.

Previous reports have indicated that proteolytic Igs utilize a serine protease-like catalytic mechanism entailing nucleophilic attack on the electrophilic carbonyl of peptide bonds (7, 9). This was the basis for the covalent phage IgV selection in this study. To confirm the mechanism, we studied the reactivity of IgV_{L2}-*t* 2E6 and IgV_L-*t'* 5D3 with the electrophilic phosphonate diester E-hapten-**1** (Fig. 6*A*), a compound originally developed as a covalent inhibitor of serine proteases (30). E-hapten-**1** inhibited ^{125}I-Aβ40 hydrolysis by both clones (Fig. 6*B*). The biotin-containing version of the phosphonate diester,

TABLE 2

Apparent kinetic parameters for IgV-catalyzed Aβ40 hydrolysis

Reaction rates were measured following incubation of increasing Aβ40 (1–100 μM) containing a constant amount of ^{125}I-Aβ40 (~300,000 cpm) with IgV_{L2}-*t* 2E6 (3.75 μg/ml) or IgV_L-*t'* 5D3 (0.15 μg/ml). Kinetic constants were obtained from nonlinear regression fits to the Michaelis-Menten equation (r^2 for IgV_{L2}-*t* 2E6 and IgV_L-*t'* 5D3, respectively, 0.99 and 0.98).

Catalyst	K_m	k_{cat}	k_{cat}/K_m
	$M \times 10^{-5}$	min^{-1}	$M^{-1}\,min^{-1} \times 10^3$
IgV_{L2}-*t* 2E6	8.0 ± 1.2	0.3 ± 0.1	3.7 ± 0.6
IgV_L-*t'* 5D3	1.7 ± 0.1	1.0 ± 0.1	59.0 ± 4.5

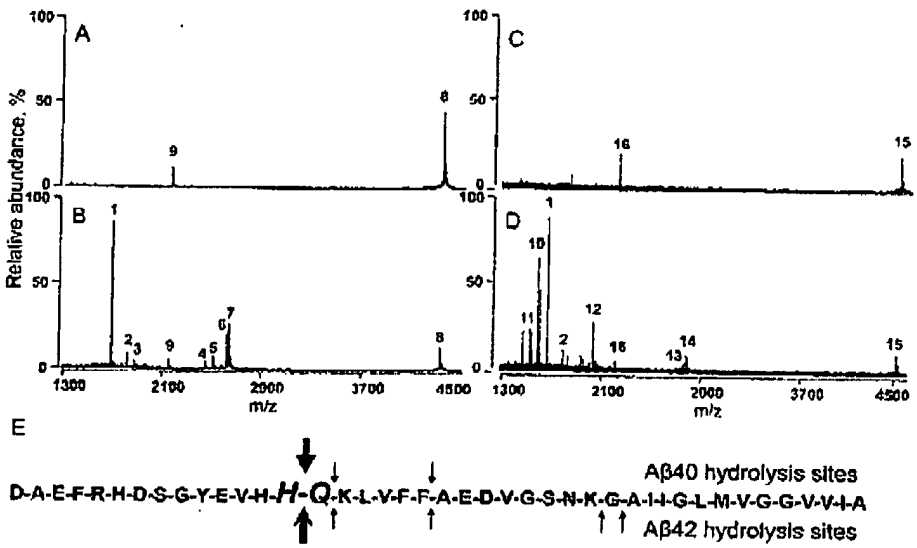

FIGURE 5. **Peptide bonds in Aβ40 and Aβ42 hydrolyzed by IgV_{L2}-*t* 2E6.** *A* and *B*, MALDI-TOF spectra of Aβ40 incubated, respectively, with diluent or IgV_{L2}-*t* 2E6. *C* and *D*, MALDI-TOF spectra of Aβ42 incubated, respectively, with diluent or IgV_{L2}-*t* 2E6. *E*, scissile bonds deduced from the spectra (*arrows*). Aβ, 100 μM; IgV_{L2}-*t* 2E6, 1 μM; 89-h incubation. Peak identities are as follows: *1*, Aβ-(1–14) (calculated (M + H)$^+$ 1698.7, observed (M + H)$^+$ 1698.8); *2*, Aβ-(1–15) (calculated (M + H)$^+$ 1826.8, observed (M + H)$^+$ 1826.9); *3*, Aβ-(21–40) (calculated (M + H)$^+$ 1886.0, observed (M + H)$^+$ 1886.1); *4*, Aβ-(1–20) (calculated (M + H)$^+$ 2461.2, observed (M + H)$^+$ 2461.2); *5*, Aβ-(16–40) (calculated (M + H)$^+$ 2520.4, observed (M + H)$^+$ 2520.4); *6*, pGluAβ-(15–40) (calculated (M + H)$^+$ 2631.4, observed (M + H)$^+$ 2631.5); *7*, Aβ-(15–40) (calculated (M + H)$^+$ 2648.5, observed (M + H)$^+$ 2648.5); *8*, full-length Aβ40 (calculated (M + H)$^+$ 4328.2, observed (M + H)$^+$ 4328.1); *9*, full-length Aβ40 (calculated (2 M + H)$^+$ 2164.6, observed (2 M + H)$^+$ 2164.6); *10*, Aβ-(15–29) (calculated (M + H)$^+$ 1638.9, observed (M + H)$^+$ 1638.9); *11*, Aβ-(15–28) (calculated (M + H)$^+$ 1581.8, observed (M + H)$^+$ 1581.8); *12*, Aβ-(21–42) (calculated (M + H)$^+$ 2070.1, observed (M + H)$^+$ 2070.2); *13*, pGluAβ-(15–42) (calculated (M + H)$^+$ 2814.6, observed (M + H)$^+$ 2814.8); *14*, Aβ-(15–42) (calculated (M + H)$^+$ 2832.6, observed (M + H)$^+$ 2832.6); *15*, full-length Aβ42 (calculated (M + H)$^+$ 4512.3, observed (M + H)$^+$ 4512.1); *16*, full-length Aβ42 (calculated (2 M + H)$^+$ 2256.7, observed (2 M + H)$^+$ 2256.6).

Downloaded from www.jbc.org by guest, on April 28, 2010

PAGE 55/92 * RCVD AT 4/28/2010 6:45:45 PM [Eastern Daylight Time] * SVR:USPTO-EFXRF-6/33 * DNIS:2738300 * CSID:7132705361 * DURATION (mm-ss):48-00

Supplemental Material can be found at: http://www.jbc.org/content/suppl/2008/11/04/M806768200.DC1.html

E-hapten-2, formed 30-kDa covalent adducts with IgV_{L2}-*t* 2E6 that were stable to boiling and SDS treatment (Fig. 6*B*, *inset*). Control hapten-3, a poorly electrophilic analog of E-hapten-2, did not form detectable adducts with the IgV_{L2}-*t*. The results support a nucleophilic catalytic mechanism.

IgV_{L2}-*t* 2E6 and IgV_L-*t'* 5D3 (20 μg/ml) did not bind detectably to immobilized Bt-Aβ40 in enzyme-linked immunosorbent assay tests (A_{490} < 0.06). Under similar conditions, the reference anti-Aβ monoclonal IgG (6E10, 0.1 μg/ml) afforded readily detected binding activity (A_{490}, 0.7 ± 0.01).

Molecular Models—Intramolecular H-bonding between triads and dyads of amino acids enhances the nucleophilicity of certain side chains responsible for enzymatic catalysis. Examples are the hydroxyl side chains of Ser, Thr, and Tyr residues activated by spatially neighboring general bases contributed by His, Lys, Arg, Tyr, Glu, and Asp residues (31–34). We screened molecular models of IgV_{L2}-*t* 2E6 and IgV_L-*t'* 5D3 for side chain hydroxyls located within 4 Å of atoms that can serve as general bases as described in Ref. 31. One triad and several dyads fulfilling this requirement were found in each of the catalysts (supplemental Fig. S5 and supplemental Table S3). The presence of the potential nucleophiles is consistent with the mechanism of IgV catalysis suggested by electrophilic inhibitor studies. Several complexes containing the candidate nucleophilic residues of IgV_{L2}-*t* 2E6 apposed to Gln^{15} of the major Aβ40 scissile bond were evaluated by molecular modeling. Among these, the complex containing VL1 domain Thr^{105} apposed to the scissile bond was the energetically most favored structure. This complex also contained various noncovalent stabilizing interactions between IgV_{L2}-*t* 2E6 and Aβ40, including VL1 domain Gly^{41} and Ala^{42} backbone atoms hydrogen bonded with, respectively, Aβ40 Asp^{23} backbone and side chain atoms.

The V_L domain of clone 5D3 is highly catalytic in the unpaired IgV_L-*t'* state and poorly catalytic when paired with a second V domain in scFv-*t* or homodimeric IgV_{L2}-*t* states. Subangstrom movements of electronegative atoms can weaken or strengthen H-bonds and thereby modulate the nucleophilic and proteolytic activities (35, 36). Frequent backbone displacements on the order of 0.5–1.7 Å were evident by energy minimization of the V_L domain modeled in the unpaired state *versus* the paired scFv-*t* or IgV_{L2}-*t* states (Fig. 7, *A* and *B*). Spatial displacement of amino acid side chains that influence H-bonding strength and increase or decrease the nucleophilic reactivity could also occur by virtue of rotation around single bonds (see supplemental Table S3 for changes of inter-residue distances within the potential nucleophilic sites in the unpaired and paired V_L domain states). The modeling results therefore suggest the feasibility of altered nucleophilic reactivity and provide a rational explanation for unequal catalysis by various V_L domain-containing molecules.

TABLE 3

Negligible hydrolysis of model peptide substrates by Aβ hydrolyzing IgVs

ND indicates not detected; one-letter amino acid code is used. Peptide-AMC substrates, 200 μM; purified IgVs and polyclonal human IgM 9010, 30 μg/ml; 37 °C. Values (means of three replicates ± S.D.) are slopes of progress curves monitored by fluorimetry as in Ref. 12.

Substrate	Hydrolysis, μM AMC/h/μM Ig		
	IgV_{L2}-*t* 2E6	IgV_L-*t'* 5D3	IgM 9010
AE-AMC	ND	ND	ND
AAA-AMC	ND	ND	ND
IIW-AMC	ND	ND	ND
AAPF-AMC	ND	ND	ND
EKK-AMC	0.030 ± 0.001	0.104 ± 0.001	13.1 ± 1.4
VLK-AMC	ND	ND	6.9 ± 0.4
EAR-AMC	0.005 ± 0.001	0.023 ± 0.001	61.9 ± 6.9
IEGR-AMC	0.010 ± 0.001	0.052 ± 0.001	2.0 ± 0.7
PFR-AMC	ND	ND	37.4 ± 0.7

DISCUSSION

Our observations indicate the superior Aβ hydrolyzing activity of V_L domains expressed in the IgV_{L2}-*t* and IgV_L-*t'* scaffolds compared with scFv-*t* constructs mimicking physiological antigen-combining sites. The catalytic activity is also strikingly superior to previously reported catalytic IgMs that contain fully natural Aβ-combining sites (18). Several IgV_{L2}-*t* and IgV_L-*t'* clones with exceptional Aβ hydrolyzing activity were identified from the library. Inclusion of full-length V_H domains in these clones uniformly suppressed the catalytic activity. Certain previous studies have presented evidence for hydrolysis of polypeptides (37) and nucleic acid (38) by isolated Ig light chain subunits. In contrast to catalysis, high affinity antigen binding by noncovalent means depends on cooperative V_L-V_H domain interactions, and heterodimeric V_L-V_H domain complexes invariably bind antigens noncovalently at levels superior to the binding activity of either V domain alone. It may be concluded that the catalytic sites are frequently present in IgV_L domains, but the physiological Ig scaffold does not favor expression of catalytic activity.

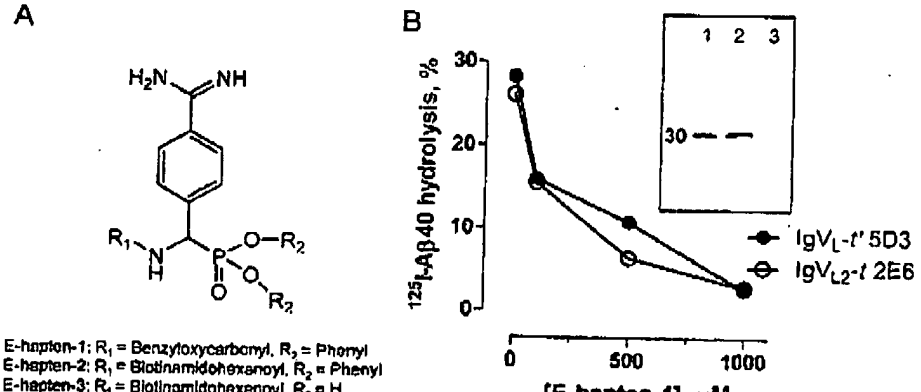

FIGURE 6. **Inhibition of IgV catalysis by E-hapten-1.** *A*, E-hapten-1 is an active site-directed inhibitor of serine proteases. E-hapten-2, a biotinylated analog of E-hapten-1, was used to detect covalent IgV adducts. E-hapten-3, the unesterified phosphonic acid analog of E-hapten-1, is the poorly electrophilic control compound. *B*, inhibition of IgV_{L2}-t 2E6 and IgV_L-*t'* 5D3 catalyzed ^{125}I-Aβ40 hydrolysis by E-hapten-1. IgV_{L2}-*t* 2E6 (0.55 μg/ml) or IgV_L-*t'* 5D3 (0.075 μg/ml) was treated with E-hapten-1 for 2 h followed by determination of ^{125}I-Aβ hydrolytic activity. *Inset*, streptavidin-peroxidase-stained blots of SDS gels showing IgV_{L2}-*t* 2E6 (20 μg/ml) treated for 18 h with 0.1 mM E-hapten-2 (*lane 2*) or E-hapten-3 (*lane 3*). *Lane 1*, IgV_{L2}-*t* 2E6 stained with silver.

Downloaded from www.jbc.org by guest, on April 28, 2010

PAGE 56/92 * RCVD AT 4/28/2010 6:45:45 PM [Eastern Daylight Time] * SVR:USPTO-EFXRF-6/33 * DNIS:2738300 * CSID:7132705361 * DURATION (mm-ss):48-00

Supplemental Material can be found at:
http://www.jbc.org/content/suppl/2008/11/04/M800766200.DC1.html

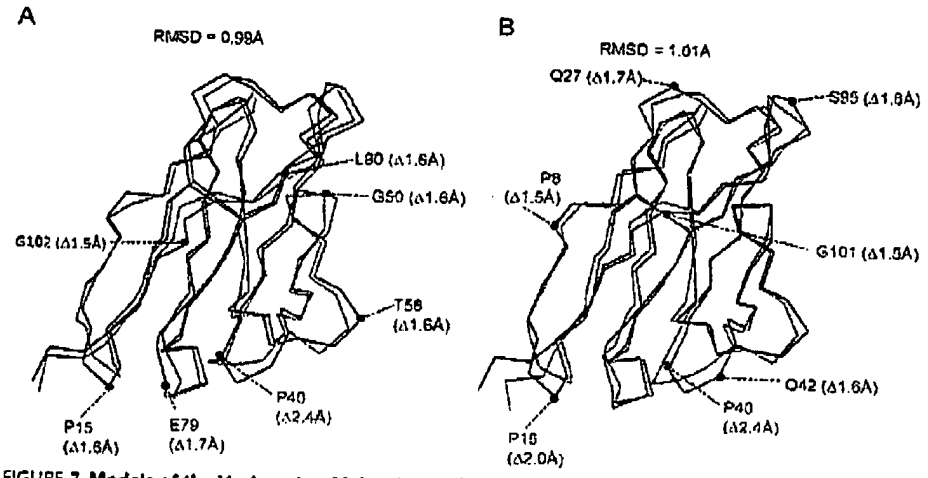

FIGURE 7. **Models of the V_L domain of IgV_L-*t*′ 5D3 (*black*) superimposed on the VL domains of its heterodimeric scFv-*t* derivative clone 5D3-E6 (*red, A*) and its homodimeric IgV_{L2}-*t* 5D3 derivative (*red, B*).** C-α atoms belonging to amino acids with r.m.s. deviation > 1.5 Å are identified, and overall r.m.s. deviations the superimposed models are indicated.

Ig light chain homodimers overproduced by cancerous B cells in multiple myeloma patients can bind certain antigens (39, 40). There is no naturally occurring Ig homolog of IgV_{L2}-*t* 2E6, a heterodimer of two V_L domains. Homodimeric IgV_{L2}-*t* constructs containing the individual V_L domains of IgV_{L2}-*t* 2E6 were without appreciable Aβ hydrolyzing activity, suggesting that both V_L domains in the heterodimer are important in maintaining the integrity of the catalytic site. Three Aβ-hydrolyzing clones with the IgV_L-*t*′ scaffold were also identified. In energy-minimized molecular models of one such clone, the small V_H domain peptide in the C-terminal segment was revealed as a disordered region without the β sheet structure typical of the Ig fold. Moreover, the proximity of the V_H peptide region to the V_L domain was insufficient to anticipate that it contributes to Aβ recognition by the V_L domain catalytic site. Noncovalent intermolecular association of the single domain IgV_L-*t*′ can be hypothesized to generate homodimeric V_L-V_L-combining sites. However, the stable homodimeric IgV_{L2}-*t* derivative containing its two V_L domains was devoid of catalytic activity, supporting attribution of catalysis to the unpaired V_L domain. No natural Igs with an unpaired, functionally active V_L domain are known. In extant organisms, the closest functional homolog of the unpaired catalytic V_L domain are certain jawed fish and camelid Igs containing a single V_H domain, which is thought to bind antigen in its unpaired state (41, 42). The V_L and V_H domains express appreciable sequence identity with each other, and modern Igs have likely evolved by duplication and sequence diversification of a common primordial gene encoding the Ig fold (43). The phylogenic origin of Ig catalysis and deterioration or improvement of the catalytic function over the course of evolution of the immune system remains to be examined.

Electrophilic compounds that react irreversibly with the active site of serine proteases inhibited the Aβ hydrolyzing activity and formed irreversible complexes with the catalytic IgVs. This suggests a nucleophilic catalytic mechanism as deduced for other proteolytic Igs from inhibitor, mutagenesis, and crystallography studies (7, 9, 10). Protein nucleophilic reactivity is generated by intramolecular activation reactions within dyads and triads formed by precisely positioned amino acids, *e.g.* by hydrogen bonding between the Ser hydroxyl side chain and an imidazole nitrogen. Even small, sub-Å side chain movements can weaken the bonding and induce loss of active site nucleophilic reactivity. Noncovalent antigen binding, on the other hand, is mediated by weak and more numerous interactions at several contact residues in Ig-combining sites (1). Loss of any single contact because of a minor conformational change may weaken noncovalent antigen binding, but an abrupt transition from the binding state to a nonbinding state is less likely. Molecular modeling of the single domain IgV_L-*t*′ 5D3 suggested the likelihood of minor structural perturbations upon pairing the catalytic V_L domain with another V domain, helping explain the poor catalytic activity of the scFv-*t* and homodimeric IgV_{L2}-*t* versions of the molecule. Compared with the suppressive effect of V_L-V_H and V_L-V_L pairing, the catalytic activity of the single domain V_L was tolerant to inclusion of the C-terminal κ constant domain. This is significant, because it opens the route to inclusion of C-terminal moieties that reduce IgV clearance, *e.g.* polyethylene glycol or the Ig Fc fragment (44–46). Engineering stable catalyst versions with sufficient longevity *in vivo* is an important goal for clinical applications. scFv-*t* constructs have short half-lives in peripheral blood (47), and in view of their small size, the IgVs may also be subject to rapid clearance *In vivo*. Another route to prolonging the lifetime of IgVs is their recloning within the physiological IgG scaffold (48). The two domain IgV_{L2}-*t* 2E6 is a heterodimeric structure that should allow development of a IgG-like structure with a combining site formed by the two V_L domains.

Drugs currently employed to treat AD do not arrest the underlying pathology and progressive cognitive decline. Aβ oligomer accumulation is thought to be a major cause of neuronal death and dysfunction in the AD brain (49, 50). Small amounts of peripherally infused Aβ binding monoclonal IgGs traverse the blood-brain barrier, and IgG-facilitated Aβ clearance has emerged as a novel therapeutic strategy with the potential to halt cognitive decline in AD patients (51). Reversibly binding IgGs can at best bind two antigen molecules. Large quantities of stoichiometrically binding monoclonal IgGs are usually required for immunotherapy. Catalytic Igs hold the potential of clearing Aβ efficiently by virtue of the specific Aβ degrading activity. For example, from its k_{cat} value in Table 1, a single IgV_L-*t*′ 5D3 molecule is predicted to digest 4320 Aβ molecules in 3 days at excess Aβ concentration. The enzyme neprilysin has received attention as a potential Aβ-clearing AD drug (52). The k_{cat} of neprilysin for Aβ is comparable with the IgVs reported here (53). Neprilysin, however, also hydrolyzes irrelevant polypeptides (54), whereas the IgVs did not degrade

Downloaded from www.jbc.org by guest, on April 28, 2010

PAGE 57/92 * RCVD AT 4/28/2010 6:45:45 PM [Eastern Daylight Time] * SVR:USPTO-EFXRF-6/33 * DNIS:2738300 * CSID:7132705361 * DURATION (mm-ss):48-00

Supplemental Material can be found at: http://www.jbc.org/content/suppl/2008/11/04/M805786200.DC1.html

non-Aβ polypeptides detectably. Aβ degradation by an IgM at a substantially lower rate than the IgVs was previously reported to inhibit Aβ aggregation and Aβ-induced neurotoxicity (18). The IgVs hydrolyze the His^{14}–Gln^{15} bond and, at lower levels, other peptide bonds located in the central Aβ region. The aggregability of various synthetic Aβ fragments is generally weaker than full-length Aβ (55–57), but the precise functional effects of IgV-catalyzed Aβ hydrolysis remain to be examined. Concerns have been raised that Aβ binding IgGs can induce inflammation (58) and vascular microhemorrhages (59, 60) caused, respectively, by immune complex-stimulated release of microglial inflammatory mediators and IgG-stimulated Aβ deposition in cerebral blood vessels. The IgVs reported here do not form immune complexes detectably. They degrade Aβ permanently, minimizing the risks of inflammatory mediator release and Aβ re-deposition in the vascular wall. The recently reported phase II clinical trial of a reversibly binding anti-Aβ monoclonal IgG in patients with mild-to-moderate AD patients highlights the importance of searching for safer and more effective immunotherapeutic reagents (61). A dose-limiting incidence of vasogenic edema in magnetic resonance images was evident in this trial. At lower doses of the IgG, cognitive performance tended to improve, but the effect did not reach statistical significance in the intent-to-treat population. However, upon exclusion of patients homozygous for the apolipoprotein E4 allele, post-hoc analysis suggested significantly improved cognitive functions in the remaining patient subgroup. The apolipoprotein E4 allele is known to predispose AD patients to increased amyloid accumulation (62).

In summary, the specific and efficient Aβ degrading activity of the IgVs supports evaluation of their efficacy and safety in attaining Aβ clearance. The potential medical utility of catalytic Igs to microbial antigens and cancer-associated antigens has been discussed previously (28), but the low catalytic rate constants of physiological Igs have been a barrier to their clinical application. Our observations suggest that enhanced catalysis can be achieved by placing the V_L domains within non-physiological two domain and single domain scaffolds. If this finding proves generally applicable, development of efficient catalysts specific for other clinically important antigens should be feasible.

Acknowledgment—We thank Karine Huard for technical assistance.

REFERENCES

1. Davies, D. R., Padlan, E. A., and Sheriff, S. (1990) *Annu. Rev. Biochem.* **59**, 439–473
2. Paul, S., Volle, D. J., Beach, C. M., Johnson, D. R., Powell, M. J., and Massey, R. J. (1989) *Science* **244**, 1158–1162
3. Lacroix-Desmazes, S., Moreau, A., Sooryanarayana, Bonnemain, C., Stieltjes, N., Pashov, A., Sultan, Y., Hoebeke, J., Kazatchkine, M. D., and Kaveri, S. V. (1999) *Nat. Med.* **5**, 1044–1047
4. Shuster, A. M., Gololobov, G. V., Kvashuk, O. A., Bogomolova, A. E., Smirnov, I. V., and Gabibov, A. G. (1992) *Science* **256**, 665–667
5. Krasnorutskii, M. A., Buneva, V. N., and Nevinsky, G. A. (2008) *J. Mol. Recognit.* **21**, 233–242
6. Kohen, F., Hollander, Z., Burd, J. F., and Boguslaski, R. C. (1979) *FEBS Lett.* **100**, 137–140
7. Paul, S., Tramontano, A., Gololobov, G., Zhou, Y. X., Taguchi, H., Karle, S., Nishiyama, Y., Planque, S., and George, S. (2001) *J. Biol. Chem.* **276**, 28314–28320
8. Hifumi, E., Mitsuda, Y., Ohara, K., and Uda, T. (2002) *J. Immunol. Methods* **269**, 283–298
9. Gao, Q. S., Sun, M., Rees, A. R., and Paul, S. (1995) *J. Mol. Biol.* **253**, 658–664
10. Ramsland, P. A., Terzyan, S. S., Cloud, G., Bourne, C. R., Farrugia, W., Tribbick, G., Geysen, H. M., Moomaw, C. R., Slaughter, C. A., and Edmundson, A. B. (2006) *Biochem. J.* **395**, 473–481
11. Oleksyszyn, J., Boduszek, B., Kam, C. M., and Powers, J. C. (1994) *J. Med. Chem.* **37**, 226–231
12. Planque, S., Bangale, Y., Song, X. T., Karle, S., Taguchi, H., Poindexter, B., Bick, R., Edmundson, A., Nishiyama, Y., and Paul, S. (2004) *J. Biol. Chem.* **279**, 14024–14032
13. White, A. R., and Hawke, S. H. (2003) *J. Neurochem.* **87**, 801–808
14. Schenk, D., Hagen, M., and Seubert, P. (2004) *Curr. Opin. Immunol.* **16**, 599–606
15. Solomon, B., Koppel, R., Frankel, D., and Hanan-Aharon, E. (1997) *Proc. Natl. Acad. Sci. U. S. A.* **94**, 4109–4112
16. Deane, R., Sagare, A., Hamm, K., Parisi, M., LaRue, B., Guo, H., Wu, Z., Holtzman, D. M., and Zlokovic, B. V. (2005) *J. Neurosci.* **25**, 11495–11503
17. DeMattos, R. B., Bales, K. R., Cummins, D. J., Dodart, J. C., Paul, S. M., and Holtzman, D. M. (2001) *Proc. Natl. Acad. Sci. U. S. A.* **98**, 8850–8855
18. Taguchi, H., Planque, S., Nishiyama, Y., Symersky, J., Boivin, S., Szabo, P., Friedland, R. P., Ramsland, P. A., Edmundson, A. B., Weksler, M. E., and Paul, S. (2008) *J. Biol. Chem.* **283**, 4714–4722
19. Liu, R., McAllister, C., Lyubchenko, Y., and Sierks, M. R. (2004) *Biochemistry* **43**, 9999–10007
20. Nishiyama, Y., Taguchi, H., Luo, J. Q., Zhou, Y. X., Burr, G., Karle, S., and Paul, S. (2002) *Arch. Biochem. Biophys.* **402**, 281–288
21. Nishiyama, Y., Karle, S., Planque, S., Taguchi, H., and Paul, S. (2007) *Mol. Immunol.* **44**, 2707–2718
22. Rondot, S., Koch, J., Breitling, F., and Dubel, S. (2001) *Nat. Biotechnol.* **19**, 75–78
23. Ko, J. K., and Ma, J. (2005) *Am. J. Physiol.* **288**, C1273–C1278
24. McLean, G. R., Nakouzi, A., Casadevall, A., and Green, N. S. (2000) *Mol. Immunol.* **37**, 837–845
25. Rosenfeld, J., Capdevielle, J., Guillemot, J. C., and Ferrara, P. (1992) *Anal. Biochem.* **203**, 173–179
26. Sun, M., Gao, Q. S., Kirnarskiy, I., Rees, A., and Paul, S. (1997) *J. Mol. Biol.* **271**, 374–385
27. Brunger, A. T., Adams, P. D., Clore, G. M., DeLano, W. L., Gros, P., Grosse-Kunstleve, R. W., Jiang, J. S., Kuszewski, J., Nilges, M., Pannu, N. S., Read, R. J., Rice, L. M., Simonson, T., and Warren, G. L. (1998) *Acta Crystallogr. Sect. D. Biol. Crystallogr.* **54**, 905–921
28. Hanson, C. V., Nishiyama, Y., and Paul, S. (2005) *Curr. Opin. Biotechnol.* **16**, 631–636
29. Björk, I., and Tanford, C. (1971) *Biochemistry* **10**, 1280–1288
30. Powers, J. C., Asgian, J. L., Ekici, O. D., and James, K. E. (2002) *Chem. Rev.* **102**, 4639–4750
31. Nishiyama, Y., Mitsuda, Y., Taguchi, H., Planque, S., Hara, M., Karle, S., Hanson, C. V., Uda, T., and Paul, S. (2005) *J. Mol. Recognit.* **18**, 295–306
32. Dodson, G., and Wlodawer, A. (1998) *Trends Biochem. Sci.* **23**, 347–352
33. Thayer, M. M., Olender, E. H., Arvai, A. S., Kolke, C. K., Canestrelli, I. L., Stewart, J. D., Benkovic, S. J., Getzoff, E. D., and Roberts, V. A. (1999) *J. Mol. Biol.* **291**, 329–345
34. Rao, G., and Philipp, M. (1991) *J. Protein Chem.* **10**, 117–122
35. Dijkstra, B. W., and Matthews, R. G. (2003) *Curr. Opin. Struct. Biol.* **13**, 706–708
36. Chakrabarti, R., Klibanov, A. M., and Friesner, R. A. (2005) *Proc. Natl. Acad. Sci. U. S. A.* **102**, 10153–10158
37. Mei, S., Mody, B., Eklund, S. H., and Paul, S. (1991) *J. Biol. Chem.* **266**, 15571–15574
38. Kanyshkova, T. G., Semenov, D. V., Khlimankov, D., Buneva, V. N., and Nevinsky, G. A. (1997) *FEBS Lett.* **416**, 23–26
39. Harris, D. L., King, E., Ramsland, P. A., and Edmundson, A. B. (2000) *J. Mol. Recognit.* **13**, 198–212
40. Edmundson, A. B., Ely, K. R., Herron, J. N., and Cheson, B. D. (1987) *Mol.*

PAGE 58/92 * RCVD AT 4/28/2010 6:45:45 PM [Eastern Daylight Time] * SVR:USPTO-EFXRF-6/33 * DNIS:2738300 * CSID:7132705361 * DURATION (mm-ss):48-00

Downloaded from www.jbc.org by guest, on April 28, 2010

Supplemental Material can be found at:
http://www.jbc.org/content/suppl/2008/11/04/M806786200.DC1.html

Immunol. **24**, 915–935
41. Dooley, H., and Flajnik, M. F. (2006) *Dev. Comp. Immunol.* **30**, 43–56
42. De Genst, E., Saerens, D., Muyldermans, S., and Conrath, K. (2006) *Dev. Comp. Immunol.* **30**, 187–198
43. Hood, L., Campbell, J. H., and Elgin, S. C. (1975) *Annu. Rev. Genet.* **9**, 305–353
44. Kubetzko, S., Balic, E., Waibel, R., Zangemeister-Wittke, U., and Pluckthun, A. (2006) *J. Biol. Chem.* **281**, 35186–35201
45. Powers, D. B., Amersdorfer, P., Poul, M., Nielsen, U. B., Shalaby, M. R., Adams, G. P., Weiner, L. M., and Marks, J. D. (2001) *J. Immunol. Methods* **251**, 123–135
46. Dumont, J. A., Low, S. C., Peters, R. T., and Bitonti, A. J. (2006) *BioDrugs* **20**, 151–160
47. Yang, K., Basu, A., Wang, M., Chintala, R., Hsieh, M. C., Liu, S., Hua, J., Zhang, Z., Zhou, J., Li, M., Phyu, H., Petti, G., Mendez, M., Janjua, H., Peng, P., Longley, C., Borowski, V., Mehlig, M., and Filpula, D. (2003) *Protein Eng.* **16**, 761–770
48. Coloma, M. J., Hastings, A., Wims, L. A., and Morrison, S. L. (1992) *J. Immunol. Methods* **152**, 89–104
49. Dahlgren, K. N., Manelli, A. M., Stine, W. B., Jr., Baker, L. K., Krafft, G. A., and LaDu, M. J. (2002) *J. Biol. Chem.* **277**, 32046–32053
50. Knobloch, M., Farinelli, M., Konietzko, U., Nitsch, R. M., and Mansuy, I. M. (2007) *J. Neurosci.* **27**, 7648–7653
51. Dodel, R. C., Du, Y., Depboylu, C., Hampel, H., Frolich, L., Haag, A., Hemmeter, U., Paulsen, S., Teipel, S. J., Brettschneider, S., Spottke, A., Nolker, C., Moller, H. J., Wei, X., Farlow, M., Sommer, N., and Oertel, W. H. (2004) *J. Neurol. Neurosurg. Psychiatry* **75**, 1472–1474
52. El-Amouri, S. S., Zhu, H., Yu, J., Marr, R., Verma, I. M., and Kindy, M. S. (2008) *Am. J. Pathol.* **172**, 1342–1354
53. Tucker, H. M., Kihiko-Ehmann, M., and Estus, S. (2002) *J. Neurosci. Res.* **70**, 249–255
54. Howell, S., Nalbantoglu, J., and Crine, P. (1995) *Peptides (Elmsford)* **16**, 647–652
55. Hosia, W., Griffiths, W. J., and Johansson, J. (2005) *J. Mass Spectrom.* **40**, 142–145
56. Barrow, C. J., Yasuda, A., Kenny, P. T., and Zagorski, M. G. (1992) *J. Mol. Biol.* **225**, 1075–1093
57. Forloni, G., Tagliavini, F., Buglani, O., and Salmona, M. (1996) *Prog. Neurobiol.* **49**, 287–315
58. Lue, L. F., and Walker, D. G. (2002) *J. Neurosci. Res.* **70**, 599–610
59. Burbach, G. J., Vlachos, A., Ghebremedhin, E., Del Turco, D., Coomaraswamy, J., Staufenbiel, M., Jucker, M., and Deller, T. (2007) *Neurobiol. Aging* **28**, 202–212
60. Morgan, D. (2005) *Neurodegener. Dis.* **2**, 261–266
61. Grundman, M., and Black, R. (2008) In *International Conference on Alzheimer's Disease, July 26–31, 2008*, Chicago, Abstr. O3-04-05, Elsevier, St. Louis
62. Schmechel, D. E., Saunders, A. M., Strittmatter, W. J., Crain, B. J., Hulette, C. M., Joo, S. H., Pericak-Vance, M. A., Goldgaber, D., and Roses, A. D. (1993) *Proc. Natl. Acad. Sci. U. S. A.* **90**, 9649–9653

Downloaded from www.jbc.org by guest, on April 28, 2010

PAGE 59/92 * RCVD AT 4/28/2010 6:45:45 PM [Eastern Daylight Time] * SVR:USPTO-EFXRF-6/33 * DNIS:2738300 * CSID:7132705361 * DURATION (mm-ss):48-00

THE JOURNAL OF BIOLOGICAL CHEMISTRY
© 2003 by The American Society for Biochemistry and Molecular Biology, Inc.
Vol. 278, No. 22, Issue of May 30, pp. 20429–20435, 2003
Printed in U.S.A.

Specific HIV gp120-cleaving Antibodies Induced by Covalently Reactive Analog of gp120*

Received for publication, January 27, 2003, and in revised form, March 26, 2003
Published, JBC Papers in Press, March 28, 2003, DOI 10.1074/jbc.M300870200

Sudhir Paul‡, Stephanie Planque, Yong-Xin Zhou, Hiroaki Taguchi, Gita Bhatia, Sangeeta Karle, Carl Hanson§, and Yasuhiro Nishiyama

From the Chemical Immunology Research Center, Department of Pathology, University of Texas, Houston Medical School, Houston, Texas 77030 and §Viral and Rickettsial Disease Lab, California Department of Health Services, Richmond, California 94804

We report the results of efforts to strengthen and direct the natural nucleophilic activity of antibodies (Abs) for the purpose of specific cleavage of the human immunodeficiency virus-1 coat protein gp120. Phosphonate diester groups previously reported to form a covalent bond with the active site nucleophile of serine proteases (Paul, S., Tramontano, A., Gololobov, G., Zhou, Y. X., Taguchi, H., Karle, S., Nishiyama, Y., Planque, S., and George, S. (2001) *J. Biol. Chem.* 276, 28314–28320) were placed on Lys side chains of gp120. Seven monoclonal Abs raised by immunization with the covalently reactive analog of gp120 displayed irreversible binding to this compound (binding resistant to dissociation with the denaturant SDS). Catalytic cleavage of biotinylated gp120 by three monoclonal antibodies was observed. No cleavage of albumin and the extracellular domain of the epidermal growth factor receptor was detected. Cleavage of model peptide substrates occurred on the C-terminal side of basic amino acids, and K_m for this reaction was ~200-fold greater than that for gp120 cleavage, indicating Ab specialization for the gp120 substrate. A hapten phosphonate diester devoid of gp120 inhibited the catalytic activity with exceptional potency, confirming that the reaction proceeds via a serine protease mechanism. Irreversible binding of the hapten phosphonate diester by polyclonal IgG from mice immunized with gp120 covalently reactive analog was increased compared with similar preparations from animals immunized with control gp120, indicating induction of Ab nucleophilicity. These findings suggest the feasibility of raising antigen-specific proteolytic antibodies on demand by covalent immunization.

Promiscuous cleavage of small peptide substrates is a heritable function of Abs[1] encoded by germ line gene variable domains (for review, see Ref. 1). Peptide bond cleaving Abs with specificity for individual polypeptides have been identified in patients with autoimmune (1) and alloimmune disease (2). Specific monoclonal Abs and Ab light chain subunits displaying proteolytic activities can be raised by routine immunization with polypeptides (3, 4). Under ordinary circumstances, however, adaptive maturation of the catalytic activity may not be a favored event. B cell clonal selection occurs by sequence diversification of genes encoding the Ab variable domains followed by selective binding of the antigen to cell surface Abs with the greatest affinity, which drives proliferation of the B cells (5). Catalysis entails chemical transformation of the antigen and release of products from the Ab, which may cause cessation of B cell proliferation when the catalytic rate exceeds the rate of transmembrane signaling necessary to stimulate cell proliferation.

Originally developed as irreversible inhibitors of conventional serine proteases, haptenic phosphonate esters are reported to bind the nucleophilic sites of natural proteolytic Abs covalently (6, 7). The haptenic phosphonates could potentially serve as covalently reactive analogs (CRAs) for inducing the synthesis of Abs with improved nucleophilicity. To the extent that Ab nucleophilicity is rate-limiting in proteolysis, its enhancement may permit more rapid peptide bond cleavage, *i.e.* if the subsequent steps in the catalytic reaction cycle (hydrolysis of the acyl-Ab complex and product release) do not pose significant energetic hurdles (see Fig. 1). The innate character of Ab nucleophilic reactivity is the central element of this approach, and there is no requirement for *de novo* formation of chemically reactive sites over the course of variable domain sequence diversification. Most previous attempts to program the structure of catalytic sites in Abs in comparison have relied on noncovalent stabilization of the oxyanionic transition state (*i.e.* by immunization with transition state analogs; Refs. 8 and 9). An Ab with esterase activity (10) and another with aldolase activity (11) utilize covalent catalytic mechanisms, but the relationship of these activities to innate Ab nucleophilicity is unclear.

An ideal antigen-specific proteolytic Ab may be conceived to combine traditional noncovalent binding interactions in the ground state of the Ab-antigen complex with nucleophilic attack on the peptide backbone. The ground state interactions are desirable to obtain specificity for individual polypeptide antigens. No impediments for catalysis are presented by the stable ground state complexes, provided the noncovalent interactions are carried over into the transition state complex and are properly coordinated with nucleophilic attack at the reaction center. In theory, synthesis of antigen-specific proteolytic Abs could be induced by an analog that presents a mimetic of the chemical reaction center in the context of classical antigenic epitopes available for noncovalent binding interactions. If the reaction proceeds by a lock-and-key stereochemical mech-

* This work was supported by National Institutes of Health Grants AI46029 and AI31268. The costs of publication of this article were defrayed in part by the payment of page charges. This article must therefore be hereby marked "*advertisement*" in accordance with 18 U.S.C. Section 1734 solely to indicate this fact.

‡ To whom correspondence should be addressed: Chemical Immunology Research Center, Dept. of Pathology, MSB 2.250, 6431 Fannin, University of Texas, Houston Medical School, Houston, TX 77030. Tel.: 713-500-5347; Fax: 713-500-0574; E-mail: Sudhir.Paul@uth.tmc.edu.

[1] The abbreviations used are: Ab, antibody; mAb, monoclonal Ab; Bt, biotin; CRA, covalently reactive antigen analog; MCA, methylcoumarinamide; VIP, vasoactive intestinal peptide; HIV, human immunodeficiency virus; exEGFR, extracellular domain of enhanced green fluorescent protein; ELISA, enzyme-linked immunosorbent assay.

Downloaded from www.jbc.org by guest, on April 28, 2010

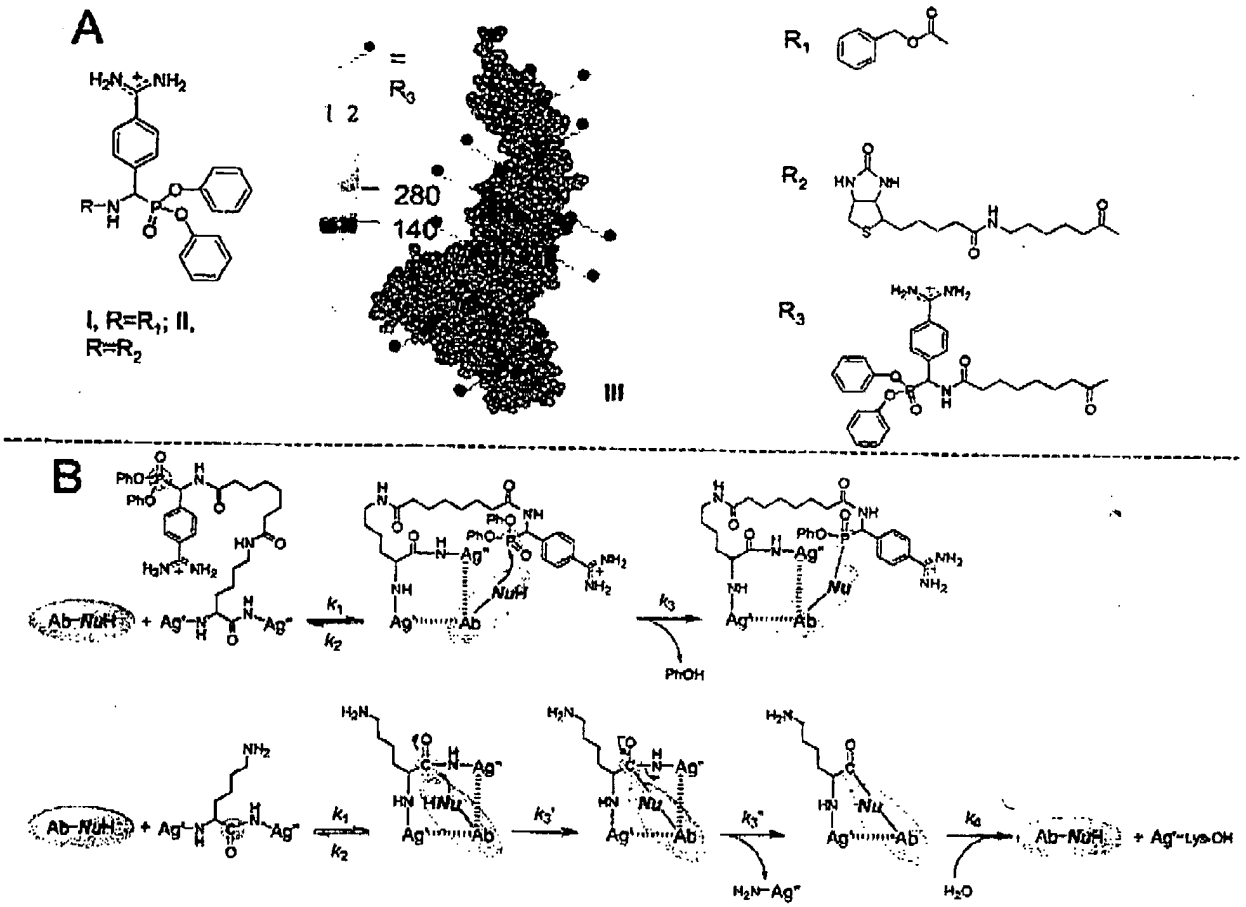

FIG. 1. **CRA structures (*A*) and their reaction with Abs (*B*). III** is a schematic representation of gp120 with R3 substituents at Lys residues. Left of **III** are streptavidin-peroxidase stained blots of SDS-electrophoresis gels showing biotinylated **III** containing 4 mol (*lane 1*) and 14 mol (*lane 2*) of phosphonate diester groups/mol gp120. *B*: *Nu*, nucleophile; Ag'-Lys-OH, N-terminal antigen fragment; NH_2-Ag", C-terminal antigen fragment; k_{cat} = k3' + k3". A catalytic Ab forms the initial noncovalent complex by conventional epitope-paratope interactions. The active site nucleophile attacks the carbonyl carbon of the scissile bond in Ag^{a+} (substrate) to form the tetrahedral transition-state complex. The C-terminal antigen fragment is released, and the acyl-Ab complex is formed. Hydrolysis of the acyl-Ab complex results in release of the N-terminal antigen fragment and regeneration of the catalytic Ab. The reaction with phosphonate-containing Ag^{a+} recapitulates the interactions in the ground and transition state Ab-Ag^{a+} complexes (noncovalent binding at peptide epitopes and nucleophilic attack by the Ab), but unlike the acyl-Ab intermediate, the phosphonyl-Ab adduct is a stable product. A potential weakness is that immunogen **III** does not contain structural features favoring synthesis of Abs capable of rapid hydrolysis of the acyl-Ab intermediate and product release (*bottom reaction scheme*).

anism, the mimetic must be located precisely at the position of the intended scissile bond in the backbone of the polypeptide antigen. In the instance of large proteins, locating the mimetic within the protein backbone is outside the range of present-day synthetic technologies. A potential solution is to place the mimetic group at amino acid side chains using chemical linker techniques. An Ab nucleophile that recognizes the side chain mimetic could facilitate proteolysis if it enjoys sufficient conformational freedom to approach the polypeptide backbone of the substrate and form the acyl-Ab complex (see Fig. 1).

We describe here the characteristics of Abs induced by a CRA of the HIV-1 coat protein gp120 (gp120-CRA) consisting of phosphonate diester groups located in Lys side chains of the protein. Enhanced serine protease-like nucleophilic reactivity of the Abs was observed. One monoclonal Ab cleaved gp120 slowly and specifically, it displayed preference for cleavage on the C-terminal side of Lys/Arg residues, and the catalytic reaction was susceptible to CRA inhibition. These findings are the first indications that Abs with proteolytic activity specific for individual proteins can be raised on demand.

MATERIALS AND METHODS

Hapten, gp120-CRAs, and Biotinylated Proteins—Synthesis of hapten CRAs I and II (see Fig. 1) and their characterization by electrospray ionization-mass spectroscopy and elemental analyses have been described previously (12). For preparation of gp120-CRA **III**, the precursor diphenyl-*N*-[*O*-(3-sulfosuccinimidyl)suberoyl]amino-(4amidinophenyl)methanephosphonate (**IV**) was synthesized by mixing a solution of diphenylamino(4-amidinophenyl)methanephosphonate (79 mg, 0.13 mmol) in *N,N*-dimethylformamide (2 ml) containing *N,N*-diisopropylethylamine (0.11 ml, 0.63 mmol) and bis(sulfosuccinimidyl)suberate disodium salt (150 mg, 0.26 mmol; Pierce) for 2 h. **IV** was obtained by reversed-phase high performance liquid chromatography (12) and lyophilized to give a colorless powder (yield 54%, 50 mg; *m/z* 715 (MH+) by electrospray ionization mass spectroscopy). **IV** (1.1 mg) was reacted with electrophoretically pure gp120 (0.5 mg; Immunodiagnostic Inc., MN strain, purified from baculovirus expression system) in 5 ml of 10 mM HEPES, 25 mM NaCl, 0.1 mM CHAPS, pH 7.5 buffer (2 h, 25 °C). Excess **IV** was removed by gel filtration (Micro Bio-Spin 6 disposable column, Bio-Rad), and the concentration of free amines in the initial protein and CRA-derivitized protein was measured using fluorescamine (13). The density of labeling was varied as needed from 4.0 to 32.6 mol of CRA/mol of gp120 by varying the concentration of **IV**. Preparation of gp120 labeled at Lys residues with biotin (Bt-gp120) was

Downloaded from www.jbc.org by guest, on April 28, 2010

by similar means using 6-biotinamidohexanoic acid *N*-hydroxysuccinimide ester (Sigma). The reaction time and reactant concentrations were controlled to yield biotin/gp120 molar ratios 0.8–1.9. Unreacted biotinylation reagent was removed using a disposable gel filtration column in 50 mM Tris-HCl, 100 mM glycine, 0.1 mM CHAPS, pH 7.8. The biotin content was determined using 2-(4′-hydroxyazobenzene)benzoic acid (14). Total protein measurements were done using the BCA method (Pierce kit). Biotinylated **III** was prepared from Bt-gp120 as described for **III**. With increasing incorporation of the hapten groups, biotinylated **III** tended to form dimers and trimers evident in SDS electrophoresis gels as bands at ~ 240 and 380 kDa (nominal mass of monomer gp120, 120 kDa). Biotinylated **III** at hapten density similar to the non-biotinylated **III** employed as immunogen (23 mol/mol of gp120) contained the monomer, dimer, and trimer species at proportions of 50, 21, and 29%, respectively. Protein-CRAs were lyophilized and stored at −20 °C until used. Bt-gp120 was stored at −70 °C in 50 mM Tris-HCl, pH 8.0, 0.1 M glycine, 0.1 mM CHAPS. Storage of **I** and **II** was at −70 °C as 10 mM solutions in *N,N*-dimethylformamide. The extracellular domain of EGFR (exEGFR) obtained from Dr. Maureen O'Connor (15) was biotinylated as described for gp120 (0.9 mol of biotin/mol of exEGFR).

Antibodies—mAbs were prepared from female MRL/MpJ-Fas^{lpr} mice (The Jackson Laboratory, Bar Harbor, ME; 4–5 weeks) immunized with gp120-CRA **III** (23 mol of phosphonate diester/mol of gp120). The mice were injected intraperitoneally on days 0, 14, and 28 days with gp120-CRA **III** (11 μg) in Ribi adjuvant (monophosphoryl lipid A + trehalose dicorynomycolate emulsion; Sigma) followed by a fourth intravenous booster without adjuvant on day 55. Blood was obtained from the retroorbital plexus over the course of the immunization schedule. Three days after the final injection, hybridomas were prepared by fusion of splenocytes with myeloma cell line (NS-1; Ref. 3). After identification of wells secreting the desired Abs by ELISA, monoclonal cell lines were prepared by two rounds of cloning by limiting dilution. Monoclonal IgG was prepared from tissue culture supernatants containing mAbs (200 ml) by affinity chromatography on immobilized protein G (3). Control mAbs (anti-VIP clone c28.5 and anti-yellow fever virus antigen clone CRL 1689; ATCC) and serum IgG were purified similarly. The IgG preparations were electrophoretically homogeneous, determined by silver staining of overloaded IgG and immunoblotting with specific Abs to mouse IgG (3). Additional immunizations of female BALB/c mice (Jackson; 4–5 weeks) with gp120 or gp120-CRA were carried out similarly. mAb heavy and light chain isotypes were determined by ELISA as described (3).

ELISA—Maxisorp 96-well microtiter plates (Nunc) were coated with gp120 or gp120-CRA (40–100 ng/well) in 100 mM bicarbonate buffer, pH 8.6. Routine ELISAs were carried out as described (16). For assay of irreversible binding, the Abs were allowed to bind the plates, and the wells were treated for 30 min with 2% SDS in 10 mM sodium phosphate, 137 mM NaCl, 2.7 mM KCl, 0.05% Tween 20, pH 7.4 (PBS-Tween) or PBS-Tween without SDS (control wells for measurement of total binding). The wells were then washed three times with PBS-Tween, and bound IgG was determined as usual using a peroxidase conjugate of goat anti-mouse IgG (Fc-specific; Sigma). Observed values of binding were corrected for nonspecific binding in wells containing nonimmune IgG or nonimmune mouse serum ($A_{490} < 0.03$). Percent residual binding in SDS-treated wells was computed as (A_{490}, SDS-treated wells) × 100/(A_{490}, PBS-Tween-treated wells).

Electrophoresis of Ab-CRA Complexes—Irreversible binding of biotinylated CRAs by purified IgG was determined by denaturing electrophoresis (6). Briefly, the reaction mixtures were incubated at 37 °C in 50 mM Tris-HCl, 0.1 M glycine, pH 8.0. SDS was added to 2%, and the mixtures were boiled (5 min) and then subjected to SDS-PAGE (4–20%, Bio-Rad, or 8–25% Phast gels, Amersham Biosciences). After electroblotting onto nitrocellulose membranes (0.22 μm, Bio-Rad), the membranes were blocked with 5% skim milk in PBS-Tween and processed for detection of IgG or biotin using peroxidase-conjugated goat anti-mouse IgG (Sigma) or peroxidase-conjugated streptavidin, respectively. Imaging and quantification were using x-ray film (Eastman Kodak Co.) with Unscan-it software (Silk scientific, Orem, UT) or a Fluoro-STM MultiImager (Bio-Rad). Biotinylated bovine serum albumin (11 mol of biotin/mol of bovine serum albumin; Sigma) was employed to construct a standard curve (0.06–1.5 pmol of biotin/lane).

Hydrolysis Assays—Biotinylated proteins were incubated with IgG in 50 mM Tris-HCl, 0.1 M glycine, 0.1 mM CHAPS, pH 8, at 37 °C, the reaction was terminated by addition of SDS to 2%, and the samples were boiled (5 min) and then analyzed by reducing SDS-gel electrophoresis (4–20%, Bio-Rad). Biotin containing protein bands in blots of the gel were identified and quantified as in the preceding section. In some blots, reaction products were identified by immunoblotting using peroxidase-conjugated goat anti-gp120 Abs (Fitzgerald, Concord, MA; catalog #60-H14) (16). N-terminal sequencing of protein bands from electrophoresis gels was done as described previously (17). Hydrolysis of peptide-MCA substrates (Peptide International, Louisville, KY or Bachem Biosciences, King of Prussia, PA) was determined in 96-well plates by fluorimetric detection of aminomethylcoumarin (Varian Cary Eclipse; λ_{ex} 360 nm, λ_{em} 470 nm) with authentic aminomethylcoumarin as standard (6). Cleavage of [Tyr$^{10-126}$I]VIP by mAb c23.5 was measured as the radioactivity rendered soluble in trichloroacetic acid (17). Kinetic parameters for cleavage of increasing concentrations of peptide-MCA substrates were determined from the Michaelis-Menten equation, $v = (V_{max}[S])/(K_m + [S])$. Because of the expense of studying gp120 cleavage at large concentrations of the protein, K_d ($-K_m$) and k_{cat} for this reaction were obtained from the general quadratic equation (17) $[CS]^2 - [CS]([C_t] + [S_t] + K_d) + [C_t][S_t] = 0$, where $[C_t]$ and $[S_t]$ are the total concentrations of catalyst and substrate, and [CS] is the catalyst-substrate concentration. The method consists of calculation of [CS] at a series of assumed K_d values. The assumed K_d value yielding the best fit (by linear regression) between the observed reaction velocity and [CS] represents the experimentally determined K_d. k_{cat} is computed as the slope of the observed velocity *versus* [CS] plot.

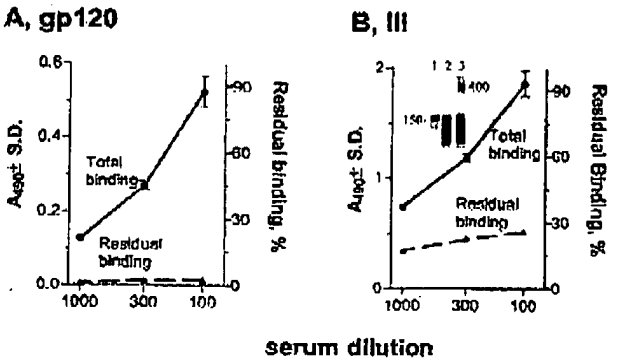

FIG. 2. **Irreversible III binding by polyclonal Abs.** *A*, immobilized gp120. *B*, immobilized **III**. Shown are ELISA values for binding of polyclonal Abs in serum of mice hyperimmunized with **III** (pooled sera, $n = 4$ mice). Binding of nonimmune mouse serum was negligible (A_{490} of 1:100 nonimmune serum in 0.001 (*A*) and −0.002 (*B*)). Residual and total binding represent A_{490} values in wells treated with and without SDS, respectively. *Inset*, anti-IgG stained blot of SDS-electrophoresis gels showing **III** (0.3 μM) treated for 48 h with nonimmune IgG (*lane 2*, 0.1 μM) and anti-**III** IgG (*lane 3*, 0.1 μM). Large Ab-containing adducts are evident at ~ 400 kDa in *lane 3*. *Lane 1* is a shorter exposure of *lane 2* showing a well defined 150-kDa band at the position of the smear evident in overexposed *lanes 2* and *3*.

RESULTS

gp120-CRA Design and Validation—Synthesis of hapten CRAs **I** and **II** (Fig. 1) and their covalent reactivity with naturally occurring proteolytic Abs has been described previously (6, 7). The electrophilic phosphonate mimics the peptide bond carbonyl group susceptible to nucleophilic attack, the positively charged amidino group adjacent to the phosphonate diester serves as a mimic of Lys/Arg P1 residues at which cleavage by germ line-encoded proteolytic Abs is observed (6), and the biotin group in **I** permits sensitive detection of Ab-phosphonate adducts. gp120-CRA **III** contains phosphonate diester groups in spatial proximity with antigenic epitopes presented by the protein. Multiple phosphonate diester groups were available per molecule of gp120, allowing presentation of the electrophilic hapten in conjunction with diverse antigenic epitopes.

Robust polyclonal Ab responses in MRL/lpr and BALB/c mice immunized with **III** were observed by routine ELISA. Abs raised to **III** were bound at somewhat greater levels by immobilized **III** than control gp120 devoid of phosphonate diester groups (Fig. 2). Conversely, Abs raised to control gp120 recognized immobilized **III**, but the binding was 3–4-fold lower than by immobilized gp120 (*e.g.* at serum dilution of 1:1000, A_{490} 0.44 ± 0.03 for immobilized **III** and 1.40 ± 0.03 for immobilized

Downloaded from www.jbc.org by guest, on April 28, 2010

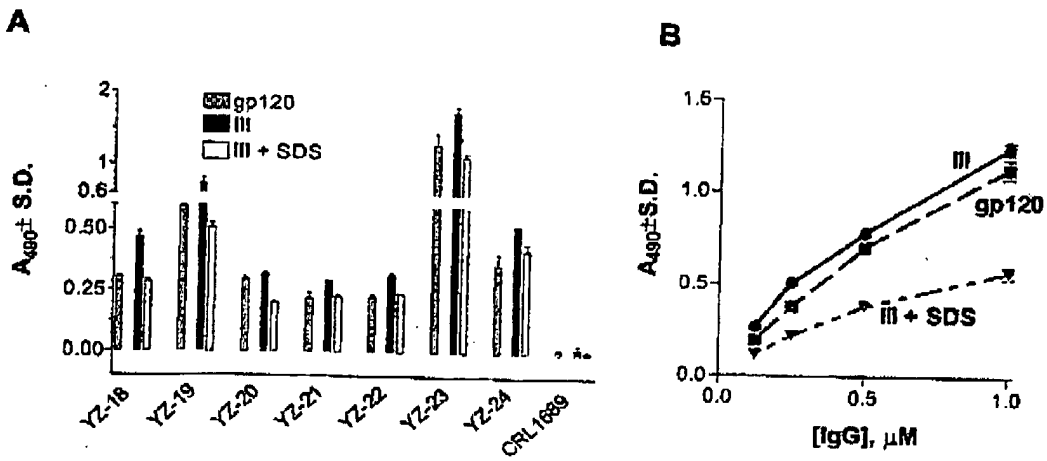

FIG. 3. **Irreversible III binding by monoclonal Abs.** ELISA showing SDS-resistant III binding by tissue culture supernatants containing mAbs (YZ series) (*A*) and monoclonal IgG purified from clone YZ18 (*B*) raised by immunization with gp120-CRA III. mAb CRL 1689 is an irrelevant monoclonal IgG with same isotype as mAbs YZ21 and YZ23. Immobilized antigens are gp120 and III. SDS-resistant III binding is indicated by *bars* and the curve labeled III + SDS.

gp120). III binding by nonimmune Abs was negligible, indicating that indiscriminate covalent binding at the hapten groups was not a problem. The observed differences in the antigenic reactivity of gp120 and III were held to be sufficiently small to proceed with further Ab studies. To facilitate high throughput screening, the feasibility of measuring irreversible III binding by Abs was studied by ELISA. After binding of polyclonal Abs anti-III Abs to the immobilized antigens, ELISA plates were treated with the denaturant SDS to remove reversibly bound Abs. SDS treatment allowed essentially complete removal of anti-III Abs bound by control gp120 devoid of hapten phosphonate groups. In comparison, 13–40% of the overall anti-III Ab binding activity consistently remained bound to immobilized III after SDS treatment in three repeat experiments. SDS-electrophoresis and immunoblotting with Abs to mouse IgG confirmed formation of irreversible Ab-III complexes in boiled reaction mixtures (Fig. 2*B*, *inset*, *lane 3*, estimated mass from extrapolated standard curve of molecular mass standards, ~400 kDa; large complexes can be formed by binding of multiple Abs to hapten groups in III).

Catalytic Activity—mAbs were prepared from MRL/lpr mice immunized with gp120-CRA III. This mouse strain develops lupus-like autoimmune disease attributable to the dysfunctional Fas-receptor gene. Spontaneous development of proteolytic Abs (18) and increased synthesis of esterase Abs in response to immunization with phosphonate monoester haptens (19, 20) have been reported in this mouse strain. Supernatants from 712 hybridoma wells (two splenocyte-myeloma cell fusions) were screened for SDS-resistant binding to III. IgG from seven wells was positive for this activity. After cloning of the cells by limiting dilution, monoclonal IgG from the supernatants of the seven cell lines was purified, and the binding assays were repeated (Fig. 3; clones YZ18, IgG2a,κ; YZ19, IgG2b,κ; YZ20, IgG2a,κ; YZ21, IgG2a,κ; YZ22, IgG2a,κ; YZ23, IgG2a,κ, and YZ24, IgG1,κ). Of total binding observed without SDS treatment of the ELISA plates, residual binding after the detergent treatment was 43–83% in 4 repeat assays. All seven mAbs were also bound by gp120 devoid of hapten CRA groups determined by routine ELISA without SDS treatment, indicating that they are not directed to neoepitopes generated by chemical modification procedures used for III preparation. An irrelevant mAb (clone CRL 1689) displayed no detectable binding of III or gp120.

Of seven mAbs with irreversible III binding activity, slow

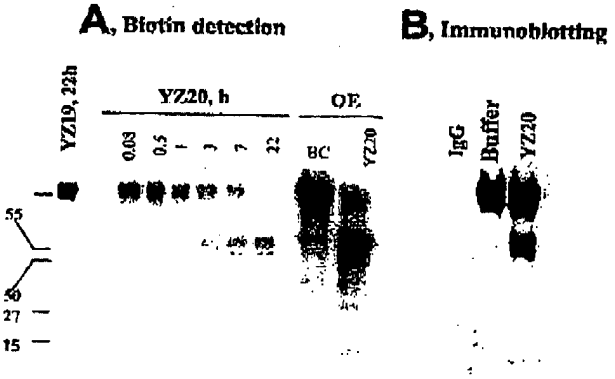

FIG. 4. **Cleavage of Bt-gp120 by mAb YZ20.** *A*, streptavidin peroxidase-stained blot of SDS-electrophoresis gels showing time-dependent Bt-gp120 cleavage by mAb YZ20 and lack of cleavage by mAb YZ19 (22 h incubation). IgG, 1 μM; Bt-gp120, 0.2 μM. *OE*, overexposed lanes showing Bt-gp120 incubated for 22 h in diluent and with YZ20 IgG (1 μM). Product bands at 27 and 15 kDa are visible in addition to the major 50–55 kDa bands. *B*, anti-gp120-peroxidase stained blot of SDS-electrophoresis gel showing gp120 (1 μM) incubated with diluent or YZ20 IgG (1 μM, 24 h).

cleavage of Bt-gp120 by three mAbs was detected (YZ18, YZ20, YZ24), determined by the appearance of biotin-containing fragments of the protein in SDS-electrophoresis gels. The electrophoretic pattern of Bt-gp120 cleaved by mAbs YZ18 and YZ24 were similar to that shown for mAb YZ20 in Fig. 4. mAb YZ20 was further studied as it cleaved Bt-gp120 ~5-fold more rapidly than the other two mAbs. The consumption of gp120 was time-dependent (Fig. 4*A*). Major biotin-containing cleavage products with apparent mass 55 and 50 kDa were observed along with less intensely stained bands at 27 and 15 kDa. A band at 35 kDa was visible in overexposed gels, but this does not represent a product of mAb cleavage, as it was present at similar density in control incubations of Bt-gp120 in diluent. A control-irrelevant mAb (clone CRL 1689) did not cleave Bt-gp120. Immunoblotting using polyclonal anti-gp120 Abs confirmed that non-biotinylated gp120 is also susceptible to cleavage by the mAb (55-kDa cleavage product, Fig. 4*B*). Both detection methods allow quantification of gp120 cleavage by measuring depletion of intact gp120. Neither method provides guidance about the complete product profile or product concen-

Downloaded from www.jbc.org by guest, on April 28, 2010

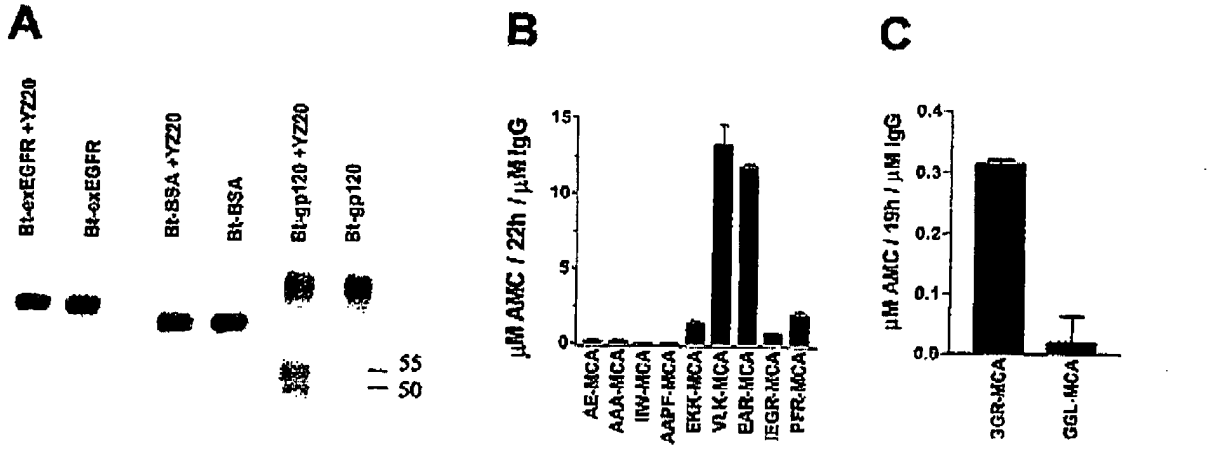

FIG. 5. **Lack of cleavage of Bt-bovine serum albumin (*BSA*) and Bt-exEGFR by mAb YZ20 (*A*) and preferential cleavage at basic residues (*B* and *C*).** *A*, streptavidin peroxidase-stained blots of biotinylated proteins (0.2 μM) incubated with mAb YZ20 (1 μM, 24 h). *B*, fluorimetric determination of mAb YZ20 (0.5 μM) catalyzed cleavage of peptide-MCA (*AMC*) substrates (200 μM, 22 h). *C*, cleavage of GGR-MCA and GGL-MCA by mAb YZ20 (0.5 μM). Concentration of both substrates was held at 12.5 μM because of limited solubility of Gly-Gly-Leu-MCA. Blocking groups at the N termini of the substrates were: succinyl, AE-MCA, AAA-MCA, AAPF-MCA, IIW-MCA; *t*-butyloxycarbonyl, EKK-MCA, VLK-MCA, IEGR-MCA, EAR-MCA; benzyloxycarbonyl, GGR-MCA, GGL-MCA. Values are the means of three replicates ± S.D.

tration, because Bt-gp120 contains minimal amounts of biotin (~1 mol/molgp120), and the polyclonal Abs used for immunoblotting do not react equivalently with the cleavage products.

mAb YZ20 did not cleave biotinylated bovine serum albumin or the extracellular domain of the epidermal growth factor (exEGFR), indicating selectivity for gp120 (Fig. 5*A*). Attempts to identify the bonds cleaved by mAb YZ20 were unsuccessful. N-terminal sequencing of the 55- and 50-kDa bands yielded identical sequences (TEKLWVTVYY), corresponding to the N-terminal residues of gp120. Sequencing of the 15-kDa band from the YZ20 reaction mixture did not yield detectable phenylthiohydantoin derivatives of amino acids, possibly because of a blocked N terminus. Identification of the 27-kDa gp120 fragment is complicated because of its comigration with the Ab light chain in reducing gels. Because identification of the precise bonds in gp120 cleaved by the mAb was not central to the present study, we turned to the use of model peptide substrates for determination of scissile bond preferences. A fluorimetric assay was employed to determine mAb-catalyzed cleavage of the amide bond linking aminomethylcoumarin to the C-terminal amino acid in a panel of peptide-MCA substrates (Fig. 5*B*). The peptide-MCA substrates were used at excess concentration (200 μM), permitting detection of even weakly cross-reactive catalytic Abs. Selective cleavage at Arg-MCA and Lys-MCA was observed, with no evident cleavage on the C-terminal side of neutral or acidic residues. To confirm that the rate differences are because of recognition of the basic residue at the cleavage site (as opposed to remote residues), we studied two tripeptide substrates identical in sequence except for the N-terminal residue at the scissile bond, Gly-Gly-Arg-MCA and Gly-Gly-Leu-MCA. The former substrate was cleaved at detectable levels by Ab YZ20 (0.31 ± 0.01 (S.D.) μM aminomethylcoumarin/19 h/μM IgG), whereas the fluorescence intensity in reaction mixtures of the latter substrate and the Ab was statistically indistinguishable from background values observed in assay diluent (0.02 ± 0.04 μM MCA/19 h/μM IgG; $p > 0.05$; student's *t* test, unpaired; Fig. 5*C*). The basic residue preference is consistent with the presence of positively charged amidino groups neighboring the phosphonate groups in the immunogen (III) and selective cleavage on the C-terminal side of Arg/Lys residues by germ line-encoded proteolytic Abs observed previously (21, 22).

Attainment of the desired catalytic properties, *i.e.* the ability to combine high affinity for individual antigens with rapid turnover, can be judged from the K_m and k_{cat} parameters (mol of antigen cleaved/mol of Ab/unit time). The K_m of mAb YZ20 for Bt-gp120 was about 200-fold smaller than its preferred peptide-MCA substrate (EAR-MCA; Table I; single letter code for amino acids), consistent with development of specificity for gp120 by immunization with III. Twelve mol of EAR-MCA were cleaved per mol of mAb YZ20 over the course of the reaction (22 h), indicating that the mAb is capable of turnover, a defining feature of a catalyst. Turnover of Bt-gp120 was ~10-fold lower than that of EAR-MCA. Previously, conventional non-Ab serine proteases were reported to cleave short peptide more rapidly than large proteins (23), presumably because the former substrates are more readily accessible to the catalytic site.

TABLE I
Kinetic parameters for cleavage of Bt-gp120 and Boc-EAR-MCA by MAb YZ20

IgG (1 μM) was incubated with Bt-gp120 (0.14–2.2 μM; 18 h) or Boc-EAR-MCA 31 (1000 μM, 6 h). Cleavage of Bt-gp120 was determined by measuring depletion of the 120-kDa intact protein band on SDS-gels run in duplicate and of EAR-MCA by fluorimetry in triplicate. Kinetic parameters for Bt-gp120 cleavage were computed using the general quadratic equation describing a one-site binding interaction and, for EAR-MCA, by fitting the data to the Michaelis-Menten equation (see "Materials and Methods").

Antigen	K_m	k_{cat}	k_{cat}/K_m
	M	min^{-1}	$M^{-1}\ min^{-1}$
Bt-gp120	2.0×10^{-6}	$3.4 \pm 0.1 \times 10^{-8}$	1.7×10^{8}
EAR-MCA	$4.0 \pm 1.2 \times 10^{-4}$	$3.3 \pm 0.4 \times 10^{-2}$	8.4×10^{1}

Nucleophilic Reactivity—gp120 hydrolysis by mAb YZ20 was inhibited by hapten CRA II (Fig. 6), confirming the serine protease-like character of the mAb. II inhibition of mAb YZ20 cleavage of gp120 was 90-fold more potent than inhibition of mAb c23.5 cleavage of VIP (IC_{50}, 0.4 and 36.0 μM, respectively). The latter mAb was obtained by immunization with VIP devoid of phosphonate diester groups (3). Superior reactivity of the hapten CRA with mAb YZ20 is consistent with the conclusion of strengthened Ab nucleophilicity in response to immunization with phosphonate groups present in the gp120-CRA immunogen.

To confirm induction of nucleophilicity, irreversible hapten CRA I binding by polyclonal IgG was measured. The hapten

Downloaded from www.jbc.org by guest, on April 28, 2010

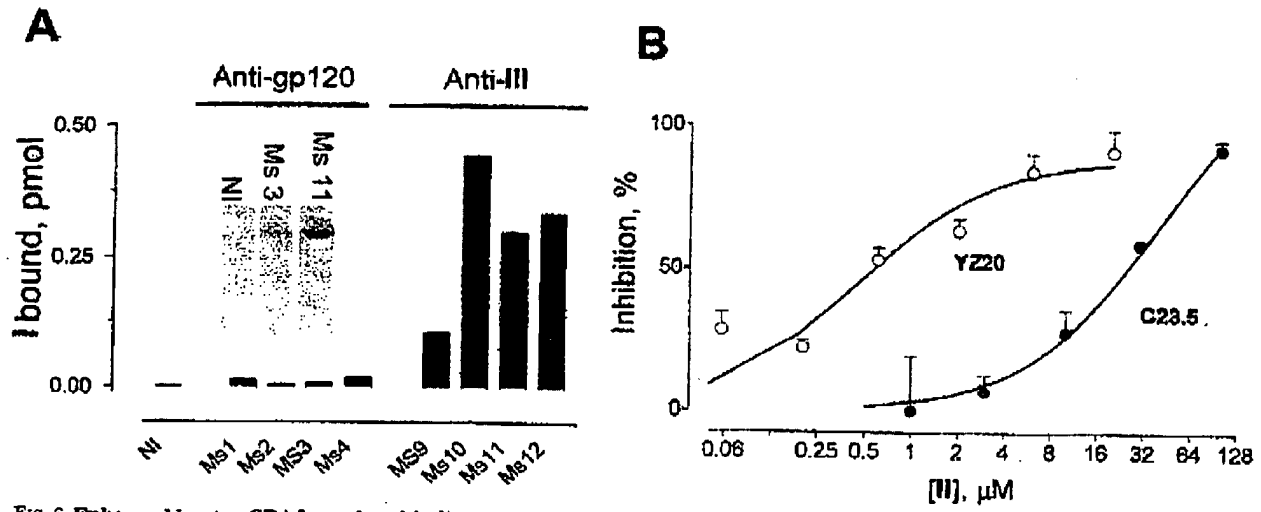

FIG. 6. **Enhanced hapten CRA I covalent binding by polyclonal IgG from mice immunized with III (*A*) and potent inhibition of mAb YZ20 cleavage of Bt-gp120 by hapten CRA II (*B*).** *A*, binding of hapten CRA I (10 μM), determined by incubation with IgG (0.4 μM) from BALB/c mice immunized with III (Ms9–12) or control gp120 (Ms1–4) for 60 min, SDS-electrophoresis, and quantification of the biotin-containing band at 150 kDa. *NI*, nonimmune IgG (pooled from 20 mice). *Inset*, representative SDS-electrophoresis lanes showing hapten CRA I binding by IgG from a mouse immunized with III (*Ms11*), a mouse immunized with gp120 (*Ms3*), and nonimmune IgG (*NI*). *B*, Bt-gp120 (0.1 μM) cleavage by mAb YZ20 (1 μM, 4 h) and [Tyr^{10}-^{125}I]VIP (~100 pM, 45,000 cpm) cleavage by mAb c23.5 (20 nM, 18 h) were measured in the presence of increasing II concentrations. In the absence of II, 15 and 40% of available Bt-gp120 and VIP, respectively, were cleaved.

CRA does not contain antigenic epitopes belonging to gp120, and noncovalent binding interactions are not anticipated to contribute to its irreversible binding by Abs. IgG samples from all four mice immunized with III displayed superior I binding compared with IgG from mice immunized with control gp120 (mean values, 0.31 and 0.01 pmol I; $p < 0.02$, Student's t test, unpaired observations) as well as pooled nonimmune IgG (Fig. 6). BALB/c mice were studied in this immunization. It may be concluded that synthesis of nucleophilic Abs in response to immunization with III is not restricted to autoimmune hosts (mAbs to gp120-CRA III were prepared from MRL/lpr mice).

DISCUSSION

The goal of this study was to strengthen the intrinsic serine protease-like reactivity of Abs and direct the reactivity to cleavage of gp120. Improved irreversible binding of hapten CRA by Abs after immunization with gp120-CRA III was evident, and the hapten CRA was a potent inhibitor of gp120 cleavage by a mAb. These observations suggest adaptive improvement of Ab nucleophilicity induced by the phosphonate diester groups. Specificity of the Abs for gp120 was obtained by traditional noncovalent mechanisms, *i.e.* recognition of gp120 epitopes located in the proximity of the phosphonate diester groups. No cleavage of unrelated proteins by the gp120-cleaving mAb was observed, and the K_m value of cleavage of a model peptide was 200-fold greater than of gp120 cleavage, indicating the absence of indiscriminate proteolysis.

Proteolysis entails Ab attack on the backbone of gp120, whereas the phosphonate electrophiles are located in Lys side chains of the immunogen. Because mAbs raised to gp120-CRA displayed proteolytic activity, the nucleophile developed to recognize the side chain electrophiles must enjoy sufficient conformational freedom to attack the polypeptide backbone. Movements of individual amino acids in Ab combining sites after binding to antigen have been reported (24, 25). Epitope mapping and mutagenesis studies of certain proteolytic Abs indicate that the catalytic residues do not participate in stabilization of the Ab-antigen ground state complex (26, 27), suggesting that the mobility of the nucleophile may not be restricted by initial noncovalent Ab-antigen interactions. Naturally occurring mAbs to VIP (17) and gp41 (4) cleave multiple peptide bonds in these antigens, which may be explained by hypothesizing formation of alternate transition states in which the nucleophile is free to initiate nucleophilic attack on spatially neighboring peptide bonds (for review, see Ref. 28). Understanding the extent of conformational freedom of Ab nucleophiles is important, because there is no viable alternative to locating the peptide bond mimetic in the side chains when large proteins must be used to induce the synthesis of catalytic Abs. In addition to direct structural analysis of nucleophile movements in available catalytic Abs, the length and flexibility of the linker utilized to attach the phosphonate groups at Lys side chains can be varied in future studies to assess the flexibility of the catalytic site. In the case of synthetic peptide immunogens, the phosphonate groups can be incorporated within the peptide backbone to better mimic the intended scissile bond (7). However, synthetic peptides often fail to assume conformations similar to their cognate determinants in full-length proteins, in which case anti-peptide Abs do not recognize the parent proteins.

The fully competent catalytic machinery found in modern non-Ab serine proteases has presumably evolved in response to selection pressures that optimized each of the rate-limiting steps in the catalytic cycle. In comparison, a CRA immunogen can at best select for Abs with the greatest covalent attack capability. No selection for hydrolysis of the acyl-Ab complex or the subsequent product release steps is anticipated, which may account for observations of limited Ab turnover. Two previous attempts to raise esterase Abs indicated the formation of irreversible substrate binding by Abs (29, 30), suggesting the need to optimize events occurring after nucleophilic attack by the Abs. Furthermore, structural refinements of the immunogen could be implemented to help guide the Ab-antigen complex toward the catalytic pathway, *e.g.* inclusion of a component that binds a water molecule and facilitates hydrolysis of the acyl-protein complexes. Notwithstanding this weakness, the results reported here represent a significant advance toward developing antigen-specific proteolytic Abs. Previously, several Abs with haptenic ester-hydrolyzing activity have been raised

Downloaded from www.jbc.org by guest, on April 28, 2010

based on the premise that catalytic sites capable of noncovalent stabilization of the oxyanionic transition states can be formed *de novo* over the course of adaptive sequence diversification of Ab variable domains (8, 9). This approach has not been successful for development of proteolytic Abs. Pollack *et al.* (31) describe the failure of a phosphonate monoester analog of Phe-Leu-Ala to induce proteolytic Ab synthesis. No attempt was made in this study to recruit the intrinsic properties of natural Abs for the purpose of protease synthesis, *i.e.* their nucleophilicity and selective recognition of basic residues adjacent to the cleavage site. Recently, phosphonate monoesters were discovered to form covalent bonds with nucleophiles in serine proteases, but their reactivity is weaker than the diester used in the present study, and no detectable reaction occurs unless an adjacent positive charge is present (6, 12).

Evidence for increased potency because of the catalytic function has recently been published in regard to Ab antagonism of the biological effects of VIP, a 28-amino acid neuropeptide (32, 33). Concerning gp120, a major hurdle has been to induce the synthesis of Abs that recognize the determinants involved in viral entry, *i.e.* the binding sites for host CD4 and chemokine receptors. Most Abs raised to monomer gp120 are directed to its variable region epitopes, and the Abs do not neutralize diverse HIV-1 strains found in different geographical locations (34). Reversibly binding Abs must bind at or near the receptor binding sites of gp120 to sterically hinder HIV entry into host cells. Proteolytic Abs offer the potential advantage of gp120 inactivation even if cleavage occurs at a site that does not itself participate in binding to host cells. Discussion of the immunotherapeutic potential of mAbs to gp120-CRA **III** is beyond the scope of the present study, but initial HIV-1 neutralization studies suggest that certain mAbs raised to gp120-CRA **III** neutralize the HIV-1 primary isolate ZA009 (peripheral blood mononuclear cell cultures; infection was measured by determining p24 antigen concentrations).[2] A potential pitfall is that proteolytic Abs to monomer gp120-CRA may not recognize trimeric gp120 on the surface of HIV-1, as observed for reversibly binding Abs to the protein (35). The CRA immunogen techniques described in the present study are readily applicable to recently developed recombinant mimetics of trimeric gp120 (36) as well as whole HIV-1 particles.

Acknowledgment—We thank the Monoclonal Antibody Core Facility of the University of Nebraska for preparing hybridomas.

REFERENCES

1. Tramontano, A., Golobov, G., and Paul, S. (2000) in *Chemical Immunology: Catalytic Antibodies* (Paul, S., ed) Vol. 77, pp. 1–17, S. Karger GmbH, Basel, Switzerland
2. Lacroix-Desmazes, S., Moreau, A., Sooryanarayana-Bonnemain, C., Stieltjes, N., Pashov, A., Sultan, Y., Hoebeke, J., Kazatchkine, M. D., and Kaveri, S. V. (1999) *Nat. Med.* 5, 1044–1047
3. Paul, S., Sun, M., Mody, R., Tewary, H. K., Stemmer, P., Massey, R. J., Gianferrara, T., Mehrotra, S., Dreyer, T., Makini, M., and Tramontano, A. (1992) *J. Biol. Chem.* 267, 13142–13145
4. Hifumi, E., Okamoto, Y., and Uda, T. (1999) *J. Biosci. Bioengin.* 88, 323–327
5. Nossal, G. J. (2002) *Immunol. Rev.* 185, 15–23
6. Paul, S., Tramontano, A., Gololobov, G., Zhou, Y. X., Taguchi, H., Karle, S., Nishiyama, Y., Planque, S., and George, S. (2001) *J. Biol. Chem.* 276, 28314–28320
7. Taguchi, H., Burr, G., Karle, S., Planque, S., Zhou, Y. X., Paul, S., and Nishiyama, Y. (2002) *Bioorg. Med. Chem. Lett.* 12, 3167–3170
8. Tramontano, A., Janda, K. D., and Lerner, R. A. (1986) *Proc. Natl. Acad. Sci. U. S. A.* 83, 6736–6740
9. Schultz, P. G., and Lerner, R. A. (1995) *Science* 269, 1835–1842
10. Wagner, J., Lerner, R. A., and Barbas, C. F., III (1995) *Science* 270, 1797–1800
11. Zhou, G. W., Guo, J., Huang, W., Fletterick, R. J., and Scanlan, T. S. (1994) *Science* 265, 1059–1064
12. Nishiyama, Y., Taguchi, H., Luo, J. Q., Zhou, Y. X., Burr, G., Karle, S., and Paul, S. (2002) *Arch. Biochem. Biophys.* 402, 281–288
13. Udenfriend, S., Stein, S., Bohlen, P., Dairman, W., Leimgruber, W., and Weigele, M. (1972) *Science* 178, 871–872
14. Green, N. M. (1965) *Biochem. J.* 94, 23–24
15. Brown, P. M., Debanne, M. T., Grothe, S., Bergsma, D., Caron, M., Kay, C., and O'Connor-McCourt, M. D. (1994) *Eur. J. Biochem.* 225, 223–233
16. Karle, S., Nishiyama, Y., Zhou, Y. X., Luo, J., Planque, S., Hanson, C., and Paul, S. (2003) *Vaccine* 21, 1213–1218
17. Sun, M., Guo, Q. S., Kirnarskiy, L., Rees, A., and Paul, S. (1997) *J. Mol. Biol.* 271, 374–385
18. Bangale, Y., Karle, S., Zhou, Y. X., Lee, L., Kalaga, R., and Paul, S. (2003) *FASEB J.* 17, 628–636
19. Tawfik, D. S., Chap, R., Green, B. S., Sela, M., and Eshhar, Z. (1995) *Proc. Natl. Acad. Sci. U. S. A.* 92, 2146–2149
20. Sun, J., Takahashi, N., Kakinuma, H., and Nishi, Y. (2001) *J. Immunol.* 167, 5775–5785
21. Kalaga, R., Li, L., O'Dell, J. R., and Paul, S. (1995) *J. Immunol.* 155, 2695–2702
22. Gololobov, G., Sun, M., and Paul, S. (1999) *Mol. Immunol.* 36, 1215–1222
23. Noda, Y., Jajiwara, R., Yamamoto, K., Fukuno, T., and Segawa, S. I. (1994) *Biopolymers* 34, 217–226
24. Jimenez, R., Salazar, G., Baldridge, K. K., and Romesberg, F. E. (2003) *Proc. Natl. Acad. Sci. U. S. A.* 100, 92–97
25. Braden, B. C., and Poljak, R. J. (1995) *FASEB J.* 1, 9–16
26. Guo, Q. S., Sun, M., Rees, A., and Paul, S. (1995) *J. Mol. Biol.* 253, 658–664
27. Paul, S., Volle, D. J., Powell, M. J., and Massey, R. J. (1990) *J. Biol. Chem.* 265, 11910–11913
28. Paul, S. (1996) *Mol. Biotechnol.* 6, 197–207
29. Rao, G., and Philipp, M. (1991) *J. Protein Chem.* 10, 117–122
30. Lefèvre, S., Debat, H., Thomas, D., Friboulet, A., and Avalle, B. (2001) *FEBS Lett.* 489, 25–28
31. Pollack, S. J., Hsiun, P., and Schultz, P. G. (1989) *J. Am. Chem. Soc.* 111, 5961–5962
32. Berisha, H. I., Bratut, M., Bangale, Y., Colasurdo, G., Paul, S., and Said, S. I. (2002) *Pulm. Pharmacol. Ther.* 15, 121–127
33. Voice, J. K., Grinninger, C., Kong, Y., Bangale, Y., Paul, S., and Goetzl, E. J. (2003) *J. Immunol.* 170, 308–314
34. Moore, J., and Trkola, A. (1997) *AIDS Res. Hum. Retroviruses* 13, 733–736
35. Kwong, P. D., Doyle, M. L., Casper, D. J., Cicala, C., Leavitt, S. A., Majeed, S., Steenbeke, T. D., Venturi, M., Chaiken, I., Fung, M., Katinger, H., Parren, P. W., Robinson, J., Van Ryk, D., Wang, L., Burton, D. R., Freire, E., Wyatt, R., Sodroski, J., Hendrickson, W. A., and Arthos, J. (2002) *Nature* 420, 678–682
36. Kwong, P. D., Wyatt, R., Sattentau, Q. J., Sodroski, J., and Hendrickson, W. A. (2000) *J. Virol.* 74, 1961–1972

[2] S. Paul, S. Karle, and C. Hanson, unpublished information.

Downloaded from www.jbc.org by guest, on April 28, 2010

THE JOURNAL OF BIOLOGICAL CHEMISTRY VOL. 282, NO. 43, pp. 31250–31256, October 26, 2007
© 2007 by The American Society for Biochemistry and Molecular Biology, Inc. Printed in the U.S.A.

Towards Covalent Vaccination

IMPROVED POLYCLONAL HIV NEUTRALIZING ANTIBODY RESPONSE INDUCED BY AN ELECTROPHILIC gp120 V3 PEPTIDE ANALOG[*]

Received for publication, August 6, 2007, and in revised form, August 15, 2007 Published, JBC Papers in Press, August 29, 2007, DOI 10.1074/jbc.M706471200

Yasuhiro Nishiyama[‡1], Yukie Mitsuda[‡], Hiroaki Taguchi[‡], Stephanie Planque[‡], Maria Salas[§], Carl V. Hanson[§], and Sudhir Paul[‡2]

From the [‡]Chemical Immunology Research Center, Department of Pathology and Laboratory Medicine, University of Texas-Houston Medical School, Houston, Texas 77030 and the [§]Viral and Rickettsial Disease Laboratory, California Department of Public Health, Richmond, California 94804

Rare monoclonal antibodies (Abs) can form irreversible complexes with antigens by enzyme-like covalent nucleophile-electrophile pairing. To determine the feasibility of applying irreversible antigen inactivation by Abs as the basis of vaccination against microbes, we studied the polyclonal nucleophilic Ab response induced by the electrophilic analog of a synthetic peptide corresponding to the principal neutralizing determinant (PND) of human immunodeficiency virus type-1 (HIV) gp120 located in the V3 domain. Abs from mice immunized with the PND analog containing electrophilic phosphonates (E-PND) neutralized a homologous HIV strain (MN) ~50-fold more potently than control Abs from mice immunized with PND. The IgG fractions displayed binding to intact HIV particles. HIV complexes formed by anti-E-PND IgG dissociated noticeably more slowly than the complexes formed by anti-PND IgG. The slower dissociation kinetics are predicted to maintain long-lasting blockade of host cell receptor recognition by gp120. Pretreatment of the anti-PND IgG with a haptenic electrophilic phosphonate compound resulted in more rapid dissociation of the HIV-IgG complexes, consistent with the hypothesis that enhanced Ab nucleophilic reactivity induced by electrophilic immunization imparts irreversible character to the complexes. These results suggest that electrophilic immunization induces a sufficiently robust nucleophilic Ab response to enhance the anti-microbial efficacy of candidate polypeptide vaccines.

Antibodies (Abs)[3] that bind human immunodeficiency virus type 1 (HIV) with irreversible character are conceptually analogous to reagents with infinite binding affinity. Rare monoclonal Abs can form unusually stable immune complexes expressing covalent character (1, 2). The combining site of such monoclonal Abs is usually intended to replicate enzyme active sites. Immunization with an Ab to β-lactamase, for example, is reported to induce an anti-idiotypic monoclonal Ab that forms a covalent intermediate with a β-lactam compound that is sufficiently stable to be detected in denaturing electrophoresis gels (1). Monoclonal Abs raised to an analog of HIV gp120 containing electrophilic phosphonate diesters (E-gp120) form noncovalent immune complexes that are subsequently converted to irreversible complexes by nucleophile-electrophile interactions (2). In this example, stimulation with the electrophilic groups is suggested to strengthen the nucleophilic reactivity of Ab combining sites by the adaptive immunological processes that are also responsible for improved noncovalent binding, *i.e.* V-(D)-J gene recombination, somatic hypermutation and combinatorial diversification. B cell clonal selection is thought to be driven by binding of antigen to the B cell receptor (BCR), *i.e.* surface Ig complexed to signal transducing proteins. As irreversible binding should permit prolonged BCR occupancy, improvement of the nucleophilic reactivity over the course of adaptive B cell differentiation is feasible. The nucleophilic reactivity is reminiscent of enzymatic active sites, in which activated groups formed by intramolecular hydrogen bonding interactions acquire an ability to conduct nucleophilic attack at electron-deficient sites in substrates. For example, the nucleophilic reactivity of the Ser-His-Asp triad in serine proteases results in the formation of enzyme-substrate covalent reaction intermediates (3). Indeed, similar nucleophilic triads have been identified in monoclonal Ab combining sites by crystallography and mutagenesis studies (4–6). Completion of the catalytic cycle following the nucleophile-electrophile reaction requires various additional accessory groups in the active site. Consequently, some but not all nucleophilic Abs proceed to catalyze chemical reactions (7).

The ability to form long-lasting immune complexes can be anticipated to enhance the antigen inactivation potency of irreversibly binding Abs compared with their reversibly binding counterparts. This leads to the hypothesis that electrophilic antigen analogs can serve as the basis for vaccine formulations capable of inducing improved protective Ab responses to microbial antigens compared with conventional vaccines. The hypothetical improvement in vaccine formulation will depend

* This work was supported by National Institutes of Health Grants, R01AI058865, R01AI067020, R21AI062455, and R21AI071951. The costs of publication of this article were defrayed in part by the payment of page charges. This article must therefore be hereby marked "*advertisement*" in accordance with 18 U.S.C. Section 1734 solely to indicate this fact.

[1] To whom correspondence may be addressed: Chemical Immunology Research Center, Dept. of Pathology and Laboratory Medicine, University of Texas-Houston Medical School, 6431 Fannin, Houston, TX 77030. E-mail: Yasuhiro.Nishiyama@uth.tmc.edu.

[2] To whom correspondence may be addressed: Chemical Immunology Research Center, Dept. of Pathology and Laboratory Medicine, University of Texas-Houston Medical School, 6431 Fannin, Houston, TX 77030. E-mail: Sudhir.Paul@uth.tmc.edu.

[3] The abbreviations used are: Ab, antibody; Bt-, biotinamidohexanoyl; BCR, B cell receptor; E-gp120, gp120 analog containing electrophilic phosphonates; E-PND, principal neutralizing determinant analog containing electrophilic phosphonates; HIV, human immunodeficiency virus; PND, principal neutralizing determinant; $TCID_{50}$, 50% tissue culture infective dose.

PAGE 67/92 * RCVD AT 4/28/2010 6:45:45 PM [Eastern Daylight Time] * SVR:USPTO-EFXRF-6/33 * DNIS:2738300 * CSID:7132705361 * DURATION (mm-ss):48-00

Downloaded from www.jbc.org by guest, on April 28, 2010

on the proportion of the induced polyclonal Ab response that displays covalent character while maintaining the correct epitope specificity necessary for recognition of the native antigen structure. In previous studies using full-length E-gp120 as the immunogen, several monoclonal Abs were identified that formed unusually stable immune complexes with gp120 devoid of exogenously introduced electrophilic groups (2). However, full-length E-gp120 expresses a multitude of epitopes, and we were unable to relate Ab covalency and HIV neutralization because of the varying Ab epitope specificities. Moreover, a rigorous covalent ELISA protocol was employed to screen hybridoma supernatants. Consequently, there is no assurance that anything more than a small minority of the overall Ab response to E-gp120 expresses the desired covalent character of the monoclonal Abs.

The immune response following HIV infection is dominated by Abs to the principal neutralization determinant (PND) of gp120 corresponding to residues 306–328 located in the V3 domain (8–10). Immunization with the synthetic PND peptide induces Ab responses that neutralize HIV strains with sequences similar to the PND immunogen (11–14). Here, we studied the comparative HIV neutralizing and binding characteristics of polyclonal Ab preparations induced by an electrophilic analog of the PND peptide (E-PND) and the control PND peptide devoid of exogenously introduced electrophiles. We observed that immunization with E-PND induced Abs that neutralized HIV more potently and dissociated from intact HIV virions more slowly than control Abs from PND-immunized mice. These results indicate the improved antigen inactivation potency due to Ab nucleophilicity and suggest the utility of electrophilic immunization as a novel vaccination strategy.

EXPERIMENTAL PROCEDURES

PND Analogs—PND peptide **1a** corresponding to gp120 residues 306–328 of HIV strain MN (YNKRKRIHIGPGRAFYTT-KNIIG) and its biotinylated analog (Bt-PND **1b**) were prepared by Fmoc-based solid phase synthesis followed by purification with reversed phase HPLC (**1a**: observed *m/z* 2705.3; calcd *m/z* 2705.2. **1b**: observed *m/z* 3043.0; calcd *m/z* 3044.6; Genemed Synthesis, South San Francisco, CA). The electrophilic phosphonate analog of PND (E-PND **2a**) was prepared by acylation of **1a** with *N*-hydroxysuccinimidyl ester of diphenyl (suberoyl)amino(4-amidinophenyl)methanephosphonate as follows. PND **1a** (10 mg, 3.7 μmol) was allowed to react with the acylating agent (33 mg, 44 μmol) in dimethyl sulfoxide (6.6 ml) and 100 mM phosphate-buffered saline, pH 8 (4.0 ml) for 1 h. Excess acylating agent was quenched by addition of 1 M glycine (2 ml). 15 min thereafter, the precipitate was collected by centrifugation, washed with cold water (4 ml × 3), and subjected to HPLC purification (YMC-Pack ODS-AM, 4.6 × 250 mm; gradient of 10% to 80% acetonitrile in 0.05% trifluoroacetic acid/water, 45 min). This yielded chromatographically pure E-PND **2a** (5.4 mg, 31%), which was characterized by electrospray ionization mass spectrometry (observed *m/z*, 1594.5, 1196.5, 957.7; calcd *m/z* for $C_{295}H_{319}N_{51}O_{50}P_4$, 1595.1 (3+), 1196.6 (4+), 957.5 (5+)). Biotinylated E-PND (Bt-E-PND **2b**) was prepared from Bt-PND **1b** in the same manner (observed *m/z*, 1151.1, 921.3, 767.9; calcd *m/z* for $C_{223}H_{314}N_{51}O_{48}P_3S$, 1151.6 (4+), 921.5 (5+), 768.0 (6+).

Antibodies—Female MRL/lpr mice (n = 5/immunogen; Jackson Laboratory, Bar Harbor, ME; 8 weeks age) were immunized intraperitoneally on days 0, 15, 29, 44, 58, and 101 with PND **1a** or E-PND **2a** (50 μg for the first 4 injections and 200 μg for the last 2 injections) in RIBI adjuvant (monophosphoryl lipid A-trehalose dicorynomycolate emulsion; Sigma-Aldrich). Blood was obtained from the retroorbital plexus over the course of the immunization schedule (days 0, 15, 29, 44, 58, 65, and 111). Development of PND-reactive IgG was examined by ELISA using Bt-PND **1b** (4 μg/ml) immobilized on streptavidin-coated plates, sera diluted 1:5000 in 10 mM PBS containing 0.025% Tween 20 and 1% bovine serum albumin, and peroxidase-conjugated goat anti-mouse IgG (Fc specific; Sigma-Aldrich) as secondary Ab. IgG was purified to electrophoretic homogeneity from serum (prepared from blood collected 10 days after the last immunization) by affinity chromatography on protein-G Sepharose (GE Healthcare, Piscataway, NJ) (15).

HIV Neutralization—Neutralization of HIV (strain MN, clade B) by serially diluted sera or purified IgG samples was determined in a "microplaque" reduction assay using cells of the MT-2 T lymphocyte cell line as hosts (16). Neutralization of strain ZA009 (clade C) was measured by the p24 capsid protein assay with human peripheral blood mononuclear cells as hosts (17). Concentrations yielding 50 and 80% inhibition (IC_{50} and IC_{80}) were obtained from the least-square-fits to a sigmoidal dose-response shown in Equation 1.

$$\%\text{Neutralization} = \text{TOP}/(1 + 10^{((\log IC_{50} - X) \times \text{HillSlope})}) \quad \text{(Eq. 1)}$$

HIV Binding Assays—Purified IgG (17 μg/ml) and HIV (MN strain, 1.6×10^4 $TCID_{50}$/ml; $TCID_{50}$, 50% tissue culture infective dose) were incubated in a mixture of 10 mM phosphate-buffered saline, pH 7.4, and RPMI1640 (1:1) containing 10% fetal bovine serum at 4 °C for 16 h. HIV-IgG complexes (and free IgG) were captured on Protein G-Sepharose (100 μl of settled gel) using Bio-Spin chromatography columns (Bio-Rad), and unbound HIV removed by washing with the reaction buffer (500 μl × 8). The captured complexes were eluted with 100 mM glycine-HCl, pH 2.7 (400 μl), HIV was lysed with Triton X-100 (10%) and p24 in the lysates was measured with Coulter HIV-1 p24 Antigen Assay kit. Values were corrected for nonspecific HIV binding to the affinity gel, determined by identical processing of control HIV treated with diluent in the absence of IgG (A490, 0.21 ± 0.01). In competition experiments, IgG and HIV were incubated in the presence of excess PND peptide **1a** (50 μg/ml) or an irrelevant peptide (gp120 residues 465–479 of MN strain; NIH AIDS Research and Reference Reagent program), and HIV-IgG complexes were measured as above. To determine dissociation kinetics, HIV-IgG complexes were allowed to form for 16 h (IgG 50 μg/ml, HIV 1.6×10^4 $TCID_{50}$/ml), excess PND **1a** (50 μg/ml) was added to the reaction mixtures to preclude reassociation of any complexes undergoing dissociation. Aliquots of the reaction mixtures withdrawn 0.5, 2, 4, 8, and 14 h thereafter were immediately subjected to pro-

Downloaded from www.jbc.org by guest, on April 28, 2010

PAGE 68/92 * RCVD AT 4/28/2010 6:45:45 PM [Eastern Daylight Time] * SVR:USPTO-EFXRF-6/33 * DNIS:2738300 * CSID:7132705361 * DURATION (mm-ss):48-00

tein G chromatography and p24 assays to determine residual immune complexes as described above.

IgG Nucleophilic Reactivity—Bt-E-PND **2b** (1 μM) was incubated with IgG (75 μg/ml) for 2 h, the reaction mixtures were boiled, subjected to reducing SDS-electrophoresis, and the covalent adducts were detected by streptavidin-peroxidase staining of the blots as described previously (18). To study the role of IgG nucleophilic reactivity in HIV binding, the IgG (1.4 mg/ml) was treated with the haptenic phosphonate 3 (1 mM; diphenyl benzyloxycarbonylamino(4-amidinophenyl)methanephosphonate, synthesis described in ref 19) at room temperature for 13 h. After removing unreacted phosphonate by gel filtration (Bio-spin 6, Bio-Rad; IgG recovery 88%), the dissociation kinetics of the HIV-IgG complexes was studied as above.

RESULTS

Immunogenicity—The E-PND immunogen **2a** corresponds to the amino acid sequence of HIV gp120 residues 306–328 (MN strain) with 4 electrophilic phosphonate diester groups located at the side chains of Lys^{308}, Lys^{310}, and Lys^{324} residues and the N terminus (Fig. 1*A*). The phosphonate groups are structurally identical to those incorporated into full-length gp120 and other polypeptides in previous studies (7, 18, 20–22). The resultant electrophilic polypeptides bind nucleophilic sites in Abs covalently (18, 20–22). We employed multiple phosphonate groups within a single E-PND molecule to increase the probability of nucleophile-electrophile pairing coordinated with noncovalent binding at the proximate peptide regions. The control immunogen PND **1a** was the identical peptide structure devoid of the phosphonate groups. Successive immunizations of mice with E-PND **2a** or PND **1a** resulted in progressively increasing PND binding activity in serum IgG obtained over days 15 to 65 (mean A_{490} ± S.D. for 1:5000-diluted pooled sera using immobilized Bt-PND **1b** increased from 0.06 ± 0.10 to 0.71 ± 0.13 in **2a**-immunized mice and from 0.01 ± 0.01 to 0.42 ± 0.28 in **1a**-immunized mice; n = 5 mice each; preimmune mouse serum binding, 0.01 ± 0.01). ELISA assays using the final bleeds obtained on day 111 indicated that each of the mice had mounted an IgG response to PND (A_{490} values for sera from individual **2a**-immunized mice at 1:1000 dilution, 0.79 ± 0.01, 0.47 ± 0.03, 1.48 ± 0.01, 0.72 ± 0.02, 2.59 ± 0.09). These results indicate that Abs to E-PND can recognize PND devoid of the electrophilic groups.

HIV Neutralization—Pooled sera from the mice (day 111) were assayed for the ability to neutralize HIV strain MN (clade B, coreceptor CXCR4-dependent) using MT-2 host cells. Serially diluted sera were incubated with the virus and the infectivity was measured by the microplaque assay (16). Dose-dependent HIV neutralization was observed, with the sera from E-PND **2a**-immunized mice displaying 44–272-fold greater neutralizing potency compared with sera from PND **1a**–immunized mice (dilution yielding 50% neutralization, 1:787 *versus* 1:34,444; dilution yielding 80% neutralization, 1:54 *versus* 1:14,692; Fig. 1*B*). The consistency of the Ab response was confirmed by assaying neutralization by sera from individual E-PND **2a**-immunized mice and PND **1a**-immunized mice (Fig. 1*C*; n = 5 and 4 mice, respectively). Mean % neutralization ± S.D. values at 1:800 dilution of sera from the E-PND and PND groups were, respectively, 92 ± 18 and 25 ± 2%; p = 0.0002, unpaired t test, two-tailed. The superior neutralizing Ab response in E-PND **2a** immunization was confirmed using pooled IgG purified by affinity chromatography on protein G-Sepharose columns (Table 1). IgG from E-PND **2a**-immunized mice was 59-fold more potent than IgG from PND **1a**-immunized mice (IC_{50} values, respectively, 2 *versus* 118 μg/ml). Serum from E-PND or PND immunized mice at dilutions as low as 1:500 failed to neutralize the clade C strain ZA009 (core-

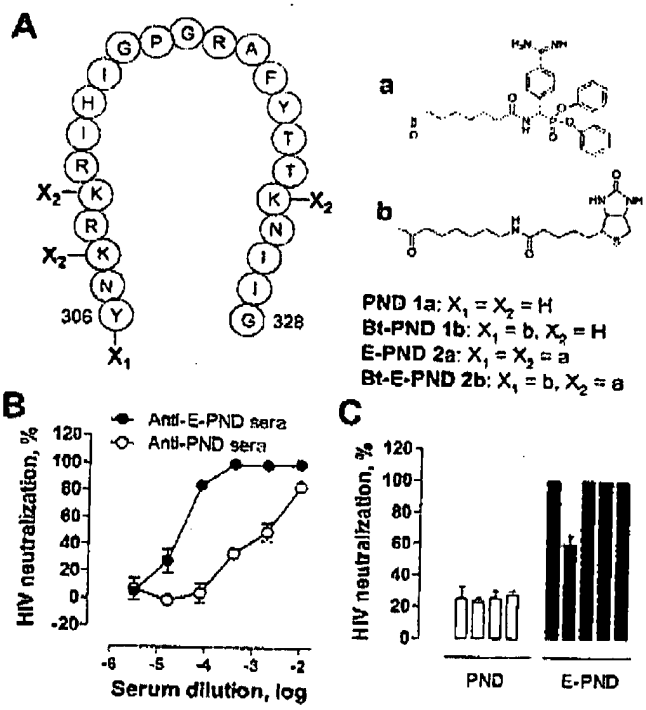

FIGURE 1. **HIV neutralizing activity.** *A*, immunogen structures. PND **1a** is the synthetic peptide corresponding gp120 residues 306–328 (MN strain). E-PND **2a** is an electrophilic analog of PND containing diphenyl amino(4-amidinophenyl)methanephosphonate groups (*a*) located at 3 Lys residues (Lys^{308}, Lys^{310}, Lys^{324}) and the N terminus. PND **1b** and E-PND **2b**, respectively, are **1a** and **2a** analogs with biotinamidohexanoyl (*b*) at the N terminus. *B*, HIV neutralization by pooled sera from mice immunized with E-PND and PND. Serially diluted pooled sera (n = 5 mice) obtained following hyperimmunization with E-PND **2a** or PND **1a** (day 111) were assayed for HIV neutralization activity by the microplaque assay using the clade B, CXCR4-dependent strain MN and MT-2 host cells (values are means ± S.E. of 4 replicates at each concentration studied in parallel). Number of plaques in the absence of sera was 27.7 ± 1.7/well. *C*, HIV neutralization by sera from individual mice immunized with E-PND **2a** or PND **1a**. Sera from the mice (day 111; 1:800 dilution) were assayed for HIV neutralization activity as in *panel B* (values are means ± S.E. of 4 replicates conducted in parallel). Number of plaques in the absence of sera was 24.8 ± 1.2/well.

TABLE 1

HIV neutralizing activity of anti-E-PND and anti-PND IgGs

Protein G-purified IgGs were assayed for HIV neutralization activity using the clade B X4 strain MN and MT-2 host cells. Concentrations yielding 50% and 80% neutralization (IC_{50} and IC_{80}) were obtained from dose response studies (four replicates at each concentration), with curve fitting as in Ref. 17.

IgG	IC_{50}	IC_{80}
	μg/ml	*μg/ml*
Preimmune	>463	>463
Anti-PND	118	362
Anti-E-PND	2	5

Downloaded from www.jbc.org by guest, on April 28, 2010

PAGE 69/92 * RCVD AT 4/28/2010 6:45:45 PM [Eastern Daylight Time] * SVR:USPTO-EFXRF-6/33 * DNIS:2738300 * CSID:7132705361 * DURATION (mm-ss):48-00

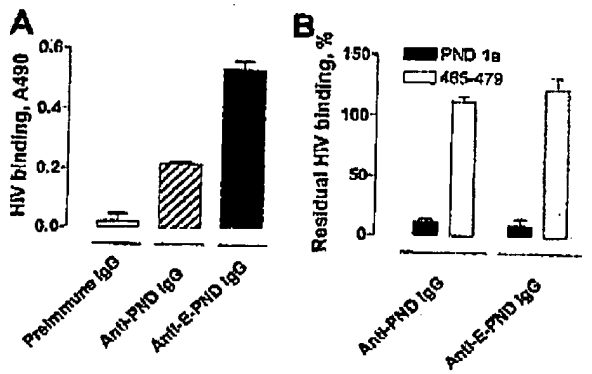

FIGURE 2. **Intact HIV-IgG binding.** *A*, HIV binding by anti-E-PND IgG and anti-PND IgG. IgG (17 μg/ml) and HIV (MN, 1.6×10^4 $TCID_{50}$/ml) were incubated at 4 °C for 16 h. Formation of HIV-IgG immune complexes was measured by capture on immobilized protein G and p24 assays (see "Experimental Procedures"). Values are means ± S.D. of duplicates corrected for nonspecific binding, determined by identical processing of HIV in the absence of IgG (A490, 0.210 ± 0.005). *B*, inhibition of HIV-IgG binding by PND peptide **1a**. IgG (50 μg/ml) and HIV (MN, 1.6×10^4 $TCID_{50}$/ml) were incubated in the presence (50 μg/ml) of the PND peptide or an irrelevant peptide control (gp120 465–479), and IgG-bound HIV was determined as in *panel A*. Values are expressed as percent of binding observed in the absence of **1a** (A490 0.49 ± 0.02, anti-PND IgG; A490 0.47 ± 0.01, anti-E-PND IgG). Shown is a representative assay of three independent assays. Residual HIV binding in the presence of **1a** in these assays were 9 ± 4% for anti-PND IgG (A490 in the absence of **1a**, 0.61 ± 0.09) and 12 ± 3% for anti-E-PND IgG (0.62 ± 0.12).

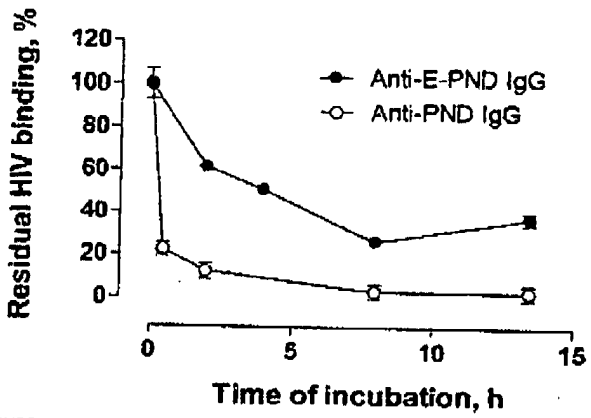

FIGURE 3. **Dissociation of HIV-IgG complexes.** Immune complexes were formed by incubating anti-E-PND or anti-PND IgG (50 μg/ml) with HIV (MN, 1.6×10^4 $TCID_{50}$/ml) for 13 h. PND peptide **1a** (50 μg/ml) was added ($t = 0$), and aliquots of the mixtures withdrawn at the indicated time points were processed for measurement of residual HIV-IgG complexes as in Fig. 2. Values are expressed as percent of binding at $t = 0$ (100% A_{490} values for anti-E-PND and anti-PND IgGs, respectively: 0.56 ± 0.01 and 0.37 ± 0.03; corrected for nonspecific binding determined using HIV-IgG mixtures in which 50 μg/ml PND peptide was present before initiating immune complex formation; values of nonspecific binding with anti-E-PND and anti-PND IgGs, respectively: 0.15 ± 0.01 and 0.16 ± 0.02). Shown is one of two independent assays (nominal $t^1/_2$ values of HIV complexes formed by anti-PND and anti-E-PND IgGs in the assay not shown here were 12 min and 2.1 h, respectively).

ceptor R5-dependent; data not shown). This is consistent with the highly divergent sequences of the strain MN PND peptide employed as immunogen and the PND expressed by strain ZA009 (respectively, YNKRKRIHIGPGRAFYTTKNIIG and NNTRKSMRIGPGQVFYATNGIIG).

HIV Binding Characteristics—To study Ab binding to the native PND structure expressed on the viral surface, we used intact, infectious HIV particles. The virion preparation (MN strain) was incubated with purified IgG, the HIV-IgG complexes were captured using immobilized protein G, the complexes were eluted at acid pH and virions were lysed with a detergent, and p24 was measured by ELISA. As shed gp120 is not associated with p24, the method detects Ab-HIV complexes without interference from free gp120 shed by the virus. Binding of the virions by IgG preparations from E-PND **2a**-immunized and PND **1a**-immunized mice was evident at levels greater than control IgG from preimmune mice (Fig. 2*A*). Near-complete competitive inhibition of the binding was observed in the presence of excess PND **1a** but not an irrelevant HIV peptide (Fig. 2*B*), indicating that virion binding by IgG induced by E-PND **2a** immunization is attributable to specific recognition of the PND region.

To study immune complex stability, we measured the dissociation rates of the HIV-IgG complexes. After the complexes had been formed, excess PND **1a** (18.5 μM) was added to the reaction mixtures to preclude reassociation of HIV that had undergone dissociation, and the residual complexes were measured periodically by the p24 assay. Dissociation of HIV complexed to IgG induced by immunization with PND **1a** occurred rapidly and proceeded at a rate consistent with the first-order dissociation equation (half-life, $t^1/_2$, 10.6 min; r^2 0.985; Fig. 3). Dissociation of anti-E-PND IgG complexes was substantially slower and suggested two subpopulations of complexes, a subpopulation that dissociated slowly over 8 h (~70% of initial complexes; nominal $t^1/_2$ assuming first order kinetics and complete dissociation over 8 h, 2.5 h, r^2 0.971) and another subpopulation that did not dissociate detectably between 8 and 14 h (~30% of initial complexes).

Ab Nucleophilic Reactivity—The strongly electrophilic phosphonate in probe E-PND **2b** (Fig. 1*A*) is known to form stable covalent bonds with Ab nucleophiles (7, 18, 20–22). In addition, this probe contains the PND peptide regions available for noncovalent Ab binding. As a test of antigen-specific nucleophilic reactivity, we measured the formation of covalent adducts of IgG and Bt-E-PND **2b**. Boiled reaction mixtures of the IgG and E-PND **2b** were analyzed by reducing SDS-electrophoresis and densitometry. Adducts of **2b** formed by the IgG heavy and light chains from E-PND-immunized mice accumulated more rapidly than the adducts from control PND-immunized mice or control non-immune IgG (Fig. 4*A*, 60 kDa heavy chain adduct intensities in arbitrary volume units from **2a**-immunized mice, **1a**-immunized mice and preimmune mice, respectively, 3881, 830, and 111; 30-kDa light chain adduct intensities, respectively, 1869, <12, and <12). In previous studies, we employed the small molecule phosphonate **3** (Fig. 4*B*) as a probe for nucleophilic reactivity of Abs independent of noncovalent binding forces responsible for specific recognition of polypeptide antigens (18, 19, 21, 23). According to our split-site model deduced from mutagenesis studies (5, 24, 25), distinct sites in antigen-specific Abs are responsible for the nucleophilic and noncovalent binding activities. Following treatment with excess phosphonate **3** and removal of the unreacted phosphonate **3**, IgG from E-PND immunized mice retained the ability to bind HIV. However, the dissociation of HIV complexes formed by phosphonate **3**-treated anti-E-PND IgG was accelerated compared with the control IgG treated with diluent, and unlike

Downloaded from www.jbc.org by guest, on April 28, 2010

PAGE 70/92 * RCVD AT 4/28/2010 6:45:45 PM [Eastern Daylight Time] * SVR:USPTO-EFXRF-6/33 * DNIS:2738300 * CSID:7132705361 * DURATION (mm-ss):48-00

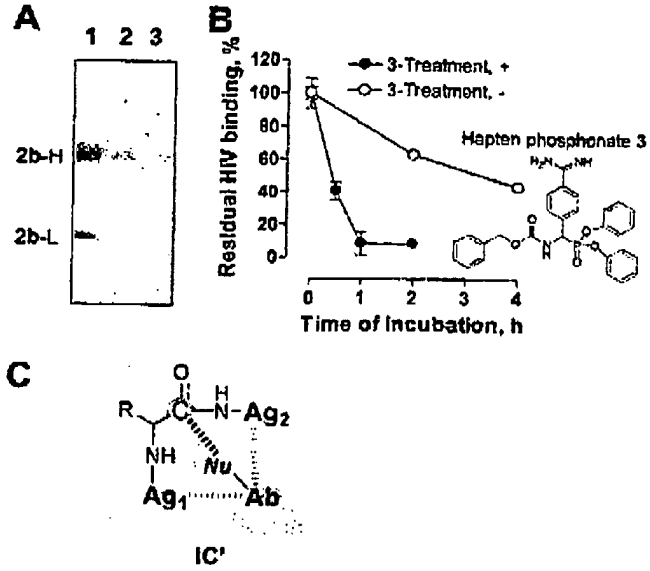

FIGURE 4. **IgG nucleophilic reactivity.** *A*, formation of IgG adducts with E-PND **2b**. The anti-E-PND IgG, anti-PND IgG, and preimmune IgG (75 μg/ml) were incubated with E-PND **2b** (1 μM) for 2 h, subjected to reducing SDS-electrophoresis and the covalent adducts were detected by streptavidin-peroxidase staining of blots. *B*, dissociation of HIV complexes formed by hapten 3-treated IgG. Anti-E-PND IgG (1.4 mg/ml) was incubated in the presence of diluent or hapten phosphonate 3 (1 mM; structure in *Inset*) for 16 h, and unreacted 3 was removed by gel filtration. Immune complexes were formed by incubating 3-treated anti-E-PND IgG or control diluent-treated anti-E-PND IgG (50 μg/ml) with HIV (MN, 1.6×10^6 $TCID_{50}$/ml) for 13 h. Dissociation of HIV-IgG complexes (means ± S.D., three replicates at each time point) were monitored periodically as in Fig. 3. Values are corrected for nonspecific binding and are expressed as percent of binding at $t = 0$ (100% values for 3-treated IgG and diluent-treated control IgG, respectively: 0.73 ± 0.06 and 0.88 ± 0.03). *C*, likely mechanism for stabilization of immune complexes. The irreversible binding character of the immune complexes may be due to accumulation of the resonant tetrahedral complex (IC'). In enzymes, such complexes proceed to form trigonal acyl-enzyme covalent intermediates with release of the C-terminal antigen fragment. NuH, nucleophile; Ag_1 and Ag_2 denote flanking regions of the antigen responsible for noncovalent binding.

the control HIV-IgG complexes, the dissociation of HIV complexes formed by phosphonate 3-treated IgG proceeded to near-completion within 1 h (Fig. 4*B*). These results suggest that nucleophilic sites in IgG from the E-PND-immunized mice are responsible for the enhanced stability of the immune complexes and superior HIV neutralization.

DISCUSSION

An effective vaccine against diverse HIV strains found in different geographical regions and escape mutants that emerge in the course of infection remains elusive. The anti-viral efficacy of various Abs directed to the neutralizing epitopes of the HIV envelope depends largely on their first order dissociation rate constants (k_{off}; $t½ = \ln 2/k_{off}$) and concentrations in biological fluids. The Ab-virus association rate constant (k_{on}) also contributes to the observed binding affinity ($K_a = k_{on}/k_{off}$), but different Abs to a given viral epitope usually display comparable k_{on} values, as this constant is controlled mainly by the rate of diffusion and the orientation of collisions between the reactants. A previous study has highlighted the correlation between the HIV neutralizing potency and dissociation rate constants of monoclonal Abs to the PND, the epitope targeted in the present study (26). We reported that rare monoclonal Abs raised to an electrophilic analog of full-length gp120 neutralized HIV and formed unusually stable immune complexes with gp120 devoid of exogenous electrophiles (2). The stability of the immune complexes was attributable to the adaptively strengthened nucleophilic groups in the Abs induced by electrophilic immunization. The nucleophilic groups are hypothesized to lend covalent character to the complexes by pairing with natural electrophilic groups in gp120. Regrettably, polyclonal IgG from the mice immunized with full-length E-gp120 failed to neutralize HIV at levels superior to IgG from non-immunized mice, presumably because the overall polyclonal immune response is dominated by Abs to irrelevant epitopes and Abs with sufficient nucleophilic reactivity to the neutralizing epitope were present only at low concentrations.

In the present study, a well characterized synthetic analog of the peptide corresponding to the principal neutralizing determinant of HIV strain MN was studied as immunogen (E-PND). Four electrophilic phosphonates were incorporated within the 23 residues peptide analog to maximize the opportunity of B cell adaptive differentiation in response to electrophilic stimulation. Polyclonal Ab preparations obtained following E-PND immunization formed complexes with intact HIV virions. The complexes were poorly dissociable or not at all dissociable. The polyclonal anti-E-PND IgG neutralized HIV ~50-fold more potently than control Abs to PND devoid of phosphonate electrophilic groups. This is consistent with the prediction that slower dissociation of the HIV-IgG complexes should prolong the duration over which the Ab-complexed virus exists in non-infectious form. Biochemical analysis confirmed the enhanced nucleophilic reactivity of the anti-E-PND Abs and the importance of the nucleophilic reactivity in prolonging immune complex longevity. It may be concluded that the nucleophilic Abs responsible for forming stable immune complexes are present in the polyclonal IgG mixtures at concentrations sufficient to achieve functionally useful viral inactivation.

Concerning epitope specificity, the PND (residues 306–328) is located in the highly mutable V3 region of gp120 (12). Consistent with the neutralization results for strains MN and ZA009 in the present study, Abs to the V3 region display type-specific neutralizing activity, that is, they neutralize the infecting HIV strain, but V3 sequence mutants resistant to infection emerge following infection (11–14). The mechanism of neutralization by anti-PND Abs is thought to involve sterically hindered recognition of gp120 by HIV coreceptors CCR5 and CXCR4 expressed by host cells (27–29). In particular, residues Pro^{316}-Arg^{318} are reported to be important for CCR5 binding (30–32). Attempts to induce broadly neutralizing Abs that recognize diverse HIV strains using mixtures of synthetic peptides with varying V3 sequences have been reported (*e.g.* Refs. 33, 34). However, V3 sequence diversity is so great that a large library of immunogenic peptides is necessary to justify hopes of inducing a broadly neutralizing Ab response. For example, the 201 known clade B virus strains available in the Los Alamos data base contain 179 distinct PND sequences. Monoclonal Abs that recognize the more conserved Gly-Pro-Gly-Arg sequence within the PND are reported to neutralize various HIV strains comparatively broadly (35, 36). To the extent that inducing a

Downloaded from www.jbc.org by guest, on April 28, 2010

PAGE 71/92 * RCVD AT 4/28/2010 6:45:45 PM [Eastern Daylight Time] * SVR:USPTO-EFXRF-6/33 * DNIS:2738300 * CSID:7132705361 * DURATION (mm-ss):48-00

broadly neutralizing Ab response to the PND or regions within the PND is feasible by these means, our results suggest that inclusion of electrophilic groups in the immunogenic peptide (or combination of peptides) will be helpful to increase the potency of neutralization. In principle, the electrophilic immunization strategy is applicable to targeting of any peptide epitope. gp120 also contains important neutralizing epitopes outside the PND, *e.g.* the conserved regions that participate in binding to host cell CD4 receptors (37). However, these epitopes are generally poorly immunogenic and they are composed of peptide regions distant in the linear sequence of the protein (conformational epitopes). No linear gp120 peptide or mimetic is available presently that reproducibly induces the synthesis of broadly neutralizing Abs to the diverse HIV strains responsible for the pandemic.

The following empirical and theoretical points are relevant in assessing the potential generality of the electrophilic immunization approach: (*a*) Electrophilic phosphonates were originally developed as covalent inhibitors of the catalytic sites of serine proteases (38). Haptenic phosphonates react covalently with all Ab preparations examined thus far, including monoclonal Abs, single chain Fv constructs (V_L and V_H domains tethered by a linker) (18, 19, 23) and Igs contained in BCRs (39). This suggests that the nucleophilic reactivity is ubiquitously distributed in Ab combining sites regardless of noncovalent binding specificity. (*b*) Noncovalent epitope recognition is reported to accelerate the covalent reaction of electrophilic phosphonate groups incorporated into several polypeptide with various polyclonal and monoclonal Abs specific for these polypeptides (18, 20–22). It appears, therefore, that the noncovalent and nucleophilic Ab subsites are within sufficient proximity to express their functions in a coordinated manner. (*c*) Only a small subset of nucleophilic Abs displays the ability to hydrolyze peptide bonds (7). This may be understood from the requirement for additional rate-limiting events for completing the catalytic cycle following the initial nucleophilic attack step, *i.e.* water attack and product release. We did not detect PND hydrolysis IgG from E-PND immunized mice.[4] Importantly, the electrophilic phosphonate is predicted to favor adaptive strengthening of Ab nucleophilicity, but the immunogen lacks structural elements that can induce the synthesis of Abs capable of completing the catalytic cycle; and (*d*) Observations using noncatalytic monoclonal Abs raised to full-length E-gp120 suggest the feasibility of immune complex stabilization by resonant nucleophile-electrophile pairing at the naturally occurring electrophilic reaction centers in the polypeptide antigen, *e.g.* the carbonyl groups of backbone peptide bonds or side chain amide bonds in structure IC′, Fig. 4*C* (2). Such interactions are hypothesized to impart partial covalent character to the complexes and impede their dissociation. Similar structures are thought to exist in the transition state of enzymatic reactions (3). To our knowledge there is no theoretical bar to stabilization of ground state protein-protein complexes by this mechanism. B cell clonal selection processes favor increased BCR occupancy by the antigen. Covalent binding of electrophilic phosphonates due to improved BCR nucleophilic reactivity is predicted to be an immunological selectable event, and the desirable consequence of the improved nucleophilicity is the ability to bind the target polypeptide antigen with covalent character.

In summary, our studies using the model E-PND immunogen indicate that electrophilic immunization induces a robust polyclonal nucleophilic Ab response with improved viral binding and inactivation potency. Concerning HIV vaccine development, the caveat remains that PND sequence divergences may limit the functional efficacy of E-PND immunization. However, the E-PND studies validate electrophilic immunization as a potentially general approach that can be applied to induce adaptive Ab responses capable of binding microbial antigens with irreversible character and help improve vaccine efficacy.

Acknowledgments—We thank Robert Dannenbring and Tomoko Yoshikawa for technical assistance.

[4] Incubation of PND 1a (0.1 mM) in the presence of IgG (1 μM) from hyperimmune mice for 3 h did not result in detectable product accumulation at levels greater than background in control incubations conducted using an equivalent concentration of preimmune IgG determined by reversed-phase HPLC with an electrospray mass detector (VyDac C18 MASS SPEC column, 2.1 × 150 mm; 3–60% acetonitrile in 0.1% formic acid and water; retention time of intact PND 1a, 14.3 min).

REFERENCES

1. Lefevre, S., Debat, H., Thomas, D., Friboulet, A., and Avalle, B. (2001) *FEBS Lett.* 489, 25–28
2. Nishiyama, Y., Karle, S., Mitsuda, Y., Taguchi, H., Planque, S., Salas, M., Hanson, C., and Paul, S. (2006) *J. Mol. Recognit.* 19, 423–431
3. Hedstrom, L. (2002) *Chem. Rev.* 102, 4501–4524
4. Zhou, G. W., Guo, J., Huang, W., Fletterick, R. J., and Scanlan, T. S. (1994) *Science* 265, 1059–1064
5. Gao, Q. S., Sun, M., Rees, A. R., and Paul, S. (1995) *J. Mol. Biol.* 253, 658–664
6. Ramsland, P. A., Terzyan, S. S., Cloud, G., Bourne, C. R., Farrugia, W., Tribbick, G., Geysen, H. M., Moomaw, C. R., Slaughter, C. A., and Edmundson, A. B. (2006) *Biochem. J.* 395, 473–481
7. Paul, S., Planque, S., Zhou, Y. X., Taguchi, H., Bhatia, G., Karle, S., Hanson, C., and Nishiyama, Y. (2003) *J. Biol. Chem.* 278, 20429–20435
8. Broliden, P. A., von Gegerfelt, A., Clapham, P., Rosen, J., Fenyo, E. M., Wahren, B., and Broliden, K. (1992) *Proc. Natl. Acad. Sci. U. S. A.* 89, 461–465
9. Boudet, F., Girard, M., Theze, J., and Zouali, M. (1992) *Int. Immunol.* 4, 283–294
10. Warren, R. Q., Anderson, S. A., Nkya, W. M., Shao, J. F., Hendrix, C. W., Melcher, G. P., Redfield, R. R., and Kennedy, R. C. (1992) *J. Virol.* 66, 5210–5215
11. Palker, T. J., Clark, M. E., Langlois, A. J., Matthews, T. J., Weinhold, K. J., Randall, R. R., Bolognesi, D. P., and Haynes, B. F. (1988) *Proc. Natl. Acad. Sci. U. S. A.* 85, 1932–1936
12. Javaherian, K., Langlois, A. J., McDanal, C., Ross, K. L., Eckler, L. I., Jellis, C. L., Profy, A. T., Rusche, J. R., Bolognesi, D. P., Putney, S. D., and Matthews, T. J. (1989) *Proc. Natl. Acad. Sci. U. S. A.* 86, 6768–6772
13. Wang, C. Y., Looney, D. J., Li, M. L., Walfield, A. M., Ye, J., Hosein, B., Tam, J. P., and Wong-Staal, F. (1991) *Science* 254, 285–288
14. Hartley, O., Klasse, P. J., Sattentau, Q. J., and Moore, J. P. (2005) *AIDS Res. Hum Retroviruses* 21, 171–189
15. Kalaga, R., Li, L., O'Dell, J. R., and Paul, S. (1995) *J. Immunol.* 155, 2695–2702
16. Hanson, C. V., Crawford-Miksza, L., and Sheppard, H. W. (1990) *J. Clin. Microbiol.* 28, 2030–2034
17. Karle, S., Planque, S., Nishiyama, Y., Taguchi, H., Zhou, Y. X., Salas, M., Lake, D., Thiagarajan, P., Arnett, F., Hanson, C. V., and Paul, S. (2004) *AIDS* 18, 329–331

Downloaded from www.jbc.org by guest, on April 28, 2010

PAGE 72/92 * RCVD AT 4/28/2010 6:45:45 PM [Eastern Daylight Time] * SVR:USPTO-EFXRF-6/33 * DNIS:2738300 * CSID:7132705361 * DURATION (mm-ss):48-00

18. Planque, S., Taguchi, H., Burr, G., Bhatia, G., Karle, S., Zhou, Y. X., Nishiyama, Y., and Paul, S. (2003) *J. Biol. Chem.* **278**, 20436–20443
19. Nishiyama, Y., Taguchi, H., Luo, J. Q., Zhou, Y. X., Burr, G., Karle, S., and Paul, S. (2002) *Arch. Biochem. Biophys.* **402**, 281–288
20. Nishiyama, Y., Bhatia, G., Bangale, Y., Planque, S., Mitsuda, Y., Taguchi, H., Karle, S., and Paul, S. (2004) *J. Biol. Chem.* **279**, 7877–7883
21. Nishiyama, Y., Mitsuda, Y., Taguchi, H., Planque, S., Hara, M., Karle, S., Hanson, C. V., Uda, T., and Paul, S. (2005) *J. Mol. Recognit.* **18**, 295–306
22. Nishiyama, Y., Karle, S., Planque, S., Taguchi, H., and Paul, S. (2007) *Mol. Immunol.* **44**, 2707–2718
23. Paul, S., Tramontano, A., Gololobov, G., Zhou, Y. X., Taguchi, H., Karle, S., Nishiyama, Y., Planque, S., and George, S. (2001) *J. Biol. Chem.* **276**, 28314–28320
24. Sun, M., Gao, Q. S., Kirnarskiy, I., Rees, A., and Paul, S. (1997) *J. Mol. Biol.* **271**, 374–385
25. Paul, S. (1996) *Mol. Biotechnol.* **5**, 197–207
26. VanCott, T. C., Bethke, F. R., Polonis, V. R., Gorny, M. K., Zolla-Pazner, S., Redfield, R. R., and Birx, D. L. (1994) *J. Immunol.* **153**, 449–459
27. Hill, C. M., Deng, H., Unutmaz, D., Kewalramani, V. N., Bastiani, L., Gorny, M. K., Zolla-Pazner, S., and Littman, D. R. (1997) *J. Virol.* **71**, 6296–6304
28. Wu, L., Gerard, N. P., Wyatt, R., Choe, H., Parolin, C., Ruffing, N., Borsetti, A., Cardoso, A. A., Desjardin, E., Newman, W., Gerard, C., and Sodroski, J. (1996) *Nature* **384**, 179–183
29. Trkola, A., Dragic, T., Arthos, J., Binley, J. M., Olson, W. C., Allaway, G. P., Cheng-Mayer, C., Robinson, J., Maddon, P. J., and Moore, J. P. (1996) *Nature* **384**, 184–187
30. Hu, Q., Trent, J. O., Tomaras, G. D., Wang, Z., Murray, J. L., Conolly, S. M., Navenot, J. M., Barry, A. P., Greenberg, M. L., and Peiper, S. C. (2000) *J. Mol. Biol.* **302**, 359–375
31. Huang, C. C., Tang, M., Zhang, M. Y., Majeed, S., Montabana, E., Stanfield, R. L., Dimitrov, D. S., Korber, B., Sodroski, J., Wilson, I. A., Wyatt, R., and Kwong, P. D. (2005) *Science* **310**, 1025–1028
32. Suphaphiphat, P., Essex, M., and Lee, T. H. (2007) *Virology* **360**, 182–190
33. Neurath, A. R., and Strick, N. (1990) *Mol. Immunol.* **27**, 539–549
34. Estaquier, J., Gras-Masse, H., Boutillon, C., Ameisen, J. C., Capron, A., Tartar, A., and Auriault, C. (1994) *Eur. J. Immunol.* **24**, 2789–2795
35. Zolla-Pazner, S., Zhong, P., Revesz, K., Volsky, B., Williams, C., Nyambi, P., and Gorny, M. K. (2004) *AIDS Res. Hum. Retroviruses* **20**, 1254–1258
36. Gorny, M. K., Williams, C., Volsky, B., Revesz, K., Wang, X. H., Burda, S., Kimura, T., Konings, F. A., Nadas, A., Anyangwe, C. A., Nyambi, P., Krachmarov, C., Pinter, A., and Zolla-Pazner, S. (2006) *J. Virol.* **80**, 6865–6872
37. Zhou, T., Xu, L., Dey, B., Hessell, A. J., Van Ryk, D., Xiang, S. H., Yang, X., Zhang, M. Y., Zwick, M. B., Arthos, J., Burton, D. R., Dimitrov, D. S., Sodroski, J., Wyatt, R., Nabel, G. J., and Kwong, P. D. (2007) *Nature* **445**, 732–737
38. Powers, J. C., Asgian, J. L., Ekici, O. D., and James, K. E. (2002) *Chem. Rev.* **102**, 4639–4750
39. Planque, S., Bangale, Y., Song, X. T., Karle, S., Taguchi, H., Poindexter, B., Bick, R., Edmundson, A., Nishiyama, Y., and Paul, S. (2004) *J. Biol. Chem.* **279**, 14024–14032

Downloaded from www.jbc.org by guest, on April 28, 2010

PAGE 73/92 * RCVD AT 4/28/2010 6:45:45 PM [Eastern Daylight Time] * SVR:USPTO-EFXRF-6/33 * DNIS:2738300 * CSID:7132705361 * DURATION (mm-ss):48-00

AIChE

Promoting α-Secretase Cleavage of Beta-Amyloid with Engineered Proteolytic Antibody Fragments

Srinath Kasturirangan
Harrington Dept. of Bioengineering, Arizona State University, Tempe, AZ 85287

Dan Brune
Dept. of Chemistry and Biochemistry, Arizona State University, Tempe, AZ 85287

Michael Sierks
Dept. of Chemical Engineering, Arizona State University, Tempe, AZ 85287

DOI 10.1021/bp.190
Published online July 1, 2009 in Wiley InterScience (www.interscience.wiley.com).

Deposition of beta-amyloid (Aβ) is considered as an important early event in the pathogenesis of Alzheimer's Disease (AD), and reduction of Aβ levels by various therapeutic approaches is actively being pursued. A potentially non-inflammatory approach to facilitate clearance and reduce toxicity is to hydrolyze Aβ at its α-secretase site. We have previously identified a light chain fragment, mk18, with α-secretase-like catalytic activity, producing the 1–16 and 17–40 amino acid fragments of Aβ40 as primary products, although hydrolysis is also observed following other lysine and arginine residues. To improve the specific activity of the recombinant antibody by affinity maturation, we constructed a single chain variable fragment (scFv) library containing a randomized CDR3 heavy chain region. A biotinylated covalently reactive analog mimicking α-secretase site cleavage was synthesized, immobilized on streptavidin beads, and used to select yeast surface expressed scFvs with increased specificity for Aβ. After two rounds of selection against the analog, yeast cells were individually screened for proteolytic activity towards an internally quenched fluorogenic substrate that contains the α-secretase site of Aβ. From 750 clones screened, the two clones with the highest increase in proteolytic activity compared to the parent mk18 were selected for further study. Kinetic analyses using purified soluble scFvs showed a 3- and 6-fold increase in catalytic activity (k_{cat}/K_M) toward the synthetic Aβ substrate compared to the original scFv primarily due to an expected decrease in K_M rather than an increase in k_{cat}. This affinity maturation strategy can be used to select for scFvs with increased catalytic specificity for Aβ. These proteolytic scFvs have potential therapeutic applications for AD by decreasing soluble Aβ levels in vivo. © 2009 American Institute of Chemical Engineers. *Biotechnol. Prog.*, 25: 1054–1063, 2009
Keywords: proteolytic antibody, beta-amyloid, alpha-secretase, single chain antibody, affinity maturation

Introduction

Alzheimer's disease (AD) is a progressive neurodegenerative disorder that affects 5 million adults over the age of 65.[1] Memory loss and dementia associated with AD seem to be caused by the accumulation of beta amyloid (Aβ) in regions of the brain associated with memory and cognition.[2] Clearance of Aβ by active immunization in human clinical trials was shown to reduce cognitive decline and decrease neuronal loss.[3] Although the clinical trials had to be stopped due to the occurrence of meningioencephalitis in 6% of the patients,[4] the promising results obtained suggest that clearance of Aβ by an alternative approach that does not generate an inflammatory response could be a viable therapeutic option.

Correspondence concerning this article should be addressed to M. Sierks at sierks@asu.edu.

Several proteases have been identified that can cleave Aβ at single or multiple sites including two metalloproteases, neprilysin (NEP) and insulin degrading enzyme (IDE), as well as trypsin and chymotrypsin.[5] The cleavage products of IDE and NEP show reduced aggregation and neurotoxicity compared to full length Aβ, suggesting that these enzymes may help regulate Aβ levels in vivo.[6] Both NEP and IDE have been found in close proximity to Aβ plaques in post mortem brain. The subsequent reduction in Aβ clearance can lead to accumulation and toxic aggregation of Aβ in AD patients.[7] Although supplementing IDE or NEP activity has been proposed as a potential therapeutic mechanism for treating AD,[8] these proteases have other preferred substrates and can cleave a variety of proteins with diverse sequences.[9] Hence, their value as therapeutic agents to specifically target and cleave Aβ may be limited.

© 2009 American Institute of Chemical Engineers

PAGE 74/92 * RCVD AT 4/28/2010 6:45:45 PM [Eastern Daylight Time] * SVR:USPTO-EFXRF-6/33 * DNIS:2738300 * CSID:7132705361 * DURATION (mm-ss):48-00

Table 1. Oligonucleotide Primers Used for PCR

Primer	Sequence	Purpose
mkNewF	5′ GAT GCT GCA CCA GGC GGC GGC GGC TCA GGC GGC GGC GGC TCA GGC GGC GGC GGC TCA GGA TCC GAG TCT GGG GGA 3′	Modify the linker and introduce BamHI site between the V_L and V_H regions
mkNewR	5′ TCC CCC AGA CTC GGA TCC TGA GCC GCC GCC GCC TGA GCC GCC GCC GCC TGA GCC GCC GCC GCC TGG TGC AGC ATC 3′	
mkYDF	5′ TCT GCT AGC GAT GTT TTG ATG 3′	Replace restriction site for yeast transformation
mkYDR	5′ TAG AAT TCC GGA TGC AGA GAC AGT GAC 3′	
mkCDR3F1	5′ GCC TTG TAT TTC TGT GGA AGA NNK NNK NNK NNK NNK NNK TGG GGC CAA GGG 3′	Generate random CDR3 region in short 200 bp fragment
pPNL6F	5′ GTACGAGCTAAAAGTACAGTG 3′	
mkCDR3R1	5′ CTTCCACAGAAATACAAGCC 3′	Amplify 800 bp fragment before CDR3 mutation
pPNL6R	5′ TAGATACCCATACGACGTTC 3′	
pPNL9F	5′ GACGTTCCAG ACTACGCTGG TGGTGGTGGT TCTGCTA 3′	Insert surface displayed scFv into secretion vector after panning and screening
pPNL9R	5′ GGGTTAGGGA TAGGCTTACC CTGTTGTTCT AGAATTCCG 3′	

N corresponds to nucleotides A, T, C, or G; K to G or T.

An alternative approach to clear Aβ is to supplement its α-secretase cleavage using proteolytic single chain variable fragments (scFvs). We showed that a recombinant antibody light chain, mk18, originally raised by immunization against vasoactive intestinal polypeptide (VIP),[10] has α-secretase like proteolytic activity against Aβ.[11] The primary products of this cleavage are the 1–16 and 17–40 amino acid fragments, although fragments corresponding to hydrolysis at other lysine (position 28) and arginine (position 5) residues could also be identified. An scFv version of the mk18 light chain, c23.5, was constructed where the catalytic residues are contained in the light chain variable region (V_L), and additional substrate specificity toward VIP are contained in the heavy chain variable region (V_H).[12] Because the heavy chain of c23.5 was selected based on binding to VIP, we expect that the catalytic activity of the c23.5 scFv toward Aβ will be lower than the original mk18 light chain. Because the original mk18 light chain has a wide range of specificities, it is not a suitable therapeutic agent; therefore, we selected the c23.5 scFv as a starting point from which to develop a proteolytic antibody with greater specificity for Aβ.

Protein stability is a critical component of an effective therapeutic,[13] and since the linker used in the original c23.5 scFv construct (-G-S-T-S-G-S-G-K-S-S-E-G-K-G-) is susceptible to proteolysis by subtilisin (hydrolytic site in bold), we replaced the linker with the more commonly used $(GGGGS)_3$ linker to provide greater stability and flexibility.[14] After changing the linker, we focused on increasing the specificity of the scFv by targeting the heavy chain domain. Randomizing the CDR3 of the V_H domain is an effective method to increase antigen binding diversity and allows for an efficient selection of antibodies with high affinities to the desired antigen because of their variations in both length and shape.[15] We therefore constructed a second generation yeast surface display library of the modified c23.5 scFv by introducing random mutations in the CDR3 region of the heavy chain.

Although numerous surface display methods are available for selecting individual clones from various libraries, including phage, bacterial, and yeast, yeast surface display is increasingly used to isolate engineered antibodies with higher specificity by affinity maturation.[16] The scFv is fused to the yeast surface agglutinin protein, enabling display of the scFv on the surface of the yeast.[17] Since yeast display selections are performed in solution, antigen concentrations can be precisely controlled and the ability to use very low antigen concentrations enables selection of high affinity clones.[18] Further, magnetic bead enrichment of the surface displayed library allows for a quantitative screening for clones with higher affinity.[19]

A difficulty in affinity maturation of proteins with improved catalytic efficiency is that the panning protocols typically screen for better binding but not better activity. Several novel approaches have been developed to circumvent this problem.[20] Transition state analogs (TSAs) that closely mimic high energy transition state intermediates can be designed for affinity maturation studies to generate antibodies that recognize the transient transition state thereby lowering the activation energy.[21] Irreversible inhibitors of conventional serine proteases, or covalently reactive analogs (CRA), where the lysine residue targeted by the serine protease is replaced with a hapten phosphonate, have been utilized to generate antibodies with improved nucleophilicity.[22] CRAs have been shown to enhance serine protease-like nucleophilic activity of antibodies targeted against the HIV-1 coat protein gp120.[23] IgV_L domains that hydrolyze Aβ with catalytic efficiencies that are 3–4 times higher than polyclonal Ig preparations have been identified using such CRAs.[24] Here we perform affinity maturation of the yeast displayed c23.5 based scFv library using CRA where the hapten phosphonate replaces the lysine at the α-secretase site of Aβ.

The yeast display library was affinity matured by two rounds of panning using magnetic bead enrichment. Two clones having the greatest increase in proteolytic activity towards a synthetic fluorogenic α-secretase substrate from a total of 750 screened clones were selected for further study. Kinetic analyses indicate 5.6- and 2.8-fold increases in the second order rate constant, or specificity constant (k_{cat}/K_M), of the two selected clones towards the α-secretase substrate compared to the original scFv.

Materials and Methods

Materials

Components used for yeast surface display, including EBY100 and YVH10 competent cells and pPNL6 and pPNL9 plasmid vectors, were obtained from Pacific National Laboratories, San Diego, CA. PCR amplification primers listed in Table 1 were synthesized by Integrated DNA Technologies, IA. All PCR experiments were performed using Platinum® Pfx DNA Polymerase, Invitrogen, CA. The biotinylated CRA corresponding to residues 6–15 of Aβ was synthesized by the Protein Analysis and Synthesis Lab at Arizona State University. Anti-biotin-coated magnetic beads, streptavidin-coated magnetic beads, and MACS separation

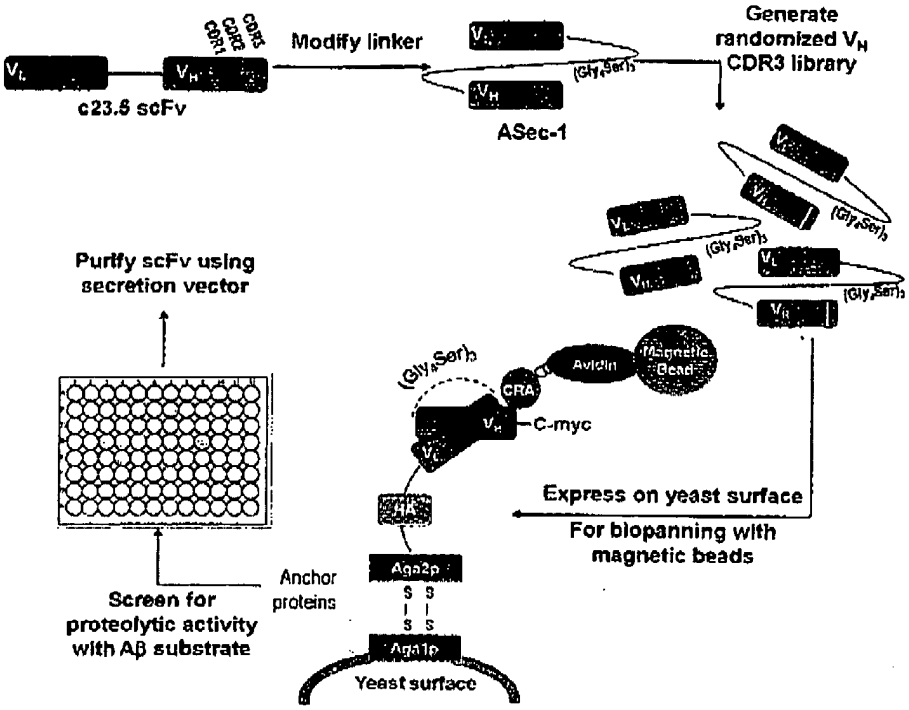

Figure 1. Schematic showing the major steps in construction and panning of the yeast displayed scFv library.

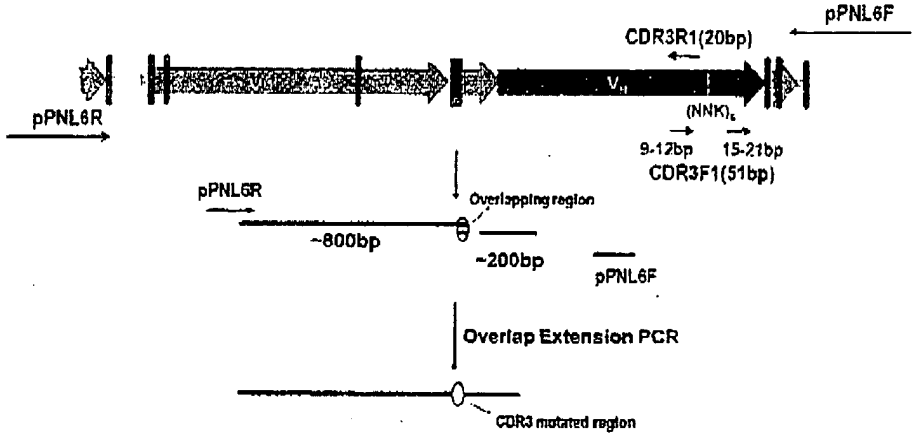

Figure 2. Introduction of random mutations in the CDR3 region of the heavy chain by overlap PCR. PCR amplification with pPNL6R and CDR3R1 generates the 800 bp fragment, whereas amplification with CDR3F1 and pPNL6F generates the shorter 200 bp fragment containing the $(NNK)_6$ CDR3 mutation. Overlap PCR followed by addition of end primers pPNL6F and pPNL6R generates the full length scFv.

columns were purchased from Miltenyi Biotec. Anti-myc-tag and goat-anti-mouse IgG (HRP conjugated) antibodies were purchased from Santa Cruz Biotechnology. 3,3′-Diaminobenzidine (DAB) substrate system was purchased from Sigma-Aldrich. Restriction enzymes and buffers were purchased from New England Biolabs.

A schematic depicting the strategy utilized to produce and screen the yeast displayed antibody library is shown in Figure 1.

Construction of ASec-1

Overlapping PCR using the forward and reverse primers mkNewF and mkNewR (Table 1) was performed to replace the linker of the original c23.5 scFv with the more commonly utilized $(GGGGS)_3$ linker. A BamH1 restriction endonuclease site was also introduced into the heavy chain to simplify future cloning operations.

Briefly the light chain fragment (V_L) was amplified from the original pCANTAB5E vector, using pCANTAB S1 forward and mkNewR reverse primers (Figure 2, Table 1). The heavy chain region (V_H) was amplified from c23.5 scFv by PCR using the mkNewF forward and S5 reverse primers (Table 1).

The V_H and V_L fragments, which have overlapping regions corresponding to the linker and BamH1 site, were combined by overlapping PCR (Figure 2) as described.[25] After five cycles of PCR with just the overlapping fragments, the outer

primers S1 and S5 were added, and a further 30 cycles of PCR were performed to amplify the overlapping product. The overlapping PCR product was ligated into the pGEMT plasmid using the pGEMT easy vector system (Promega Corp., WI) and the DNA sequence of the product was obtained to verify proper construction. The new scFv containing the $(GGGGS)_3$ linker in place of the original linker is termed ASec-1.

Library construction and yeast transformation

The CDR and FR regions of the ASec-1 scFv were determined by Kabat sequence alignment. After replacing the flanking SfiI and NotI sites with NheI and EcoR1 sites, respectively, mkCDR3F1 primer was utilized to introduce random mutations in the CDR3 region of the scFv (Table 1) by replacing the original 4 amino acids in the CDR3 region (GIAY) with a series of 6 NNK repeats. The primer was 51 base pairs (bp) long, and contained a 15–21 nucleotide anchor sequence flanking the $(NNK)_6$ mutation (Table 1). Using NNK degenerate codons, where N is A, T, C, or G and K is G or T reduces the chance of introducing a stop codon and increases library diversity.[26] The reverse primer (mkCDR3R1) was 20 bp long and had a short region of complementarity with the forward primer to promote hybridization of the fragments by overlap extension PCR (Figure 2) to reconstruct the full length scFv containing the CDR3 mutation.

The PCR amplicon of ASec-1 scFv containing the randomized V_H CDR3 region was subcloned into the surface display vector pPNL6 by gap repair.[27] The gap was generated by digesting the pPNL6 plasmid with NheI and NotI restriction enzymes (NEB, MA). Co-transformation into EBY100 yeast competent cells was accomplished by lithium acetate method using the Yeastmaker yeast transformation system (Clontech Laboratories, CA).[28] The pPNL6 plasmid without the insert and EBY100 cells alone were used as controls. The ASec-1 PCR amplicon without the CDR3 mutation was co-transformed with pPNL6 surface display vector into EBY100 cells to serve as controls for all the subsequent panning and screening experiments.

Selection of clones containing the gap repaired plasmid was performed on synthetic dextrose plus casein amino acids (SDCAA)—agar plates lacking tryptophan, which were grown at room temperature.[29]

Synthesis of covalently reactive analog

To select for clones with increased specificity for the Aβ, we utilized a CRA containing a phosphonate diester linked to the Aβ sequence N-Terminal to the α-secretase site. The inactive analog intermediate, diphenyl [*N*-(benzyloxycarbonyl) amino](4-amidinophenyl)methanephosphonate, was generously provided by Dr Sudhir Paul (University of Texas, Houston Health Science Center). The analog was activated to diphenyl amino(4-amidinophenyl)methanephosphonate by dissolving 0.15 mg in 5 mL HBr for 2 h followed by precipitation with diethyl ether. Activated compound was dried under vacuum, purified by HPLC and stored at −20°C.[30] The Aβ 6–15 peptide was synthesized on PAL-PEG-polystyrene resin using standard Fmoc procedures and biotinylated at its N terminus. The C-terminal carboxyl group of the protected peptide was activated in the presence of the phosphonate diester causing an amide bond formation between the carboxyl group and the free amino group of the TSA. The de-protected peptide was purified by HPLC and verified by mass spectrometry (MS). The resulting protein was 95% pure with some contamination with non-biotinylated peptide. The hapten phosphonate diester mimicking the Lys16 α-secretase cleavage site is covalently linked to the C-terminus of the biotinylated Aβ peptide and serves as a CRA for screening α-secretase activity.

Affinity maturation using covalently reactive analogs

Affinity maturation of the yeast library was performed by magnetic bead enrichment using the CRA.[19] Starting cultures of 10^{10} yeast cells were rinsed with wash buffer (50 mL ice-cold PBS, pH 7.4 containing 2 mM EDTA, 0.5% BSA), co-incubated with 1 μM of the CRA for 1 h at room temperature with gentle mixing, chilled on ice, rinsed with 50 mL wash buffer, and resuspended in 2 mL of the same buffer. Enrichment with magnetic beads was performed using a Miltenyi LS column with either streptavidin or anti-biotin coated microbeads (Miltenyi Biotec, Auburn, CA).[29] The process of loading the column with cells, removing the column briefly from the magnet to re-arrange the iron particles, and rinsing with wash buffer was continued until the entire sample was loaded on to the column. The column was then washed three times with wash buffer, the yeast were eluted with 5 mL SDCAA selection media and grown for 3 h to separate the cells from the cell-bead complex, and plated onto SDCAA agar plates to obtain single colonies for screening studies.

Yeast library screening

The internally quenched fluorogenic substrate [Ac-Arg-Glu(EDANS)-Val-His-His-Gln-Lys-Leu-Val-Phe-Lys(DABCYL)-Arg-OH] (Calbiochem, CA) was used to screen for α-secretase activity by monitoring the increase in fluorescence resulting from hydrolysis of the peptide at excitation max 355 and emission max 480.[31] The substrate was dissolved in DMSO to a stock concentration of 5 mM. Before use, it was diluted to a final concentration of 5 μM in HEPES buffer pH 7.4.

Colonies selected from the SDCAA plate after magnetic bead enrichment were grown for 24 h at 30°C with shaking in 96 well plates followed by induction in SGRCAA induction media (same as SDCAA except glucose was replaced with 20 g/L of galactose) at 25°C overnight. A 150 μL aliquot of 5 μM α-secretase substrate (HEPES buffer pH 7.4) was added to each well and incubated for 30 min at 37°C. After spinning down the cells, the supernatant was removed and added to opaque bottom 96 well assay plates (NUNC, NY) and the fluorescence was measured at an excitation 355 nm and emission 480 nm. Fluorescence was expressed as the percentage of fluorescence compared to the value obtained with the parent clone ASec-1. A clone displaying a random scFv which does not resemble the Asec-1 was used as a negative control.

The proteolytic activity of selected clones was also determined using a second substrate, 50 μM N-a-carbobenzoxy-L-lysine p-nitrophenyl ester (Z-Lys-ONp, Sigma Aldrich, MO) in HEPES buffer pH 7.4. Hydrolysis of the substrate by the surface displayed scFvs was analyzed by incubating at 37°C for 15 min and monitoring ONp release at 405 nm. The sequence integrity of clones with increased α-secretase activity compared to the parent ASec-1 scFv were verified by DNA sequencing.

Secretion and purification of soluble scFvs

To obtain purified soluble scFv, the scFv genes were removed from the yeast surface expression vector, pPNL6, and

inserted into the yeast expression vector, pPNL9, by gap repair after co-transformation into YVH10 yeast competent cells.[27]

For large scale expression,[32] overnight cultures of the clones in 10 mL SDCAA plus Trp growth media was used to inoculate 200 mL of the same media containing 100 U/mL penicillin G, 200 U/mL streptomycin and grown for 16 h at 30°C with shaking at 250 rpm. The cells were harvested and resuspended in 500 mL Yeast extract/peptone/galactose/raffinose containing 2% galactose and 2% raffinose induction medium (YEPGR) and induced for 48–72 h at 25°C with shaking. After centrifugation, to remove cells, the supernatant was concentrated to a final volume of 50 mL using a Pellicon tangential flow system with 10 kDa cut off filter and dialyzed against PBS. The 6xHis tagged scFv were purified by mixing with 1 mL Nickel NTA sepharose beads (Qiagen, CA) for 2 h, followed by elution with an imidazole gradient. Fractions containing scFv antibodies were pooled and dialyzed into 1× PBS. Protein expression and purity was checked with SDS-PAGE and western blotting. A BCA protein assay was used to determine scFv concentration.

Preparation of Aβ

Aβ40 was synthesized in the Proteomics and Protein Chemistry Laboratory at Arizona State University, purified by HPLC, lyophilized, and stored as its Trifluoroacetate salt Aβ40 at −20°C. Samples were prepared as previously described.[33] Briefly, Aβ40 was solubilized in 1,1,1,3,3,3-hexafluoro-2-propanol (HFIP) at a concentration of 1 mg/mL to avoid aggregates. Aliquots of 250 μL were air dried and stored at −20°C. Before use, the aliquots were re-suspended in dimethyl-sulfoxide (DMSO) and diluted to final concentration in 1× phosphate buffered saline (PBS), pH 7.4.

Analysis of proteolytic cleavage products

MS was used to identify cleavage products of Aβ after incubation with the purified soluble scFv samples. To initiate hydrolysis, a 250 nM sample of scFv (PBS, pH 7.4) was reacted with 50 μM Aβ40 in 1× PBS, pH 7.4 at 37°C for 24 h and analyzed by MS. For MS analyses, 4 μL of the reaction mixture matrix was added to 5 μL of α-cyano-4-hydroxy cinnamic acid in 50% acetonitrile containing 0.5% trifluoroacetic acid. A 2 μL aliquot of the above mixture was taken and spotted onto a stainless steel MS sample plate. MS analysis was performed using a Voyager-DE STR Biospectrometry Workstation operated in the positive ion mode and using the reflectron. The accelerating voltage was 20,000 V and data were acquired over a mass range of 1–6000 Da. Each spectrum was typically the average of 100 laser shots. Control samples were taken with 50 μM Aβ40 without any scFv to rule out the possibility of Aβ40 self-degradation after 24 h in 1× PBS solution.

Kinetic characterization of soluble scFv

The kinetic constants of the purified soluble scFvs toward hydrolysis of the internally quenched α-secretase substrate and the Z-Lys-ONp fluorogenic substrate were determined as described above. Different concentrations of the substrate (0.1, 0.25, 0.5, 1, 5, 10, and 20 μM) in HEPES buffer pH 7.4 were incubated with 50 nM of the purified scFvs. Fluorescence resulting from hydrolysis of the peptide was followed as a function of time at excitation max 355 and emission max 480 using a spectrophotometer. The Michaelis–Menten kinetic parameters, k_{cat} and K_M, were calculated using Graphpad Prism software.

LDH release cytotoxicity assay

A human neuroblastoma cell line, SH-SY5Y, was grown and maintained as previously described.[33] Cells were plated onto a 96 well tissue culture treated plates (Corning) at ~ 2 × 10^4 cells/well in 100 μL of medium, and incubated for 24 h to allow attachment to the bottom of the wells. Media was aspirated off and replaced with 100 μL of serum-free media. Samples of c23.5, ASec-1, ASec-1A, and ASec-1B scFv were added to the cells were 0.5 μM final concentrations. 1× PBS buffer was used as a control. Plates were incubated for an additional 48 h at 37°C. LDH release was measured using an LDH release toxicity kit (Sigma) as per the manufacturer's protocol. Absorbance was measured as a difference between 490 nm and 690 nm wavelengths. LDH release was determined by dividing the absorbance of treated wells by the absorbance of untreated wells. The data are reported as percentage of control value obtained from three independent experiments.

Results and Discussion

Increased accumulation of Aβ in senile plaques in the brains of AD patients is thought to be a critical factor in AD pathology, and numerous approaches to decrease Aβ levels are being studied. There is considerable evidence that AD is an inflammatory disease,[34] and antibody-mediated clearance by phagocytosis induced by active immunization could potentially exacerbate brain inflammation and damage. Clinical trials using an Aβ vaccine showed promising improvements in cognition and reduced memory loss,[3] however, inflammation in the central nervous system was detected in 6% of the test individuals[4] and the mobilization of the plaques by Aβ antibodies results in increased vascular Aβ deposition and the appearance of micro-hemorrhages.[35] The positive outcomes from the vaccine trials however indicate that non-inflammatory clearance of Aβ has potential therapeutic value.

Increased cleavage of Aβ by physiological proteases such IDE and NEP can compensate for a reduction in other Aβ clearance mechanisms providing a means to regulate Aβ aggregation and neurotoxicity.[7] Depressed levels of IDE expression have been observed in the post mortem brains of AD patients[36] suggesting a role for proteolytic degradation of Aβ in AD, and increasing proteolytic cleavage of Aβ by supplementing IDE levels was shown to reduce extra-cellular levels of Aβ.[37,38] However, IDE is active on a wide range of substrates, and this activity is influenced by insulin levels,[39] both factors complicating its potential application in treating AD. Furthermore, natively folded recombinant IDE was shown to form a stable complex with Aβ, which may potentially interfere with clearance pathways and promote AD pathogenesis.[40]

Although proteolytic degradation of Aβ represents a promising therapeutic approach, the catalytic activity should be targeted specifically to Aβ to avoid potential complicating effects. A proteolytic antibody fragment lacking the Fc region engineered to specifically target and cleave Aβ can increase clearance of Aβ without inducing an inflammatory response or initiating other unwanted side-reactions. scFvs are the potent interventional agents that can be used for targeted therapeutics.[41] They can be efficiently expressed in bacteria, yeast, or plant systems and retain the antigen binding capabilities of the parent antibody.[42] Since scFvs lack

Biotechnol. Prog., 2009, Vol. 25, No. 4

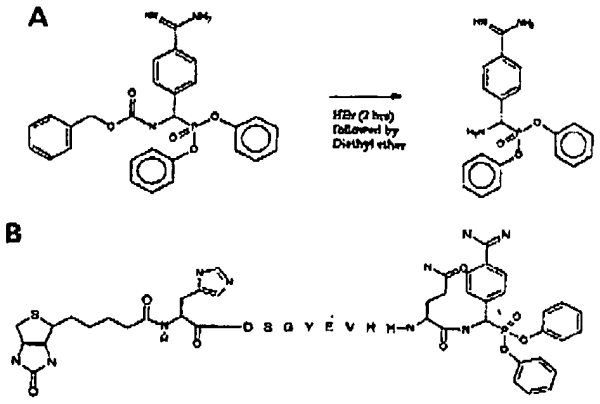

Figure 3. C-terminus TSA.

(A) Inactive hapten was activated by treatment with HBr for 2 h followed by precipitation with diethyl ether. (B) The activated hapten phosphonate diester—Diphenyl amino(4-amidinophenyl)methanephosphonate was attached to biotinylated short Aβ peptide replicating the α-secretase site. The resulting compound is the CRA.

the constant region, thereby reducing retention by Fc receptors, the use of these proteolytic scFv will reduce the chances of a cellular response mediated by the Fc receptors.[43] Because of their small size (1/6th the size of intact IgG), low kidney uptake, and rapid blood clearance, scFvs are being increasingly used in cancer research as carrier of radionuclei and drugs to tumors.[44] Therefore, an scFv that specifically hydrolyzes Aβ represents a promising therapeutic option for treating AD. We previously identified a light chain antibody mk18, and the scFv derivative c23.5, both of which have α-secretase-like activity.[11]

Since the original linker in the c23.5 scFv is susceptible to proteolysis,[45] we replaced that linker with the $(GGGGS)_3$ linker, which increases flexibility between the heavy and light chain domains, facilitates the functional folding of the antigen combining site, and resists proteolytic cleavage. Replacement of the existing linker between the VH and VL domains with the $(GGGGS)_3$ linker and replacement of the flanking SfiI and NotI sites with NheI and EcoRI sites, respectively, was verified by DNA sequencing. The resulting modified c23.5 scFv clone is termed ASec-1.

To increase the specificity of the Asec-1 scFv towards Aβ, we constructed a second generation library by replacing the 4 amino acid CDR3 region of the ASec-1 scFv by 6 random amino acids using a NNK mutation (Figure 2). Using a NNK mutation reduces the chances of introducing 2 of the 3 stop codons and covers all 20 amino acids.[46] Triplet oligonucleotides encoded by NNK leads to $4 \times 4 \times 2 = 32$ possible codons and with the randomization of 6 amino acids all possible combinations will be represented in a theoretical library diversity of $.10^9$. The catalytic residues of c23.5 are located in V_L domain whereas additional binding specificity is contained in the V_H domain.[47] The CDR3 heavy chain region was targeted initially because this region is predominantly responsible for binding activity and antigen recognition specificity.[48] It tolerates a large range of lengths and structural shapes,[49] and highly diverse CDR3 antibody libraries have been effectively utilized.[50]

Although numerous surface display technologies are available, yeast surface display provides several powerful advantages for affinity maturation of engineered antibodies.[18]

Table 2. Relative Activity of Selected Clones towards 5 μM α-Secretase Substrate in HEPES Buffer pH 7.4 at 37°C

Clone	Percentage of mk18 Cleavage of α-Secretase Substrate (Ex:355 Em:480)
p1D3	105
p2g6	115
p3g8	123
p4b7	115
P6E4 (ASec-1A)	**150**
P6G9	149
P7E2	150
P9E4	104
P9F8	124
P10D9	125
P11D3	149
P11G8(ASec-1B)	**190**
P12C5	138
P12C9	145
P12D4	143
ASec-1	**100**

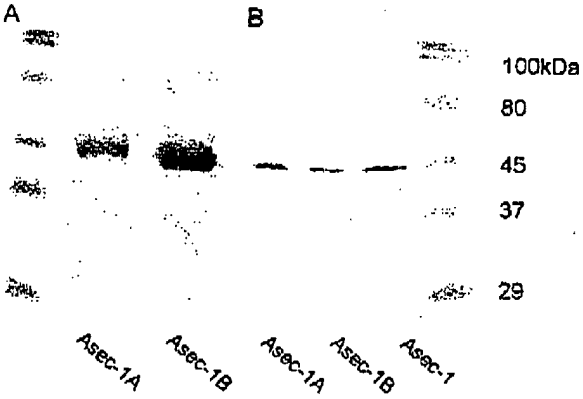

Figure 4. Purification of scFv from yeast.

Pure protein can be seen as a band corresponding to 42 kDa on (A) SDS-PAGE gel and (B) Western blot analysis using mouse anti-V5 primary and goat anti-mouse IgG HRP secondary antibody.

Transformation into yeast was confirmed by plating onto SDCAA selection plates and the library size was determined to be $\sim 10^8$. The diversity of the library was checked by sequencing 20 random clones, out of which 16 clones had a unique sequence, indicating a library diversity of $\sim 10^7$.

Originally developed as probes for enzymatic nucleophiles, electrophilic phosphonates have been used as irreversible serine protease inhibitors.[24] CRAs containing a haptenic phosphonate diester can be used for isolating serine proteases with improved nucleophilicity to their target antigen.[51] The CRA, used as an antigen for magnetic bead enrichment (Figure 3), was synthesized and purified by HPLC. The resulting product was 95% pure with some contamination due to non-biotinylated peptide. After 2 rounds of magnetic bead enrichment using the CRA, 4×10^6 cells were recovered as determined by cell count on SDCAA plates. Anti-biotin coated magnetic beads were used during the second round of panning to reduce chances of isolating streptavidin binding clones. Since our goal is to isolate scFvs with improved catalysis toward Aβ rather than just improved binding, we only performed two rounds of panning with the CRA.

After selection with the CRA, we screened 750 single clones for increased proteolytic activity toward Aβ using an

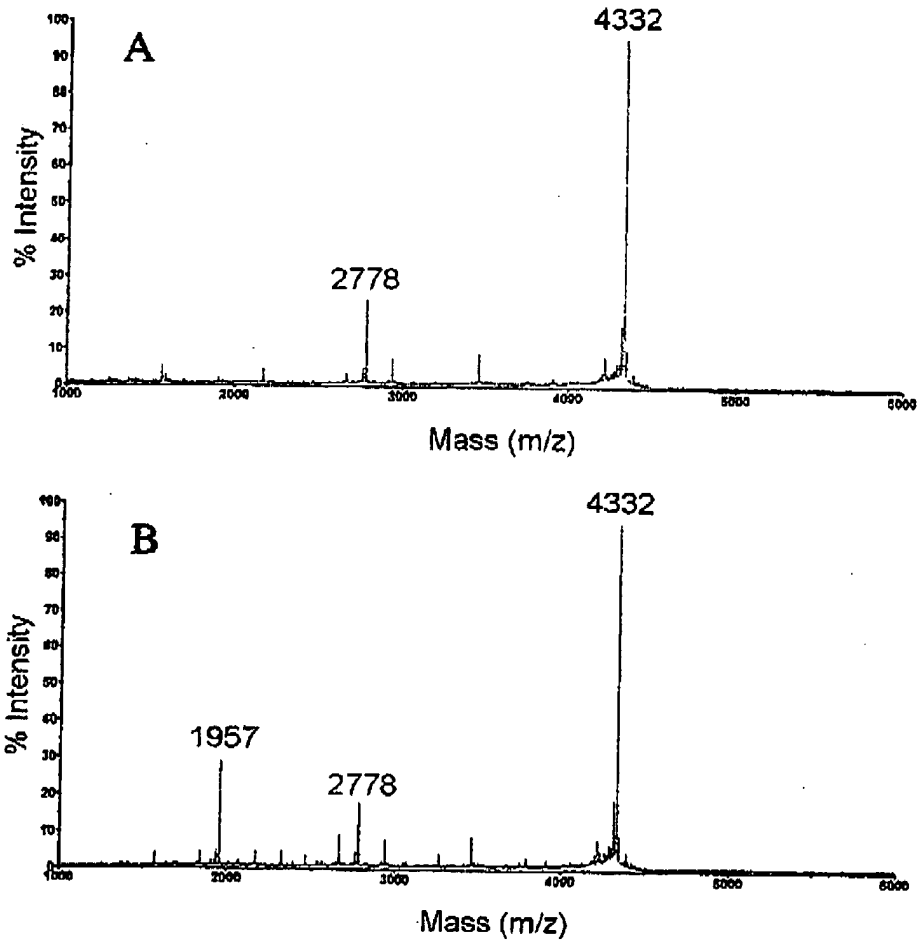

Figure 5. Proteolytic degradation of Aβ40 with antibody fragment ASec-1A.

A 50 μM aliquot of Aβ40 was incubated with alone (A) or with 250 nM ASec-1A yeast scFv in PBS (pH 7.4) (B), at 37°C. MS analysis was performed on aliquots taken after 24 h. Peaks corresponding to Aβ 1–16 (m/z = 1957) and full-length 1–40 (m/z = 4333) along with a major contaminant (m/z = 2778) are indicated.

internally quenched α-secretase substrate. Of the 750 clones tested, 15 unique clones showed increased α-secretase-like activity compared to the ASec-1 scFv expressed on the yeast surface (Table 2). A random clone selected as a control scFv showed no activity toward the substrate. Sequences of positive clones were verified by DNA sequencing. The 15 clones with increased proteolytic activity were also tested for α-secretase-like activity using Z-Lys-ONp substrate to verify that the activity was targeted to the α-secretase Lys-Leu cleavage site. The two clones corresponding to wells 6E4 and 11G8, having the highest activity toward both the α-secretase and Z-Lys-ONp substrates, were selected for further studies and renamed ASec-1A and ASec-1B respectively.

The selected scFvs were inserted into pPNL9 expression vector by gap repair after co-transformation into YVH10 competent cells. After growing the cells in SDCAA media containing Trp, the highest scFv expression levels were observed after induction by YEPGR media for 48 h as evidenced by dot blot (data not shown). Purified soluble scFv was analyzed by SDS-PAGE (Figure 4A) and western blot analysis using anti-V5 primary antibody to verify the presence of a 42 kDa band (Figure 4B). Increased proteolytic stability of the ASec-1, ASec-1A, and ASec-1B scFvs compared to the parent c23.5 scFv was evident as all of the scFvs with the modified linker show only a single 42 kDa band after purification whereas the parent c23.5 scFv contains an additional 14 kDa cleavage fragment in SDS PAGE and Western blots (data not shown).

The cleavage products of Aβ40 substrate with both scFvs were similar to those of the parent mk18 light chain antibody as determined by MS, where Aβ1-16 is the predominant product (Figure 5). The C-terminal fragment corresponding to Aβ17–40 was not detected likely due to precipitation before fractionation by MS as previously noted.[52]

The kinetic parameters k_{cat} and K_M were determined using different substrate concentrations of the Z-Lys-ONp substrate (Table 3) and the fluorogenic Aβ substrate (Table 4). When the c23.5 scFv of the mk18 light chain was constructed, the hydrolytic activity toward the Lys-ONp substrate decreased 6-fold compared to mk18 due to both an increase in K_M and decrease in k_{cat} (Table 3). The decrease in k_{cat} was mostly recovered when the V_H/V_L linker was replaced with the standard $(GGGGS)_3$ linker to generate the ASec-1 scFv (Table 3) possibly because of a reduction in strain between the two antibody domains. The two selected scFvs, ASec-1A, and ASec-1B, both showed decreases in K_M and

Table 3. Kinetic Constants of scFvs for Hydrolysis of Z-Lys-ONp in HEPES Buffer pH 7.4 and 37°C

	K_M (μM)	k_{cat} (per min)	k_{cat}/K_M (μM/min)
ASec-1	7.24 ± 0.21	766.68 ± 2.35	105.9
ASec-1A	3.62 ± 0.28	1187.14 ± 1.75	327.94
ASec-1B	4.80 ± 0.37	1345.71 ± 3.02	280.36
mk18 from bacteria	2.71 ± 0.13	1012.50 ± 0.87	373.62
c23.5 from bacteria	8.08 ± 0.45	495.10 ± 1.11	61.3

Table 4. Kinetic Constants of scFvs for Hydrolysis of α-Secretase Aβ Fluorogenic Substrate in HEPES Buffer pH 7.4 and 37°C

	K_M (μM)	k_{cat} (per min)	k_{cat}/K_m (μM/min)
ASec-1	6.12 ± 0.31	66.41 ± 1.26	10.85
ASec-1A	0.6 ± 0.08	34.84 ± 0.1	58.07
ASec-1B	1.51 ± 0.12	61.02 ± 0.22	40.41

increases in k_{cat} toward the Lys-ONp substrate, more closely reflecting the values obtained with the original mk18 light chain antibody (Table 3).

The specificity constant (k_{cat}/K_M) toward the Aβ substrate for ASec-1A is 5.6-fold greater and for ASec-1B is 2.8-fold greater than the parent ASec-1 scFv (Table 4). The increase in activity against Aβ for both scFvs is due to decreases in K_M compared to ASec-1, rather than increases in k_{cat}. All three scFvs, even the parent ASec-1 containing the $(GGGGS)_3$ linker, had a higher specificity constant compared to the original c23.5 scFv. The increase in the specificity constant due to the improved K_M values toward the Aβ substrate was expected because the randomized CDR3 heavy chain library was designed to increase binding to the desired substrate without affecting the catalytic residues in the light chain domain. The light chain mk18 of the parent c23.5 scFv was observed to cleave VIP with K_M 0.2 μM and k_{cat} 0.01/min.[53] The lower K_M for VIP cleavage compared to Aβ is expected because the light chain mk18 was originally derived from an antibody raised by immunization with VIP. However, addition of a random heavy chain to the mk18 light chain to generate a full length scFv reduced its binding affinity to VIP. Affinity maturation of this full length scFv against a CRA based on the VIP peptide resulted in a significant enhancement of its binding affinity.[12] A similar increase in binding specificity towards the Aβ substrate is observed in the case of our ASec-1A and ASec-1B scFv following affinity maturation against phosphonate diesters.

The effect of the recombinant scFv on SH-SY5Y neuroblastoma cells was determined and compared with the toxicity induced by the parent c23.5 scFv (Figure 6). Although the parent c23.5 scFv is toxic to the SH-SY5Y cells, all the variants containing the $(GGGGS)_3$ linker instead of the original linker are not.

Proteolytic processing of amyloid precursor protein (APP) by the non amyloidogenic pathway involves cleavage by α and γ secretases and precludes Aβ formation, instead yielding a soluble N-terminal fragment, sAPP that is neuroprotective and possesses neurotrophic properties.[54-55] Thus, strategies to enhance α-secretase cleavage of APP could be a significant therapeutic approach in ameliorating the progression of the disease, and to reverse memory loss. Because the proteolytic scFvs reported here have been engineered to target the α-secretase site, in addition to clearing the existing Aβ, they could also potentially be used to enhance APP processing to reduce further production of Aβ while stimulating production of the neuroprotective sAPP protein.

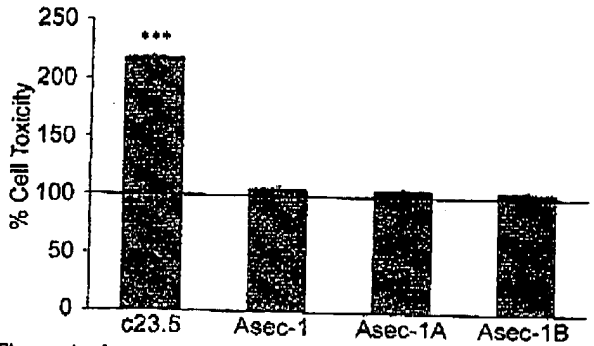

Figure 6. LDH release assay. Modifying the c23.5 scFv greatly reduces its toxicity towards SHSY-5Y neuroblastoma cells. Data are expressed as percentage of control wells containing cells with medium alone. Line at 100% indicates buffer only control. ***$P < 0.001$ using paired Student's t-test. Error bars indicate SEM.

The substrate specificity of the scFv can be increased further by additional manipulation of the CDR regions. The binding site of proteases is determined by the proteolytic site (P1–P1′) and interactions with amino acids to each side of the hydrolytic site.[56] For example, trypsin has a deep, narrow binding pocket on the C-terminal side of the lysine/arginine cleavage site (P1′) and will selectively cleave proteins or peptides that have amino acids with long positively charged side chains.[57] The substrate specificity of the proteolytic scFv can be further increased by generating additional scFv libraries with randomized CDR regions that specifically accommodate the amino acids surrounding the α-secretase site of Aβ. In vitro affinity maturation of the proteolytic scFvs should provide a general means of increasing the specificity constant and producing a highly selective scFv, which would have potential applications for treating AD.

Acknowledgments

The authors thank Dr. Sudhir Paul, University of Texas, Houston Health Science Center, for the hapten precursor, John Lopez for his help in synthesis of the CRA and MS, and to Dr. Bin Yuan and Philip Schulz for technical assistance. This work was supported by grants from the Arizona Department of Health Services for the Arizona Alzheimer's Consortium and the Alzheimer's Association.

Literature cited

1. Apostolova LG, Thompso PM. Mapping progressive brain structural changes in early Alzheimer's disease and mild cognitive impairment. *Neuropsychologia*. 2008;46:1597–1612.
2. Haass C, Selkoe DJ. Soluble protein oligomers in neurodegeneration: lessons from the Alzheimer's amyloid beta-peptide. *Nat Rev Mol Cell Biol*. 2007;8:101–112.
3. Nicoll JA, Wilkinson D, Holmes C, Steart, P, Markham, H, Weller RO. Neuropathology of human Alzheimer disease after immunization with amyloid-beta peptide: a case report. *Nat Med*. 2003;9:448–452.
4. Check E. Nerve inflammation halts trial for Alzheimer's drug. *Nature*. 2002;415:462.
5. Chander H, Chauhan A, Chauhan V. Binding of proteases to fibrillar amyloid-beta protein and its inhibition by Congo red. *J Alzheimers Dis*. 2007;12:261–269.
6. Farris W, Mansourian S, Chang Y, Lindsley L, Eckman EA, Frosch MP, Eckman CB, Tanzi RE, Selkoe DJ, Guenette S. Insulin-degrading enzyme regulates the levels of insulin, amyloid beta-protein, and the beta-amyloid precursor protein intracellular domain in vivo. *Proc Natl Acad Sci USA*. 2003;100:4162–4167.

7. Miners JS, Baig S, Palmer J, Palmer LE, Kehoe PG, Love S. Abeta-degrading enzymes in Alzheimer's disease. *Brain Pathol.* 2008;18:240–252.
8. Betts V, Leissring MA, Dolios G, Wang R, Selkoe DJ, Walsh DM. Aggregation and catabolism of disease-associated intra-Abeta mutations: reduced proteolysis of AbetaA21G by neprilysin. *Neurobiol Dis.* 2008;31:442–450.
9. Bennett RG, Duckworth WC, Hamel FG. Degradation of amylin by insulin-degrading enzyme. *J Biol Chem.* 2000;275:36621–36625.
10. Gao QS, Sun M, Tyutyulkova S, Webster D, Rees A, Tramontano A, Massey RJ, Paul S. Molecular cloning of a proteolytic antibody light chain. *J Biol Chem.* 1994;269:32389–32393.
11. Rangan SK, Liu R, Brune D, Planque S, Paul S, Sierks MR. Degradation of beta-amyloid by proteolytic antibody light chains. *Biochemistry.* 2003;42:14328–14334.
12. Sun M, Gao QS, Kimarskiy L, Rees A, Paul S. Cleavage specificity of a proteolytic antibody light chain and effects of the heavy chain variable domain. *J Mol Biol.* 1997;271:374–385.
13. Whitlow M, Bell BA, Feng SL, Filpula D, Hardman KD, Hubert SL, Rollence ML, Wood JF, Schott ME, Milenic DE. An improved linker for single-chain Fv with reduced aggregation and enhanced proteolytic stability. *Protein Eng.* 1993;6:989–995.
14. Shan D, Pres OW, Tsu TT, Hayden MS, Ledbetter JA. Characterization of scFv-Ig constructs generated from the anti-CD20 mAb 1F5 using linker peptides of varying lengths. *J Immunol.* 1999;162:6589–6595.
15. Xu JL, Davis MM. Diversity in the CDR3 region of V(H) is sufficient for most antibody specificities. *Immunity.* 2000;13:37–45.
16. Wang XX, Shusta EV. The use of scFv-displaying yeast in mammalian cell surface selections. *J Immunol Methods.* 2005;304:30–42.
17. Chao G, Lau WL, Hackel BJ, Sazinsky SL, Lippow SM, Wittrup KD. Isolating and engineering human antibodies using yeast surface display. *Nat Protoc.* 2006;1:755–768.
18. Feldhaus MJ, Siegel RW. Yeast display of antibody fragments: a discovery and characterization platform. *J Immunol Methods.* 2004;290:69–80.
19. Yeung YA, Wittrup KD. Quantitative screening of yeast surface-displayed polypeptide libraries by magnetic bead capture. *Biotechnol Prog.* 2002;18:212–220.
20. Xu Y, Yamamoto N, Janda KD. Catalytic antibodies: hapten design strategies and screening methods. *Bioorg Med Chem.* 2004;12:5247–5268.
21. Tanaka F. Catalytic antibodies as designer proteases and esterases. *Chem Rev.* 2002;102:4885–4906.
22. Paul S, Planque S, Zhou YX, Taguchi H, Bhatia G, Karle S, Hanson C, Nishiyama Y. Specific HIV gp120-cleaving antibodies induced by covalently reactive analog of gp120. *J Biol Chem.* 2003;278:20429–20435.
23. Planque S, Nishiyama Y, Taguchi H, Salas M, Hanson C, Paul S. Catalytic antibodies to HIV: physiological role and potential clinical utility. *Autoimmun Rev.* 2008;7:473–479.
24. Taguchi H, Planque S, Nishiyama Y, Szabo P, Weksler ME, Friedland RP, Paul S. Catalytic antibodies to amyloid beta peptide in defense against Alzheimer disease. *Autoimmun Rev.* 2008;7:391–397.
25. Gao C, Mao S, Kaufmann G, Wirsching P, Lerner RA, Janda KD. A method for the generation of combinatorial antibody libraries using pIX phage display. *Proc Natl Acad Sci USA.* 2002;99:12612–12616.
26. Bond CJ, Marsters JC, Sidhu SS. Contributions of CDR3 to V H H domain stability and the design of monobody scaffolds for naive antibody libraries. *J Mol Biol.* 2003;332:643–655.
27. Orr-Weaver TL, Szostak JW. Yeast recombination: the association between double-strand gap repair and crossing-over. *Proc Natl Acad Sci USA.* 1983;80:4417–4421.
28. Fujita Y, Ito J, Ueda M, Fukuda H, Kondo A. Synergistic saccharification, and direct fermentation to ethanol, of amorphous cellulose by use of an engineered yeast strain codisplaying three types of cellulolytic enzyme. *Appl Environ Microbiol.* 2004;70:1207–1212.
29. Siegel RW, Coleman JR, Miller KD, Feldhaus MJ. High efficiency recovery and epitope-specific sorting of an scFv yeast display library. *J Immunol Methods.* 2004;286:141–153.
30. Nishiyama Y, Taguchi H, Luo JQ, Zhou YX, Burr G, Karle S, Paul S. Covalent reactivity of phosphonate monophenyl esters with serine proteinases: an overlooked feature of presumed transition state analogs. *Arch Biochem Biophys.* 2002;402:281–288.
31. Komano H, Rockwell N, Wang GT, Krafft GA, Fuller RS. Purification and characterization of the yeast glycosylphosphatidylinositol-anchored, monobasic-specific aspartyl protease yapsin 2 (Mkc7p). *J Biol Chem.* 1999;274:24431–24437.
32. Miller KD, Weaver-Feldhaus J, Gray SA, Siegel RW, Feldhaus MJ. Production, purification, and characterization of human scFv antibodies expressed in *Saccharomyces cerevisiae*, *Pichia pastoris*, and *Escherichia coli*. *Protein Expr Purif.* 2005;42:255–267.
33. Zameer A, Kasturirangan S, Emadi S, Nimmagadda SV, Sierks MR. Anti-oligomeric Abeta single-chain variable domain antibody blocks Abeta-induced toxicity against human neuroblastoma cells. *J Mol Biol.* 2008;384:917–928.
34. Akiyama H, Barger S, Barnum S, Bradt B, Bauer J, Cole GM, Cooper NR, Eikelenboom P, Emmerling M, Fiebich BL, Finch CE, Frautschy S, Griffin WS, Hampel H, Hull M, Landreth G, Lue L, Mrak R, Mackenzie IR, McGeer PL, O'Banion MK, Pachter J, Pasinetti G, Plata-Salaman C, Rogers J, Rydel R, Shen Y, Streit W, Strohmeyer R, Tooyoma I, Van Muiswinkel FL, Veerhuis R, Walker D, Webster S, Wegrzyniak B, Wenk G, Wyss-Coray T. Inflammation and Alzheimer's disease. *Neurobiol Aging.* 2000;21:383–421.
35. Racke MM, Boone LI, Hepburn DL, Parsadainian M, Bryan MT, Ness DK, Piroozi KS, Jorda WH, Brown DD, Hoffman WP, Holtzman DM, Bales KR, Gitter BD, May PC, Paul SM, DeMattos RB. Exacerbation of cerebral amyloid angiopathy-associated microhemorrhage in amyloid precursor protein transgenic mice by immunotherapy is dependent on antibody recognition of deposited forms of amyloid beta. *J Neurosci.* 2005;25:629–636.
36. Cook DG, Leverenz JB, McMillan PJ, Kulstad JJ, Ericksen S, Roth RA, Schellenber GD, Ji LW, Kovacina KS, Craft S. Reduced hippocampal insulin-degrading enzyme in late-onset Alzheimer's disease is associated with the apolipoprotein E-epsilon4 allele. *Am J Pathol.* 2003;162:313–319.
37. Qiu WQ, Walsh DM, Ye Z, Vekrellis K, Zhang J, Podlisn MB, Rosner MR, Safavi A, Hersh LB, Selkoe DJ. Insulin-degrading enzyme regulates extracellular levels of amyloid beta-protein by degradation. *J Biol Chem.* 1998;273:32730–32738.
38. Leissring MA, Farris W, Chang AY, Walsh DM, Wu X, Sun X, Frosch MP, Selkoe DJ. Enhanced proteolysis of beta-amyloid in APP transgenic mice prevents plaque formation, secondary pathology, and premature death. *Neuron.* 2003;40:1087–1093.
39. Leissring MA, Selkoe DJ. Structural biology: enzyme target to latch on to. *Nature.* 2006;443:761–762.
40. Llovera RE, de Tullio M, Alonso LG, Leissring MA, Kaufman SB, Roher AE, de Prat Gay G, Morelli L, Castano EM. The catalytic domain of insulin-degrading enzyme forms a denaturant-resistant complex with amyloid beta peptide: implications for Alzheimer's disease pathogenesis. *J Biol Chem.* 2008;283:17039–17048.
41. Arafat WO, Gomez-Navarro J, Buchsbaum DJ, Xiang J, Wang M, Casado E, Barker SD, Mahasreshti PJ, Haisma HJ, Barnes MN, Siegal GP, Alvarez RD, Hemminki A, Nettelbeck DM, Curiel DT. Effective single chain antibody (scFv) concentrations in vivo via adenoviral vector mediated expression of secretory scFv. *Gene Ther.* 2002;9:256–262.
42. Kim SH, Schindler DG, Lindner AB, Tawfik DS, Eshhar Z. Expression and characterization of recombinant single-chain Fv and Fv fragments derived from a set of catalytic antibodies. *Mol Immunol.* 1997;34:891–906.
43. Clark M. Antibody humanization: a case of the "Emperor's new clothes"? *Immunol Today.* 2000;21:397–402.
44. Kim DJ, Chung JH, Ryu YS, Rhim JH, Kim CW, Suh Y, Chung HK. Production and characterisation of a recombinant

scFv reactive with human gastrointestinal carcinomas. *Br J Cancer.* 2002;87:405–413.
45. Argos P. An investigation of oligopeptides linking domains in protein tertiary structures and possible candidates for general gene fusion. *J Mol Biol.* 1990;211:943–958.
46. Tominaga T, Hatakeyama Y. Determination of essential and variable residues in pediocin PA-1 by NNK scanning. *Appl Environ Microbiol.* 2006;72:1141–1147.
47. Noel D, Bernardi T, Navarro-Teulon I, Marin M, Martinetto JP, Ducancel F, Mani JC, Pau B, Piechaczyk M, Blard-Piechaczyk M. Analysis of the individual contributions of immunoglobulin heavy and light chains to the binding of antigen using cell transfection and plasmon resonance analysis. *J Immunol Methods.* 1996;193:177–187.
48. Davis MM, Boniface JJ, Reich Z, Lyons D, Hampl J, Arden B, Chien Y. Ligand recognition by alpha beta T cell receptors. *Annu Rev Immunol.* 1998;16:523–544.
49. Chothia C, Lesk AM. Canonical structures for the hypervariable regions of immunoglobulins. *J Mol Biol.* 1987;196:901–917.
50. Hoet RM, Cohen EH, Kent RB, Rookey K, Schoonbroodt S, Hogan S, Rem L, Frans N, Daukandt M, Pieters H, van Hegelsom R, Neer NC, Nastri HG, Rondon IJ, Leeds JA, Hufton SE, Huang L, Kashin I, Devlin M, Kuang G, Steukers M, Viswanathan M, Nixon AE, Sexton DJ, Hoogenboom HR, Ladner RC. Generation of high-affinity human antibodies by combining donor-derived and synthetic complementarity-determining-region diversity. *Nat Biotechnol.* 2002;3:344–348.
51. Taguchi H, Burr G, Kurle S, Planque S, Zhou YX, Paul S, Nishiyama Y. A mechanism-based probe for gp120-Hydrolyzing antibodies. *Bioorg Med Chem Lett.* 2002;12:3167–3170.
52. Liu R, McAllister C, Lyubchenko Y, Sierks MR. Proteolytic antibody light chains alter beta-amyloid aggregation and prevent cytotoxicity. *Biochemistry.* 2004;43:9999–10007.
53. Gao QS, Sun M, Rees AR, Paul S. Site-directed mutagenesis of proteolytic antibody light chain. *J Mol Biol.* 1995;253:658–664.
54. Fahrenholz F. Alpha-secretase as a therapeutic target. *Curr Alzheimer Res.* 2007;4:412–417.
55. Postina R. A closer look at alpha-secretase. *Curr Alzheimer Res.* 2008;5:179–186.
56. Perona JJ, Craik CS. Structural basis of substrate specificity in the serine proteases. *Protein Sci.* 1995;4:337–360.
57. Olsen JV, Ong SE, Mann M. Trypsin cleaves exclusively C-terminal to arginine and lysine residues. *Mol Cell Proteomics.* 2004;3:608–614.

Manuscript received Aug. 8, 2008, and revision received Dec. 12, 2008.

THE JOURNAL OF BIOLOGICAL CHEMISTRY
© 2004 by The American Society for Biochemistry and Molecular Biology, Inc.

Vol. 279, No. 9, Issue of February 27, pp. 7877–7883, 2004
Printed in U.S.A.

Toward Selective Covalent Inactivation of Pathogenic Antibodies

A PHOSPHONATE DIESTER ANALOG OF VASOACTIVE INTESTINAL PEPTIDE THAT INACTIVATES CATALYTIC AUTOANTIBODIES*

Received for publication, October 3, 2003, and in revised form, December 11, 2003
Published, JBC Papers in Press, December 15, 2003, DOI 10.1074/jbc.M310950200

Yasuhiro Nishiyama‡, Gita Bhatia§, Yogesh Bangale, Stephanie Planque, Yukie Mitsuda, Hiroaki Taguchi, Sangeeta Karle, and Sudhir Paul‡

From the Chemical Immunology and Therapeutics Research Center, Department of Pathology and Laboratory Medicine, University of Texas-Houston Medical School, Houston, Texas 77030

We report the selective inactivation of proteolytic antibodies (Abs) to an autoantigen, the neuropeptide vasoactive intestinal peptide (VIP), by a covalently reactive analog (CRA) of VIP containing an electrophilic phosphonate diester at the Lys^{20} residue. The VIP-CRA was bound irreversibly by a monoclonal Ab that catalyzes the hydrolysis of VIP. The reaction with the VIP-CRA proceeded more rapidly than with a hapten CRA devoid of the VIP sequence. The covalent binding occurred preferentially at the light chain subunit of the Ab. Covalent VIP-CRA binding was inhibited by VIP devoid of the phosphonate diester group. These results indicate the importance of noncovalent VIP recognition in guiding Ab nucleophilic attack on the phosphonate group. Consistent with the covalent binding data, the VIP-CRA inhibited catalysis by the recombinant light chain of this Ab with potency greater than the hapten-CRA. Catalytic hydrolysis of VIP by a polyclonal VIPase autoantibody preparation that cleaves multiple peptide bonds located between residues 7 and 22 essentially was inhibited completely by the VIP-CRA, suggesting that the electrophilic phosphonate at Lys^{20} enjoys sufficient conformational freedom to react covalently with Abs that cleave different peptide bonds in VIP. These results suggest a novel route to antigen-specific covalent targeting of pathogenic Abs.

Specific antigen recognition by the variable domains underlies the pathogenic effects of certain Abs[1] produced as a result of autoimmune, allergic, and anti-transplant reactions. For instance, Abs found in myasthenia gravis (reviewed in Ref. 1) and hemophilia (reviewed in Ref. 2) bind important epitopes of the acetylcholine receptor and Factor VIII, respectively, that interfere with the biological activity of these proteins by a steric hindrance mechanism. Other Abs utilize their constant region to mediate pathogenic effects, but antigen recognition by Ab variable domains is the stimulus initiating these effects, *e.g.* Ab recognition of erythrocyte antigens stimulates complement activation by the constant region in autoimmune hemolytic anemia and incompatible blood transfusions. Similarly, allergen recognition by IgE bound to receptors for the constant region on the surface of mast cells stimulates their degranulation. In other diseases, the mechanism of Ab pathogenicity is less clear. For example, Abs to nucleic acids in lupus (reviewed in Ref. 3) and to thyroglobulin in Hashimoto's thyroiditis (reviewed in Ref. 4) are unambiguously disease-associated but additional immune abnormalities are also evident in these diseases and the precise functional effects of the Abs remain debatable. Recently, a novel variable domain mechanism underlying Ab pathogenicity has emerged, *viz.* the catalytic cleavage of antigens. Hydrolytic catalysts such as Abs to polypeptides (5–8) and nucleic acids (9) hold the potential of permanent antigen inactivation. Moreover, catalysts are endowed with turnover capability, *i.e.* a single Ab molecule can hydrolyze multiple antigen molecules, suggesting that such Abs may exert functional effects that are more potent than Abs dependent on stoichiometric antigen recognition.

Abs that catalyze the cleavage of VIP have been identified in patients with autoimmune disease (10). VIP is a 28 amino acid peptide with important biological actions including immunoregulation via actions on T lymphocytes (reviewed in Ref. 11) and control of blood and airflow via actions on the smooth muscle (reviewed in Ref. 12). A model proteolytic Ab interferes with cytokine synthesis by cultured T cells accompanied by depletion of cellular VIP (13), and administration of the Ab to mice interferes with relaxation of airway smooth muscle (14). Proteolytic Abs to VIP appear to utilize a covalent catalytic mechanism reminiscent of serine proteases. This is suggested by studies in which replacement of the active site Ser residue resulted in the loss of catalytic activity (15) and by inhibition of catalysis by haptenic phosphonate diesters (10). These compounds form adducts with the activated nucleophiles of enzymes by virtue of the covalent reactivity of the electrophilic phosphorus atom (reviewed in Ref. 16) and have been developed recently as probes for the active site nucleophiles in Abs displaying serine protease and serine esterase activity (17, 18), designated covalently reactive antigen analogs (CRAs).

As in the case of ordinary Abs, traditional noncovalent antigen recognition is hypothesized to underlie the specificity of the proteolytic Abs for VIP. Therefore, CRAs of the VIP sequence represent a potentially specific means to target the Abs by virtue of offering a reaction surface that combines covalent

* This work was supported by National Institutes of Health Grant AI31268. The costs of publication of this article were defrayed in part by the payment of page charges. This article must therefore be hereby marked "*advertisement*" in accordance with 18 U.S.C. Section 1734 solely to indicate this fact.

‡ To whom correspondence may be addressed: Dept. of Pathology and Laboratory Medicine, University of Texas-Houston Medical School, 6431 Fannin, Houston, TX 77030. Tel.: 713-500-7342 (to Y. N.) or 713-500-5347 (to S. P.); Fax: 713-500-0574; E-mail: Yasuhiro.Nishiyama@uth.tmc.edu (Y. N.) or Sudhir.Paul@uth.tmc.edu (S. P.).

§ Present address: Dept. of Biochemistry and Molecular Genetics, University of Colorado Health Sciences Center, 4200 E. Ninth Ave., Denver, CO 80262.

[1] The abbreviations used are: Ab, antibody; AMC, 7-amino-4-methylcoumarin; CHAPS, 3-[(3-cholamidopropyl)dimethylammonio]-1-propanesulfonic acid; CRA, covalently reactive analog; DMF, *N,N*-dimethylformamide; Me_2SO, dimethyl sulfoxide; V_{app}, apparent reaction velocity; VIP, vasoactive intestinal peptide; DFP, diisopropyl fluorophosphate.

Downloaded from www.jbc.org by guest, on April 28, 2010

PAGE 84/92 * RCVD AT 4/28/2010 6:45:45 PM [Eastern Daylight Time] * SVR:USPTO-EFXRF-6/33 * DNIS:2738300 * CSID:7132705361 * DURATION (mm-ss):48-00

binding to the Ab active site with noncovalent binding at neighboring peptide epitope(s). Here we describe the antigen-specific covalent reaction of monoclonal and polyclonal Abs with a synthetic VIP-CRA compound. Despite positioning of the phosphonate group at a single site, Lys^{20}, the covalent reaction resulted in irreversible inhibition of polyclonal Abs that cleave VIP at several peptide bonds located between residues 7 and 22. The results suggest the feasibility of targeted inactivation of individual Ab populations based on their antigenic specificity.

MATERIALS AND METHODS

CRAs—Diphenyl *N*-(6-biotinamidohexanoyl)amino(4-amidinophenyl)methanephosphonate (compound 1) was prepared from diphenyl-amino(4-amidinophenyl)methanephosphonate (19, 20) and 6-biotinamidohexanoic acid (Anaspec, San Jose, CA) by the aid of (benzotriazolo-1-yl)oxytris(pyrrolidino)phosphonium hexafluorophosphate (PyBOP) (Novabiochem, San Diego, CA). The HPLC-purified material (retention time 20.76 min, purity 95% (220 nm); YMC ODS-AM column (4.6 × 250 mm), 0.05% trifluoroacetic acid in water (A):0.05% trifluoroacetic acid in acetonitrile (B), from 90:10 to 20:80 in 45 min (1.0 ml/min)) was characterized by electrospray ionization-mass spectrometry (observed *m/z* 721.3 (MH^+; calculated MH^+ for $C_{36}H_{48}N_6O_6PS$, 721.3)) and stored as 10 mM solution in DMF at −70 °C. The active ester 2 was prepared by acylating the same precursor amine with disuccinimidyl suberate (Pierce, Rockford, IL) and characterized in the same way (observed *m/z* 635.3 (MH^+; calculated MH^+ for $C_{32}H_{39}N_4O_6P$, 635.2)). VIP-CRA (compound 3) was synthesized as follows. The VIP sequence with N-terminal biotin was constructed on Rink amide MBHA resin (0.72 mmol/g, Novabiochem) by the standard 9-fluorenylmethoxycarbonyl protocol (21) with the exception that 4-methyltrityl (22) was used for side-chain protection of Lys^{20}. The peptide resin was treated with 1% trifluoroacetic acid in dichloromethane (5 min × 10) to remove the 4-methyltrityl group, and the deprotected amino group of Lys^{20} was acylated with compound 2 in 1-methyl-2-pyrrolidinone containing 0.1 mM *N,N*-diisopropylethylamine. The peptide resin was treated with trifluoroacetic acid-ethanedithiol-thioanisole-phenol (90:1:1:8) at room temperature for 2 h. After removing the resin by filtration, diethyl ether was added to the solution to afford a precipitate, which was collected by centrifugation and washed with diethyl ether. The HPLC-purified material (retention time 50.25 min, purity 96% (220 nm); Vydac 214TP C4 column (4.6 × 250 mm); A:B from 90:10 to 60:40 in 60 min (1.0 ml/min)) was characterized by electrospray ionization-mass spectrometry (observed *m/z* 4071.4 (MH^+; calculated MH^+ for $C_{180}H_{283}N_{49}O_{49}PS_2$, 4072.0)) and stored as 10 mM solution in Me_2SO at −70 °C.

Abs—Monoclonal anti-VIP IgG clone c23.5 and control isotype-matched IgG clone UPC10 (IgG2a, κ, Sigma) were purified from ascites by affinity chromatography on immobilized protein G-Sepharose (23). Polyclonal IgG from the serum of a human subject with chronic obstructive pulmonary disease (designated HS-2 in Ref. 24) was also purified by protein G-Sepharose chromatography. The recombinant light chain of anti-VIP Ab clone c23.5 (GenBank™ accession number L34775) was expressed in bacterial periplasmic extracts and purified by the binding of the His_4 tag to a nickel-affinity column (15). All of the Abs were electrophoretically homogeneous. Protein concentrations were determined with Micro BCA protein assay kit (Pierce).

CRA Adducts—Covalent binding assays were carried out as described previously (17, 20). IgG (1 μM) was incubated with compound 1 or 3 (10 μM) in 10 mM sodium phosphate, 0.137 M NaCl, 2.7 mM KCl, pH 7.4, containing 1 mM CHAPS and 0.1% Me_2SO (in compound 3 binding experiments) or 0.1% DMF (in compound 1 binding experiments) at 37 °C. In some experiments, the reaction was conducted in the presence of human plasma collected in EDTA (pooled from eight healthy blood donors; 1% v/v). Aliquots of the reaction mixtures at 10, 20, 40, 60, 90, and 120 min were boiled in 2% SDS containing 3.3% 2-mercaptoethanol in a water bath (5 min) and then subjected to electrophoresis (4–20% polyacrylamide gels, Bio-Rad). Following electroblotting onto nitrocellulose membranes (TransBlot, Bio-Rad), biotin-containing adducts were stained with a streptavidin-peroxidase conjugate and a chemiluminescent substrate kit (Supersignal, Pierce). Band density was expressed in arbitrary area units (AAU) determined using a Fluoro-STM Multi-Imager (Bio-Rad), ensuring that the densities were within the linear response range.

Catalysis Assays—Pro-Phe-Arg-AMC (0.2 mM, Peptides International, Louisville, KY) was incubated with Ab (0.8 μM) in 96-well plates in 50 mM Tris·HCl, 0.1 M glycine, pH 8.0, containing 0.6% Me_2SO and 0.025% Tween 20 at 37 °C, and the release of AMC was determined by fluorometry (λ_{em} 470 nm; λ_{ex} 360 nm, Cary Eclipse spectrometer, Varian, Palo Alto, CA). Preparation and assay of cleavage of [Tyr^{10-125}I]VIP were described previously (24). To determine whether the CRAs inhibit Abs irreversibly, IgG (2 μM) was incubated (37 °C) with compound 1 or 3 for 16 h in 50 mM Tris·HCl, 0.1 M Gly, pH 8.0, containing 2.5% Me_2SO and 0.025% Tween 20. Unreacted compound 1 or 3 was then removed by chromatography of the reaction mixtures (0.2 ml) on protein G columns as described previously (23) (50 μl of settled gel; washed with 0.8 ml of 50 mM Tris·HCl, pH 7.4; eluted with 0.2 ml of 0.1 M Gly·HCl, pH 2.7; neutralized with 1 M Tris·HCl, pH 9). 50-μl aliquots of the recovered IgG (and IgG-CRA complexes) were incubated with [Tyr^{10-125}I]VIP (86,000 cpm) for 18 h, and peptide cleavage was determined by measuring the radioactivity soluble in trichloroacetic acid. Control IgG samples were incubated without CRA, chromatographed, and analyzed for VIP-cleaving activity in the same way.

RESULTS

VIP-CRA—Important features in design of the VIP-CRA (compound 3 in Fig. 1*A*) are as follows. (*a*) Inclusion of the electrophilic phosphonate diester group capable of selective reaction with activated nucleophiles, for example, is found in serine proteases (16). (*b*) The location of the positively charged amidino group is in proximity to the phosphonate to allow recognition by the model proteolytic IgG clone c23.5, which cleaves peptide bonds preferentially on the C-terminal side of basic amino acids (Arg/Lys) (23, 25). (*c*) The incorporation of these groups is on the side chain of Lys^{20} in the sequence of VIP. Hapten CRA 1 contains the phosphonate diester and amidino groups but is devoid of the VIP sequence. Location of the covalently reactive moiety at Lys^{20} is based on observations that the Lys^{20}-Lys^{21} peptide bond is one of the bonds cleaved by monoclonal Ab clone c23.5 (23) and polyclonal human IgG preparations containing Abs to VIP (24). Peptide inhibitors of proteases customarily contain the covalently reactive group located within the peptide backbone or at the peptide termini (*e.g.* Refs. 26 and 27). In this study, our purpose was to maximize the opportunity for approach of the phosphonate group within covalent binding distance of the nucleophile contained in diverse Ab active sites. For this reason, the phosphonate group was placed at the side chain of Lys^{20} using a flexible linker, which allows rotation at several C–C bonds (as opposed to inclusion of the phosphonate within the peptide backbone, which may impose a greater level of conformational constraints on accessibility of this group).

VIP-CRA 3 was synthesized by the regioselective on-resin acylation as outlined in Fig. 1*B*. The VIP sequence was constructed by solid-phase peptide synthesis with standard 9-fluorenylmethoxycarbonyl chemistry with the exception that the 4-methyltrityl group was used for side-chain protection of Lys at position 20 (compound 4a). After selective removal of 4-methyltrityl, peptide resin 4b was acylated with compound 2, which was prepared from diphenyl amino(4-amidinophenyl)-methanephosphonate and disuccinimidyl suberate. The resulting peptide resin 4c was treated with anhydrous trifluoroacetic acid to give compound 3, which was purified with HPLC, yielding a single species with the anticipated mass (*m/z*, 4071.4; calculated value, 4072.0).

Covalent Ab Labeling—Monoclonal Ab c23.5, raised by hyperimmunization with VIP, is characterized by strong recognition of the ground state of VIP (K_d 1.9 nM; K_m 0.34 nM) made possible by traditional noncovalent Ab paratope-epitope interactions (23). The catalytic site of the Ab is located in the light chain subunit and is composed of a serine protease-like catalytic triad (15). Here, we compared the covalent binding of this Ab by VIP-CRA 3 and hapten CRA 1. The isotype-matched Ab UPC10 (IgG2a, κ) served as the control to determine background Ab nucleophilic reactivity independent of noncovalent

Downloaded from www.jbc.org by guest, on April 28, 2010

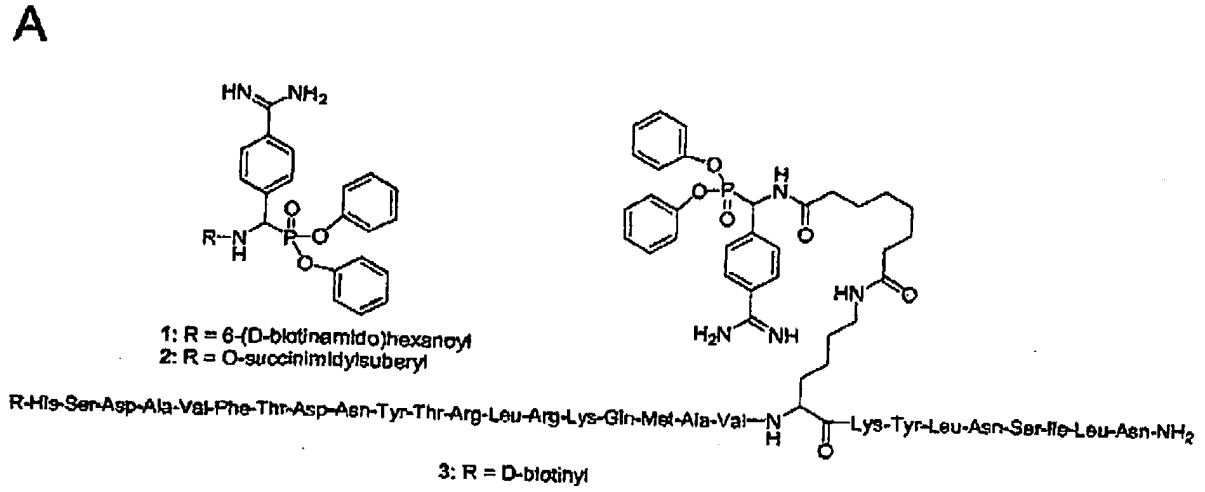

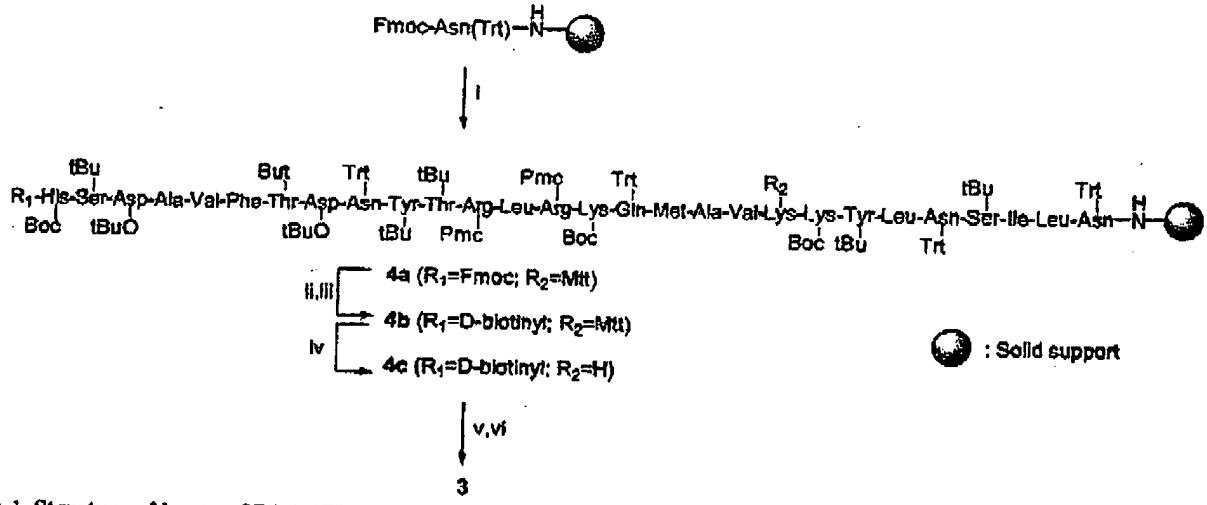

FIG. 1. **Structure of hapten CRA 1, VIP-CRA 3, and synthetic intermediate 2 (*panel A*), and scheme for synthesis of VIP-CRA 3 (*panel B*).** Reagents and conditions for *steps i–vi* in *panel B* are as follows. *Step i*, solid-phase peptide synthesis by 9-fluorenylmethoxycarbonyl (Fmoc) chemistry (deprotection, 20% piperidine in DMF (3 min × 2; 20 min × 1); coupling, Fmoc-amino acid (2.5 eq), PyBOP (2.5 eq), 1-hydroxybenzotriazole (2.5 eq), and *N,N*-diisopropylethylamine (7.5 eq) in DMF (60 min)); *step ii*, 20% piperidine in DMF (3 min × 2; 20 min × 1); *step iii*, D-biotin (2.5 eq), PyBOP (2.5 eq), 1-hydroxybenzotriazole (2.5 eq), and *N,N*-diisopropylethylamine (7.5 eq) in DMF (60 min); *step iv*, 1% trifluoroacetic acid in CH_2Cl_2 (5 min × 10); *step v*, compound 2 (3 eq), 0.1 mM *N,N*-diisopropylethylamine in DMF (overnight); and *step vi*, trifluoroacetic acid-ethanedithiol-thioanisole-phenol (90:1:1:8, 2 h). All of the steps were done at room temperature. Protecting groups: *Boc*, *t*-butoxycarbonyl; *tBu*, *tert*-butyl; *Pmc*, 2,2,5,7,8-pentamethylchroman-6-sulfonyl; *Trt*, trityl; *Mtt*, 4-methyltrityl.

recognition of VIP. The covalent reaction was visualized by boiling the reaction mixtures followed by denaturing SDS-electrophoresis and detection of biotin-containing adducts (Fig. 2*A*, *inset*). Accumulation of covalent VIP-CRA 3 adducts with the anti-VIP Ab increased linearly as a function of time[2] with the light chain subunit accounting for the majority of the adducts (nominal mass 29 kDa determined by comparison with molecular mass standards). Adducts of VIP-CRA 3 with the control Ab were formed at lower levels. Similarly, hapten CRA 1 reacted with anti-VIP and control Abs slowly compared with the VIP-CRA and there was no preference for covalent binding of the hapten CRA at the light chain subunit. Apparent reaction velocities (V_{app}) were obtained from the slopes of linear regression curves fitted to the progress data by least square analysis ([Ab-CRA] = $V_{app} \times t$, where [Ab-CRA] represents the intensity of Ab-CRA adduct band in AAU and t is the reaction time). V_{app} values are compiled in Table I. For the anti-VIP Ab, V_{app} of the VIP-CRA 3 reaction with the light chain was 6.6-fold greater than the heavy chain. Hapten CRA 1 V_{app} values for the two subunits of this Ab were nearly equivalent. V_{app} for the reaction of VIP-CRA with the anti-VIP light chain was 66-fold greater than the corresponding reaction with the control Ab light chain. These observations indicate the selective nucleophilic reactivity of the anti-VIP light chain. Inclusion of VIP

[2] The CRA-Ab reactions were predicted to follow the second-order rate law, but linear adduct accumulation occurred in the initial stage of the reaction.

Downloaded from www.jbc.org by guest, on April 28, 2010

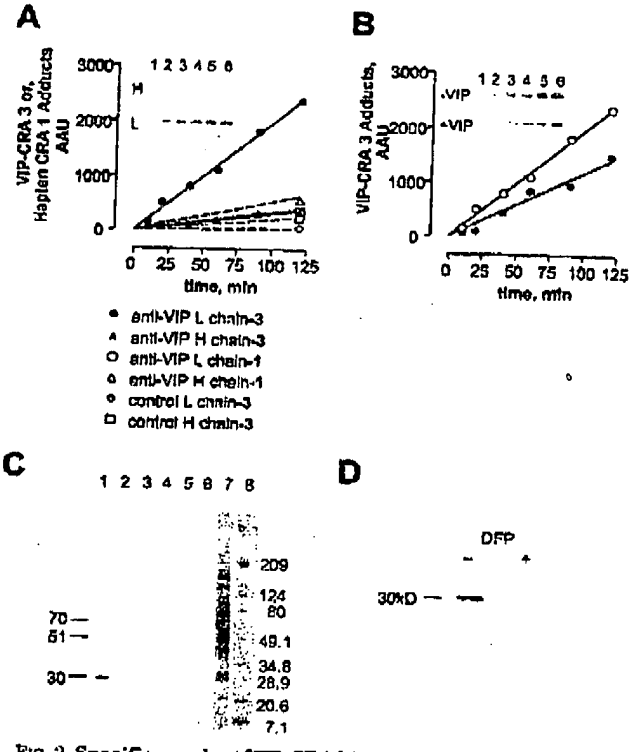

FIG. 2. **Specific covalent VIP-CRA binding by monoclonal anti-VIP IgG (clone c23.5).** *Panel A*, accumulation of VIP-CRA 3 or hapten CRA 1 adducts shown in arbitrary area units (*AAU*) of the adduct bands determined by electrophoresis and densitometry. Reaction conditions: 1 μM IgG, 10 μM CRA, at 37 °C. Data are means of closely agreeing duplicates. Correlation coefficients for curves fitted to progress curves by linear regression were 0.9 or greater. All of the reactions were analyzed at 6 time points as shown for anti-VIP L chain. For clarity, only the final data points at 120 min are shown for anti-VIP H chain and control Ab H and L chains (UPC10 IgG). *Inset*, streptavidin-peroxidase-stained blots of SDS gels showing 3-adducts of the c23.5 light (29 kDa) and heavy (58 kDa) chains. *Lanes 1–6* correspond to the reaction time shown in the graph (10, 20, 40, 60, 90, and 120 min). *Panel B*, representative plot showing inhibition by VIP (10 μM) of formation of anti-VIP light chain adducts with VIP-CRA 3. Percent inhibition was determined as follows: $100 - 100(V_{app}^{+VIP}/(V_{app}^{-VIP})$, where +VIP and −VIP refer to the presence and absence of VIP, respectively. *Inset*, streptavidin-peroxidase-stained electrophoresis cutouts showing light chain adducts formed in the absence and presence of VIP. *Headers 1–6* correspond to the progressively increasing reaction time shown in the graph. *Panel C*, streptavidin-peroxidase-stained blots of SDS-electrophoresis gels showing CRA binding to anti-VIP Ab in the presence of human plasma (1% v/v, 1 h; 10 μM each of CRAs; 10 μM exogenously added Abs). Exogenous Abs and CRAs used are as follows: anti-VIP c23.5 IgG + VIP-CRA 3 (*lane 1*); Control UPC10 IgG + VIP-CRA 3 (*lane 2*); VIP-CRA 3 alone (*lane 3*); anti-VIP c23.5 + hapten 1 (*lane 4*), UPC10 IgG + hapten 1 (*lane 5*); and hapten 1 alone (*lane 6*). Biotin-containing bands in *lanes 1–6* were detected as in *panel A*. *Lanes 7* and *8* are silver-stained blots of human plasma (1% v/v) and molecular weight standards, respectively. *Panel D*, streptavidin-peroxidase-stained blots of reducing SDS-electrophoresis gels showing inhibition of VIP-CRA binding to anti-VIP c23.5 light chain by DFP. Anti-VIP IgG c23.5 (1 μM) was incubated with or without DFP (5 mM) for 5 min and then was allowed to react with VIP-CRA 3 (2 μM) for 60 min.

devoid of the phosphonate group in the reaction mixture inhibited the formation of VIP-CRA 3 adducts with the anti-VIP light chain (Fig. 2*B*; inhibition in three repeat experiments, 41.0 ± 7%). It may be concluded that selective covalent binding of VIP-CRA 3 by the anti-VIP Ab is made possible by noncovalent interactions due to the presence of the VIP sequence.

Pooled plasma from healthy humans was included in the reaction along with VIPase c23.5 to investigate further the selectivity of the VIP-CRA. As expected, the predominant VIP-CRA 3 adduct appeared at the position of the light chain subunit of the VIPase Ab (Fig. 2*C*). Little or no reaction of the VIP-CRA with plasma proteins and the control IgG subunits was observed. Similarly, the reaction mixtures of hapten CRA 1 yielded little or no adduct formation with plasma proteins or the exogenously added monoclonal Abs. Faint biotin bands were observed upon prolonged exposure in each of the *lanes* shown in Fig. 2*C* at a mass of 67–70 kDa. These bands presumably reflect a low level adduct formation of the hapten-CRA and VIP-CRA with albumin, the major protein present in plasma (see *silver-stained electrophoresis lane* in Fig. 2*C*). Covalent reactions of albumin with organophosphorus compounds have been reported previously (28, 29).

TABLE I
Initial velocities (V_{app}) for the formation of VIP-CRA 3 and hapten-CRA 1 Ab adducts

V_{app} values were determined as shown in Fig. 2 legend. AAU, arbitrary area units.

Ab	Subunit	V_{app} ± S.D., AAU min^{-1}	
		VIP-CRA 3	Hapten CRA 1
Anti-VIP IgG, c23.5	Light	19.8 ± 0.4	3.3 ± 0.4
Anti-VIP IgG, c23.5	Heavy	3.0 ± 0.3	5.3 ± 0.7
Control IgG, UPC10	Light	0.3 ± 0.1	ND[a]
Control IgG, UPC10	Heavy	2.0 ± 0.3	ND[a]

[a] ND, not determined.

Diisopropyl fluorophosphate (DFP), a well established serine hydrolase inhibitor, was previously reported to inhibit catalysis by anti-VIP light chain c23.5 (15). In this study, DFP inhibited the covalent VIP-CRA binding to the light chain (Fig. 2*D*), consistent the presence of a serine protease-like binding site(s).

Inhibition of Catalytic Activity—The cleavage of the model peptide substrate Pro-Phe-Arg-AMC by the recombinant light chain of anti-VIP Ab c23.5 has been reported previously (15). Site-directed mutagenesis studies have suggested that the light chain contains a catalytic triad similar to the active site of serine proteases (15). Here, the progress of Pro-Phe-Arg-AMC cleavage by the light chain was measured fluorimetrically by determining AMC generated due to cleavage at the Arg-AMC amide bond. As expected, a linear increase of AMC fluorescence was evident (Fig. 3*A*). Inclusion of VIP-CRA 3 in the reaction mixture inhibited the reaction in a time-dependent manner. The deviation of the progress curve from linearity in the presence of VIP-CRA suggests an irreversible inhibition mode (30). Inhibitory potency comparisons using VIP-CRA 3 and hapten CRA 1 indicated the superior potency of the former compound (IC_{50} = 1.5 and 27 μM, respectively; Fig. 3*B*). The superior potency of VIP-CRA 3 is consistent with the covalent adduct data reported in the preceding section and may be attributed to improved noncovalent recognition of the peptidyl component of VIP-CRA 3. The stoichiometry of the inhibition was determined by titration with limiting amounts of VIP-CRA 3 ([3]/[light chain] ratio = 0.0375–3.75 in Fig. 3*C*). The *x*-intercept of the residual activity (%) *versus* [VIP-CRA 3]/[light chain] plot was 0.89, suggesting a 1:1 stoichiometry. This finding is consistent with the observed molecular mass of the light chain:VIP-CRA adduct, *i.e.* 29 kDa (light chain, 25 kDa; VIP-CRA, 4 kDa).

Next, we turned to a human polyclonal IgG preparation isolated from a subject with airway disease (designated HS-2 in Ref. 24). Cleavage of VIP by this preparation has been attributed to IgG autoantibodies based on retention of the activity in Fab fragments, adsorption of the activity by IgG binding reagents, and absence of VIP cleavage by control identically purified human IgG preparations. N-terminal sequencing of VIP fragments generated by this IgG has identified the following scissile bonds: Thr^{7}-Asp^{8}, Arg^{14}-Lys^{15}, Gln^{16}-Met^{17}, Met^{17}-Ala^{18}, Ala^{18}-Val^{19}, Lys^{20}-Lys^{21}, and Lys^{21}-Tyr^{22} (24). Here, we

Downloaded from www.jbc.org by guest, on April 28, 2010

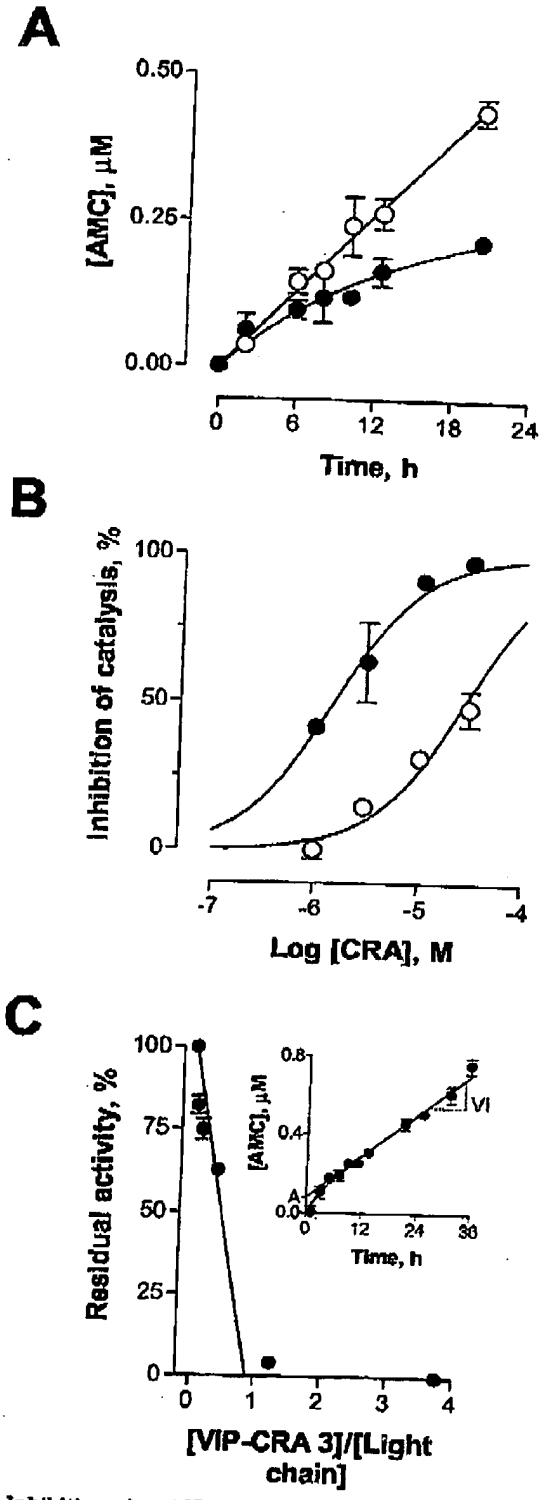

FIG. 3. **Inhibition of anti-VIP light chain c23.5 catalyzed Pro-Phe-Arg-AMC hydrolysis by VIP-CRA 3.** *Panel A*, progress curves of Pro-Phe-Arg-AMC (0.2 mM) cleavage by the light chain (0.8 μM) in the absence (○) and presence (●) of VIP-CRA 3 (3 μM). Curves are least-square fits to the equation $[AMC] = V \times t$ (r^2 0.99) (○) or $[AMC]/[AMC]_{max} = 1 - e^{-k_{obs} \times t}$ (r^2 0.89) (●), where V is the velocity of AMC release, $[AMC]_{max}$ is the extrapolated maximum value of AMC release, and k_{obs} is the observed first-order rate constant. Data are means of three replicates ± S.D. Fluorescence values expressed as released AMC by comparison with a standard curve constructed using authentic AMC. Background fluorescence in the absence of catalyst corresponded to 0.05 ± 0.03 μM AMC. *Panel B*, comparison of VIP-CRA 3 (●) and hapten CRA 1 (○) inhibition of light chain-catalyzed Pro-Phe-Arg-AMC hydrolysis. Curves are fitted to the equation, percent inhibition = $100/(1 + 10^{(\log EC_{50} - \log[CRA])})$, where EC_{50} is the concentration yielding 50% inhibition (r^2 0.98). Reaction conditions are as in *panel A* with the exception that varying CRA concentrations were employed (1, 3, 10, and 30 μM). Percent inhibition was computed as, $100(V - V_{13})/V$, where V_{13} represents the residual activity after incubation for 13 h (tangents of the least-square fit progress curves obtained as in *panel A*). Values are means of three replicates ± S.D. In the absence of CRAs, the reaction rate was 22 nM AMC h^{-1}. *Panel C*, stoichiometry of antibody light chain (c23.5) reaction with VIP-CRA 3. Shown is the plot of residual catalytic activity (Pro-Phe-Arg-AMC hydrolysis) of the light chain in the presence of varying VIP-CRA 3 concentrations (reaction conditions as in *panel B* with the exception that the VIP-CRA concentrations were 0.03, 0.1, 0.3, 1.0, and 3.0 μM and reaction time was 36 h). Residual activity was determined as $100Vi/V$, where V is the velocity in the absence of inhibitor and Vi is a computed value of the velocity under conditions of complete inhibitor consumption. Vi values were obtained from least-square fits to the equation $[AMC] = Vi \times t + A(1 - e^{-k_{obs} \times t})$, where A and k_{obs} represent, respectively, the computed AMC release in the stage when inhibitor consumption is ongoing and the observed first-order rate constant, respectively (r^2 for individual progress curves, >0.97). The equation is valid for reactions with an initial first-order phase and a subsequent zero-order phase. The x-intercept shown in the plot was determined from the least-square fit for data points at [VIP-CRA 3]/[light chain] ratio <1. *Inset*, example progress curve from which Vi values were computed. VIP-CRA 3, 0.03 μM.

initially confirmed the ability of the polyclonal IgG preparation to cleave multiple peptide bonds in VIP. Three new radioactive peaks were generated from [Tyr^{10}-^{125}I]VIP by treatment with the IgG (Fig. 4*A*). The observed radioactive product peaks in Fig. 4*A* probably represent mixtures of peptide fragments, as the VIP fragments generated by cleavage at the aforestated peptide bonds have previously been noted to elute from the HPLC with similar retention times (24).

To determine whether VIP-CRA 3 is an irreversible inhibitor, aliquots of the IgG treated with varying concentrations of this compound (10, 20, 40, and 80 μM) were subjected to affinity chromatography on protein G to remove the unreacted inhibitor followed by assay of the cleavage of [Tyr^{10}-^{125}I]VIP (Fig. 4*B*). Control IgG was subjected to an identical incubation without VIP-CRA followed by the chromatographic procedure. Dose-dependent inhibition of catalytic activity was evident, and near-complete inhibition of catalysis was observed at VIP-CRA concentrations >20 μM. The observed irreversible inhibition suggests that VIP-CRA forms covalent adducts with the polyclonal Abs, similar to its behavior with the monoclonal Ab examined in the preceding section. Selectivity of the VIP-CRA inhibitory effect was confirmed by comparison with hapten CRA 1. As expected, the VIP-CRA inhibited the cleavage of VIP more potently than the hapten CRA (IC_{50} = 7 and 36 μM, respectively).

DISCUSSION

The following conclusions may be drawn from these data. (*a*) Functionally coordinated noncovalent and covalent interactions allowed nucleophilic anti-VIP Abs to form specific and covalent adducts with the VIP-CRAs. (*b*) The VIP-CRA inhibits each of the reactions involving cleavage of VIP at several peptide bonds, indicating its potential as a universal inhibitor of diverse anti-VIP catalytic Abs. The importance of noncovalent Ab paratope-antigen epitope binding in directing the VIP-CRA to the Ab nucleophile is evident from the following observations: lower reactivity of the anti-VIP monoclonal Ab with the hapten CRA devoid of the VIP sequence; limited reactivity of the irrelevant isotype-matched Ab and plasma proteins with the VIP-CRA; and inhibition of the anti-VIP Ab covalent reaction with the VIP-CRA by VIP devoid of the CRA moiety.

Downloaded from www.jbc.org by guest, on April 28, 2010

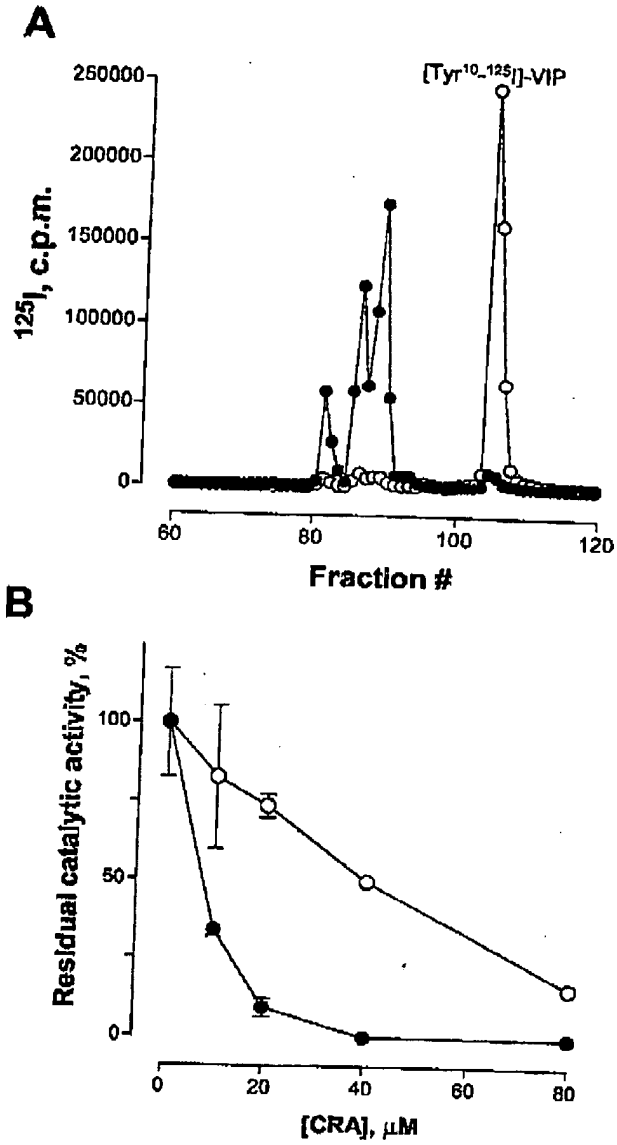

FIG. 4. **Inhibition of polyclonal antibody catalyzed VIP cleavage by VIP-CRA 3 and hapten CRA 1.** *Panel A*, reversed-phase HPLC profiles showing cleavage of [Tyr^{10}-^{125}I]VIP at multiple sites by human IgG HS-2. [Tyr^{10}-^{125}I]VIP incubated in the presence (●) or absence (○) of HS-2 IgG (2 μM) for 16 h and subjected to HPLC (Novapak C_{18} 3.9 × 150 mm; 0.1% trifluoroacetic acid in water-0.1% trifluoroacetic acid in 80% acetonitrile 95:5 for 10 min, from 95:5 to 30:70 in 55 min, from 30:70 to 0:100 in 5 min, and 0:100 for 5 min (0.5 ml/min)). Shown are values of ^{125}I-radioactivity recovered in the HPLC fractions (0.5 ml). *Panel B*, irreversible inhibition of HS-2 IgG-catalyzed [Tyr^{10}-^{125}I]VIP cleavage by VIP-CRA 3 and hapten CRA 1. IgG (2 μM) was preincubated for 16 h in the absence or presence of increasing concentrations of VIP-CRA 3 (●) or hapten CRA 1 (○). Following the removal of unreacted CRA by chromatography on immobilized protein G, the residual catalytic activity of the IgG was measured using [Tyr^{10}-^{125}I]VIP as substrate. Data are the means ± S.D. Control HS-2 IgG that was incubated in the absence of CRAs cleaved 2791 cpm [Tyr^{10}-^{125}I]VIP.

Recently, CRA derivatives of other polypeptide antigens (human immunodeficiency virus glycoprotein 120 and epidermal growth factor receptor) have also been reported to form covalent adducts with specific Abs directed to these antigens with only minor levels of reactions evident with Abs directed to irrelevant Abs (31, 32). Taken together, these considerations open the route toward permanent inhibition of individual Ab subpopulations based on their antigenic specificity.

The light chain subunit accounted for most of the covalent reactivity of the anti-VIP monoclonal Ab with the VIP-CRA. Reactivity with the hapten CRA serves as an index of Ab nucleophilicity independent of traditional noncovalent forces responsible for Ab-antigen complexation. Hapten CRA reactivities of the anti-VIP heavy and light chain subunits were comparable, suggesting that differences in intrinsic nucleophilic reactivity do not account for rapid formation of adducts of the light chain with the VIP-CRA. It may be concluded that the light chain nucleophile is in the immediate vicinity of the Ab noncovalent binding site and that the noncovalent binding interactions facilitate covalent binding. This statement is consistent with observations that the purified light chain of this Ab is capable of specifically catalyzing the cleavage of VIP (25). Previously, the purified light and heavy chain subunits of the Ab were reported to bind VIP independently determined by a conventional assay for noncovalent Ab-antigen complexes (K_d for light chain, heavy chain, and intact IgG, respectively, 10.1, 6.8, and 1.9 nM) (33). In addition to the light chain, the heavy chain subunit appears to contribute noncovalent binding energy for Ab complexation with VIP but the heavy chain nucleophile does not seem to be sufficiently in register with the phosphonate group of the VIP-CRA to participate in the covalent reaction.

Additional evidence for irreversible and specific Ab recognition by the VIP-CRA is available from the catalysis assays. VIP-CRA adducts of the Abs obtained following the removal of unreacted VIP did not display catalytic activity. Catalytic cleavage of Pro-Phe-Arg-AMC by the recombinant light chain of the monoclonal Ab has been documented previously (15). This reaction is characterized by 57.5-fold higher K_m than the cleavage of VIP by the light chain and is attributed to cross-reactivity of the catalytic site with peptide substrates devoid of an antigenic epitope capable of participating in high affinity noncovalent binding. Pro-Phe-Arg-AMC cleavage by the light chain was inhibited more potently by the VIP-CRA than the hapten CRA. Similarly, the cleavage of VIP by polyclonal human autoantibodies to VIP was inhibited more potently by the VIP-CRA than the hapten-CRA.

Ab diversity poses an interesting challenge in achieving antigen-specific covalent inactivation of pathogenic Abs. Structural differences in the variable domains underlies Ab specificity for individual antigenic epitopes, and even Abs to small molecules presenting a limited surface area can contain structurally distinct binding sites (*e.g.* Refs. 34 and 35). Catalytic IgG preparations from patients with autoimmune disease cleave several backbone bonds in polypeptide (7, 24) and oligonucleotide (9) antigens. This may be due to the presence of multiple Ab species in polyclonal IgG preparations, each with a distinct scissile bond specificity. We have suggested previously that the nucleophiles enjoy some measure of mobility within Ab active sites that is not subject to restriction when noncovalent binding of Abs and antigens takes place (31, 32). To the extent that this hypothesis is valid, Abs with differing peptide bond specificity could react covalently with the VIP-CRA even if the phosphonate group is located somewhat imprecisely in the antigenic epitope. In this study, the placement of the phosphonate on the Lys^{20} side chain (as opposed to the peptide backbone) and inclusion of a flexible linker represent attempts to expand further the conformational space available for the covalent reaction. Complete inhibition of catalytic hydrolysis of VIP by polyclonal Abs that cleave several bonds between VIP residues 7 and 22 by the VIP-CRA was evident. Therefore, promising means to

Downloaded from www.jbc.org by guest, on April 28, 2010

obtain antigen-specific covalent inhibition of diverse Abs include the exploitation of intrinsic conformational properties of Ab catalytic sites and the provision of enhanced access to the phosphonate group by manipulating the linker structure. In comparison, if Ab antigen binding is conceived as a rigid body interaction involving inflexible surface contacts, covalent inhibitor design must entail close topographical simulation of the transition state of each scissile bond and individual inhibitors must be developed to effectively inhibit different catalytic Abs. The importance of evaluating conformational factors in inhibitor design is supported by previous reports suggesting a split-site model of catalysis (31, 32) in which antigen binding at the noncovalent subsite imposes little or no conformational constraints on the catalytic subsite, allowing the catalytic residue to become positioned in register with alternate peptide bonds as the transition state is formed.

As noted previously, catalytic Abs are proposed to contribute in the pathogenesis of autoimmune disease. Specific covalent inhibitors represent a novel means to help define the precise functional effects of the Abs. Such inhibitors may serve as prototypes for the development of therapeutic agents capable of ameliorating harmful Ab effects. In addition to inactivation of secreted Abs, reagents such as the VIP-CRA may be useful in targeting antigen-specific B cells. The feasibility of this goal is indicated by evidence that CRAs bind covalently to Abs expressed on the surface of B cells as components of the B cell receptor (36). Ab nucleophilicity may be viewed as an indication of their competence in completing the first step in covalent catalysis, *i.e.* formation of an acyl-Ab reaction intermediate. This is supported by observations that the magnitude of Ab nucleophilic reactivity is correlated with their proteolytic activity (31). A recent study suggests that noncatalytic Abs also contain nucleophiles but are unable to facilitate steps in the catalytic cycle following covalent attack on the antigen, *viz.* water attack on the acyl-Ab intermediate and product release (31). Regardless of the physiological functions of nucleophiles expressed by noncatalytic Abs, their presence may allow CRA targeting of Ab populations with established pathogenic roles, *e.g.* anti-factor VIII Abs in hemophilia.

Acknowledgement—We thank Robert Dannenbring for technical assistance.

REFERENCES

1. Vincent, A. (2002) *Nat. Rev. Immunol.* 2, 797–804
2. Gilles, J. G., Vanzieleghem, B., and Saint-Remy, J. M. (2000) *Semin. Thromb. Hemostasis* 26, 151–156
3. Rekvig, O. P., and Nossent, J. C. (2003) *Arthritis Rheum.* 48, 300–312
4. Tomer, Y. (1997) *Clin. Immunol. Immunopathol.* 82, 3–11
5. Paul, S., Valle, D. J., Beach, C. M., Johnson, D. R., Powell, M. J., and Massey, R. J. (1989) *Science* 244, 1158–1162
6. Matsuura, K., and Sinohara, H. (1996) *Biol. Chem.* 377, 587–589
7. Lacroix-Desmazes, S., Moreau, A., Sooryanarayana, Bonnemain, C., Stiniljes, N., Paehov, A., Sultan, Y., Hochoke, J., Kazatchkine, M. D., and Kaveri, S. V. (1999) *Nat. Med.* 5, 1044–1047
8. Hatiuchi, K., Hifumi, E., Mitsuda, Y., and Uda, T. (2003) *Immunol. Lett.* 86, 249–257
9. Shuster, A. M., Gololobov, G. V., Kvashuk, O. A., Bogomolova, A. E., Smirnov, I. V., and Gabibov, A. G. (1992) *Science* 256, 665–667
10. Bangale, Y., Karle, S., Planque, S., Zhou, Y. X., Taguchi, H., Nishiyama, Y., Li, L., Kalnga, R., and Paul, S. (2003) *FASEB J.* 17, 628–636
11. Voice, J. K., Dorsam, G., Chan, R. C., Grinninger, C., Kong, Y., and Goetzl, E. J. (2002) *Regul. Pept.* 109, 199–208
12. Maggi, C. A., Ginchetti, A., Dey, R. D., and Said, S. I. (1995) *Physiol. Rev.* 75, 277–322
13. Voice, J. K., Grinninger, C., Kong, Y., Bangale, Y., Paul, S., and Goetzl, E. J. (2003) *J. Immunol.* 170, 308–314
14. Berisha, H. I., Bratut, M., Bangale, Y., Colasurdo, G., Paul, S., and Said, S. I. (2002) *Pulm. Pharmacol. Ther.* 15, 121–127
15. Gao, Q. S., Sun, M., Rees, A. R., and Paul, S. (1995) *J. Mol. Biol.* 253, 658–664
16. Oleksyszyn, J., and Powers, J. C. (1994) *Methods Enzymol.* 244, 423–441
17. Paul, S., Tramontano, A., Gololobov, G., Zhou, Y. X., Taguchi, H., Karle, S., Nishiyama, Y., Planque, S., and George, S. (2001) *J. Biol. Chem.* 276, 28314–28320
18. Kolesnikov, A. V., Kozyr, A. V., Alexandrova, E. S., Koralewski, F., Demin, A. V., Titov, M. I., Avalle, B., Tramontano, A., Paul, S., Thomas, D., Gabibov, A. G., and Friboulet, A. (2000) *Proc. Natl. Acad. Sci. U. S. A.* 97, 13526–13531
19. Oleksyszyn, J., Boduszek, B., Kam, C. M., and Powers, J. C. (1994) *J. Med. Chem.* 37, 226–231
20. Nishiyama, Y., Taguchi, H., Luo, J. Q., Zhou, Y. X., Burr, G., Karle, S., and Paul, S. (2002) *Arch. Biochem. Biophys.* 402, 281–288
21. Wellings, D. A., and Atherton, E. (1997) *Methods Enzymol.* 289, 44–67
22. Aletras, A., Barlos, K., Gatos, D., Koutsogianni, S., and Mamos, P. (1995) *Int. J. Pept. Protein Res.* 45, 488–496
23. Paul, S., Sun, M., Mody, R., Tewary, H. K., Stemmer, P., Massey, R. J., Gianferrara, T., Mehrotra, S., Dreyer, T., Meldal, M., and Tramontano, A. (1992) *J. Biol. Chem.* 267, 13142–13145
24. Paul, S., Mei, S., Mody, B., Eklund, S. H., Beach, C. M., Massey, R. J., and Hamel, F. (1991) *J. Biol. Chem.* 266, 16128–16134
25. Sun, M., Gao, Q. S., Kirnarskly, L., Rees, A., and Paul, S. (1997) *J. Mol. Biol.* 271, 374–385
26. Oleksyszyn, J., and Powers, J. C. (1991) *Biochemistry* 30, 485–493
27. Sampson, N. S., and Bartlett, P. A. (1991) *Biochemistry* 30, 2256–2263
28. Means, G. E., and Wu, H. L. (1979) *Arch. Biochem. Biophys.* 194, 526–530
29. Schwartz, M. (1982) *Clin. Chim. Acta* 124, 213–223
30. Marangoni, A. G. (2003) *Enzyme Kinetics: A Modern Approach*, John Wiley & Sons, Inc., New York
31. Planque, S., Taguchi, H., Burr, G., Bhatia, G., Karle, S., Zhou, Y. X., Nishiyama, Y., and Paul, S. (2003) *J. Biol. Chem.* 278, 20436–20443
32. Paul, S., Planque, S., Zhou, Y. X., Taguchi, H., Bhatia, G., Karle, S., Hanson, C., and Nishiyama, Y. (2003) *J. Biol. Chem.* 278, 20429–20435
33. Sun, M., Li, L., Gao, Q. S., and Paul, S. (1994) *J. Biol. Chem.* 269, 734–738
34. Kaartinen, M., Penttonen, J., and Makela, O. (1988) *Eur. J. Immunol.* 18, 98–105
35. Mitchell, T. J., and Reilly, T. M. (1990) *Pept. Res.* 3, 277–281
36. Planque, S., Bangale, Y., Song, X. T., Karle, S., Taguchi, H., Poindexter, B., Bick, R., Edmundson, A., Nishiyama, Y., and Paul, S. (January 15, 2004) *J. Biol. Chem.*, 10.1074/jbc.M312152200

Downloaded from www.jbc.org by guest, on April 28, 2010